Alma Mater Studiorum – Università di Bologna

DOTTORATO DI RICERCA IN

SCIENZE BIOTECNOLOGICHE E FARMACEUTICHE

Ciclo XXXII

Settore Concorsuale: 03/D1

Settore Scientifico Disciplinare: CHIM/08

NOVEL DUAL D3R/GSK-3β MODULATORS: AN INNOVATIVE MULTITARGET STRATEGY FOR BIPOLAR DISORDER

Presentata da: **Francesca Seghetti**

Coordinatore Dottorato   **Supervisore**

Prof.ssa Maria Laura Bolognesi   **Prof.ssa Federica Belluti**

Esame finale anno 2020

TABLE OF CONTENTS

Abstract

NOVEL DUAL D3R/GSK-3β MODULATORS: AN INNOVATIVE MULTITARGET STRATEGY FOR BIPOLAR DISORDER

Among the psychiatric diseases, bipolar disorder (BD) is the sixth leading cause of disability with a prevalence up to 4 % worldwide. BD is a complex neuropsychiatric condition which alternates episodes of mania with symptoms of depression. Although the neurobiological pathways are not completely clarified, the dopamine (DA) hypothesis, recognized as the leading theory explaining the pathophysiology of the malady, states that the dramatically compromised homeostatic regulation of dopaminergic circuits leads to alternated changes in DA neurotransmission. Modulation of D2 and D3 receptors (D2/3R) through partial agonists represents the first-line therapeutic strategy for psychiatric diseases. Moreover, a deregulation of the enzyme glycogen synthase kinase-3β (GSK-3β) has been reported as peculiar feature of BD. In this scenario, the concomitant modulation of D3R and GSK-3β, by employing multifunctional or multitarget compounds, could offer promises to achieve an effective cure of this illness. In the light of these findings, we rationally envisaged the pharmacophoric model at the basis of the design of several D3R partial agonists, suitable to be exploited for the dual D3R/GSK-3β ligand design. Thus, synthetic efforts were addressed to develop a first set of hybrid molecules able to concurrently modulate the selected targets. For a chemical structure point of view, we employed different spacers to combine a substituted aryl-piperazine moiety, reported in previously discovered D3R modulators, with a pyrazole-based fragment, already identified in GSK-3β inhibitors. A fluorescent and a cellular functional assays were carried out to assess the activity of all synthetized compounds against GSK-3β and on D3R, respectively. Most of the derivatives proved to effectively modulate both GSK-3β and D3R with potencies in the low-µM and low-nM range, respectively. The consistent biological data obtained allowed us to identify some lead candidates worth to be further

modified with the aim to optimize their biological profile and to perform a structure-activity relationship (SAR) study.

List of abbreviations

ADHD attention deficit hyperactivity disorder

AC adenylyl cyclase

AKT protein kinase B

PKC protein kinase C

5-HTT serotonin transporter

DAT dopamine transporter

BDNF brain-derived neurotrophic factor

COMT catechol-*O*-methyltransferase

BD bipolar disorder

Boc₂O di-*tert*-butyl-dicarbonate

cAMP cyclic adenosine monophosphate

DA dopamine

D2R dopamine D2 receptor

D3R dopamine D3 receptor

DIPEA *N*,*N*-diisopropylethylamine

DMAP 4-Dimethylaminopyridine

DMF *N*,*N*-dimethylformamide

ICL intracellular protein loop

ECL extracellular protein loop

EDC *N*-(3-Dimethylaminopropyl)-*N*′-ethylcarbodiimide hydrochloride

Et₂O diethyl ether

EtOAc ethyl acetate

EtOH ethanol

GPCR G protein-coupled receptor

GSK-3β glycogen synthase kinase-3β

GSH glutathione

5-HT serotonin

HATU 1-[Bis(dimethylamino)methylene]-1*H*-1,2,3-triazolo[4,5-b]pyridinium 3-oxid hexafluorophosphate

HVA homovanillic acid

HOBt Hydroxybenzotriazole

IMPase inositol-1(or 4)-monophosphatase

IPP inositol-1,4 bisphosphate 1-phosphatase

LDA Lithium diisopropylamide

MAO monoamine oxidase

MW microwave

NH$_{3(aq)}$ Ammonia aqueous solution 32%

OBS orthosteric binding site

6-OHDA 6-hydroxydopamine

PKA protein kinase A

PE petroleum ether

ROS reactive oxygen species

rt room temperature

SBP secondary binding pocket

TEA triethylamine

TFA trifluoroacetic acid

THF tetrahydrofuran

THP tetrahydropyranyl

TM transmembrane helices

1. INTRODUCTION

1.1. BIPOLAR DISORDER: THE BURDEN OF A COMPLEX MENTAL ILLNESS

Fluctuations in mood are frequent during human life, especially when a person faces stressful events. However, when mood changes became persistent and result in notable distress or impairment, could underlie an affective disorder. Bipolar disorders (BDs) refer to a group of affective disorders typically characterized by recurrent episodes of mania and depression.[1] BD, previously known as maniac depressive illness, is a neuroprogressive and chronic mental illness with a variable course that often results in central nervous system (CNS) functional and cognitive impairment, by reducing the quality of life.[2] The malady affects about 1 % of the world's population with equal prevalence in males and females and represents one of the leading causes of disability among young people.[3] The recurrent mood changes between mania or hypomania, namely elevated and irritable mood, and depression symptoms like anhedonia, cognitive disorders, and suicidal thoughts, represent a diagnostic hallmark of the malady (Figure 1).
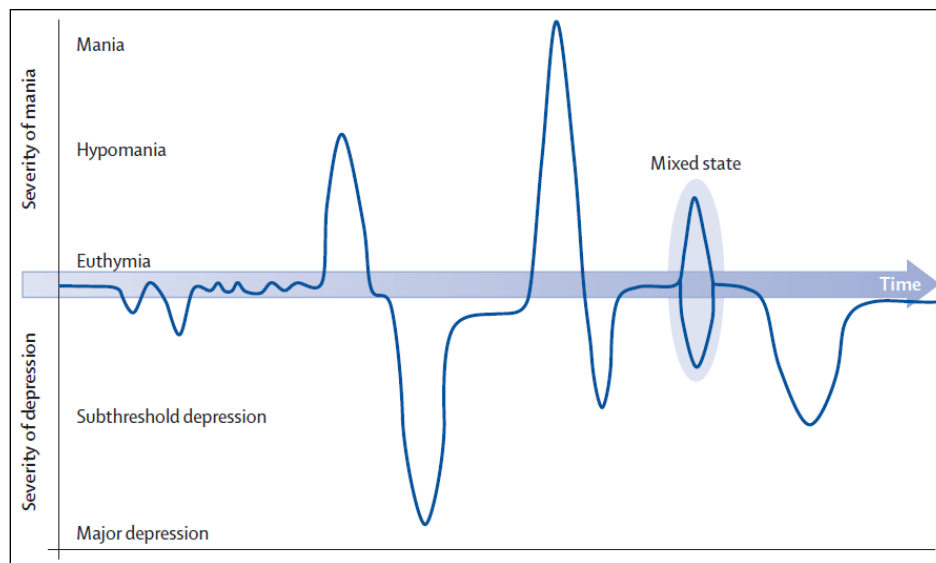

Figure 1. Life chart showing the progression of BD.[4]

According to the longitudinal course of the disease, which is characterised by the presence of symptom below or above the state of euthymia (normal mood state), BD is classified in four main subtypes:

- BD type I (Figure 2), defined by at least one episode of mania or mixed episode, although major depressive episodes are typical but not needed for diagnosis. Manic symptoms include irritability or euphoria together with insomnia, impulsive behaviour, increased talkativeness, hasty thoughts, hyperactivity, and distractibility. Mixed episodes include manic symptoms and simultaneous depressive symptoms lasting for at least one week.

- BD type II (Figure 2), characterized by several protracted periods of major depression and at least one hypomanic episode, but without maniac symptoms. Hypomania presents the same symptoms as mania but lasts for shorter intervals (four or more days instead of weeks for maniac episode). Depressive symptoms include intense sadness or loss of interests, accompanied by fatigue, insomnia, psychomotor agitation or retardation, weight gain or loss, cognitive dysfunction, feelings of worthlessness, and suicidal thoughts or attempts.
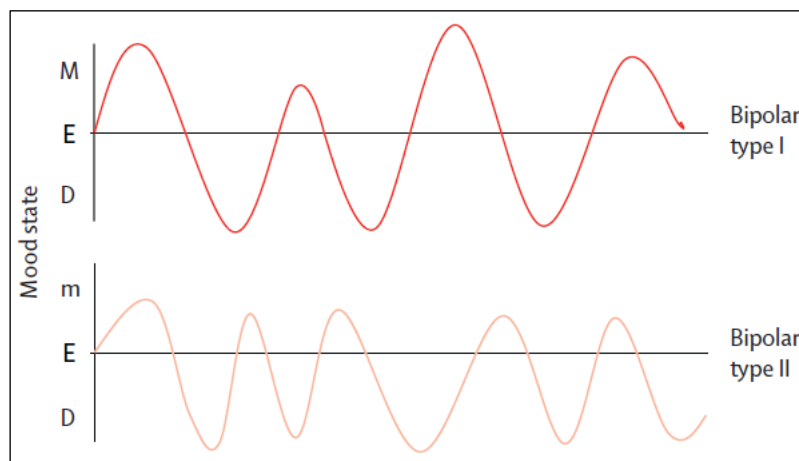

Figure 2. Mood fluctuations in BD type I and BD type II.[5] M = mania; m = hypomania; d = depression; E = euthymia.

- Cyclothymic disorder, described by several periods of hypomanic and depressive symptoms that do not meet diagnostic criteria for hypomania or major depression for at least two years.

- Bipolar disorder not otherwise specified: depressive and hypomanic-like symptoms and episodes that might alternate rapidly, but do not meet the full diagnostic criteria for any of the above disorders.

Over the past decade, this complex disorder has been consistently associated with clinical comorbidities that contribute to premature mortality, particularly death by suicide.[6] Among the medical comorbidities, cardiovascular disease, hypertension, obesity, metabolic syndrome and diabetes are highly prevalent in patients with BD,[7] while psychiatric comorbidities, including attention deficit hyperactivity disorder (ADHD), anxiety, personality disorders, eating disorder and drug addiction,[8] are reported in 90 % of patients with BD.[9]

Considering the high number of comorbid conditions, BDs are complicated to diagnose accurately in clinical practice, especially in their early stages. Indeed, only 20 % of diseased patients who are experiencing a depressive episode are diagnosed with BD within the first year of seeking treatment,[10] and the mean delay between the illness onset and diagnosis is 5-10 years.[11]

1.2. PATHOLOGICAL NETWORK OF BD

Although the neurobiology of this complex disease is still not completely clarified, the identification of key biomarkers led to the development of several hypotheses.[12] In detail, multiple findings provided by neuroimaging, genetic, neurophysiological, and neurochemical studies conducted on BD patient's brain, allowed to identify a number of interconnected pathological hallmarks involved in the progression of this disorder. These include genetic changes, structural and functional brain damage, impaired mood regulation neuronal circuits, altered synaptic neurotransmission, mitochondrial dysfunction, oxidative stress, impaired cellular signalling, apoptosis, and chronic neuroinflammation (Figure 3).

In the light of this complex scenario, BD represents a multifactorial disease that arises from compromised synaptic and neuronal plasticity of circuits involved in affective and cognitive functions. Thus, BD could be conceptualized as a disorder of synapses and circuits, rather than an imbalance in neurotransmitters.[13]
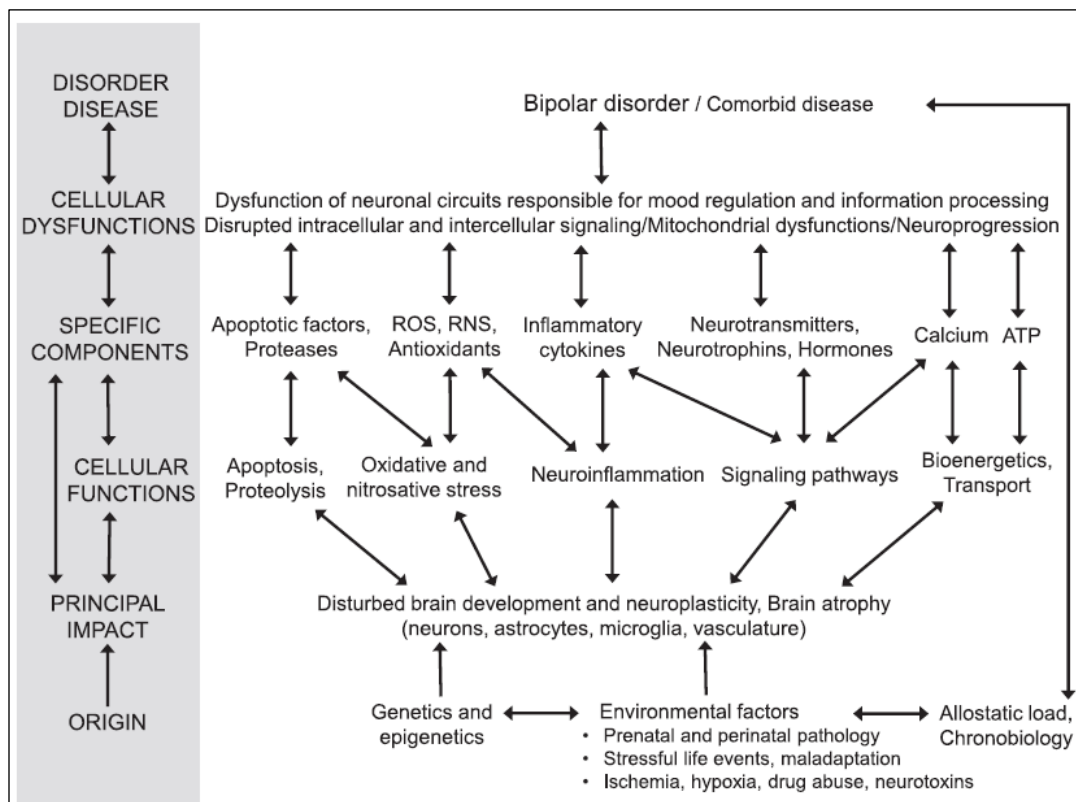

Figure 3. Map of pathogenic events leading to BD.[12]

Herein, an overview of the biochemical pathways underpinning both the onset and course of the malady has been described. Particular emphasis was devoted to explaining the role played by the impaired neuroplasticity in BD pathophysiology and treatment. This preliminary investigation allowed the identification of potential biological targets whose modulation may stabilize neuroprogression through reduction of the frequency and the severity of mood fluctuations.

➢ **Genetic and epigenetic factors**

BD is among the most heritable human disorder. Based on twins studies, heritability was estimated at 85 %.[14] Genetic and environmental factors are implicated in the development of the disease, which could be considered as a polygenic disorder. In this respect, genetic analyses have confirmed that many chromosomal regions and genes are related to susceptibility to BD, with each gene exerting a mild to moderate effect.[15] In detail, genetic polymorphisms of several signaling pathways such as serotonin transporter (5-HTT), dopamine transporter (DAT), brain-derived neurotrophic factor (BDNF), and catechol-O-methyltransferase (COMT), along with various mutations of mitochondrial DNA have been identified. [16]

In addition, also environmental and social factors, namely drug addiction or sexual abuse,[17] have shown to play a significant role in the manifestation and course of BD.

➢ **Neuroanatomical brain modifications**

Neuroimaging studies in BD patients allowed identifying several structural and functional abnormalities of CNS implicated in the control of mood states and emotions encompassing limbic, striatal, and frontal regions (Figure 4).
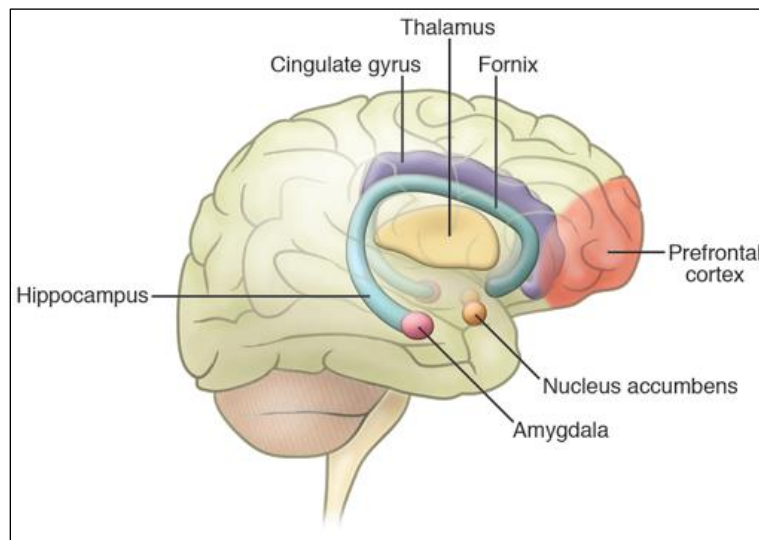
Figure 4. Neuroanatomical brain regions implicated in BD.[18]

In detail, several studies have found region-specific structural modifications, namely increased ventricular size and decrease hippocampal and frontal cortical volume.[19-21] Moreover, white matter hyperintensities around the ventricles have been identified.[22] In parallel with structural studies, from functional imaging findings an excessive activation in the brain region associated with emotional regulation that include *amygdala*, *striatum*, and *thalamus* has been identified.[23]

➢ **Neurotransmitter system**

Pharmacological evidence, studies on neurotransmitter metabolites, and PET imaging experiments supported the crucial role of the altered neurotransmission in the pathophysiology of mood disorders; unfortunately, they did not demonstrate the primary role of the neurotransmitter levels in the onset of the disease. However, deregulation of a number of neurotransmitters, such as dopamine (DA), serotonin (or 5-hydroxytryptamine, 5-HT) and glutamate, has been associated with BD. The original hypothesis states that both maniac and depressive episodes arise from an imbalance in monoaminergic neurotransmission that, in turn, is induced not only by compromised amounts of monoamines, but also by altered functions of neurotransmitter receptors, transporters, catabolizing enzymes, and by other brain neurobiological systems.[24, 25]

In this context, evidence suggest that increased levels of DA D2 and D3 receptors (D2/3R) and hyperactive reward system lead to mania, while elevated striatal DAT availability conducts to depression. Thus, the compromised homeostasis of DA circuits, leading to cyclical changes in DA neurotransmission, was reported as a key pathological event of BD.[26] Moreover, it is proved that increased DA levels affect not only neurotransmission but also oxidative balance, due to dopaminergic metabolic pathways (Figure 6).[27] Indeed, DA can be metabolized *via* monoamine oxidase (MAO) or can go through not enzymatic hydroxylation, in presence of Fe^{2+} and hydrogen peroxide (H_2O_2). The interaction of DA with MAO leads to the release of reactive oxygen species (ROS) and H_2O_2,[28] while the oxidation of this neurotransmitter by Fe^{2+} produces 6-hydroxydopamine (6-OHDA) and *p*-quinone that might inhibit mitochondrial electron transport chain[27] or activate caspase-8 pathway, respectively,[29] resulting in oxidative damage and apoptosis (Figure 6). The aberrant production of *p*-quinone leads to depletion of glutathione (GSH), the primary antioxidant defence in CNS, thus leaving cells more vulnerable to oxidation.[30]

A reduced serotoninergic tone is common to both depressive and maniac symptoms; indeed, elevated MAO density and reduced 5-HTT levels have been detected during the major depression, confirming that the severity of depressive episodes is proportionate to a modified monoamine transporter activity.[31, 32]

The glutamatergic system has also been found to be implicated, due to the detection of the increased level of glutamate in prefrontal cortex of BD patients during the manic phase.[33] Similarly to DA, glutamate plays an important role in cellular redox homeostasis, as increased glutamate levels results in intracellular calcium-mediated excitotoxicity, followed by ROS production.[34]

> **Neurotrophic factors**

Neurotrophic factors such as BDNF, bcl-2, and vascular endothelial growth factor (VEGF) regulate cellular apoptotic pathways, thus promoting neuroplasticity and neurogenesis. Alterations in neurotrophins and the related impairment in CNS plasticity are well-documented conditions in BD.[35] Besides, the characteristic

neuroprogression of the malady has been strongly associated with a low activity of BDFN and bcl-2. For example, several studies reported that peripheral BDNF levels are consistently reduced during acute episodes of mania and depression;[36] and, after therapeutic treatment, patients show a recover in plasma BDNF levels.[37] Based on these findings, BDNF may represent a reliable state-marker of the clinical trend of BD.

> ➢ **Neuroinflammation**

Inflammation is part of a complex biological response to cellular injury; it is characterized by some main events namely activation of cytokine cascades, onset of cellular immune responses, increased levels of acute phase proteins and complement factors. When the inflammatory process takes place in the CNS, microglial cell activation was observed, aimed at repairing the damaged area and preserving the neuronal environment. However, in the presence of multiple harmful stimuli, the chronic inflammatory condition triggers complex interconnected pathways culminating in synaptic degeneration and neuronal loss.[38]

Microglial cells are the resident macrophages of the CNS, playing critical roles in physiological and pathological functioning of the brain, and in neurogenesis.[39] In detail, the regulation of the inflammatory response through the release of neurotrophic factors and anti-inflammatory mediators is one of the most essential activities of microglial cells. However, under chronic neuroinflammation, the protracted activation of microglia can induce neurotoxicity through the production of pro-inflammatory cytokines, namely interleukin-1β (IL-1β), IL-6, IL-12, interferon gamma (INF-γ) and tumor necrosis factor-α (TNF-α), and the synthesis and the release of ROS and nitric oxide (NO).[40]

Several neuropsychiatric and neurodegenerative disorders are related to impaired neuroplasticity caused by chronic neuroinflammation. In this context, there is increasing evidence for a pivotal role of the inflammatory system in the pathophysiology of BD, including the progressive impairment of cognitive function and medical comorbidity. In detail, post-mortem studies on BD patients have shown increased pro-inflammatory and decreased anti-inflammatory markers in the prefrontal

cortex.[41, 42] Recently, manic episodes have been associated with a pro-inflammatory state with amplified levels of IL-6, INF-γ, TNF-α, and free radicals. After therapeutic treatment, while IL-6 is restored to normal levels, TNF-α amount remains elevated, indicating IL-6 as a possible marker of the manic episode.[43]

Figure 5 summarises the hypothetical role of neuroinflammation in BD. After the first acute episode, neuronal injury activates microglia to release proinflammatory cytokines and neurotrophic factors, which, in turn, induce synaptic modifications in order to preserve the neuronal environment. After several episodes, chronically activated microglia leads to increased production of inflammatory cytokines, and the imbalance between pro-inflammatory and anti-inflammatory states culminates in neurodegeneration and systematic toxicity.
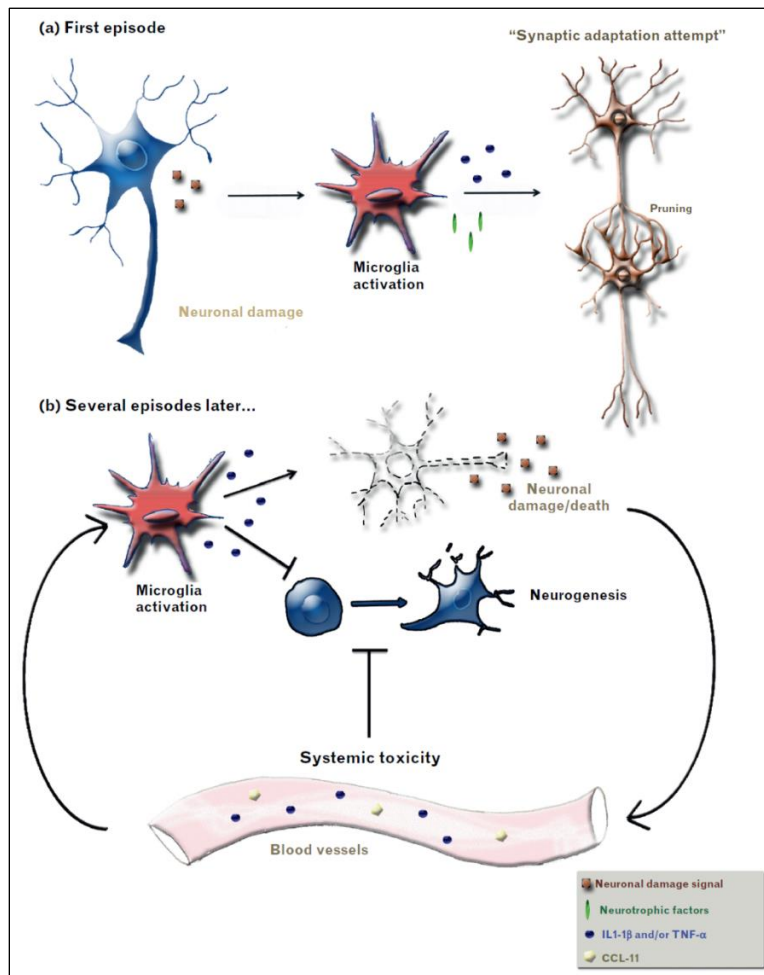

Figure 5. Schematic mechanisms of neuroinflammation in BD.[44]

➢ **Oxidative stress**

Oxidative stress has been recognized as the main pathological feature of several CNS disorders, among them BD, caused by an imbalance between oxidant and antioxidant agents. This disequilibrium leads to oxidative damage of macromolecules and ultimately impairs neuronal survival, plasticity, and signal transmission.[45] This imbalance may also be associated with several conditions such as low BDFN levels, activation of inflammatory pathways, glutamate and DA toxicity due to the depletion of intracellular glutathione, and mitochondrial dysfunction, all leading to increased levels of ROS and NO. Thus, accumulation of oxidative damage, followed by neuronal cell death, is thought to play a pivotal role in determining the impairment in mood-stabilizing mechanisms.
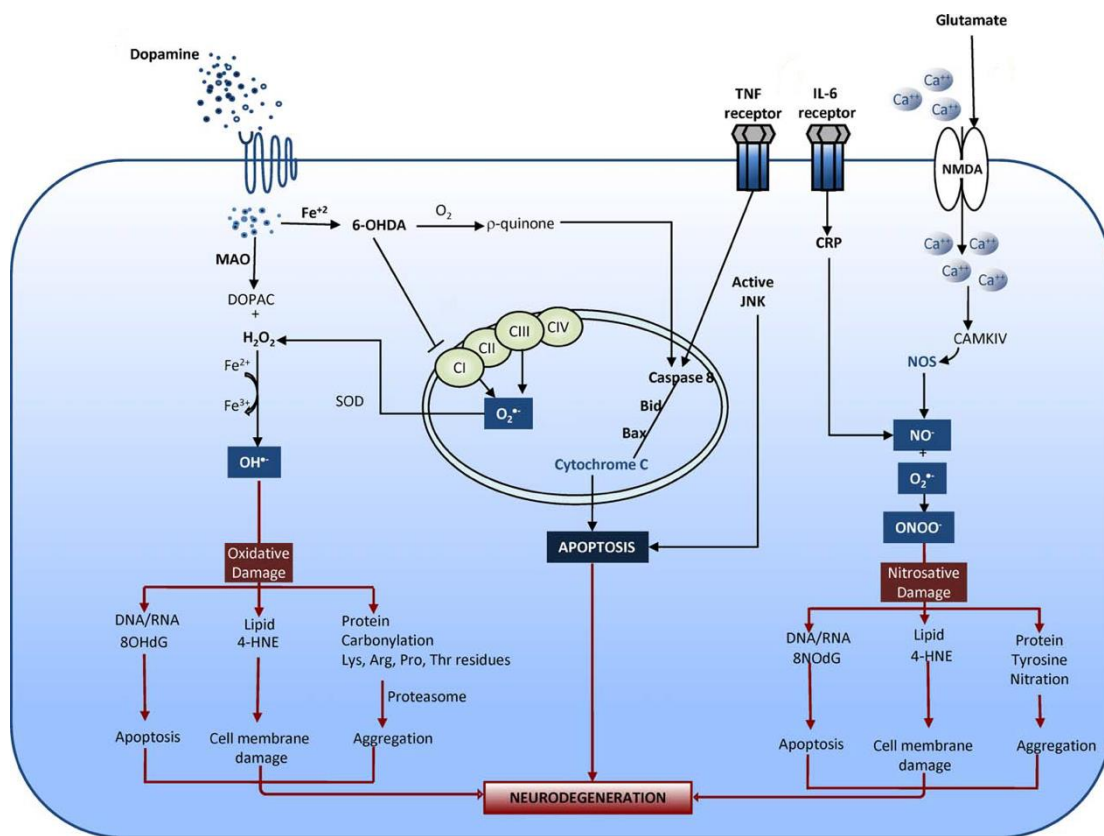

Figure 6. Interconnected pathways leading to oxidative damage and neurodegeneration in BD.[46]

In detail, in BD patients during a mania episode, the activity of superoxide dismutase (SOD), the main component of the anti-oxidant defence system, increases, suggesting

a compensatory response to oxidative stress.[47] High peripheral levels of NO, a potent oxidant agent, is also observed especially during manic eposides.[48] The peripheral detection of thiobarbituric acid reactive substances (TBARS) and protein carbonyl content (PCC), considered as serum biomarkers of lipid peroxidation and oxidative damage of protein respectively, confirmed the uncompensated status of oxidative stress.[49]

1.3. THERAPEUTIC STRATEGIES

The pharmacological treatment of BD is particularly challenging due to the multifactorial and heterogeneous nature of the disease, that includes medical and psychiatric comorbidities. The therapeutic approaches differ considerably depending on the mood state (mania, hypomania, depression or mixed episodes), on acute episode or maintenance.[50] Acute state treatment aims to stabilize symptoms with minimal adverse effects and to ensure patient's safety. For long-term maintenance therapy, the main goals are prevention of recurrence of episodes and reduction of the symptom's severity.

Several therapeutic agents such as mood stabilizers, antipsychotics and antidepressants (Figure 7) have been approved by Food and Drug Administration (FDA) for the treatment of BD.[51] Generally, to contrast the progressive course of the malady, a common clinical practice consists in a multiple-medication therapy, namely combination of drugs belonging to the same or to different pharmacological classes, with mood stabilizers as the most frequently prescribed. Despite the abundant availability of therapeutic options, the FDA approved drugs are not optimal as many patients suffer from severe side-effects such as residual symptoms, high comorbidities, polarity shifts, cognitive impairment and disability. In this respect, there is an increasing need to develop effective and safe drugs able to inhibit the neurotoxic processes while promoting the neuroprotective pathways. In this scenario, new successful therapeutic approaches for BD should encompass polypharmacological strategies. Thus, multitarget or multipotent drugs *i.e.* molecules concurrently capable of interacting with diverse targets involved in the pathology could allow preventing and reversing many impaired cellular dysfunctions.

➢ **Treatment of mania**

Mood stabilising drugs (*i.e.* lithium, valproic acid, and lamotrigine) and atypical antipsychotic agents (*i.e.* quetiapine, olanzapine, risperidone, aripiprazole, brexpiprazole, and cariprazine) are valid therapeutic options for acute mania.[52] In

particular, lithium, administered as lithium carbonate, remains the first-line treatment, despite its side-effects[51] such as weight gain, sedation, stomach irritation, thirst, motor tremors, and kidney clearance complications. Regarding the typical antipsychotic drugs (*i.e*. chlorpromazine and haloperidol), notwithstanding their effectiveness in alleviating manic symptoms, the eliciting of a depressive mood switch represents a drawback.[53]
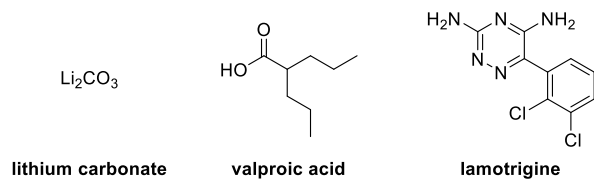
➢ **Treatment of bipolar depression**

Although a large number of first-line acute treatments are available for manic episode, only a few therapeutic agents are suitable to treat acute bipolar depression. In this respect, the only medications currently approved by the FDA are olanzapine, in combination with fluoxetine, quetiapine, and cariprazine.[50, 54] Lithium and valproic acid, combined with a selective serotonin reuptake inhibitor, are also employed.[55] Moreover, modest beneficial effects are reported for lamotrigine only upon acute and long term management.[56] Even though the standard antidepressants, when administered as monotherapy, can cause rapid cycling and manic switch,[57] their combination with mood stabilizers seems to be relatively effective.[58]
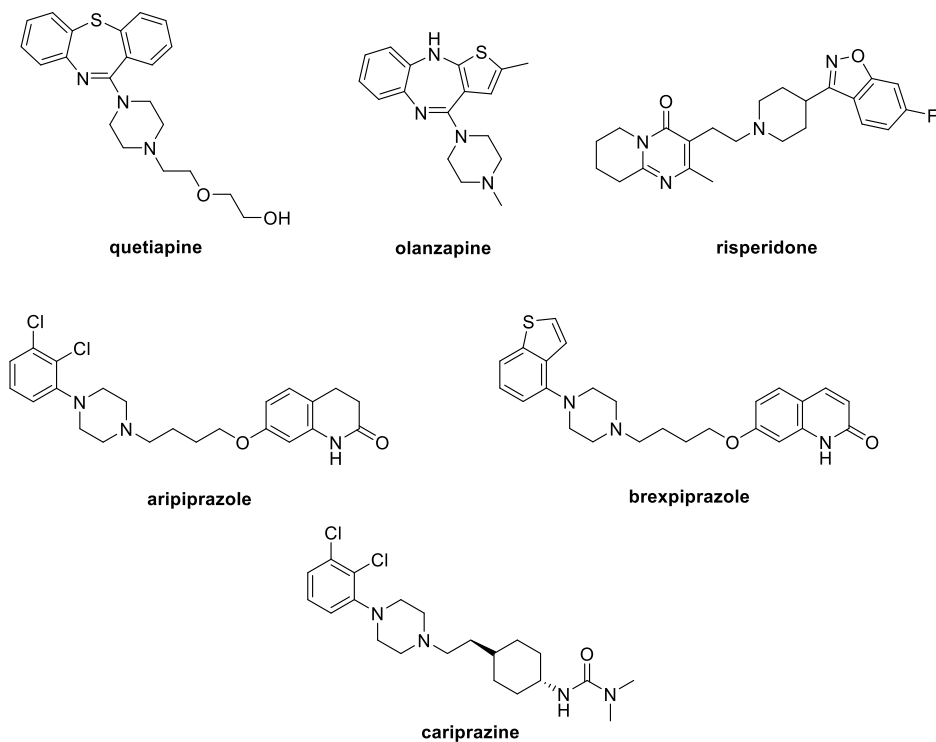
➢ **Maintenance**

Lithium is largely recommended as the first-line option for maintenance therapy due to its efficacy in preventing manic/depressive episodes, along with relapse and recurrence of BD. [51] Indeed, it has been shown to significantly reduce the risk of suicide. In addition, a combination of a mood stabiliser with an atypical antipsychotic is also effective.[52]

MOOD STABILIZING AGENTS

Li$_2$CO$_3$

lithium carbonate   valproic acid   lamotrigine

ATYPICAL ANTIPSYCHOTICS

quetiapine   olanzapine   risperidone

aripiprazole   brexpiprazole

cariprazine

TYPICAL ANTIPSYCHOTICS

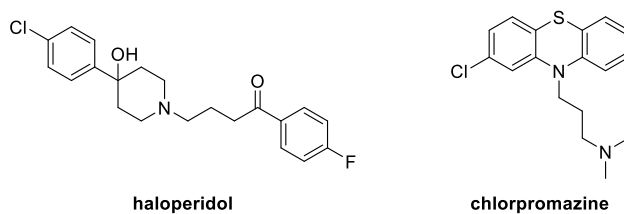haloperidol   chlorpromazine

Figure 7. Common pharmacological classes of BD therapeutics.

1.3.1. Neuroprotective effects of bipolar agents

Neuroprotection may also represent a feasible therapeutic strategy since it permits to achieve reduced BD incidence and impact. In this context, pharmacological evidence

shows that the approved psychotropic drugs are also able to induce a number of neuroprotective pathways; this last effect could be likely responsible for an increasing in clinical effect. Moreover, the peculiar pharmacodynamic profile of these agents allowed deeper insight on the illness onset and progression.

> **Lithium**

As previously reported, the mood stabilizer lithium is considered the most effective drug for BD treatment; it exerts neuroprotective and neurotrophic CNS effects by affecting neurotransmitter/receptor-mediated signalling, ion transport, and signal transduction cascades.[59] However, its specific mechanism in stabilizing mood is not completely clarified.

Imaging studies conducted on brain patients after lithium treatment showed increased grey matter volumes in the amygdala, hippocampus and prefrontal cortical regions, thus providing evidence for the occurrence of neuroprotective effects.[60-62] At the molecular level, lithium has been shown to control neuronal functions by decreasing the excitatory neurotransmission, through the modulation of glutamate and DA pathways, and by increasing inhibitory neurotransmission, via affecting GABA system.[63] Particular attention was paid to the effects of lithium modulation of signaling pathways that, operating within neurons, alter neurotransmission and ultimately promote cell viability. In detail, lithium affects inositol recycling through the inhibition of the enzymes inositol-1,4 bisphosphate 1-phosphatase (IPP) and inositol-1(or 4)-monophosphatase (IMPase). The consequent decrease in inositol intracellular level attenuates the deregulated calcium response responsible for the hyperexcitability of serotonergic neurons.[64] Furthermore, lithium exerts a direct inhibition of the enzyme glycogen synthase kinase-3β (GSK-3β) with subsequent activation of glycogen synthesis and Wnt/β-catenin-dependent transcription.[65-67] As discussed below, GSK-3β, due to its modulation activity of neurogenesis, neuronal survival, mood-related behaviours, and circadian rhythms could be regarded as a key mediator of lithium's clinical effects. In addition to these putative mechanisms, lithium has been shown to reduce oxidative stress by increasing GSH levels,[68] along with to promote neurotrophic

effect by inducing BDNF and bcl-2 expression.[69] In conclusion, it is evident that complex and inter-related processes underpin the therapeutic actions of lithium.

> **Anticonvulsant agents**

It is still unclear whether anticonvulsants act with the same mechanism of action than therapeutics for epilepsy and BD. However, the effects of the latter consist of diminishing excitation and enhancing inhibition in the mesolimbic system and other brain circuits responsible for mood regulation. For example, for BD, the lamotrigine's effect is mediated by attenuation of glutamate release and regulation of voltage-dependent calcium current.[70, 71] On the other hand, the therapeutic outcome of valproic acid results from several mechanisms of action, such as inhibition of sodium and calcium channels and increase of inhibitory GABAergic neurotransmission.[72] It has also been proved that anticonvulsant drugs promote neuroplasticity by enhancing mitochondrial functions, reducing oxidative stress, decreasing apoptosis *via* GSK-3 inhibition and increase of neuroprotective factors levels (BDNF, bcl-2).[69, 73, 74]

> **Antipsychotic drugs**

The typical antipsychotic drugs belong to the class of DA antagonists that, by interacting with D2R, modulate the DA tone. Notwithstanding their usefulness in treating BD manic symptoms, several unwanted effects such as extrapyramidal symptoms (*i.e*. restlessness and sedation), tardive dyskinesia, and depressive switch, this latter due to a full D2R antagonism, frequently occur.

On the other side, the atypical antipsychotic agents exert both anti-manic and anti-depressive activities without eliciting extrapyramidal side-effects. This 'atypicality' is related to their characteristic pharmacodynamic profile that consists of a combined modulation of DA and 5-HT receptors, namely 5-HT$_{2A}$ antagonism,[75] 5-HT$_{1A}$ partial agonism,[76] and D2/3R antagonism or partial agonism.[77] Furthermore, this new class of antipsychotics, on the contrary to typical antipsychotics, induces neuroplasticity and synaptic modifications in specific brain regions such as *striatum*, prefrontal *cortex* and *hippocampus*, along with an anti-inflammatory effect via microglial modulation, which

further contributes to BD clinical effects.[78] Additionally, these drugs proved to reduce oxidative stress, not only by blocking DA receptor but also by eliciting direct effects on oxidative defence mechanisms.[79]

1.4. THE DOPAMINE HYPOTHESIS OF BD

Considering the pivotal role of DA in brain areas involved in mood regulation, dysregulation of this neurotransmitter has been closely associated with the behavioural and cognitive manifestations of BD. According to the DA hypothesis, dated back at least to the 1970s, the impaired dopaminergic neurotransmission represents the principal BD abnormality; thus, the opposite changes in DA function cause the mood fluctuation characteristic of the disorder. In detail, a hyperdopaminergic state underlies the development of manic symptoms, while a hypodopaminergic condition causes the depressive phase of the illness.[80-82] Since this theory did not explain how hyper- or hypo-dopaminergia would arise, subsequent versions have been proposed linking the disorder to compromised homeostatic regulation of DA circuits, leading to cyclical changes in dopaminergic neurotransmission.[79, 83] In detail, in mania, an increased DA transmission conducts overtime to a secondary downregulation of DA receptor sensitivity. This effect, in turn, elicits a hypodopaminergic state, corresponding with the depressive phase, and a repetition of the cycle, switching back to mania. Moreover, both pharmacological and imaging studies report an increased striatal D2/3 receptor density together with a hyperactive reward circuit in mania, while elevated levels of striatal DAT are found in bipolar depression condition (Figure 8),[26] thus supporting DA hypothesis.

Finally, for BD treatment, the successful use of the atypical antipsychotic agents emphasizes the role of the dopaminergic system. As the blockade of D2/3 receptors is their common mechanism of action,[84] it is likely that a reduced DA neurotransmission, at least, contributes to the clinical efficacy of these drugs.

In the light of these findings, the DA hypothesis of BD not only clarifies the phenomenology of the malady but also provides a useful rationale for the development of anti-BD drugs.
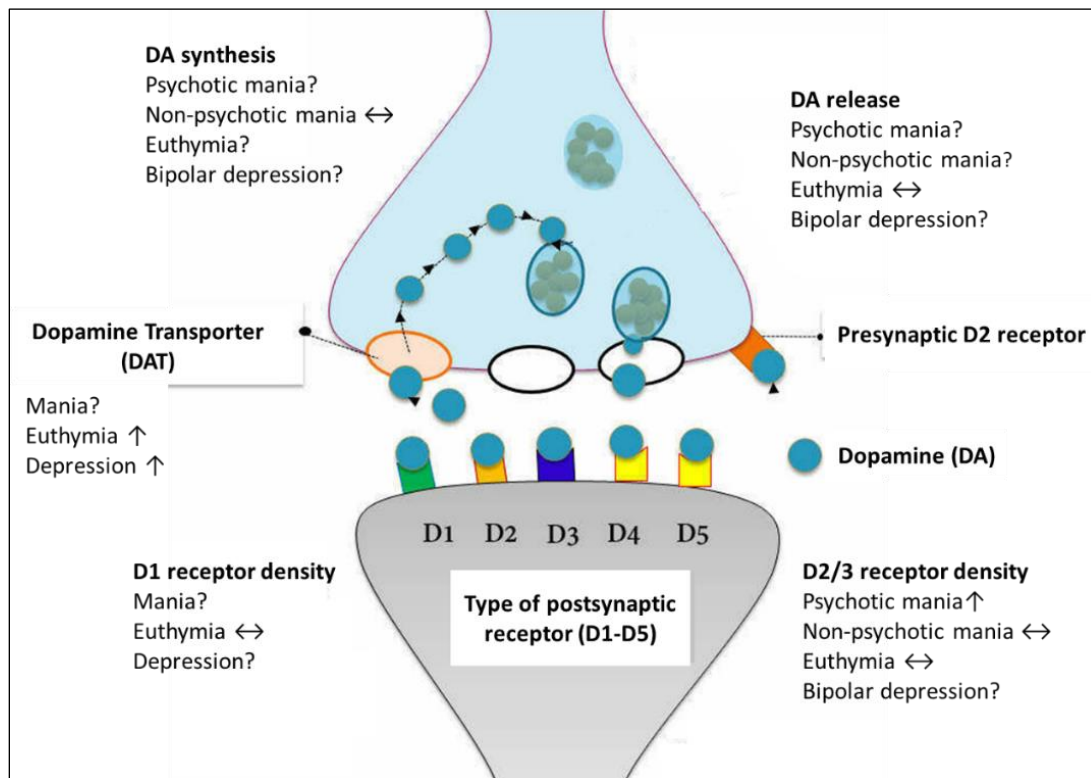
Figure 8. Summary of dopamine hypothesis in BD.

1.4.1. Dopaminergic system

DA is a widely distributed neurotransmitter (both in the vertebrate and invertebrate species) that is produced in several brain areas starting from L-tyrosine hydroxylation, to give L-DOPA, followed by its decarboxylation by DOPA decarboxylase, and serves as a precursor for noradrenaline and adrenaline synthesis. After its release into the synaptic cleft, many processes terminate DA action: (i) enzymatic breakdown *via* MAO and COMT, to produce homovanillic acid (HVA), (ii) direct cellular reuptake through DAT, (iii) diffusion away from receptor sites (Figure 9).
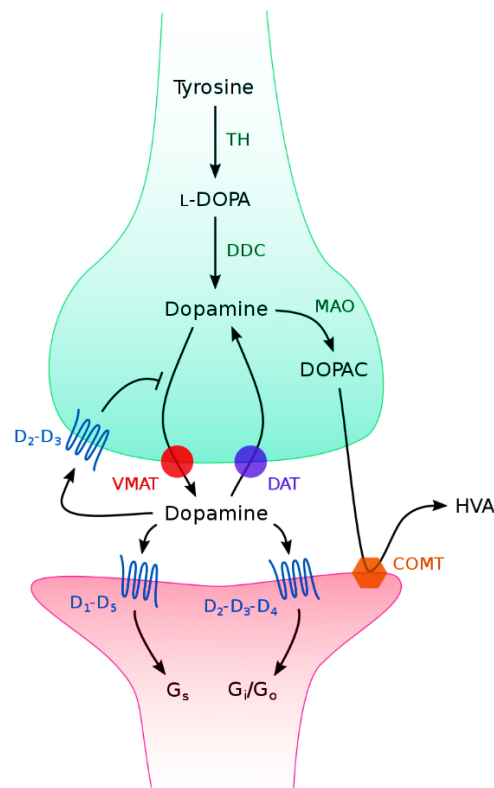
Figure 9. Schematic representation of a dopaminergic synapse.

Due to its dissimilar distribution in the brain, DA is implicated, upon interacting with its proper receptors, in a variety of physiological processes including movement, learning, reward, motivation, emotion, cognition, food intake and endocrine regulation. An impairment in dopaminergic neurotransmission and DA receptor levels underlies different neurological and psychiatric disorders, for example, Parkinson's disease, Huntington's disease, BD, schizophrenia and drug addiction.

DA receptors belong to the class of G protein-coupled receptors (GPCRs) presenting the characteristic seven transmembrane helical domains. DA receptors, based on their similarity in amino-acidic sequence in signal transduction, can be grouped into two main families, namely D1-like and D2-like. The D1-like receptors, that include D1 and D5 receptors (D1R and D5R, respectively), are coupled to stimulatory Gs proteins and activate adenylyl cyclase (AC), leading to accumulation of intracellular cyclic adenosine monophosphate (cAMP) and activation of the protein kinase A (PKA). The D2-like receptor group consists of the dopamine D2, D3, and D4 receptors (D2R, D3R,

and D4R, respectively) and are coupled to inhibitory Gi/0 proteins that, once activated, suppress cAMP levels and related downstream pathways (Figure 9).[85]

Each receptor subtype is characterised by an extracellular amino terminus, an intracellular carboxyl terminus and seven transmembrane helices (TM), linked by intracellular and extracellular protein loops (ICL and ECL, respectively). Structurally, the D1-like receptors present a short third intracellular loop and a long carboxyl-terminal tail, whereas the D2-like receptors display opposite features, bearing a long third loops and a short carboxyl terminus (Figure 10).[86]
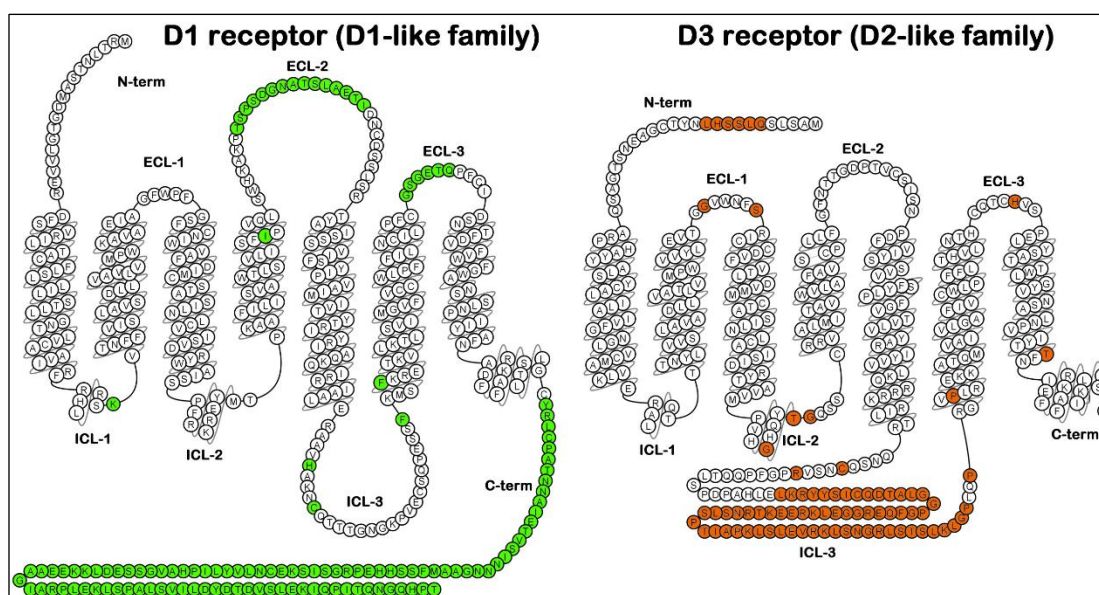
Figure 10. Structural representation of D1R, as an example of D1-like family, and D3R, as an example of D2-like family, with the non-conserved residues in green for D1R and in orange for D3R.[87]

Within the D2-like receptor subfamily, D2R and D3R display pronounced structural homology, sharing, in the transmembrane domain and the putative ligand binding site, an extensive sequence of amino acids (up to 75%).[88] Pharmacological similarity is the consequence of the sequence identity. Thus, the development of subtype-selective compounds endowed with drug-like physicochemical properties represents an arduous challenge. In the last years, detailed information about the DA receptors structure, also provided by crystallographic studies on D3R[89], greatly facilitate the design of selective ligands.

1.4.2. Dopamine D3 receptor as potential target for BD treatment

Anatomical, pharmacological and genetic findings suggest that a D3R dysfunction may be associated with several neurological disorders including BD, schizophrenia, restless leg syndrome, Parkinson's disease, and drug addiction.[90] Moreover, the selective distribution of D3R in limbic regions of the brain, especially the nucleus accumbens,[91] has prompted to consider this receptor as a potential target for the development of CNS-targeting drugs devoid of the motor side effects, classically elicited by the D2R antagonists. For instance, antipsychotic drugs exert their action by blocking both D3R and D2R, thus producing multiple adverse effects. Then, it was hypothesized that agents able to selectively target D3R could represent effective BD therapeutics without eliciting remarkable side effects.

The D3R was first cloned and characterised in 1990 by Sokoloff *et al.*[92] Among DA receptors, D3Rs are relatively few but they show a high abundance in brain regions associated with emotional and cognitive functions including ventral *striatum*, *nucleus accumbens*, *thalamus*, *hippocampus*, and *cortex*.[86] This receptor subtype possesses high affinity for DA that is 420-fold higher in comparison to that of D2Rs. Thus, small changes in D3Rs number or function produce dramatic effects on synaptic transmission, suggesting for these, a critical role in the modulation of the normal dopaminergic function.

Recently, the crystal structure of the human D3R complexed with eticlopride (Figure 11A), a potent D2/D3 antagonist,[89] provided essential insights that helped the rational design of D3R selective ligands. This study revealed a binding site located in the upper half of the transmembrane domain, defined as orthosteric binding site (OBS), to which DA binds, surrounded by TMs III, IV, VI, and VII (Figures 11B and 11C). The tertiary amine of the ethyl pyrrolidine ring of eticlopride, positively charged at physiological pH, forms a salt bridge with the carboxylate of $Asp110^{3.32}$, which is highly conserved in all aminergic GPCRs (Figure 11C); this interaction is essential for conferring a high binding affinity for aminergic subfamily of GPCRs.
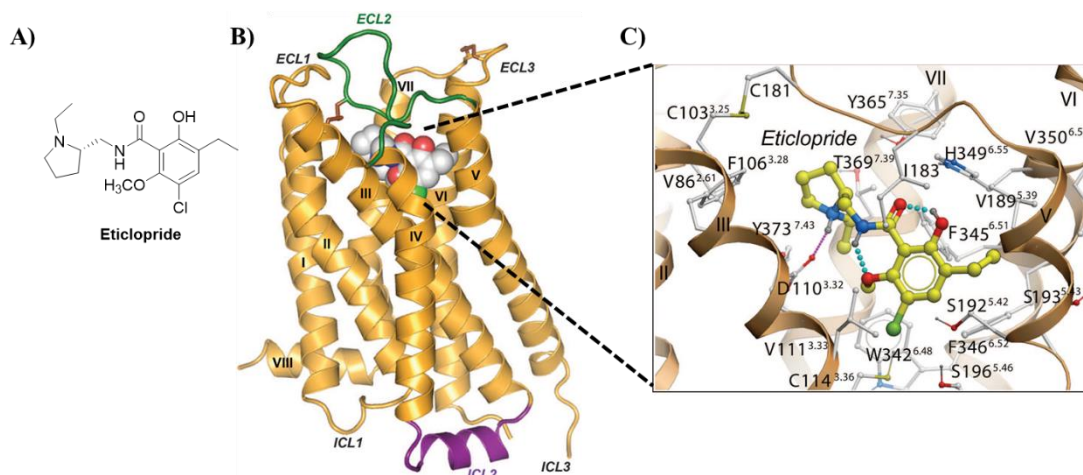
Figure 11. Crystal structure of the human D3R in complex with eticlopride.[89] A) chemical structure of eticlopride; B) overall D3R structure with eticlopride; C) Close-up of the eticlopride binding site showing the protein-ligand interaction with D3R.

Moreover, docked pose of the D3R selective antagonist **R-22** in the crystal structure of human D3R[93] (Figure 12A) reveal that the 2,3-dichloro-phenylpiperazine core occupies essentially the same region in which eticlopride is lodged, whereas the indole-2-carboxamide synthon is oriented toward the secondary binding pocket (SBP), consisting of ECL2, ECL1 and TMs I, II, and VII. The latter differs among the highly homologous D2R and D3R. Moreover, the ligand **R-22** makes contact with several conserved key residues, that include Asp110[3.32] and Tyr373[7.43] at the OBS, and Glu90[2.65] at the SBP (Figure 12B). These findings provide direction to the design of selective D3R-targeting agents for neuropsychiatric medications.
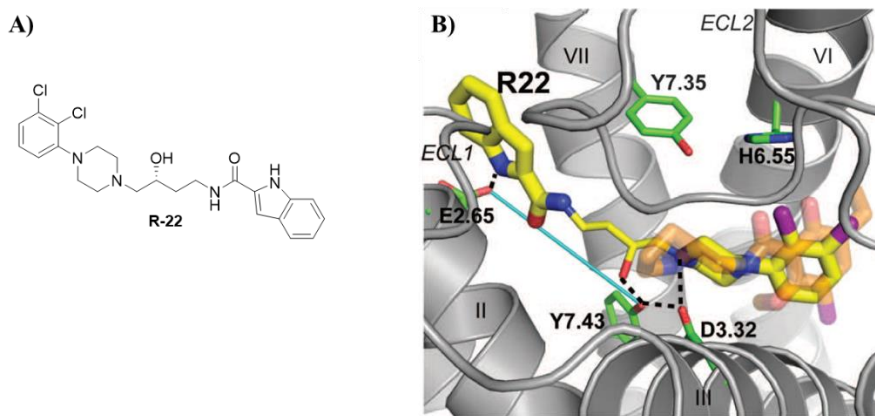
Figure 12. A) chemical structure of **R-22**; B) Docking pose of **R-22** (in yellow) and eticlopride (in orange) in the D3R.

1.4.3. D3R antagonists and partial agonists

The D3R has been recognized to be involved in the molecular mechanisms at the basis of various neurological disorders. D3R antagonists have shown efficacy in the treatment of psychosis such as schizophrenia. Moreover, D3R partial agonists are supposed to be beneficial in Parkinson's disease, BD, and drug addiction therapy. In this scenario, in the last two decades, many efforts have been dedicated to the development of selective D3R ligands. Among them, several promising compounds have been developed in the early 2000s (Figure 13). In particular, **BP897** is a potent and selective D3R partial agonist (Ki = 0.92 nM) with more than 70-fold preference for D3R rather than for D2R. This compound also demonstrated to reduce cocaine-seeking behaviour in rats, without producing reinforcement on its own, thus highlighting the useful role of D3R for the treatment of cocaine abuse.[94] A number of **BP897** analogues were developed in which the 2-methoxyphenyl function was replaced with a 2,3-dichlorophenyl one. Among them, **NGB2904** exhibited a selective D3R antagonism profile (Ki = 0.90 nM) with greater than 150-fold selectivity over other DA receptor subtypes.[95] Pharmacological studies demonstrated its beneficial effect in animal models of drug addiction.[96] Substitution of the di-hydrofluorene moiety of **NGB2904** with a benzothiophene fragment allowed to obtain **FAUC 365**, a D3R antagonist with D2/3R selectivity ratio of 7200 and D3R affinity of 0.5 nM.[97] The replacement of the arylpiperazine synthon with the 1,2,3,4-tetrahydroisoquinoline moiety, as in **SB277011A**, proved to be favourable since the compound showed nanomolar D3R affinity (10 nM) and 100-fold selectivity for D3R over the others receptors subtypes, along with a relatively high oral bioavailability (43%) and good CNS penetration.[98] Although these ligands showed interesting *in vitro* profiles, none of them reached the market, probably due to their weak physicochemical profile, characterized by a low water solubility.
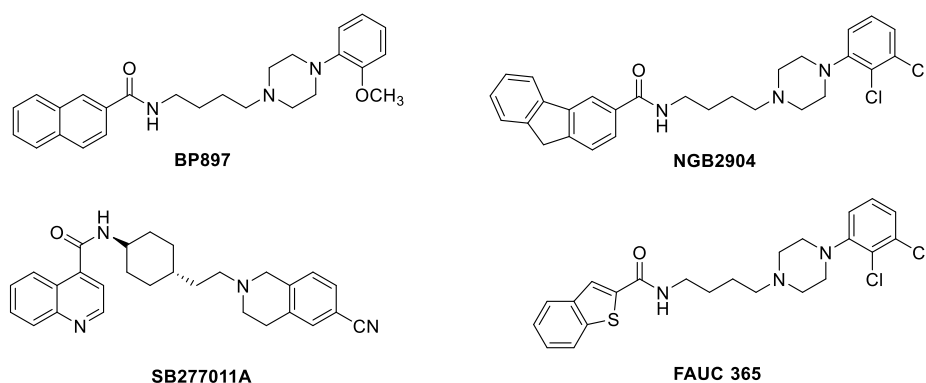
Figure 13. Early identified D3R selective ligands.

The structural analogies found among the different D3R antagonists prompted to propose a pharmacophore model, a useful tool for guiding the design of D3R selective ligands. In detail, it consists in four portions (Figure 14): a) an aromatic region (Ar1); b) an H-bond acceptor moiety (frequently an amide function); c) a spacer of appropriate length (usually a four-methylene unit); d) a fragment bearing a basic nitrogen atom (commonly a piperazine); e) an additional aromatic group (Ar2), connected to the d-portion. The general formula, simplified as 1,4-disubstituted aromatic piperazine (1,4-DAP), is considered a privileged structure because it binds not only DA receptors but also other monoamine GPCRs. Thus, several modification efforts of the proposed pharmacophore have been undertaken, aimed to modulate affinities of the obtained ligands to the corresponding GPCRs.
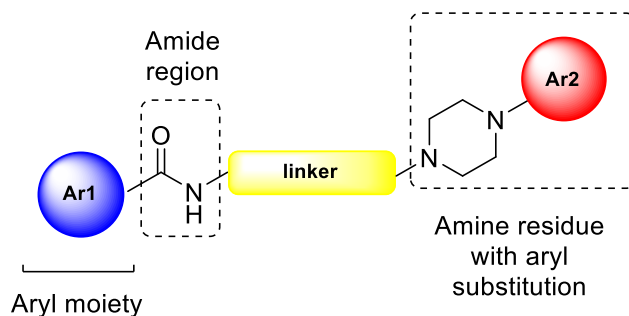
Figure 14. Pharmacophore model for D3R selective antagonist and partial agonist.

In this respect, to improve the properties of these scaffolds, researchers focused their design efforts on modifying the aryl moiety (a) and changing the nature and the length of the spacer (c), while the basic region (d) was initially unexplored, as a substituted

arylpiperazine synthon was maintained. Among the obtained compounds, interesting derivatives were obtained, among others **PG01037**[99] (Figure 15), where the presence of the bi-aryl system as portion (a) is coupled with an alkene spacer portion (c). In particular, the presence of a pyridine ring on the benzamide moiety was well tolerated, as demonstrated by biological data, namely *Ki* value of 0.7 nM for D3R, D2/3R selectivity ratio of 133, and favourable ClogP value. Moreover, the alkene-based four-carbon linker switched activity from a full antagonism, observed with a saturated butyl spacer, to a partial agonism. The insertion of a triple bond in the same four-carbon linker caused a decrease in affinity and a loss of selectivity over D2Rs. An example of modification of both linker and aromatic region is found in derivative **R-22**[93] (Figure 15), bearing an indole moiety and a 3-hydroxybutyl spacer. The ligand showed high affinity for D3R (*Ki* = 1.12 nM) and 400-fold selectivity over the D2R. It is a D3 enantioselective ligand as, between the R- and S-enantiomers, it showed the highest D3 affinity and a remarkable D3 receptor selectivity over the D2 receptor subtype. In contrast, the **S-22** enantiomer, although D3-selective, was significantly less active at D3 than its **R-22** counterpart and enantioselectivity was less pronounced at D2. This enantioselectivity aspect represents a valuable characteristic to be considered for achieving a D3R ligand selectivity. Significant elaboration of the main template allowed the identification of **RGH-188** (Figure 15),[100] known as cariprazine, that demonstrated a antagonist–partial agonist activity at both D2R and D3R, with sub-nanomolar and nanomolar affinity, respectively. Cariprazine was approved in 2015 in the USA for the treatment of schizophrenia and BD (Vraylar®). The structural innovation of this compound resides in both linker and aryl moiety which are a hydrophobic cyclohexyl ring system and a *N*-dimethyl-ureido moiety, respectively.
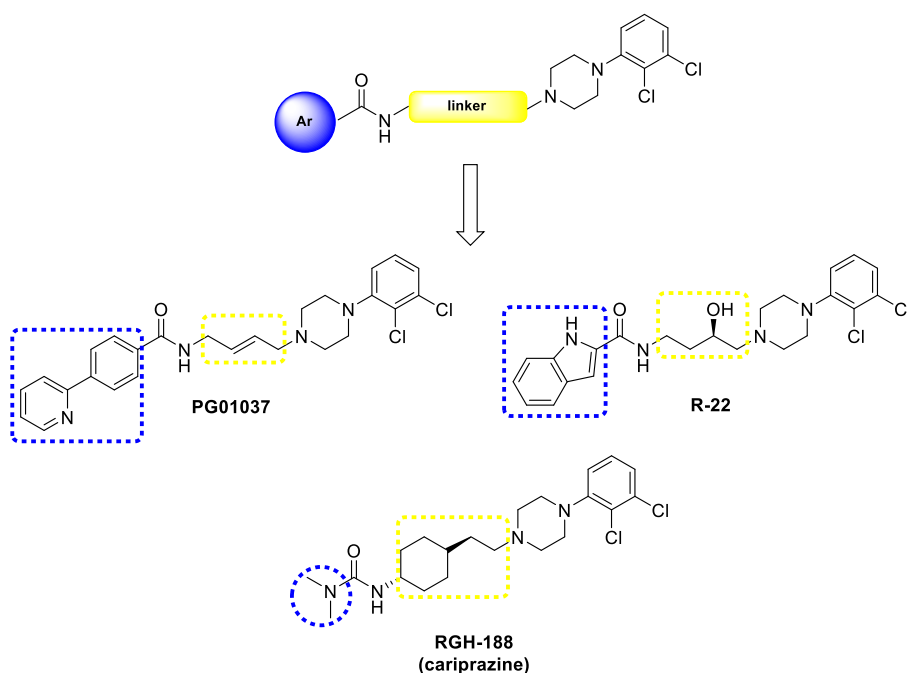
Figure 15. Arylpiperazine-based derivatives modified at both linker and aromatic region.

In order to clarify the structural features responsible for D2 and D3R selectivity and efficacy, Newmann and co-workers deconstructed into pharmacophoric elements a series of selective D3R 4-substituted-arylpiperazine compounds. They focused their attention on **R-22**, and performed computational simulations and binding evaluations to analyse the molecular determinants for D3R selectivity and efficacy.[101] From these studies, they identified the aryl piperazine moiety as a primary pharmacophore (PP) targeting OBS, and the arylamide function as a secondary pharmacophore (SP), directed to SBP. In detail, the binding mode of **R-22** in D3R (Figure 16) showed the interaction of the indole ring (SP) with a hydrophobic pocket at the interface of TMs II, III, ECL1 and ECL2 (defined as Ptm23). Moreover, the authors found that selectivity arises from divergent interactions within SBP, whereas efficacy depends on the binding mode in the OBS. Indeed, the nature of the linker, in combination with the substitution pattern on the phenyl piperazine motif, can affect the orientation of the PP in the OBS, which consequently influences the orientation of SP. Therefore, the structures of PP and linker are critical for optimal binding of the SP.
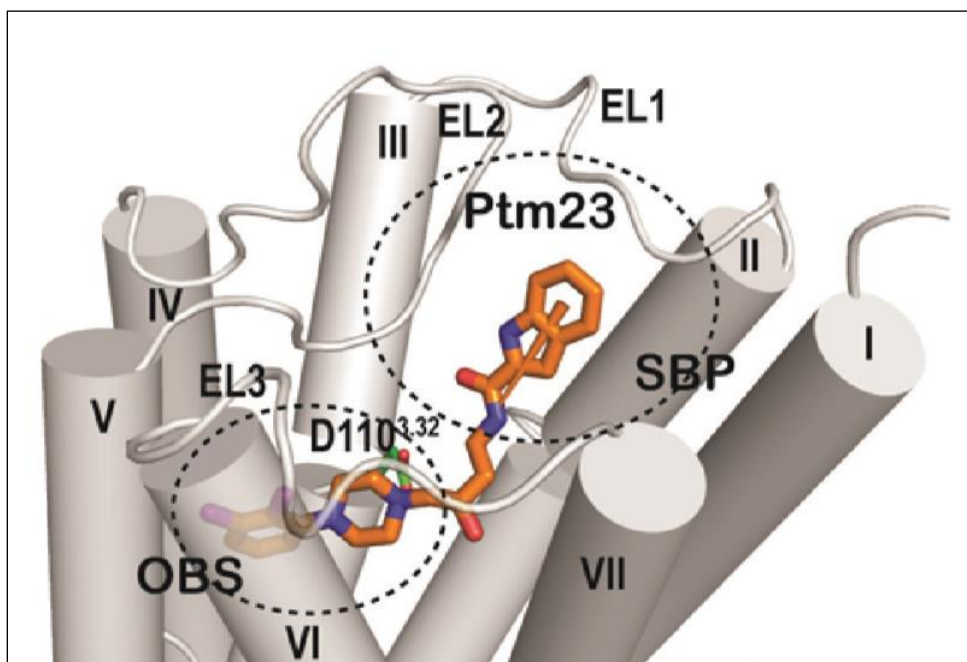
Figure 16. Predicted binding mode of R-22 (in orange) in D3R.[101]

Based on these promising outcomes, the phenylpiperazine function proves to be a valuable option for the design of selective D3R ligand, endowed with an antagonist or partial agonist activity. However, in the last decade, alternative scaffolds emerged as an optimal alternative to the more conventional aryl-piperazine based pharmacophore. In detail, as first replacement attempt, a series of compounds bearing a *tert*-butyl-trifluoromethylpyrimidine moiety connected to a piperazine were developed. The lead compound **ABT-925** (Figure 17) proved to be a highly potent and selective D3R antagonist, with low nanomolar affinity and 100-fold selectivity over D2R.[102] One example of significant modifications regarding the piperazine motif, the aromatic region, the H-bond acceptor portion, and the linker nature, is represented by derivative **SB-414796** (Figure 17). This tetrahydro-1*H*-3-benzazepine showed an effective D3R antagonism profile with high oral bioavailability and blood-brain barrier permeability.[103] This compound was employed as a starting point for the development of D3R antagonists bearing a thiotriazole scaffold. Among them, the oxazolyl derivative **GSK598809** (Figure 17) showed good D3R affinity and selectivity coupled with optimal pharmacokinetic properties.[104]
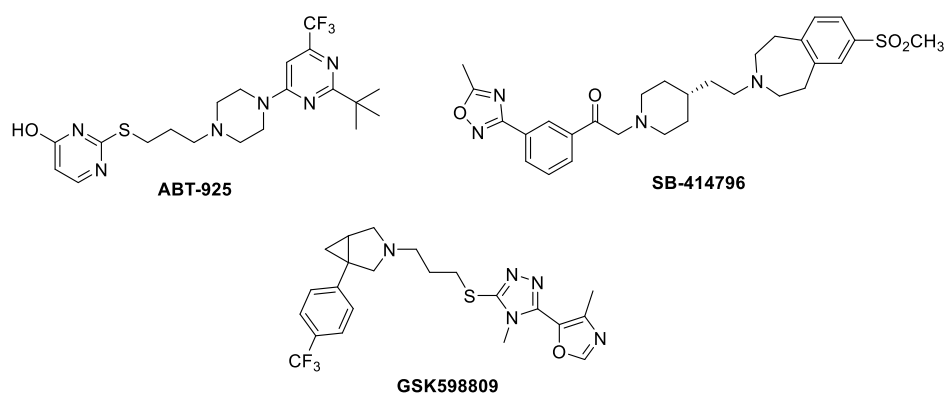
Figure 17. Examples of new D3R ligands.

1.5. ROLE OF GSK-3β ON BD ETIOPATHOGENESIS

1.5.1. Glycogen Synthase Kinase-3β

Glycogen synthase kinase-3 (GSK-3) enzyme, expressed in all human tissues, is a member of the protein kinase family, that catalyses the transfer of a phosphate group from adenosine triphosphate (ATP) to target substrates. This serine/threonine kinase transfers a phosphate group to either the serine or threonine residues of its substrates. Firstly identified as the kinase that phosphorylates glycogen synthase, it is now known to be involved in multiple signaling pathways, including cellular division, proliferation, differentiation and adhesion. In humans, GSK-3 is encoded by two different and independent genes, generating GSK-3α and GSK-3β proteins, with molecular weights of about 51 and 47 kDa, respectively. The two isoforms share nearly identical sequences in their kinase domains (95% homology of the catalytic domain) while differ substantially for a glycine-rich-N-terminus-domain of GSK-3α.

In the CNS, GSK-3β is widely expressed, especially in the cerebral *cortex*, *hippocampus* and Purkinje cells, where it has a fundamental role in neuronal signaling, regulating the Wnt pathway (by β-catenin deactivation) and tau protein function.[105] GSK-3β is unique among other kinases because it is constitutively active in resting cells being dephosphorylated.[106] The regulatory mechanisms of GSK-3β are mainly based on its inactivation through N-terminal phosphorylation of Ser9 residue by means of other protein kinases such as PKA[107], protein kinase B (AKT)[108] and protein kinase C (PKC).[109] Moreover, GSK-3β can phosphorylate itself resulting in autoinhibition. In contrast, positive regulation of the enzyme is achieved by phosphorylation of Tyr216. GSK-3β activity is also controlled by the Wnt signaling cascade whose activation inhibits the enzyme, thus preventing β-catenin phosphorylation induced by active GSK-3β and consequently its degradation.[110]

Structurally, GSK-3β contains two major domains: a β-strand domain, presenting at the N-terminus between amino acid residues 25-138, and an α-helical domain, presenting at the C-terminus between amino acid residues 139-343 (Figure 18). The

ATP-binding site is present at the interface of the α-helical and β-strand domains and is bordered by the glycine-rich loop and the hinge region.[111]
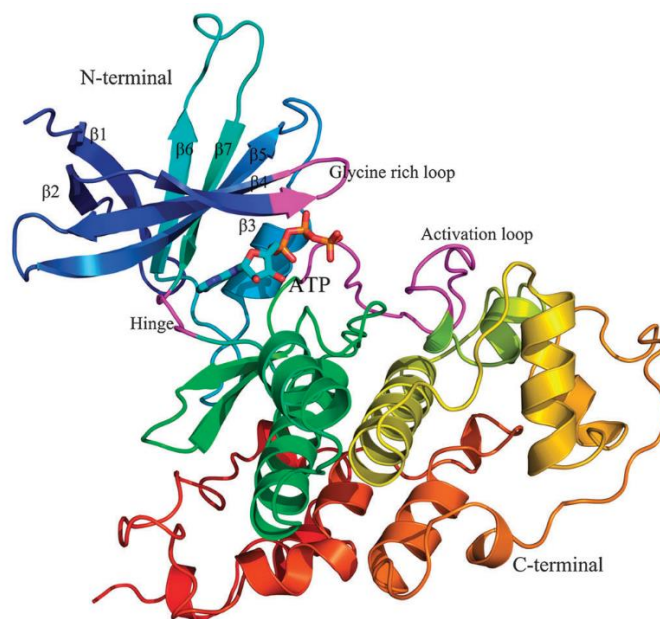

Figure 18. The structure of GSK-3β in a binary complex with AMP-PNP (PDB code 1PYX).[112]

Several evidence strongly suggest that dysregulation of GSK-3β, particularly resulting in increased kinase activity, is involved in the development of BD. In detail, Figure 19 shows the impact of GSK-3β dysfunction in different BD status. In depression, deficiencies in signals that normally maintain inhibition of GSK-3β, such as signaling induced by serotonin or neurotrophins, can cause up-regulation of GSK-3β activity, which, in turn, could further promote the susceptibility to depression. Mania may involve excessive dopaminergic signaling, which induces the activation of GSK-3β. Part of the therapeutic actions of antidepressants and mood stabilizers may derive from their direct or indirect effects on enzyme inhibition.[113]
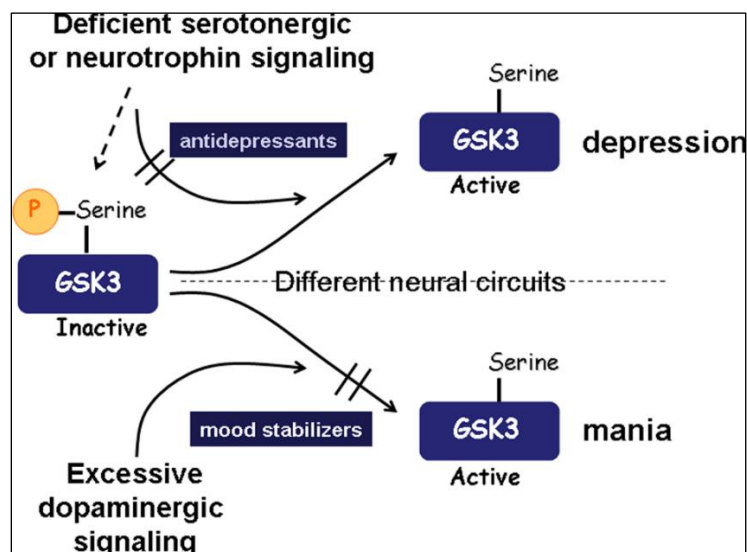
Figure 19. Overview of the involvement of GSK3 in BD.[113]

For example, the mood stabilizer lithium is hypothesized to exert its effects through direct inhibition of GSK-3β and, indirectly, an increase in GSK-3β's inhibition of serine phosphorylation. The direct mechanism consists in competitively inhibiting Mg^{2+} binding to the active site of the enzyme, which is fundamental for the catalytic activity of GSK-3β,[114] while the indirect reduction of GSK-3β activity is controlled through lithium-mediated AKT activation.[115] These findings suggest that, for mood disorders treatment, inhibition of overactive GSK-3β may normalize the enzyme signalling dysfunction, and thus may represent a promising therapeutic strategy for BD treatment.[116]

1.5.2. GSK-3β inhibitors

Due to the pivotal role of GSK-3β in cell signalling, protein regulation, metabolism and cellular transport, its inhibition has become an attractive strategy for therapeutic intervention. In the past decade, a large number of GSK-3β inhibitors have been identified, based on chemically different molecular scaffolds, and acting with diverse mechanisms of actions, such as ATP competition, allosteric modulation and enzyme irreversible inhibition. In detail, ATP-competitive inhibitors can block GSK-3β by adopting an "ATP-like" binding mode through the formation of hydrogen bonds with the key "hinge" residues Asp133 and Val135. Generally, these compounds demonstrate

overlapping interactions with other protein kinases, since they share a high degree of identity in the catalytic sites. Therefore, this lack of selectivity could be responsible for adverse secondary effects, particularly disadvantageous upon chronic treatment. Several ATP-competitive inhibitors, highly specific for GSK-3β, have been discovered, namely the thiazole-based **AR-A014418** and the structurally-related malemides **SB-216763** and **SB-415286**, showing IC_{50} values of 140, 100 and 200 nM, respectively (Figure 20). In addition to enzyme inhibition, **SB-216763** and **SB-415286** demonstrate *in vitro* neuroprotective properties, and **AR-A014418** shows an *in vivo* antidepressant effect (animal models).[117] One way to gain kinase selectivity could be an allosteric modulation of the enzyme. In this contest, the non-ATP competitive inhibitors demonstrate target selectivity and thus represent the majority of currently available inhibitors. These compounds modulate the kinase activity without competing with ATP for binding to the GSK-3β catalytic domain. They are likely to bind to unique regions of the kinase, thus avoiding adverse side effects developed by ATP-competitive agents.[118] The 2,4-disubstituted thiadiazolidiones (**TDZDs**, Figure 20) are the first class of non-ATP competitive GSK-3β inhibitors, showing high potency and selectivity.[119] Despite their mechanism of action is not yet completely confirmed, it is postulated they play a role in the modification of a cysteine key residue found in the active site of GSK-3β.[120] Halomethylketones (**HMKs**, Figure 20) represent another class of non-ATP competitive GSK-3 inhibitors, recently described as acting through an irreversible mechanism of action. In this case, the inactivation of the enzyme is due to the formation of an irreversible covalent bond between the key Cys199, located at the entrance of the ATP site of GSK-3β, and the HMK moiety.[121]

ATP-competitive inhibitors
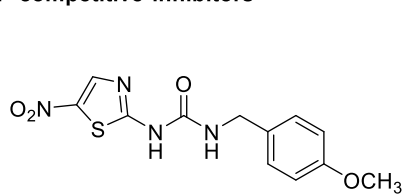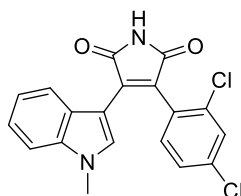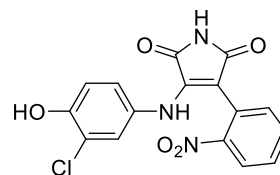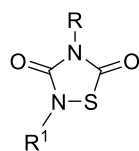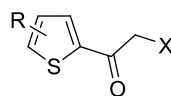
Non-ATP competitive inhibitors

Figure 20. Examples of known GSK-3β inhibitors.

2. AIM OF THE THESIS

2.1. BACKGROUND

Among the psychiatric diseases, BD is the sixth leading cause of disability with a prevalence up to 4 % worldwide. BD is a complex condition which alternates episodes of mania with depression. Although the neurobiological pathways at the basis of the disorder are not completely clarified, the DA hypothesis is recognized as the leading theory for explaining the pathophysiology of the malady. It states that the homeostatic regulation of DA circuits is dramatically compromised in BD, leading to alternated changes in DA neurotransmission. In detail, increased striatal D2/3 receptor density and hyperactive reward circuit cause mania, along with elevated levels of striatal DAT that are conducive to depression. Thus, modulation of D2/3R, by means of partial agonists (namely cariprazine, aripiprazole and brexipiprazole, Figure 7), demonstrates a relevant clinical application.[122] Unfortunately, a number of undesired side-effects, *i.e.* hyperprolactinemia and extrapyramidal symptoms, mainly due to D2R antagonism, frequently occur, underlining the need for developing new and safer therapeutic options. In this respect, D3R-selective ligands could provide a better outcome. The mood stabilizers lithium and valproic acid, employed for first-line treatment and maintenance, exert neurologic effects through modulating multiple interconnected pathways among others, inhibition of the enzyme GSK-3β activity and increase of its inhibitory phosphorylation (PI3K/AKT pathway), respectively. These evidence highlights the deregulation of GSK-3β,[123] as other BD feature. The roles of D3R and GSK-3β in both cognition and mood regulation inspired the idea that a concomitant modulation of these two targets could represent a viable therapeutic strategy to achieve an effective cure.

2.2. DESIGN STRATEGY FOR DUAL D3R/GSK-3β MODULATORS

Selective D3R antagonists and partial agonists share a common pharmacophore model that comprises three main portions (Figure 21)

i. a primary pharmacophore (PP) consisting in a basic moiety with an aromatic head group, directed to the D3R OBP and crucial in both establishing a key interaction with Asp110 residue and controlling the receptor intrinsic activity;[124]

ii. a secondary pharmacophore (SP), characterized by a heteroaryl amide function able to contact, trough H-bond interactions, the D3R SBP and to confer ligand affinity and subtype selectivity *versus* D2-like receptors;

iii. an alkyl linker which chemical nature and length influence D2/3R-selectivity.
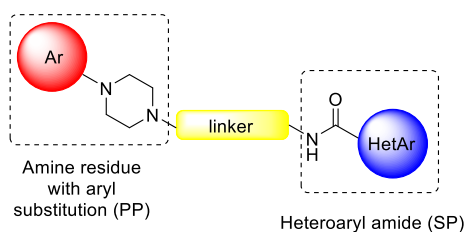
Figure 21. Pharmacophore model for D3R selective ligands.

Taking the above-described model into account and aimed at developing dual GSK-3β inhibitors and D3R partial agonists, rational drug design was applied. In this respect, the chemical synthons described at the points i) and ii) points were selected and a first set of hybrid molecules encompassing the following chemical features was obtained (Figure 22):

i. an aryl-piperazine function, a widely recognised PP;

ii. a substituted pyrazole-based moiety as SP;

iii. a linker of appropriate chemical nature and length connecting the above main pharmacophores.

Both the functions described at points i) and ii) points could be suitable for targeting both GSK-3β and D3R.
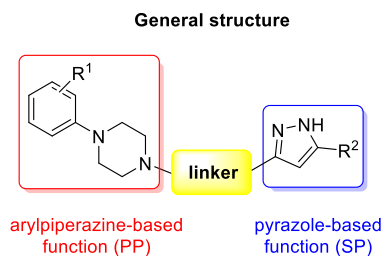
Figure 22. General structure of D3R/GSK-3β modulators.

In detail:

i. 2,3-dichloro and 2-methoxy phenylpiperazine were selected as PP function;

ii. *N*-(5-methyl-1*H*-pyrazol-3-yl)acetamide **I** (Figure 23), previously identified as GSK-3β inhibitor,[125] was selected as GSK-3β fragment. This molecule when tested *in vitro* against GSK-3β showed a mild potency (IC_{50} = 69.6 µM); moreover, docking studies demonstrated its capability to contact the enzyme hinge region, trough H-bond interactions, with the backbone of Asp133 and Val135. Accordingly, in order to increase potency and explore the chemical space of GSK-3β, this fragment was regarded as a hit compound for an optimisation campaign. Thus, a small library of pyrazole-based fragments **1-7** (Figure 23, Table 1) was synthetised. In detail, a first approach consisted in performing modifications at 3- and/or 5-positions of the pyrazole scaffold by introducing different aliphatic acyl groups and aromatic substituents, respectively. Compounds **1** and **2** were obtained by maintaining the 5-methyl substituent and introducing at 3-position a propionyl or a valeryl group, respectively. For derivatives **3**, **5**, **6** and **7** the 3-acetyl function was maintained and at the 5-position phenyl (**3**), *para*-bromobenzene (**5**), *para*-nitrobenzene (**6**), and 2-pyridyl (**7**) moieties were introduced. Finally, analogue **4** presents the phenyl and the valeryl functions at 5- and 3-positions, respectively.
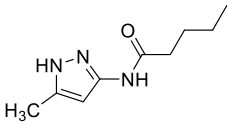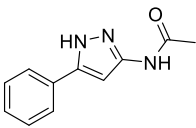
GSK-3β inhibitor

IC_{50} = 69.6 μM

pyrazole-based fragments

1: R^1 = CH_3, R^2 = CH_2CH_3
2: R^1 = CH_3, R^2 = $(CH_2)_3CH_3$
3: R^1 = Ph, R^2 = CH_3
4: R^1 = Ph, R^2 = $(CH_2)_3CH_3$
5: R^1 = 4-Br-Ph, R^2 = CH_3
6: R^1 = 4-NO_2-Ph, R^2 = CH_3
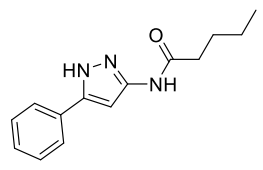**7:** R^1 = 2-pyridyl, R^2 = $(CH_2)_3CH_3$
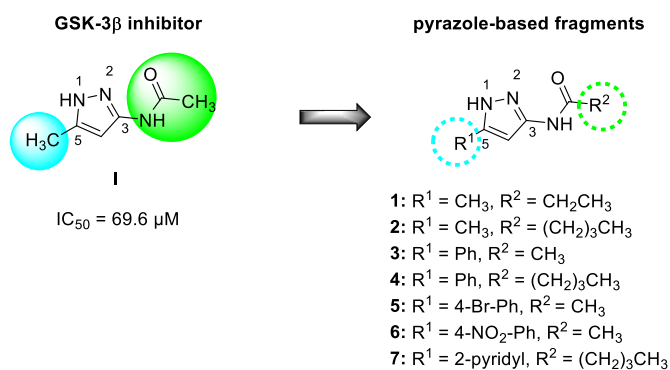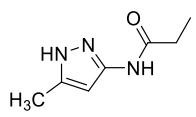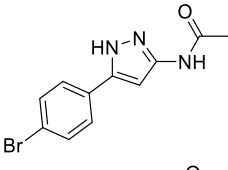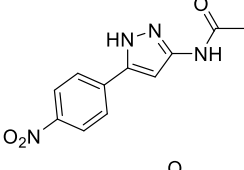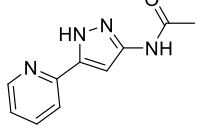
Figure 23. Design strategy for pyrazole-based fragments **1-7**

comp	Chemical structure
1[a]	
2[a]	
3[b]	
4[a]	
5[a]	
6[a]	
7	

[a]trifluoroacetate salt; [b]hydrochloride salt

Table 1. Pyrazole-based fragments **1-7**.

For this set the ability to inhibit *in vitro* GSK-3β was determined to identify the synthon/s suitable to be combined through different linkers with the arylpiperazine D3R-PP.

Methyl-aminopyrazole was selected for obtaining a preliminary set of hybrid molecules, while the 2,3-dichlorophenyl piperazine moiety was kept in all analogues (**8**, **10-12**, **27**, Figure 24, Table 2). Moreover, we examined the effects elicited by the nature of the spacer, by inserting oxalyl, amido or ureido groups, and the length by using polimethylene functions (I, II and III, respectively; Figure 24).

In detail:

- compounds **8**, **10** and **11** are characterized by an oxalyl-based linker bearing a two, three, and four-methylene alkyl chain;

- derivative **12** contains an amido-four-methylene linker;

- **27** comprises an ureido-based linker and a propyl moiety.

The methyl group of **8** was replaced with a phenyl giving compound **9**.
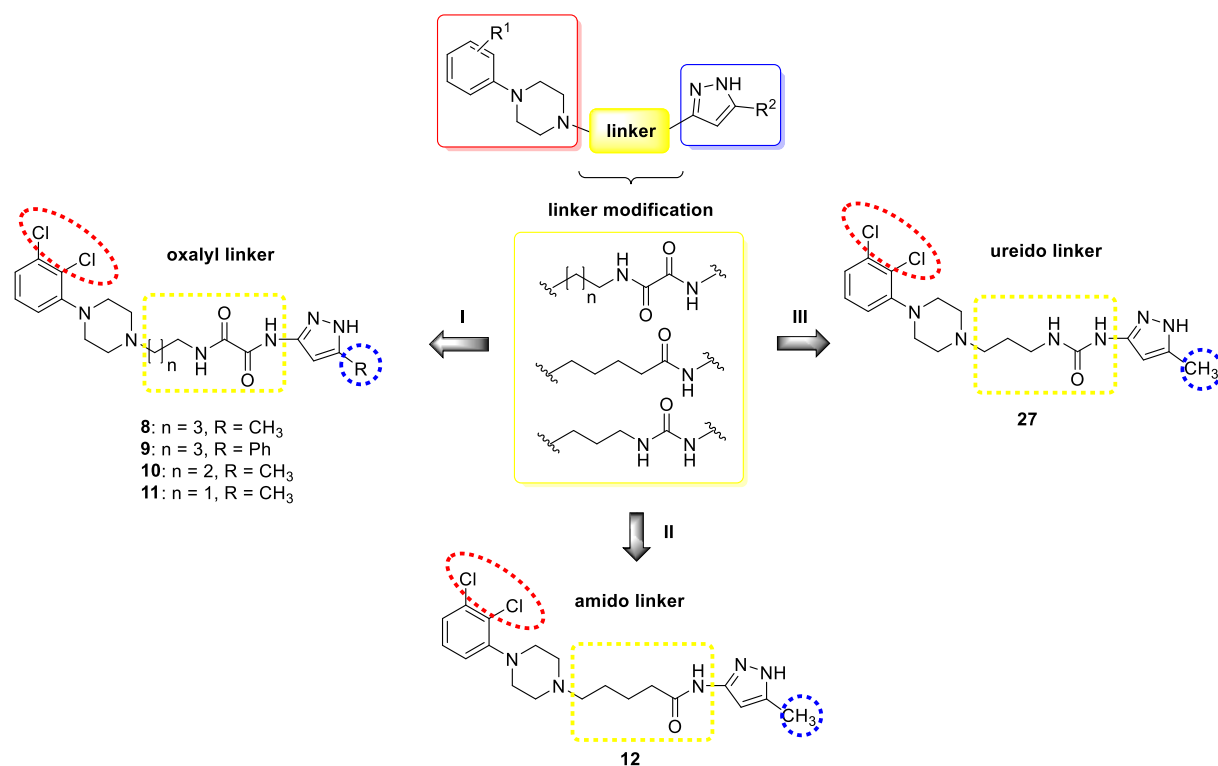
Figure 24. Design strategy for series I.

Consistent biological data were obtained for compound **12** that emerged as the most active dualistic modulator of GSK-3β and D3R of the first series. Properly structural modifications were addressed to PP and SP of analogue **12**, aiming at exploring the chemical space of the selected targets, performing preliminary structure-activity relationship (SAR) studies and identifying the key molecular features responsible for targets dualistic modulation. Therefore, derivatives **13-26** were obtained by connecting through the amido linker the 2,3-dicloro (**13-19**) or 2-methoxy (**20-26**) phenylpiperazine synthon with the substituted pyrazole-based scaffold. In detail, different substituents were inserted at the 5-position of the pyrazole core, namely methyl, phenyl, para-substituted phenyl, 2-thienyl, 2- and 3-pyridyl groups (Figure 25, Table 2).
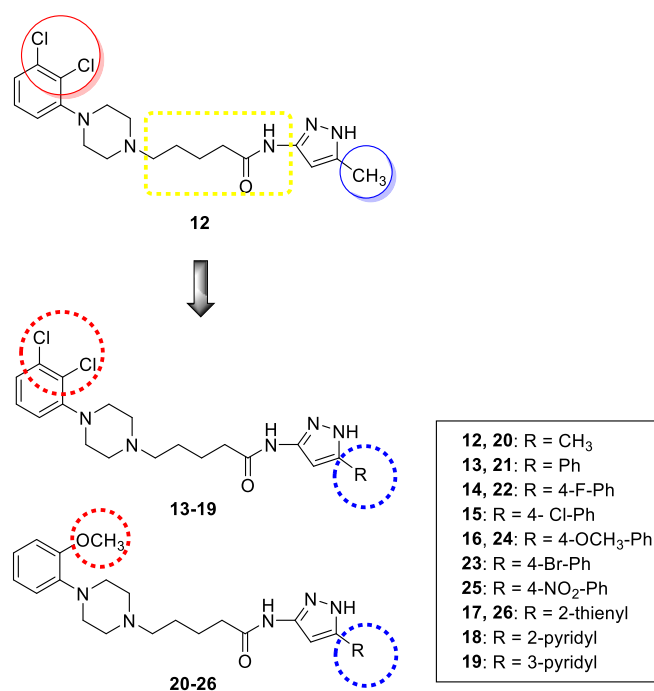
Figure 25. Design strategy for hybrid molecules bearing amido linker (**13-26**).

Similarly to compound **12**, interesting results were shown for analogue **27** (Serie I, Figure 24) bearing an ureido function on a three-methylene spacer, that was selected for an optimization process. Structural variations were carried out at the alkyl spacer of the linker by adding a methylene group, to obtain ureido-based analogues **28-30**

characterized by 2,3-dicloro or 2-methoxyphenyl as PP substituent, and methyl or phenyl group at the pyrazole-SP (Figure 26, Table 2).
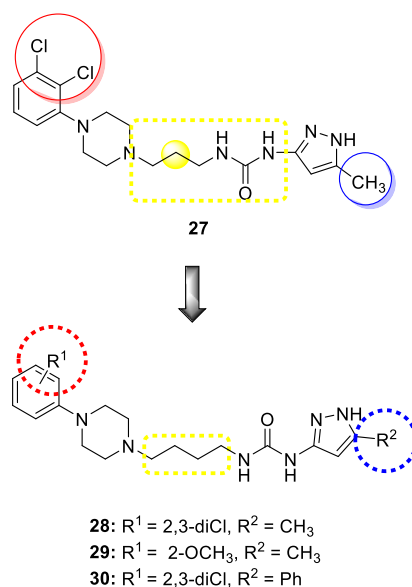

28: R^1 = 2,3-diCl, R^2 = CH$_3$
29: R^1 = 2-OCH$_3$, R^2 = CH$_3$
30: R^1 = 2,3-diCl, R^2 = Ph

Figure 26. Design strategy for hybrid molecules bearing ureido linker (**28-30**).

In summary, during my PhD course, the first set of hybrid molecules, able to concurrently modulate the selected targets, was synthetised (Figure 27). In detail, in order to explore the chemical space of the selected targets, properly addressed chemical modifications were performed at the main pharmacophoric portions, by varying the nature of the linker and the substitution pattern of the arylpiperazine and the pyrazole moieties.
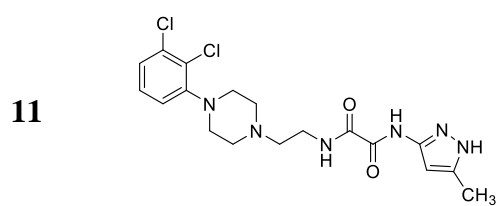
General structure

arylpiperazine-based function
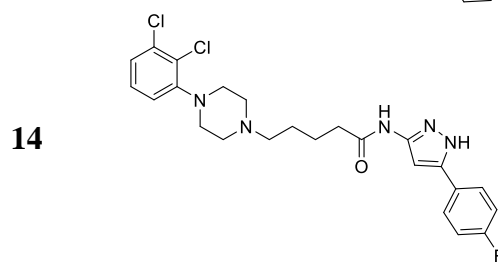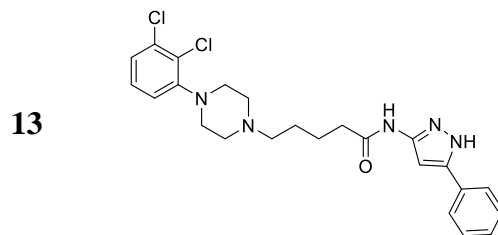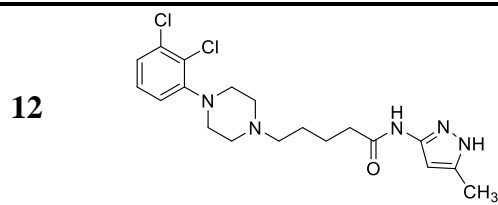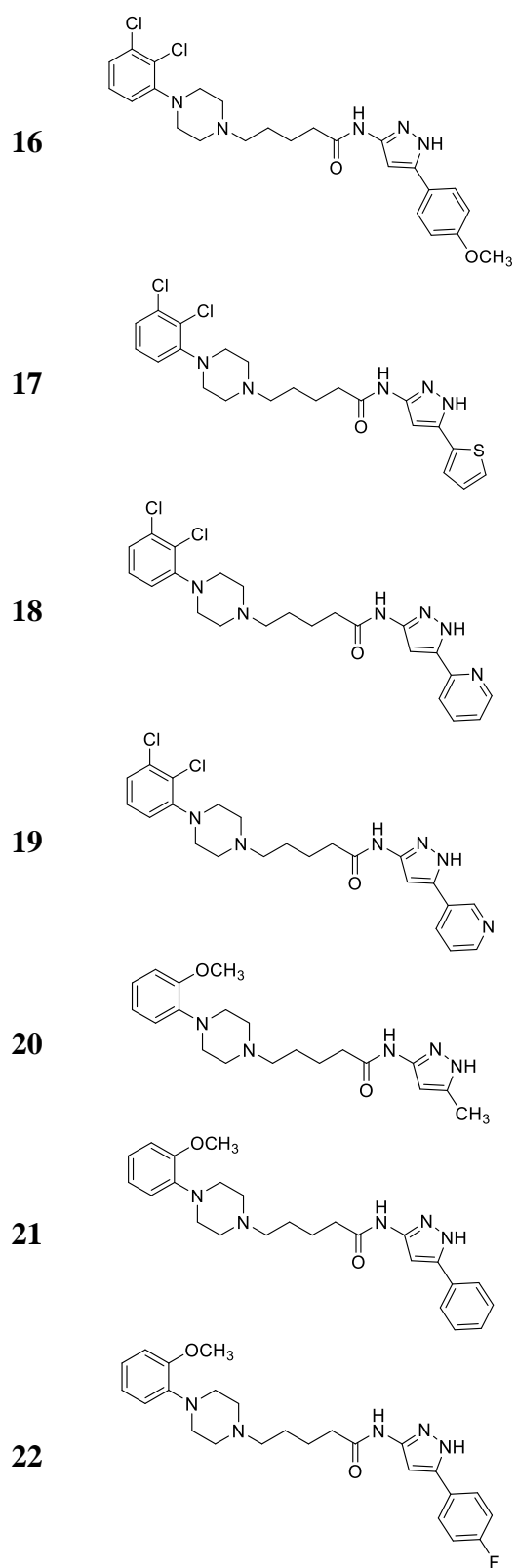
12-30

pyrazole-based function

R^3: H, F, Cl, Br, OCH$_3$, NO$_2$
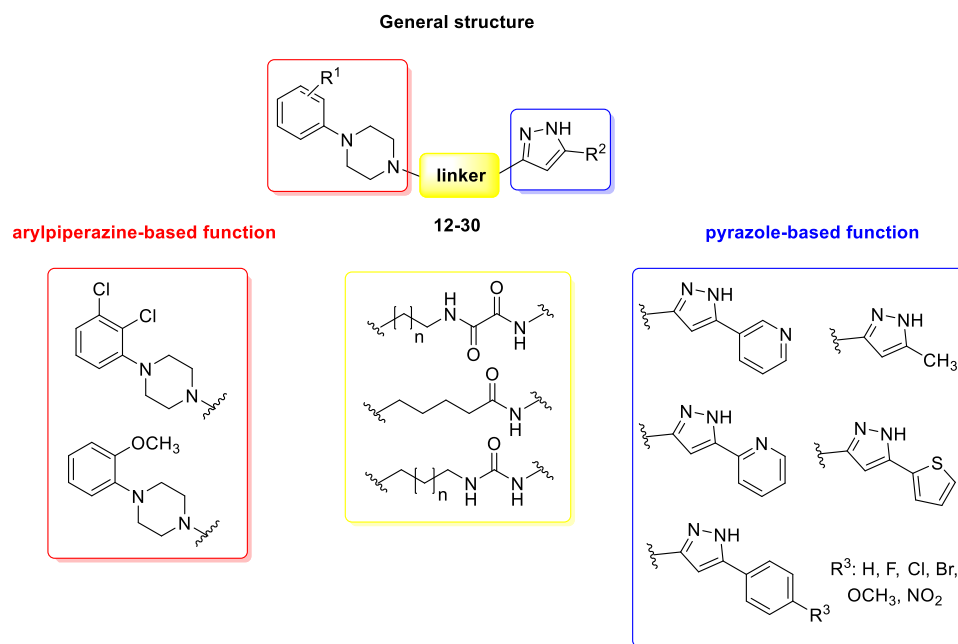
Figure 27. General structure of hybrid molecules **8-30**.

comp	Chemical structure
8	
9	
10	

11

comp	Chemical structure
12	
13	
14	
15	

16

17

18

19

20

21

22

comp	Chemical structure
23	
24	
25	
26	

comp	Chemical structure
27	
28	

29

30
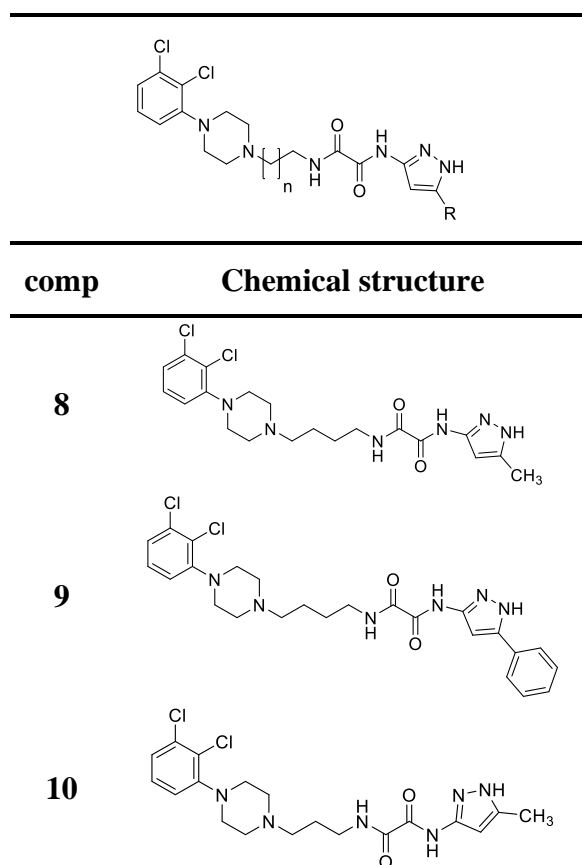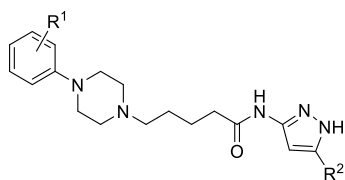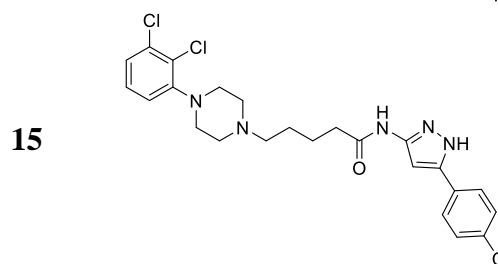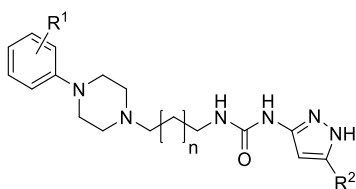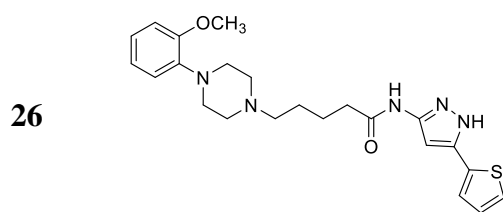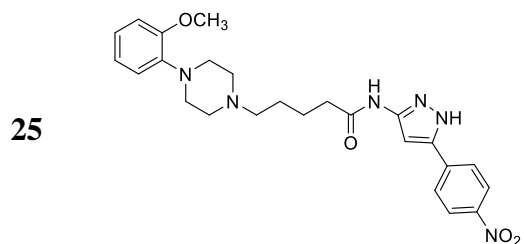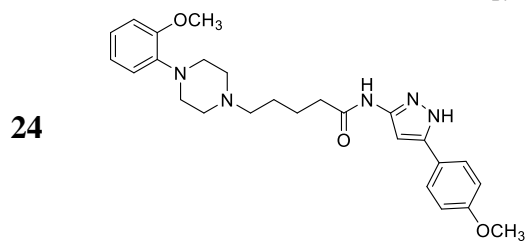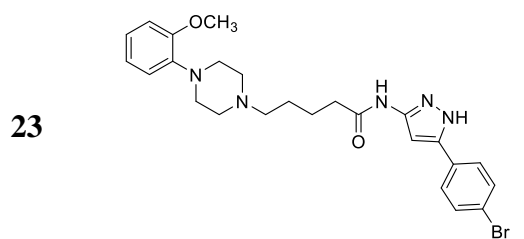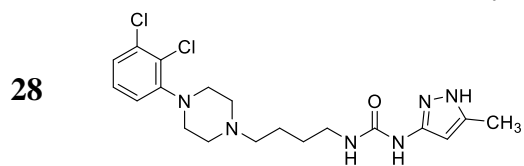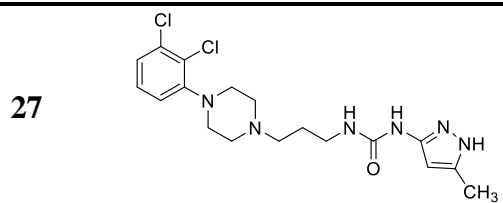
Table 2. Hybrid molecules **12-30**.

2.3. DESIGN STRATEGY FOR QUINOLINE-BASED ANALOGUES 31-38 AS NOVEL D3R LIGANDS

During the last 10 years, the arylpiperazine function, regarded as privileged structure, have proved to be a valuable option in the field of D3R drug discovery, thus obtaining a number of promising ligands endowed with high affinity, potency, selectivity over the subtypes D2-like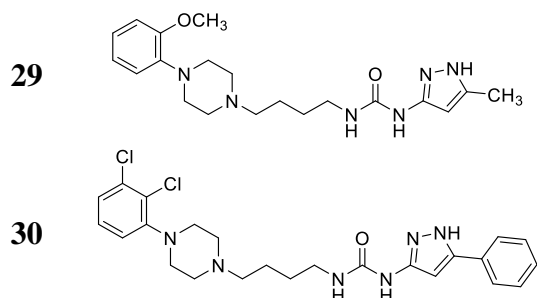 receptors, as well as adjusted intrinsic activity. However, selectivity profiles towards other biogenic GPCRs and pharmacokinetic properties require an optimization process.

A drug discovery campaign aimed at identifying novel D3R ligands as an alternative of the conventional arylpiperazine compounds was undertaken. Thus, from high-throughput screening efforts on a library of commercially available quinoline-based analogues, a hit compound **II** was identified (Figure 28), showing a mild *in vitro* D3R antagonism activity, with an IC_{50} value of 8.4 μM.

In detail, by observing the structure of this molecule, some considerations could be drawn:

- the 2-(piperidin-1-ylmethyl)quinoline fragment should act as PP;
- the acetamido function should represent the classical SP.

Therefore, in order to increase activity and perform a preliminary SAR study, a small library of compounds (**31-38**, Figure 28, Table 3) was designed, in which the 8-chloro-quinoline motif was maintained and different portions of the piperidine-3-ethylacetamide were subjected to modifications. In detail, the benzamido analogue (**31**)

of the hit compound **II** was obtained. Then, due to synthetic accessibility and to avoid stereoisomerism, the piperidine core was functionalized at the 4-position with: a) an ethyl group bearing the phthalimide (**32**), acetamide (**33**), benzamide (**34**) or *para*-fluorine benzamide (**35**) moiety; b) a methyl group bearing acetamide (**36**), bis-acetamide (**37**) or benzamide (**38**) function.

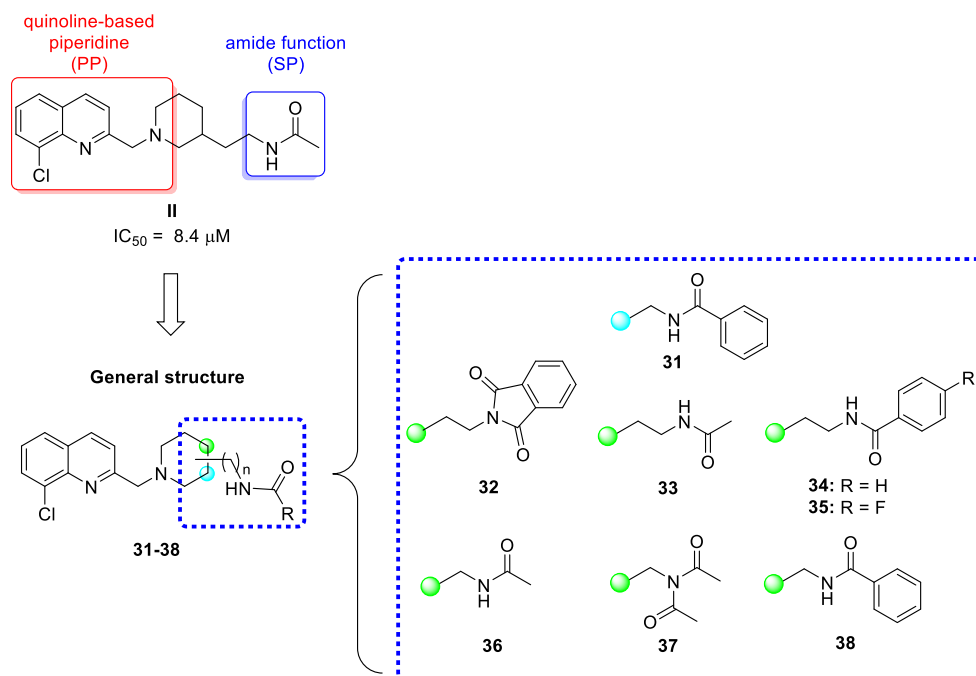**Figure 28.** Design strategy for quiniline-based analogues **31-38**.

comp	Chemical structure
31	
32	

33

34

35

36
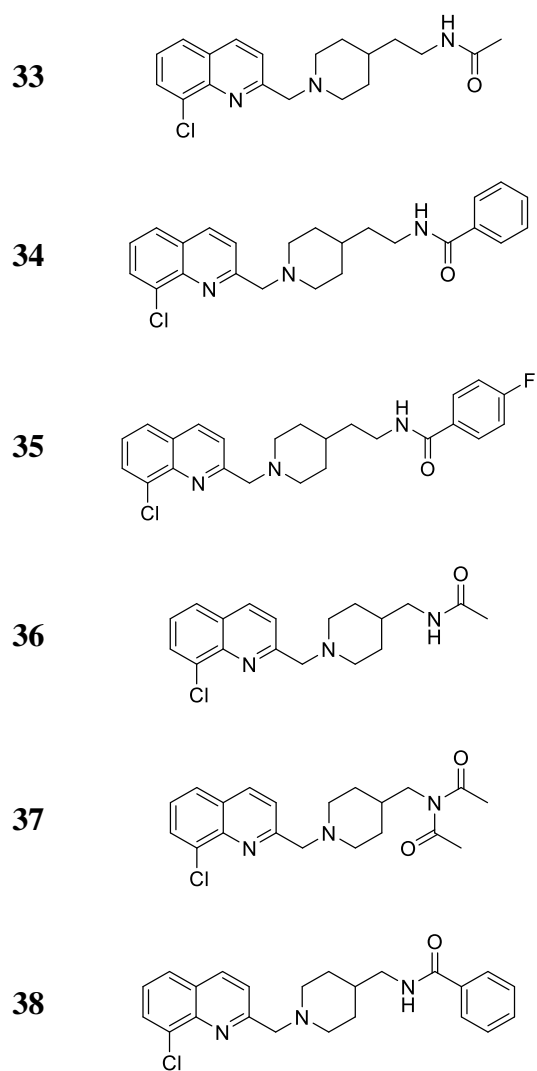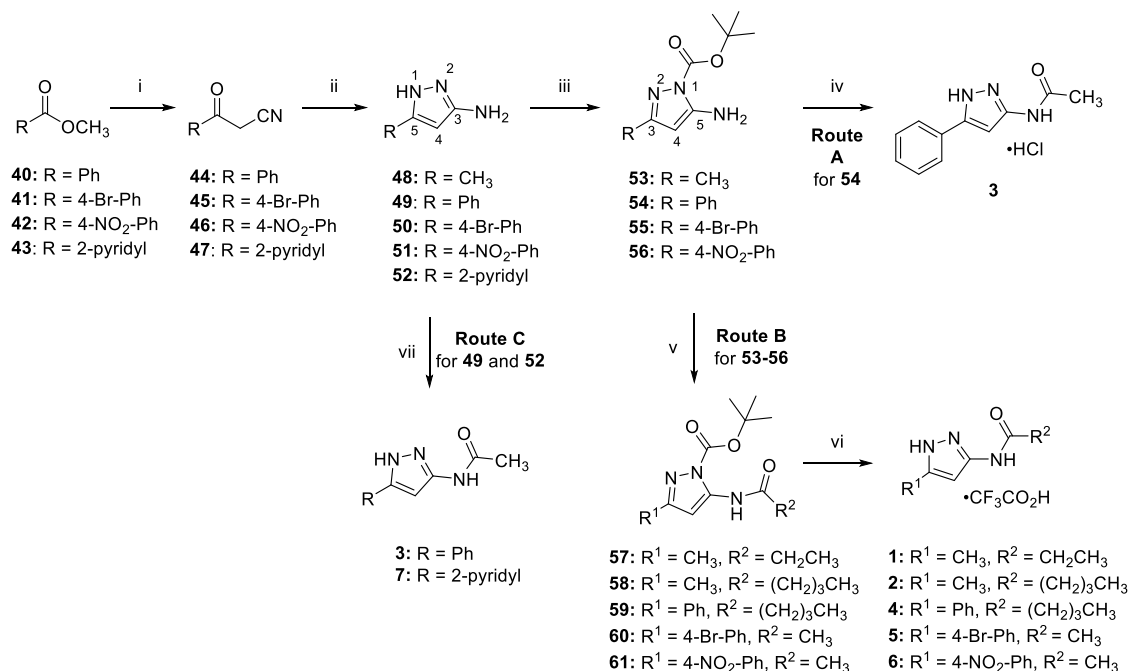
37

38

Table 3. Quinoline-based analogues **31-38**.

3. CHEMISTRY

3.1. SYNTHESIS OF PYRAZOLE-BASED FRAGMENTS 1-7

The 3-acylaminopyrazole fragments **1-7** were obtained by following the synthetic routes outlined in Scheme 1. In particular, the introduction of the acyl moiety was achieved by applying different protocols (Routes A, B, and C). The synthesis of 3-amino-5-aryl-pyrazole intermediates **49-52** was accomplished by two steps: first, the LDA-assisted Claisen condensation of the commercially available methyl esters **40-43** with CH_3CN afforded the β-ketonitriles **44-47**, which were then cyclized with hydrazine monohydrate to provide the 3-amino-5-aryl-pyrazoles **49-52**. Afterwards, the endocyclic NH group of **48-51** was protected through carbamoylation, with Boc_2O, to afford the N^1-Boc-protected 5-aminopyrazole intermediates **53-56**.[126] Then, by following Route A, **54** was reacted with acetyl chloride in CH_3CN and under reflux to obtain the final product **3** as hydrochloride salt. This procedure allowed, in a single step, to concurrently perform both acetylation of the exocyclic NH_2 and deprotection of the endocyclic NH groups. Unfortunately, this step-economic method proved to be unsuitable for synthesising the other derivatives of the series, as complex mixtures of compounds, difficult to purify, were obtained. Aimed at minimizing purification efforts, an alternative procedure was therefore applied (Route B). In detail, N^1-Boc-protected 5-aminopyrazoles **53-56** underwent an *N*-acylation reaction, by using acetyl or valeroyl chloride in presence of DIPEA as base, to achieve **57-61** that were then Boc-deprotected by acidic treatment (TFA in CH_2Cl_2) to obtain 3-acylaminopyrazoles **1**, **2**, and **4-6** as trifluoroacetate salt. Alternatively, a direct acetylation of the exocyclic NH_2 group of **49** and **52** with acetyl chloride in CH_3CN, in presence of K_2CO_3 as base and under reflux, afforded compounds **3** and **7**, as free bases (Route C). This last strategy provided the best results in terms of yield (around 90 %) and step-economy.

**Scheme 1.** Synthetic strategy for compounds **1-7**[a]

40: R = Ph
41: R = 4-Br-Ph
42: R = 4-NO$_2$-Ph
43: R = 2-pyridyl

44: R = Ph
45: R = 4-Br-Ph
46: R = 4-NO$_2$-Ph
47: R = 2-pyridyl

48: R = CH$_3$
49: R = Ph
50: R = 4-Br-Ph
51: R = 4-NO$_2$-Ph
52: R = 2-pyridyl

53: R = CH$_3$
54: R = Ph
55: R = 4-Br-Ph
56: R = 4-NO$_2$-Ph

Route A for **54**

3

Route C for **49** and **52**

Route B for **53-56**

3: R = Ph
7: R = 2-pyridyl

57: R^1 = CH$_3$, R^2 = CH$_2$CH$_3$
58: R^1 = CH$_3$, R^2 = (CH$_2$)$_3$CH$_3$
59: R^1 = Ph, R^2 = (CH$_2$)$_3$CH$_3$
60: R^1 = 4-Br-Ph, R^2 = CH$_3$
61: R^1 = 4-NO$_2$-Ph, R^2 = CH$_3$

1: R^1 = CH$_3$, R^2 = CH$_2$CH$_3$
2: R^1 = CH$_3$, R^2 = (CH$_2$)$_3$CH$_3$
4: R^1 = Ph, R^2 = (CH$_2$)$_3$CH$_3$
5: R^1 = 4-Br-Ph, R^2 = CH$_3$
6: R^1 = 4-NO$_2$-Ph, R^2 = CH$_3$

[a]**Reagents and conditions:** i) CH$_3$CN, LDA, dry THF, N$_2$, -78 °C to rt; ii) hydrazine monohydrate, EtOH, reflux; iii) Boc$_2$O, CH$_2$Cl$_2$/THF (4:1), rt; iv) acetyl chloride, CH$_3$CN, reflux; v) acetyl or valeroyl chloride, DIPEA, CH$_2$Cl$_2$, rt; vi) TFA, dry CH$_2$Cl$_2$, 0 °C to rt; vii) acetyl chloride, K$_2$CO$_3$, CH$_3$CN, reflux.

The structures of the N^1-Boc-protected 5-aminopyrazoles **53-56** were confirmed by comparison their ^{1}H-NMR chemical shift (δ) signals with those reported for similar aminopyrazoles. Moreover, when the protection reaction occurred at the N^1-position of the 5-aminopyrazoles, an intramolecular H-bond between the NH$_2$ and the Boc carbonyl could take place and lead to a down-field shift of the ^{1}H-NMR NH$_2$ signal (δ = 5.2–5.4 ppm) with respect to the corresponding NH$_2$ signal (δ = 4.8–5.0 ppm) of the starting reagents (**48-52**).[126]

3.2. SYNTHESIS OF HYBRID MOLECULES 8-30

3.2.1. Compounds bearing the oxalyl linker (8-11): synthetic route optimization

The general retrosynthetic pathway for the synthesis of compounds **8-11** is depicted in Figure 29. In detail, the insertion of the oxalyl moiety (in black) within amino-pyrazole and amino-terminal piperazine synthons (in blue and red, respectively) was carried out by applying two different synthetic strategies (Methods I and II). The two main building blocks and oxalyl chloride were combined in a one-pot acylation-deprotection reaction (Method I, compounds **8** and **9**); unfortunately, a number of undesired bi-products were also obtained with a detrimental effect on the yield. To overcome these drawbacks, a protection/deprotection stepwise approach was envisaged to be more advantageous (Method II, **10** and **11**). Initially, oxalyl chloride and aminopyrazole synthons, both bearing a protecting group (PG), were combined to afford an intermediate, which was then selectively deprotected at the oxalyl side to allow the subsequent coupling with the piperazine-synthon. Then, the aminopyrazole PG was removed leading to the desired target compounds in good yield.

Figure 29. General retrosynthetic strategy for compounds **8-11**
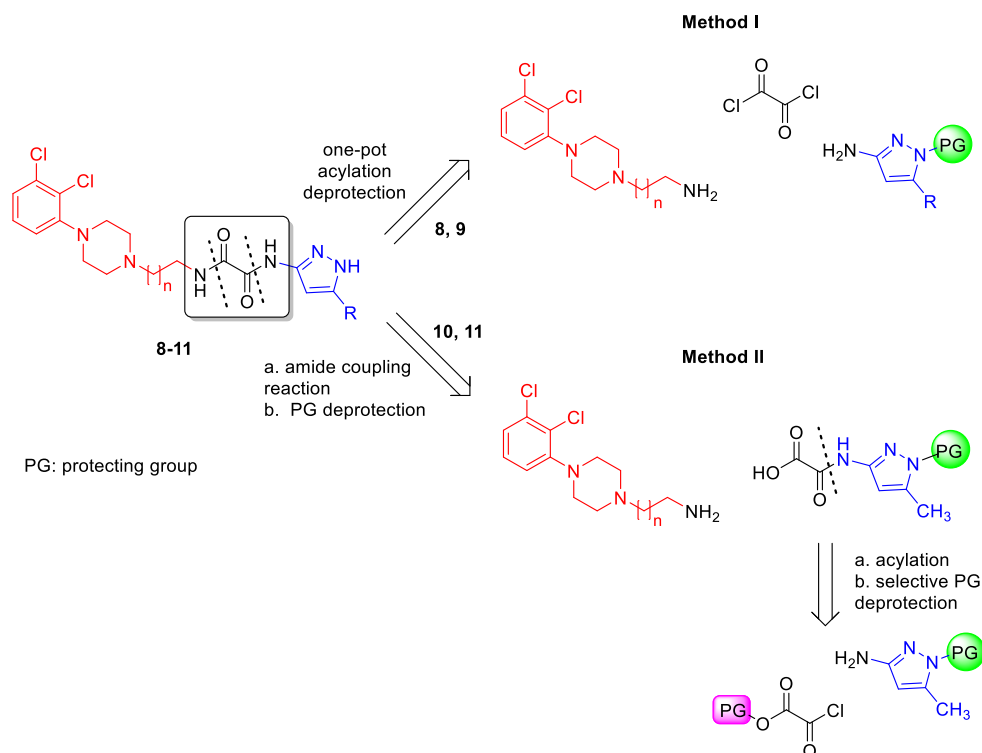
The target compounds **8-11** were obtained as depicted in Scheme 2 by following three synthetic routes (Methods I, IIa, and IIb). In Method I, a one-pot reaction between the amino-terminal-piperazine **137**, oxalyl chloride, and the N^1-Boc-protected 5-aminopyrazole (**53** or **54**), provided the final compounds **8** and **9**, respectively in low yield (slightly superior to 10 %). Moreover, regarding Method II, the aminopyrazole-based synthon underwent to two different protection strategies outlined as IIa and IIb. In Method IIa, the Boc-protected aminopyrazole **53** was reacted with mono ethyl oxalyl chloride**,** to afford derivative **62**. Hydrolysis of ethyl ester group, to provide the carboxylic acid function (compound **63**), was carried out under mild basic condition (LiOH, rt, in 50% THF/H_2O). Finally, the coupling reaction of acid **63** with the key amine **135** was performed *via* HATU activation, to give the **11** in 23 % yield (Method IIa). With the aim overcome the yield drawback, the tetrahydropyrane moiety (THP) was employed, being a favourable protective group for the N^1-position of the 3-aminopyrazole scaffold.[127] In Method IIb, the selective NH_2-acetylation of commercially available 3-amino-5-methyl-pyrazole **48**, under the previously described

condition (see Scheme 1), to obtain the 3-acetamidopyrazole **73**, was followed by the protection of the endocyclic NH group with 3,4-dihydro-2*H*-pyran, in presence of TFA as catalyst, to afford the N^1-THP-protected intermediate **79b**. The selective cleavage of the acetyl group, performed with KOH in EtOH/H_2O (2:3) and under reflux, gave the 3-amino-N^1-THP protected compound **89**, which was then treated with mono ethyl oxalyl chloride in presence of DIPEA as base to afford **64**. Afterward, the ester function of **64** was hydrolysed under basic condition (LiOH, rt, in 50% THF/H_2O), and the resulting compound **65** was reacted at the oxalyl acid moiety with the amine **136,** in presence of HATU, to afford intermediate **66**. The final cleavage of the THP PG, by TFA treatment, followed by a basic work-up, allowed obtaining the final compound **10** as free base.
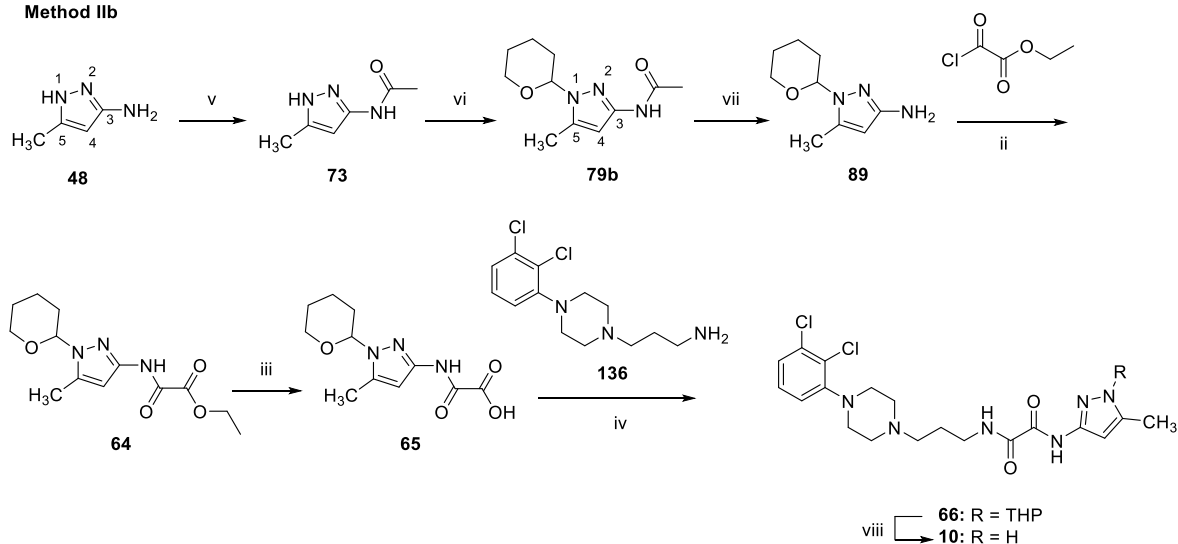
**Scheme 2.** Synthetic strategy for compounds **8-11**^a

Method IIb
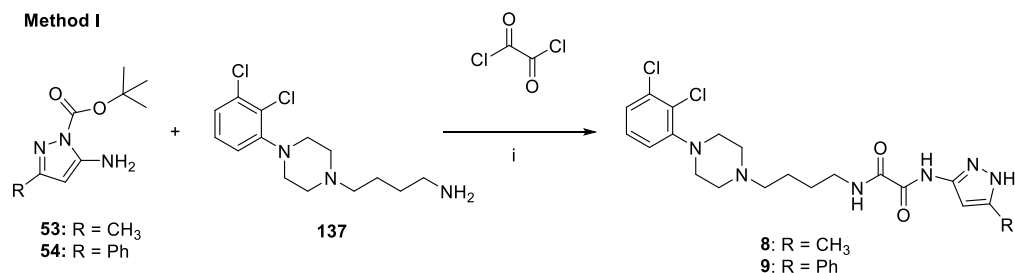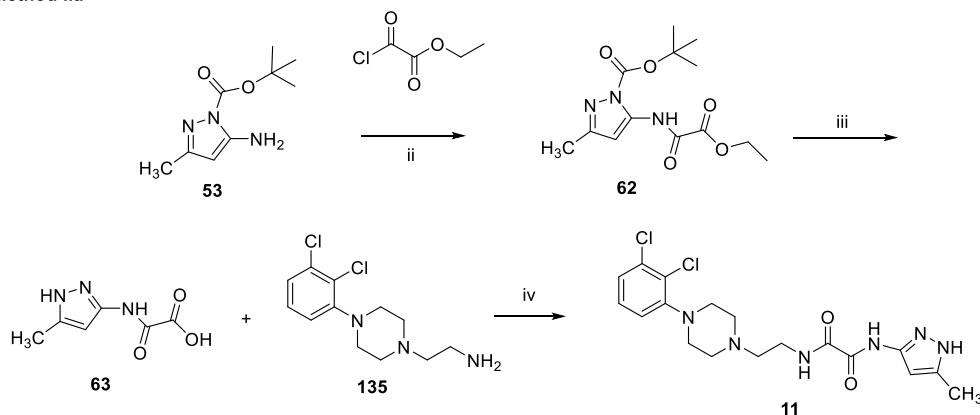
ªReagents and Conditions: i) DIPEA, CH_2Cl_2, N_2, 0°C to rt; ii) DIPEA, CH_2Cl_2, rt; iii) LiOH, THF/H_2O (1:1), rt; iv) HATU, DIPEA, dry DMF, rt; v) acetyl chloride, K_2CO_3, CH_3CN, reflux; vi) 3,4-dihydro-2*H*-pyran, TFA, CH_3CN, reflux; vii) KOH, $EtOH/H_2O$ (2:3), reflux; viii) TFA, dry CH_2Cl_2, 0 °C to rt.

3.2.2. Compounds bearing amido linker (12-26): synthetic route optimization

To synthetize the hybrids molecules (**12-26**) the retrosynthetic analysis (Figure 30) suggests, as an easily affordable strategy, a coupling reaction between the carboxy-terminal piperazine synthon and the N^1-protected-aminopyrazole. For this last, Boc or THP were used as PGs, thus exploring reactivity behaviour. Then, removal of PG through deprotection protocol leads to the target compounds.

Figure 30. General retrosynthetic strategy for compound**s 12-26**

a. amide coupling reaction
b. deprotection
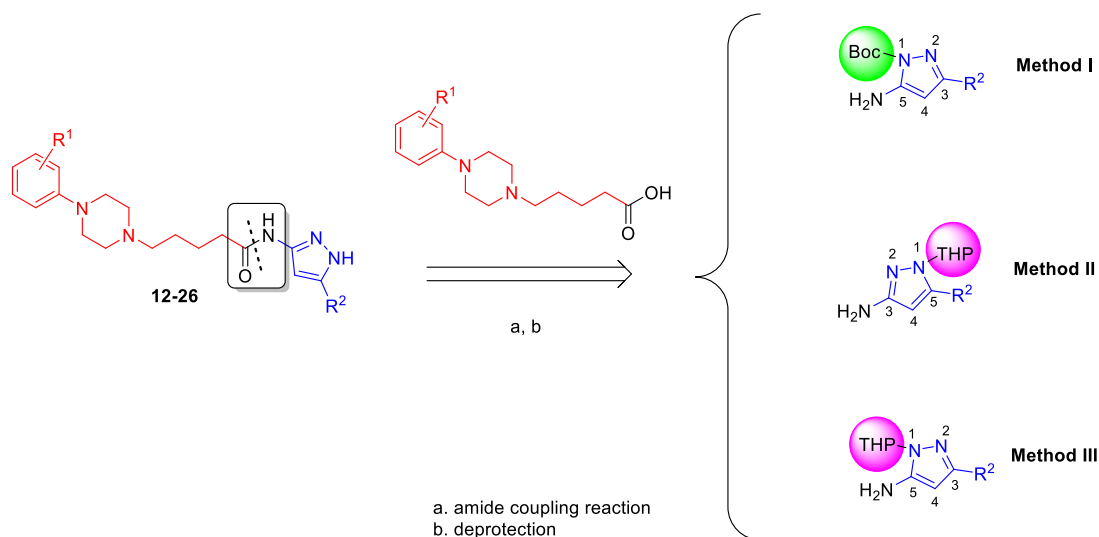
Method I. The N^1-Boc-protected 5-aminopyrazole intermediates, obtained with high regioselectivity and yield, were selected to be combined, through a coupling reaction, with the appropriate carboxylic acid-functionalized piperazine. Unfortunately, reactivity of these intermediates was revealed to be not appropriate for the purpose. In detail, the reaction between **129** and **53** to obtain intermediate **67** was performed by using different reagents and conditions, summarised in Table 4. However, none of these attempts led to the desired key intermediate. A steric hindrance effect or a hydrogen bond between the 5-NH_2 and the Boc carbonyl could be responsible for the lack of reactivity.
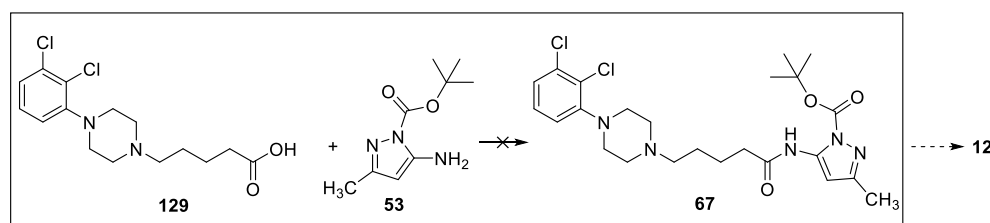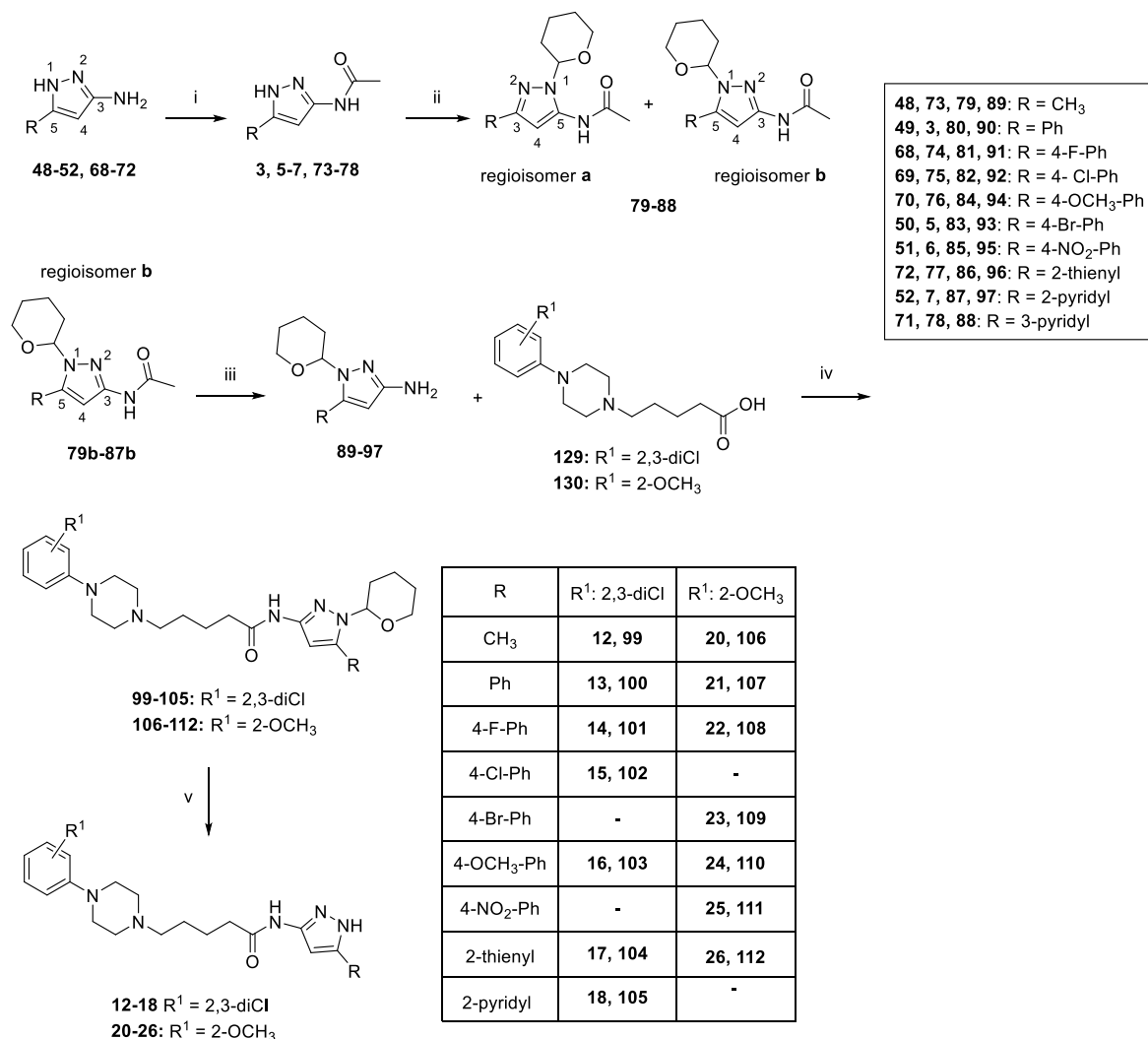

Entry	Amide coupling reagent	Base	Reaction condition
A	EDC/DMAP	-	dry CH_2Cl_2, N_2, 0 °C to rt, 18 h

B	EDC	NEt$_3$	dry CH$_2$Cl$_2$, N$_2$, 0 °C to rt, 18 h
C	EDC	NEt$_3$	dry CH$_2$Cl$_2$, N$_2$, 0 °C to reflux, 6 h
D	EDC/HOBt	NEt$_3$	dry CH$_2$Cl$_2$/DMF (4:1), N$_2$, 0 °C to rt, 18 h
E	HATU	DIPEA	dry DMF, rt, 48 h
F	HATU	DIPEA	dry DMF, 50 °C, 12 h

Table 4. Reaction conditions explored for obtaining key intermediate **67**.

Method II. The N^1-THP-3-aminopyrazole adduct proved to be a favourable key intermediate as this protection strategy gave straightforward access to a series of structurally related analogues. As depicted in Scheme 3, the synthetic route for compounds **12-26** comprises a first selective NH$_2$-acetylation of the 3-amino-5-substituted-pyrazoles, obtaining 3-acetamidopyrazoles **3**, **5-7** and **73-78**. A subsequent THP-protection of the endocyclic NH, by using the previously described conditions, afforded the N^1-THP-protected **79**-**88**. A mixture of regioisomers (designated as **a** and **b**) were obtained for compounds **80-87**, that were isolated by flash column chromatography. The regioisomer **b** of compounds **79-87** was treated with KOH providing the corresponding key aminopyrazoles **89-97**. These intermediates underwent an HATU-mediated amide coupling reaction with the appropriated carboxylic acid (**129** or **130**). The final compounds **12-18** and **20-26**, as free bases, were obtained upon TFA treatment followed by basic workup.

Scheme 3. Synthetic strategy for compounds **12-18** and **20-26**[a]

48, 73, 79, 89	: R = CH$_3$
49, 3, 80, 90	: R = Ph
68, 74, 81, 91	: R = 4-F-Ph
69, 75, 82, 92	: R = 4- Cl-Ph
70, 76, 84, 94	: R = 4-OCH$_3$-Ph
50, 5, 83, 93	: R = 4-Br-Ph
51, 6, 85, 95	: R = 4-NO$_2$-Ph
72, 77, 86, 96	: R = 2-thienyl
52, 7, 87, 97	: R = 2-pyridyl
71, 78, 88	: R = 3-pyridyl

R	R^1: 2,3-diCl	R^1: 2-OCH$_3$
CH$_3$	12, 99	20, 106
Ph	13, 100	21, 107
4-F-Ph	14, 101	22, 108
4-Cl-Ph	15, 102	-
4-Br-Ph	-	23, 109
4-OCH$_3$-Ph	16, 103	24, 110
4-NO$_2$-Ph	-	25, 111
2-thienyl	17, 104	26, 112
2-pyridyl	18, 105	-

[a]**Reagents and Conditions:** i) acetyl chloride, K$_2$CO$_3$, CH$_3$CN, reflux; ii) 3,4-dihydro-2*H*-pyran, TFA, CH$_3$CN, reflux; iii) KOH, EtOH/H$_2$O (2:3), reflux; iv) HATU, DIPEA, dry DMF, rt; v) TFA, dry CH$_2$Cl$_2$, 0 °C to rt.

Method III. The regioisomer **a** of compound **88** underwent KOH deacetylation, to obtain **98**, was reacted with **129**, and formation of the desired **113** did not occur (Scheme 4). This finding suggests that the reactivity of the pyrazole exocyclic NH$_2$ group is negatively influenced by the PG on the adjacent endocyclic nitrogen. As an alternative synthetic route, carboxylic acid **129** was converted in acyl chloride **139**, by treatment with oxalyl chloride, and then reacted with amine **98** to afford the target

compound **113**. The final THP-deprotection under acidic condition (TFA) allowed obtaining the final compound **19**.

Scheme 4. Synthetic strategy for compound **19**[a]
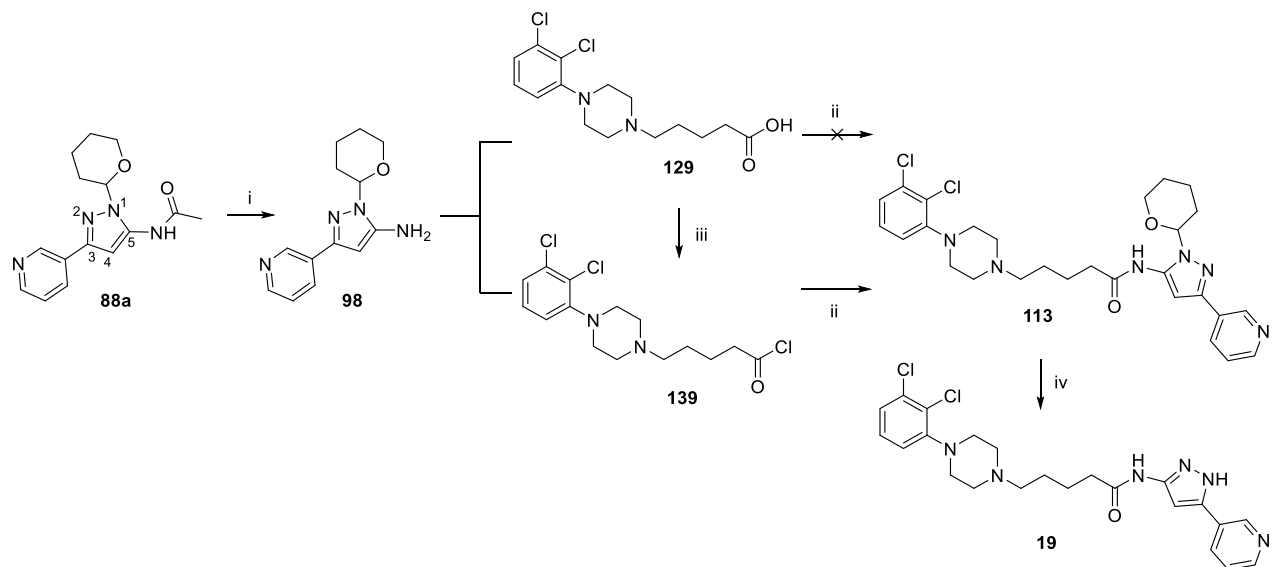
[a]**Reagents and Conditions:** i) KOH, EtOH/H_2O (2:3), reflux,; ii) HATU, DIPEA, dry DMF, rt; iii) oxalyl chloride, dry CH_2Cl_2, 0 °C to rt; iv) TFA, dry CH_2Cl_2, 0 °C to rt.

3.2.3. Aminopyrazole regioisomer: chemical and structural studies

The aminopyrazole heterocycle is known to adopt different tautomeric forms that in solution readily interconvert with each other; the ratio between regioisomers is affected by a combination of electronic and steric factors exerted by the substituents.[128] This behaviour is observed for the aminopyrazole when THP was introduced at endocyclic NH; in this context, both the acetamido group and R substituent proved to influence the regioisomer proportion. Regarding the N^1-THP-protection, only one isomer was obtained for 5-methyl- (**73**) and 5-(pyridin-3-yl)-acetamidopyrazole (**78**), affording **79b** and **88a**, respectively. On the contrary, for the same reaction a mixture of regioisomers **80-87** were observed by reacting acetamidopyrazoles **3**, **5-7** and **74-77** (Table 5).
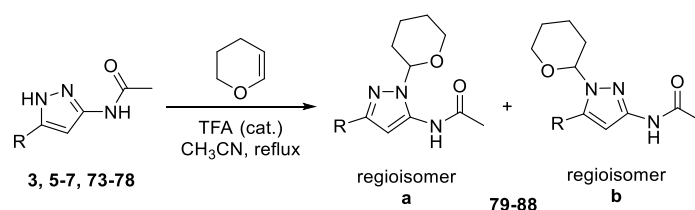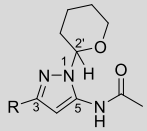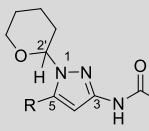
R	Products (yield)[a]		Ratio (A/B)[a]
CH_3	-	**79b** (46 %)	-
Ph	**80a** (28 %)	**80b** (21 %)	57:43
4-F-Ph	**81a** (6 %)	**81b** (38 %)	14:86
4-Cl-Ph	**82a** (6 %)	**82b** (15 %)	29:71
4-Br-Ph	**83a** (24 %)	**83b** (11 %)	69:31
4-OCH$_3$-Ph	**84a** (19 %)	**84b** (27 %)	41:59
4-NO$_2$-Ph	**85a** (60 %)	**85b** (9 %)	87:13
2-thienyl	**86a** (20 %)	**86b** (21 %)	49:51
2-pyridyl	**87a** (26 %)	**87b** (26 %)	50:50
3-pyridyl	**88a** (40 %)	**-**	-

[a] value refers to purified products

Table 5. Yields and Ratio between regioisomers **79-88.**

The structure of isolated isomers (**79-88**) was determined by ^{1}H-NMR analysis. To confirm compound regiochemistry, additional 2D experiments (^{1}H–^{1}H COSY, ^{1}H–^{13}C HSQC, NOESY) were performed on some pairs of regioisomers (**79**, **80** and **88**) (see *Appendix*). By observing the ^{1}H-NMR spectra of the aminopyrazole, the chemical shift value of H-2′ signal (Table 6) was found to provide useful information for elucidating

the isomer conformation; indeed, for regioisomer **a** it was observed a marked [1]H-downfield shift of the above mentioned signal, likely due to an anisotropic effect exerted by the acetamido carbonyl group. A cross-correlation of this behaviour was consistently found throughout the ^{1}H-NMR spectra of the regioisomer forms of compounds **79-88**. An exception was observed in the ^{1}H-NMR spectra of 2-pyridyl-substituted pyrazole (**87**) regioisomers, where the H-2′ proton of regioisomer **b** resonates at lower field (6.33 ppm) than the corresponding signal of the regioisomer **a** (5.59 ppm); the nitrogen atom of the pyridyl group could be likely responsible for this behaviour.

	δ_H (H-2′)[a]		δ_H (H-2′)[a]
-	-	CH$_3$	5.14
Ph	5.44[b]	Ph	5.14[b]
4-F-Ph	5.52	4-F-Ph	5.07
4-Cl-Ph	5.53	4-Cl-Ph	5.08
4-Br-Ph	5.52	4-Br-Ph	5.07
4-OCH$_3$-Ph	5.52	4-OCH$_3$-Ph	5.12
4-NO$_2$-Ph	5.57	4-NO$_2$-Ph	5.09
2-thienyl	5.51	2-thienyl	5.30
2-pyridyl	5.59	2-pyridyl	6.33
3-pyridyl	5.48	-	-

[a]Chemical shift value in CDCl$_3$; [b]Chemical shift value in DMSO-d_6

Table 6. Chemical shifts for H-2 proton of regioisomer A and B of key intermediates **79-88**

3.2.4. Compound bearing an ureido linker (27-30): synthetic route optimization

The retrosynthetic strategy to obtain hybrid molecules **27-30**, bearing an ureido function in the linker, is outlined in Figure 31. At a first glance, reaction between the appropriate isocyanate and the NH_2 function of the N^1-Boc-protected pyrazole was envisaged to be suitable for an easy access to a series of ureido-based analogues (Figure 31).

Figure 31. General retrosynthetic strategy for compounds **27-30.**
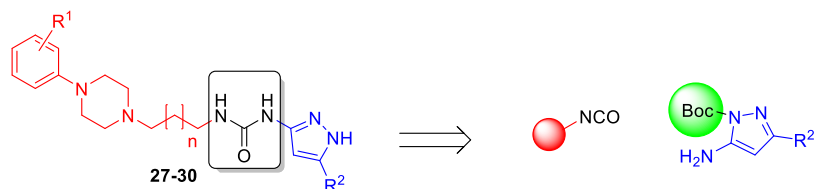
In detail, a model reaction between butyl isocyanate and N^1-Boc-protected 5-aminopyrazole **53** was performed and the undesired product **163** was obtained as a consequence of the reaction at endocyclic NH (Scheme 5).

Scheme 5.
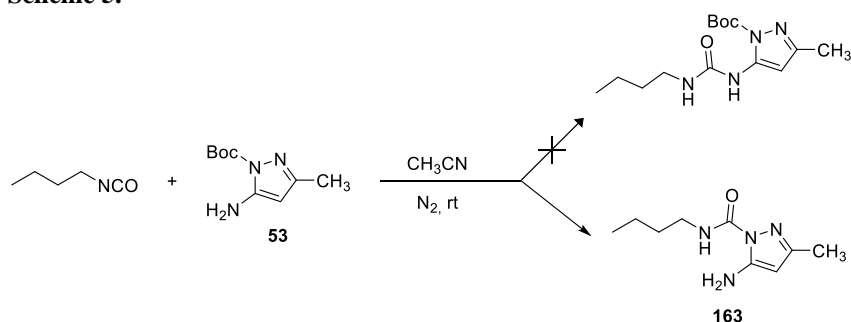
Thus, an alternative approach in which pyrazole NH_2 activation by phenyl carbamate was followed by a coupling with the appropriate amine, could be promising to obtain the desired analogues **27-30** (Figure 32).

Figure 32. General retrosynthetic strategy for compounds **27-30.**
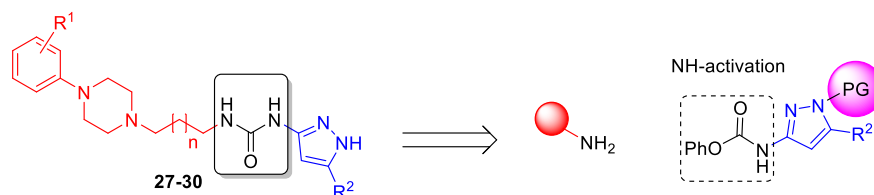
As outlined in Scheme 6A, unprotected 3-methyl-5-amino-1H-pyrazole **48** was first reacted with phenyl chloroformate, to obtain intermediate **114** in low yield (9 %) and then functionalized with amine **136**, to afford the desired compound **27** (28 %).The yields were improved by employing the THP protection strategy of aminopyrazole (Scheme 6B). Thus, the N^1-THP-protected aminopyrazoles **89** and **115** were converted in the corresponding phenyl carbamates **116** and **117**, respectively. Then, **116** reacted with the key amines **137** and **138**, to obtain the ureido-based intermediate **118** and **119**, and **117** reacted with **137** to give **120** The final THP-cleavage of **118-120**, under the previously described conditions, afforded the desired compounds **28-30**.

Scheme 6. Synthetic strategy for compounds **27-30**[a]

A)

B)
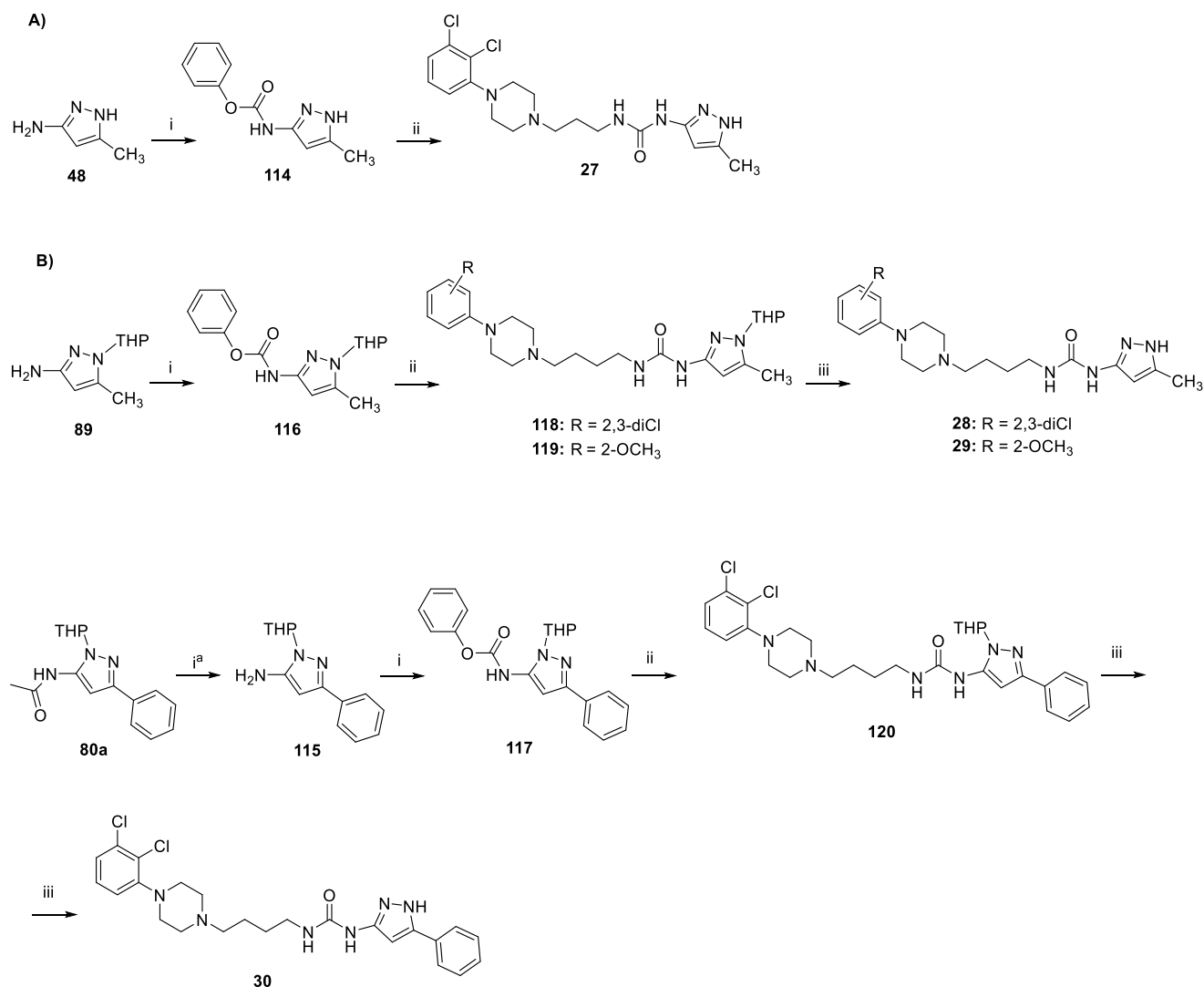
[a]**Reagents and Conditions:** i) phenyl chloroformate, pyridine, N_2, 0°C to rt; i[a]) KOH, EtOH/H_2O (2:3), reflux; ii) corresponding amine (**136**, **137**, **138**), TEA, $CHCl_3$, reflux; iii) TFA, dry CH_2Cl_2, 0 °C to rt.

3.2.5. Synthesis of aryl piperazine-based key intermediates 129, 130 and 135-138

Synthetic route for obtaining key intermediates with the aryl piperazine function (**129**, **130** and **135-138**) is outlined in Scheme 7. The *N*-alkylation of the commercially available aryl piperazines **122** and **123** was performed, under conventional reflux or microwave irradiation, with the properly functionalized alkyl halides, namely ethyl 5-

bromovalerate (**121**) and ω-halo-alkylphtalimide (**124-126**). The ester intermediates (**127** and **128**) were transformed into the carboxylic acids **129** and **130** by hydrolysis under basic condition (LiOH), while the phthalimide intermediates **131-134** were treated with hydrazine, to give the key primary amines **135-138**.

Scheme 7. General synthetic method for key intermediates **129**, **130** and **135-138**[a]
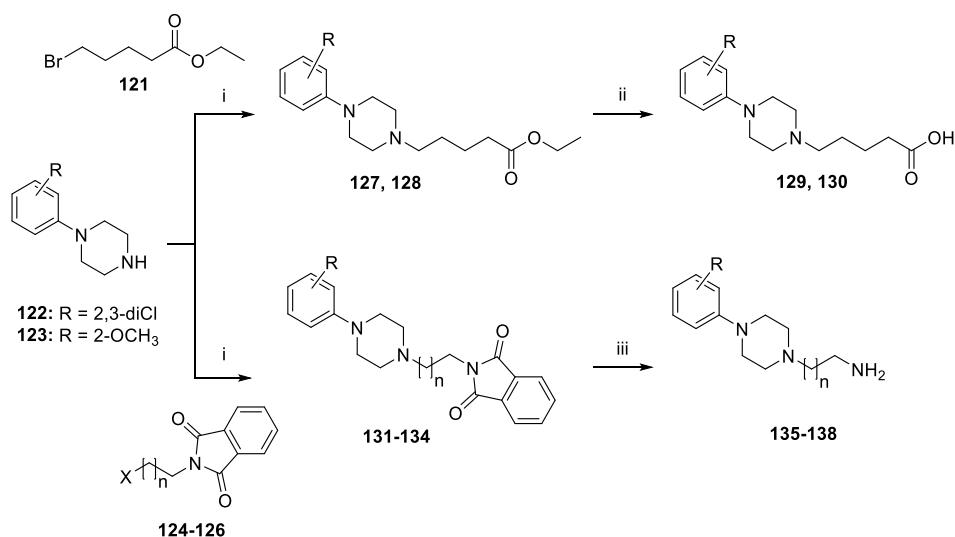
[a]**Reagents and Conditions:** i) a) K$_2$CO$_3$, CH$_3$CN, reflux; or b) NEt$_3$, CH$_3$CN, 100 °C (MW), 40 min; ii) LiOH, THF/H$_2$O (1:1), rt; iii) Hydrazine monohydrate, EtOH, reflux.

3.3. SYNTHESIS OF QUINOLINE-BASED COMPOUNDS 31-38

Quinoline based-compounds **31-38** were obtained by following the synthetic routes shown in Scheme 8 for the synthesis of **31**, **36-38** and Scheme 9 for the preparation of **32-35**.

As shown in Scheme 8, chlorination of 8-chloro-2-methylquinoline **140** employing *n*-tetrabutylammonium iodide (TBAI), 1,2- dichloroethane (DCE) and urea under microwave irradiation gave intermediate **141** which was then reacted with piperidine synthons **142** and **143**, in presence of NEt$_3$ as base and under reflux, to afford compounds **144** and **145**. These intermediates were then subjected to a Boc-deprotection reaction by 4 M HCl solution yielding the key amines **146** and **147**, respectively. Reaction of intermediate **147** with acetyl chloride gave the final

compound **36** and **37**. A HATU-mediated coupling reaction between benzoic acid and amine **146** or **147** afforded the desired product **31** and **38**, respectively.

Scheme 8. Synthetic strategy for compound **31, 36-38**[a]

140   141   142: i.p.: 3   144: i.p.: 3
               143: i.p.: 4   145: i.p.: 4

146: i.p.: 3   31: i.p.: 3; R = Ph; R^1 = H
147: i.p.: 4   36: i.p.: 4; R = CH$_3$; R^1 = H
                37: i.p.: 4; R = R^1 = CH$_3$
                38: i.p.: 4; R = Ph; R^1 = H
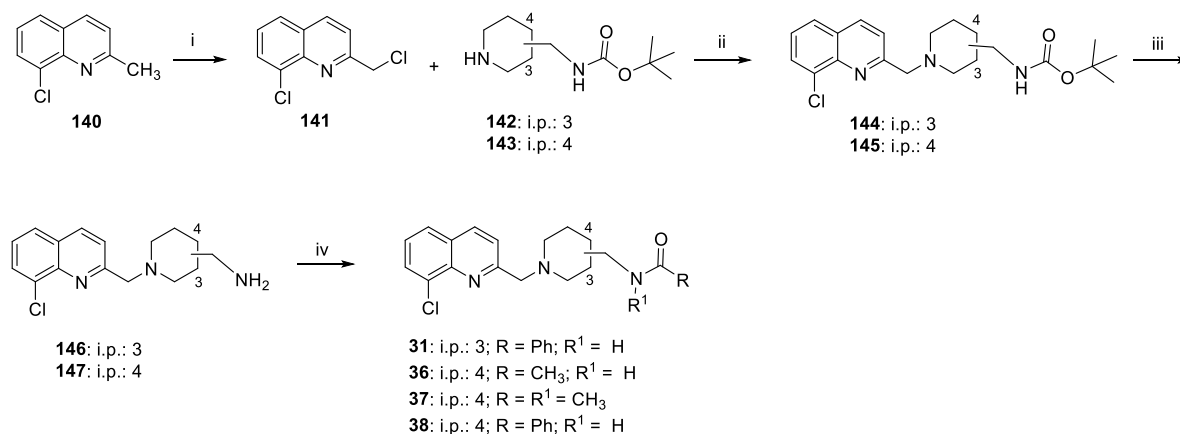
[a]**Reagents and Conditions:** i) urea, TBAI, DCE, 100 °C (MW), 30 min; ii) NEt$_3$, CH$_3$CN, reflux; iii) HCl in 1,4-dioxane (4 M), CH$_2$Cl$_2$/THF (1:1), rt; iv) a) acetyl chloride, DIPEA, CH$_2$Cl$_2$, rt or b) benzoic acid, HATU, DIPEA, dry DMF, rt.

Final compounds **32-35** were prepared by following the synthetic strategy outlined in Scheme 9. Compound **141** was reacted with 4-piperidine-ethanol, in presence of NEt$_3$ as base and under reflux, to afford intermediate **148**. The hydroxy function was substituted with chlorine, as a good leaving group, by using SOCl$_2$ to give **149** which, after treatment with potassium phthalimide, was converted in the desired compound **32**. The phthalimide function was removed with hydrazine hydrate to give the key amine **150**. Analogue **33** was obtained by acylation reaction of **150** with acetyl chloride. Compounds **34** and **35** were afforded through HATU-mediated coupling reaction of **150** with the appropriate benzoic acids.

Scheme 9. Synthetic strategy for compounds **32-35**[a]
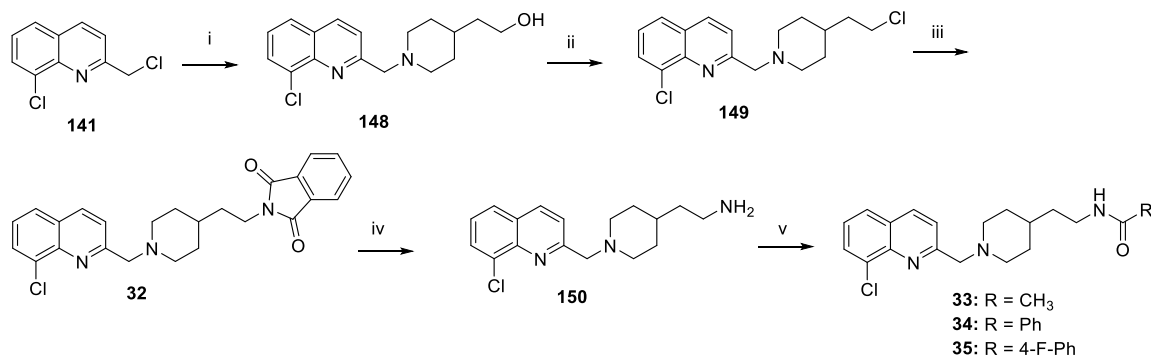
[a]**Reagents and Conditions: i)** 4-piperidine-ethanol, NEt$_3$, CH$_3$CN, reflux; **ii)** SOCl$_2$, dry CH$_2$Cl$_2$, 0 °C to rt; **iii)** potassium phthalimide, DMF, reflux; **iv)** hydrazine hydrate, EtOH, reflux; **v)** a) acetyl chloride, DIPEA, CH$_2$Cl$_2$, rt or b) appropriate benzoic acid, HATU, DIPEA, dry DMF, rt.

3.3.1. Synthesis of Boc-protected aminopiperidine intermediates 142 and 143

Synthetic route for preparing NH-Boc protected piperidine **142** and **143** is shown in Scheme 10. In detail, 3-piperidine-methanol underwent to a benzylation reaction on NH group with benzyl bromide under reflux to obtain intermediate **152**. The hydroxyl function was converted in the more reactive mesylate group, by using CH$_3$SO$_2$Cl to give **153**, and then reacted with potassium phthalimide yielding intermediate **154**. Treatment of phthalimide derivative **154** with hydrazine hydrate allowed obtaining the benzylpiperidine methyl amine **155**. Synthesis of N-benzyl piperidine **156** was performed by a selective NH-benzylation of commercially available 4-methylamine-piperidine **159**. The amine group of **155** and **156** was protected through carbamoylation with Boc$_2$O, to afford the NH-Boc benzylpiperidine intermediates **157** and **158**. A final debenzylation of piperidine ring, performed with hydrazine hydrate in presence of Pd/C as a catalyst, gave the desired intermediates **142** and **143**.

Scheme 10. General synthetic method for key intermediates **142** and **143**[a]
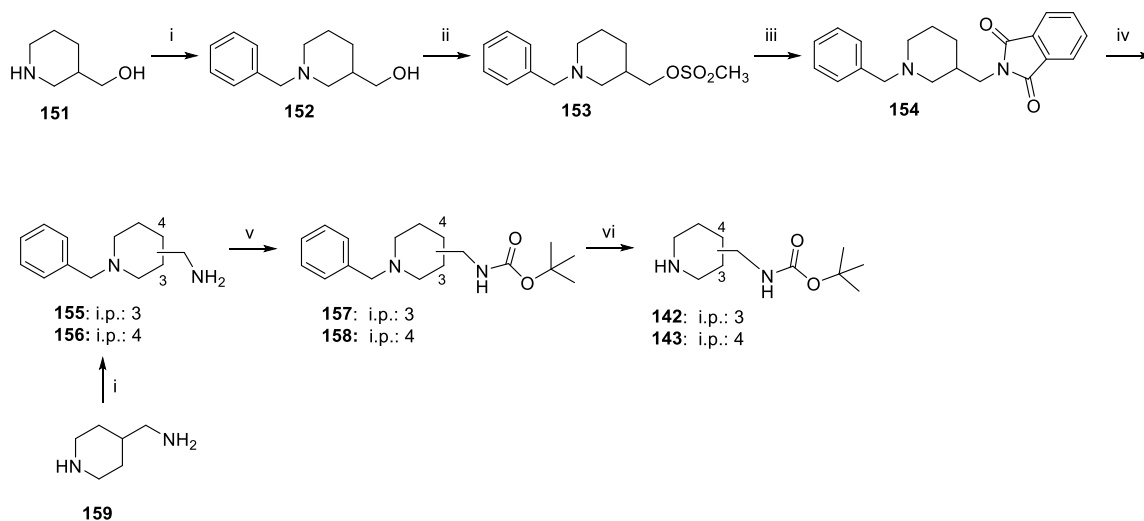
[a]**Reagents and Conditions:** i) benzyl bromide, NEt$_3$, CH$_3$CN, reflux; ii) CH$_3$SO$_2$Cl, CH$_2$Cl$_2$, 0 °C to rt; iii) potassium phthalimide, DMF, 80 °C; iv) hydrazine hydrate, EtOH, reflux; v) Boc$_2$O, CH$_2$Cl$_2$/THF (4:1), rt; vi) hydrazine hydrate, 10 % Pd/C, EtOH, 80 °C.

4. RESULTS AND DISCUSSION

4.1. D3R MODULATION

Compounds' activity on D3R was assessed by a Homogeneous Time-Resolved Fluorescence (HTRF) cAMP functional assay on stably transfected human-D3R expressing CHO-K1 cells. Biological results were obtained for hybrid molecules **8-13**, **15-19**, **21**, **22**, **24**, and **27**. As shown in Table 7, all tested compounds demonstrated potent agonistic activities on D3R, with effective concentration (EC_{50}) values in the one- or two-digit nanomolar range. The observed efficacy (expressed as a percent of the control response to 300 nM DA) ranging from 15 % to 77 % was mainly consistent with a partial agonist profile.

In detail, derivatives **8**-**11**, bearing a 2,3-dichlorophenylpiperazine, a methyl or phenyl group at the pyrazole ring and an oxalyl-based linker of different length, proved to effectively modulate D3R with nanomolar potencies (EC_{50} values ranging from 3.9 to 19.0 nM). Moreover, different extents of efficacy were observed for **8**, **10** and **11**, all bearing the methyl-pyrazole moiety, suggesting as it could be remarkably affected by the alkyl portion of the spacer. Efficacy switched from 77 % for **8** (butyl) to 33 % for **10** (propyl), while reached the value of 55 % for compound **11**, endowed with the shorter two-methylene spacer. For derivative **9**, as analogue of **8** encompassing a phenyl- instead of the methyl-pyrazole, a substantial decrease in efficacy was shown (38 %) indicating that also the steric hindrance could impact this property.

The set of derivatives characterized by an amido-four-methylene linker and a 2,3-di-Cl-phenylpiperazine (**12**, **13**, **15-19**) or a 2-methoxy phenylpiperazine (**21**, **22**, and **24**); and different substituents on the aminopyrazole, allowed us exploring the roles of PP and SP in D3R modulation. An interesting partial agonist profile was observed. In general, the substitution pattern on the pyrazole ring did not determine a remarkable effect on D3R activation. Specifically, decoration of this scaffold with a methyl group (compound **12**) allowed obtaining a potent D3R modulation (EC_{50} = 8.0 nM); its

replacement with a phenyl ring proved to be slightly detrimental for activity (compound **13**, EC_{50} = 14.1 nM). Insertion of *para*-chloro (compound **15**) or *para*-methoxy substituent (compound **16**) at the phenyl group maintained a good D3R activation with EC_{50} values of 13.0 and 8.5 nM, respectively. The presence of a thiophene ring did not affect receptor activation (compound **17**, EC_{50} = 12.0 nM), while with the insertion of a 2- or a 3-pyridyl moiety, EC_{50} values of 3.8 (compound **18**) and 2.9 nM (compound **19**), respectively, were observed. With respect to **13** and **16**, the 2-methoxy-substituted counterparts **21** and **24** (EC_{50} = 3.6 and 1.0 nM, respectively) showed improved potency. Moreover, compound **22**, bearing and 4-fluorophenyl pyrazole, turned out to be endowed with low nanomolar activity (EC_{50} = 1.0 nM). The influence of the arylpiperazine substitution on the D3R efficacy was evaluated. All 2,3-dichloro-substituted compounds, except for analogues **15** (23 % efficacy), showed a very similar percentage of efficacy values ranging from 43 to 56 % and behaved as partial agonists. Compounds bearing the 2-methoxyphenylpiperazine displayed low efficacy values varying from 15 % to 28 %.

Consistent results were obtained for compound **27**, characterized by an ureido-based linker, showed a high affinity binding at D3R (EC_{50} = 2.6 nM) and a partial agonist profile (efficacy 47 %), thus emerging a very promising compound.

Derivative **12** (Figure 33A), as prototype compound, and **19** (Figure 33B), as one of the most active of the series, were subjected to docking studies at D3R binding pocket. The obtained results contributed to support SAR studies, thus confirming the experimental outcomes. In detail, the predicted bond conformations showed the ability of the selected molecules to simultaneously engage both the OBP and the SBP. Moreover, analogue **19**, bearing a 3-pyridyl group, was likely lodged in the D3R subpocket formed between TM I and II.
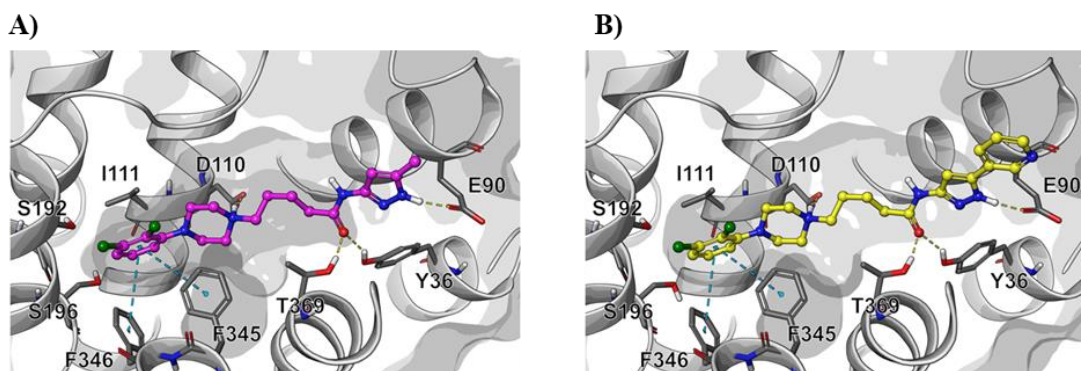
Figure 33. Predicted bound conformations of **12** (pink carbon atoms, A) and **19** (yellow carbon atoms, B) at D3R. The protein structure is reported in grey ribbons. The binding pocket is highlighted by a transparent grey mesh. Amino acids interacting with the ligand are reported in grey sticks and labelled explicitly.

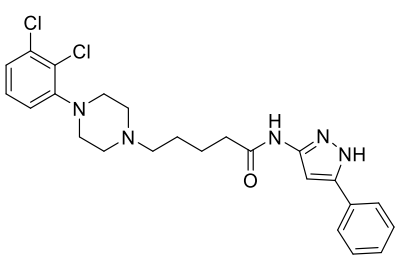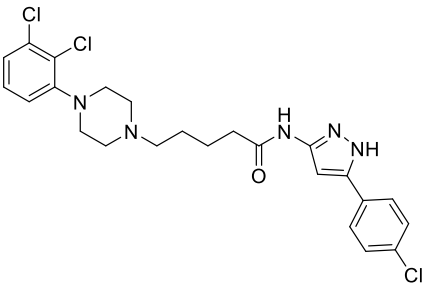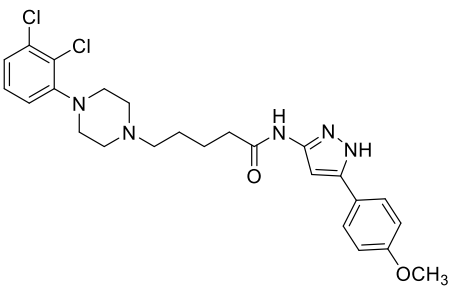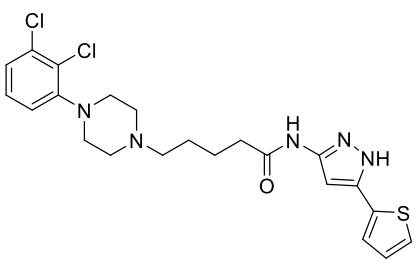In light of these results, some conclusions could be drawn:
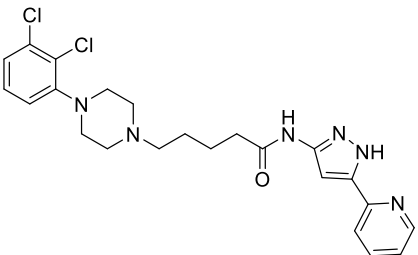
- The amido-four-methylene and the ureido-three-methylene units allowed to obtain derivatives with an effective partial agonist profile, thus emerging as promising linkers to be used for connecting the main PP and SP;

- 2,3-dichloro and 2-methoxy-substitution on the aryl-piperazine confirmed their usefulness in obtaining a partial agonist profile against D3R;

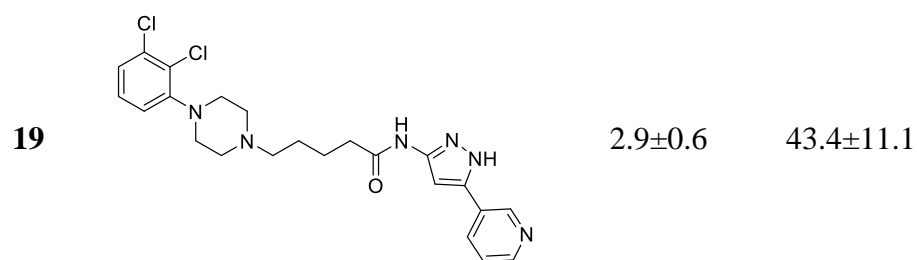- decoration of the pyrazole scaffold did not play a remarkable role in affecting activity.

Table 7. Results of D3R cell-based assay for compounds **8-13, 15-19, 21, 22, 24,** and **27.**

Comp	Chemical structure	D3R	
		EC$_{50}$ (nM)^a	**Efficacy %^{b}**
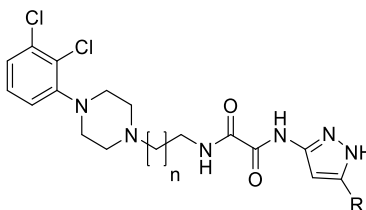
8		3.9±0.3	76.9±2.2
9		19.0±5.8	38.1±5.0
10		15.0±3.3	33.2±2.9
11		7.6±3.7	55.3±12.2

		D3R	
Comp	**Chemical structure**	EC_{50} **(nM)**[a]	**Efficacy %**[b]
12		8.0±1.8	47.0±7.5

71

13 14.1±2.5 56.3±7.6

15 13.0±1.2 23.1±1.1

16 8.5±1.5 46.5±4.8

17 12.0±1.9 45.8±2.9

18 3.8±0.3 48.7±3.4

19		2.9±0.6	43.4±11.1
21[c]		3.6	15.3
22[c]		1.0	23.9
24[c]		1.0	28.3

		D3R	
Comp	**Chemical structure**	**EC₅₀ (nM)**[a]	**Efficacy %**[b]

19		2.9±0.6	43.4±11.1
21[c]		3.6	15.3
22[c]		1.0	23.9
24[c]		1.0	28.3

		D3R	
Comp	**Chemical structure**	**EC_{50} (nM)**[a]	**Efficacy %**[b]

27   2.6±0.7   47.5±2.3

---

[a]EC$_{50}$ values are reported as a mean value of three determinations; [b]vs. 300 nM DA; [c]Preliminary data (n = 1).
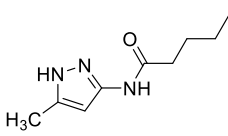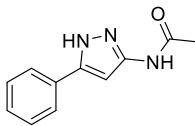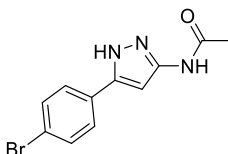
4.2. GSK-3β INHIBITION

The GSK-3β inhibitory potency of pyrazole-based fragments and hybrid molecules was evaluated by a LANCE® Ultra Time-Resolved Fluorescence Resonance Energy Transfer (TR-FRET) assay. Biological data are shown in Table 8 and 9. For those compounds which did not give a full inhibitory curve, we reported the percentage of inhibition at 100 µM or, where indicated, at the highest dose tested due to reduced compounds' solubility in the assay buffer. The obtained results were expressed as a percentage of inhibition of the control enzyme activity (inhibition %). Regarding the pyrazole-based fragments (**1**, **2**, **3**, **5**; Table 8), all the compounds, except **3**, were able to inhibit GSK-3β, with micromolar potencies. Due to their increase in size, that could account for increased interactions with the target, these analogues were more potent than the hit compound **I** (IC$_{50}$ = 69.6 µM). Analogue **3** showed only a 67 % inhibition at 59 µM, that is the highest dose tested, due to its poor solubility in the assay buffer. These preliminary data pointed out that the structural modifications on **I** had, in general, favourable effects on GSK-3β inhibition.

Table 8. Results of GSK-3β inhibition for pyrazole-based fragments **1-3** and **5**.

Comp	Chemical structure	GSK-3β[a]	
		inhib %	IC$_{50}$ (µM)
1[b]			23.5±0.12

2[b] 12.0±0.99

3[c] 67.5±2.8

(at 59 µM)

5[b] 2.6±0.14

[a]IC_{50} values are reported as a mean value of three determinations;
[b]trifluoroacetate salt; [c]hydrochloride salt.

With regards to hybrid molecules, heterogeneous GSK-3β inhibitory effects were observed for analogues **8-13**, **15-19**, **21**, **22**, **24** and **27** (Table 9). The oxalyl-based subset of compounds (**8-11**) displayed a low potency likely due to their very low solubility in the assay buffer. When tested at 100 µM, they inhibited the enzymatic activity with percentage values comprised between 16 to 44 %.

On the contrary, derivative characterised by an amido-based linker, diversely substituted pyrazoles and the 2,3-di-Cl-phenylpiperazine (**12**, **13**, **15-19**) showed a slightly improved inhibition. Among this set, the methyl-substituted **12** exerted a good GSK-3β inhibitory effect in the low micromolar range (IC_{50} = 10.1 µM), while the 3-pyridyl derivative **19**, showing a one-digit micromolar potency (IC_{50} = 2.6 µM), emerged as the most active of this series. Unexpectedly, the introduction of 2-pyridine substitution (compound **18**) was detrimental for enzyme inhibition (34 % at 100 µM). Similar effects were observed upon for the remaining compounds **13**, **15-17**. In detail, the phenyl-substituted analogue **13** was not effective up to 100 µM, while preliminary data of compounds **15-17** showed a slight inhibitory activity on the enzyme (15-54 % at 100 µM).

Interesting results were obtained for the analogues characterized by 2-methoxy phenylpiperazine (**21**, **22**, and **24**). Compounds **21** and **24** showed a good inhibitory

activity of the enzyme (IC_{50} =13.9 and 23.3 µM, respectively; only preliminary data are available), remarkably higher than the 2,3-dichloro-substituted counterparts **13** and **16**. Moreover, compound **22**, bearing a 4-fluorophenyl pyrazole, exerted a inhibitory effect in the low micromolar range (IC_{50} = 3.5 µM).

Compound **27**, characterized by the ureido-based linker and the methylpyrazole motif, turned out to be a two-digit micromolar inhibitor with IC_{50} value of 48.6 µM.

Molecular modelling studies, performed on **12** and **19** (Figure 34A and 34B, respectively) at the binding site of GSK-3β, demonstrated that the pyrazole scaffold engages the hinge region of the enzyme, forming the typical H-bond pattern of kinase inhibitors, while the 2,3-di-Cl-phenylpiperazine group projectes outside the pocket. Additionally, the 3-pyridine ring of **19** is favourably lodged toward the conserved residue LYS85 without, however, directly contacting it. These data reinforced the importance of the pyrazole moiety for an optimal modulation of the enzyme.
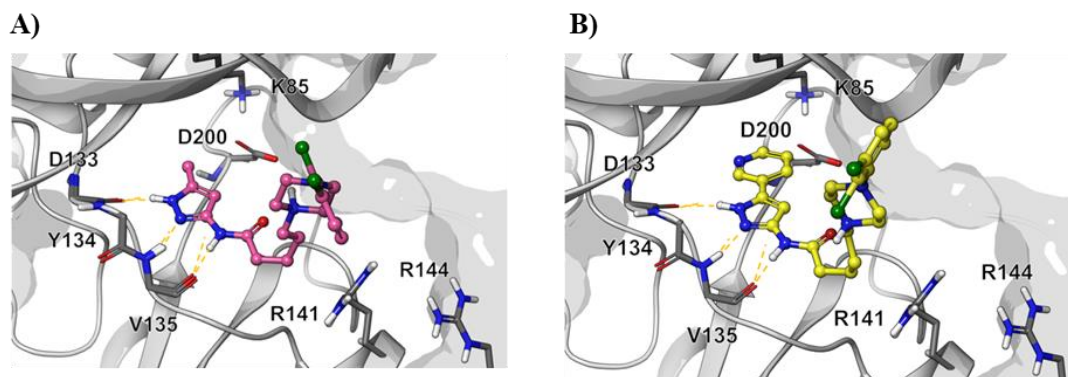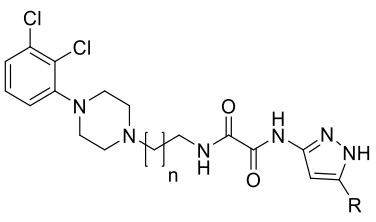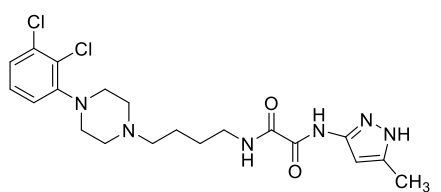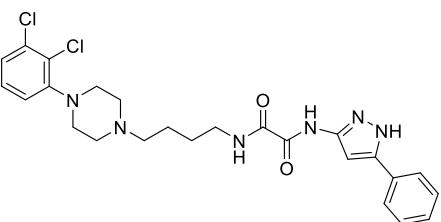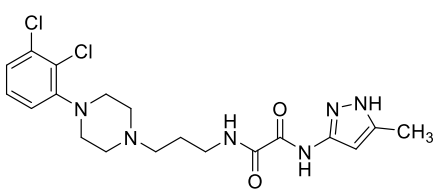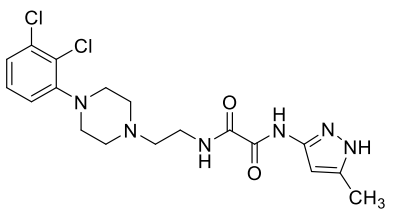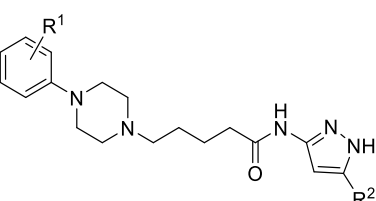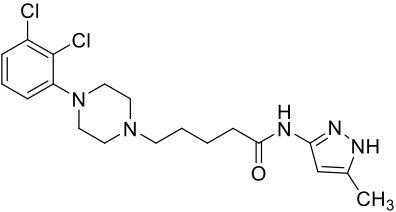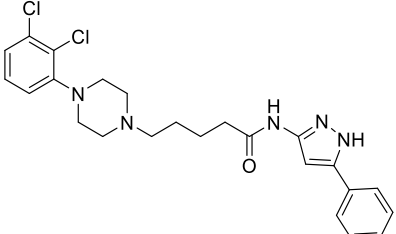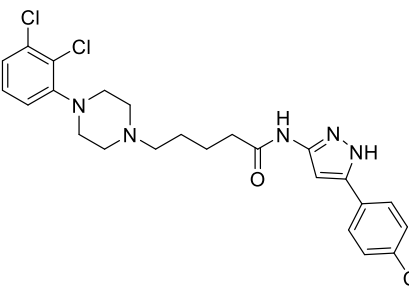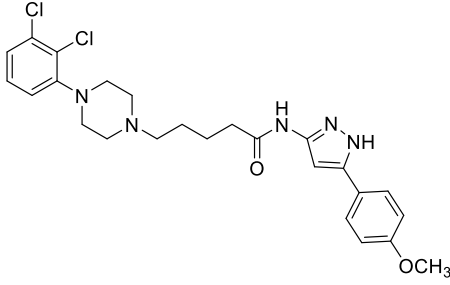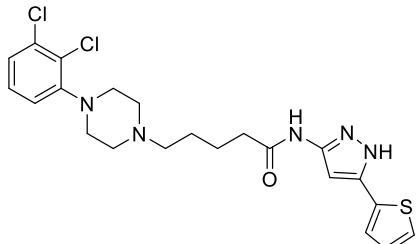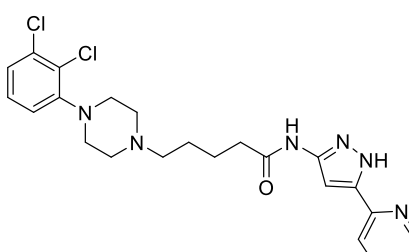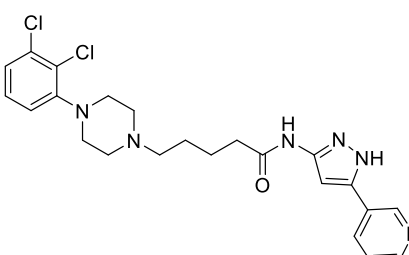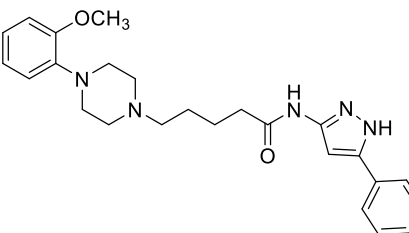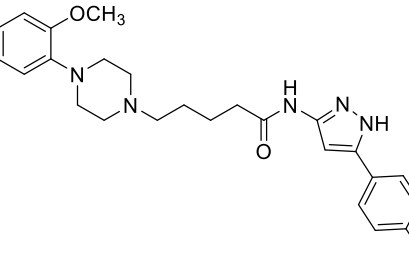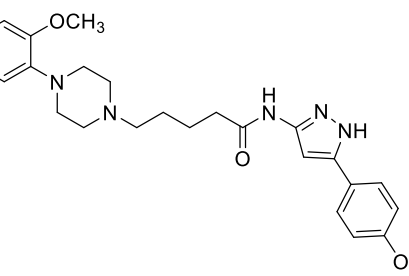

Figure 34. Predicted bound conformations of **12** (pink carbon atoms, A) and **19** (yellow carbon atoms, B) at GSK-3β. The protein structure is reported in grey ribbons. The binding pocket is highlighted by a transparent grey mesh. Amino acids interacting with the ligand are reported in grey sticks and labelled explicitly.
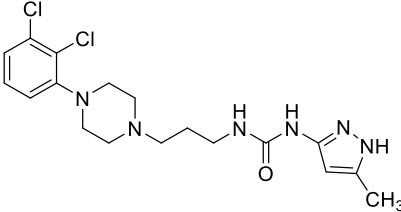
In summary, by observing the diversity of the obtained results, both the nature of the linker and the substitution pattern on the pyrazole ring remarkably affected the inhibitory profile of the hybrid molecule.

Table 9. Results of GSK-3β inhibition for hybrids molecules **8-13, 15-19, 27**.

comp	Chemical structure	GSK-3β	
		inhib %[a]	IC$_{50}$ (µM)[b]
8		44.4±5.5 (at 72 µM)	
9[c]		26.1 (at 26 µM)	
10		36.3±5.4 (at 30 µM)	
11[c]		15.8	

comp	Chemical structure	GSK-3β	
		inhib %[a]	IC$_{50}$ (μM)[b]
12			10.1±2.9
13		n.i.	n.i.
15[c]		53.8	
16[c]		41.0	
17[c]		14.9	

18 34.2±0.4

19 77.7±1.4 (at 10 µM) 2.6±0.2

21 86.1±1.5 13.9^c

22 70.5±1.4 3.5^c

24 77.2±1.2 23.3^c

Comp	Chemical structure	GSK-3β	
		inhib %[a]	IC$_{50}$ (µM)[b]
27		75.0±0.1	48.6±7.3

[a]Percentage of inhibition was determined at a concentration of 100 µM; [b]IC$_{50}$ values are reported as a mean value of three determinations; n.i.= not inhibiting up to a concentration of 100 µM; [c]Preliminary data (n = 1).

By observing these interesting results, we discovered some promising prototype compounds as dualistic modulators of D3R and GSK-3β. In detail, in a multi-target context, compounds **12**, **19**, **21**, **22**, **24**, and **27**, characterized by low-nanomolar and micromolar potencies against D3R and GSK-3β, respectively, showed an apparent not-balanced dualistic effect. However, to achieve a safe therapeutic effect, a smooth low-micromolar inhibition of GSK-3β has been recently preferred to a potent one, since it is supposed to be adequate to return CNS upregulated enzyme activity to the physiological levels.[129] Moreover, partial inhibition of the enzyme activity could not only be necessary to avoid toxicity, but also be optimal for a therapeutic effect, since lithium only partially inhibits GSK-3β (20–25%).[130] A more balanced dualistic profile was observed for **19** and **22** that emerged as the most promising compounds of this set, worth to be further optimized.

5. CONCLUSION

Main goal of this thesis was the identification of dual D3R/GSK-3β modulators as novel therapeutic strategy for BD treatment.

The complex pathological mechanisms of BD direct attention to polypharmacology as suitable strategy in achieving a successful therapeutic outcome. Thus, multitarget or multipotent drugs *i.e.* molecules concurrently capable of interacting with diverse targets involved in the pathology, could allow preventing and reversing a number of impaired cellular dysfunctions. In this scenario, the pivotal roles of D3R and GSK-3β in both cognition and mood regulation inspired the idea that a concomitant modulation of these two targets could represent a viable BD therapeutic strategy. From a medicinal chemistry standpoint, we rationally envisaged the pharmacophore model at the basis of the design of several D3R antagonists, suitable to be exploited for the design of dualistic D3R/GSK-3β ligands. Therefore, several synthetic efforts were dedicated at obtaining a first set of hybrid molecules, encompassing an aminopyrazole synthon joined to an arylpiperazine framework trough a suitable functionalized spacer (amido, ureido, and oxalyl), able to concurrently modulate the selected targets. The newly synthetized compounds were tested against GSK-3β and D3R and a large number of effective derivatives were identified. In detail, compounds **12**, **19**, **21**, **22**, and **24** turned out to be effective dualistic modulators of GSK-3β and D3R (potencies in the low-µM and low-nM range, respectively). The analogues possess an amido four-methylene spacer that emerged as promising linker by which exploring the chemical space of the selected targets, aimed to obtain novel drug candidates for BD cure. In addition, derivative **27** endowed with a more rigid ureido spacer than the amido-based one, exhibited a good dualistic modulatory effect. In conclusion, among the newly identified led compounds, analogue **19** and **22** could be regarded as the most promising, emerging as a valuable dualistic candidate worth to be further optimized through several approaches.

Biological investigations are still in progress to evaluate the potential of these hybrid molecules as effective multifunctional compounds for BD treatment. Moreover, future chemical efforts will be carried out on the selected lead compounds devoted to: i) performing different structural variations of the three pharmacophore regions, to accomplish a S.A.R. study ii) carrying out a deeper characterization, in order to assess the off-target activities (including the activity on other DA receptor subtypes), thus exploring the selectivity prolife.

6. EXPERIMENTAL PART

6.1. General chemical methods

Solvents and reagents were obtained from commercial suppliers and were used without further purification. Chromatographic separations were performed on silica gel columns using the flash method (Kieselgel 40, 0.040-0.063 mm, Merck). Reactions were followed by thin layer chromatography (TLC) on precoated silica gel plates (Merck Silica Gel 60 F254) and then visualized with a UV lamp. Microwave assisted synthesis was performed by using CEM Discover® SP apparatus (2.45 GHz, maximum power of 300W), equipped with infrared temperature measurement. NMR experiments were recorded on Varian Gemini 400 MHz or on Bruker Avance III 400 system (400.13 MHz for 1H, and 100.62 MHz for 13C). Chemical shifts are reported as parts per million (ppm δ value) relative to the peak for tetramethylsilane (TMS) as internal standard. Standard abbreviations indicating spin multiplicities are given as follows: s (singlet), d (doublet), t (triplet), br (broad), q (quartet), dd (doublet of doublet) or m (multiplet). UPLC/MS analyses were run on a Waters ACQUITY UPLC/MS system consisting of a SQD (Single Quadrupole Detector) Mass Spectrometer equipped with an Electrospray Ionization interface and a Photodiode Array Detector. PDA range was 210-400 nm. The analyses were performed on an ACQUITY UPLC BEH C_{18} (50x2.1 mmID, particle size 1.7μm) with a VanGuard BEH C_{18} pre-column (5x2.1 mmID, particle size 1.7 μm) (LogD>1). The mobile phase was 10mM NH_4OAc in H_2O at pH 5 adjusted with AcOH (A) and 10mM NH_4OAc in CH_3CN-H_2O (95:5) at pH 5 (B). Electrospray ionization in positive and negative mode was applied in the mass scan range 100-500Da. Depending on the analysis method used, a different gradient increasing the proportion of mobile phase B was applied. For analysis method A, the mobile-phase B proportion increased from 5 % to 95 % in 3 min. For analysis method B, the mobile-phase B proportion increased from 50 % to 100 % in 3 min. Compounds were named using the naming algorithm developed by CambridgeSoft Corporation and

used in ChemDraw professional 18.0. All final compounds displayed ≥ 95% purity as determined by NMR and UPLC/MS analysis.

### General procedure of *N*-Boc deprotection: synthesis of final compounds 1, 2, 4-6 (Scheme 1)

The appropriate *N*-Boc protected intermediate **57-61** (1.00 mmol) was treated with TFA (40.0 molar equiv) in dry CH_2Cl_2 (10.0 mL) at 0°C. The ice-bath was removed, and the resulting mixture was stirred at rt for 1-3h. Upon reaction completion, the mixture was concentrated under reduced pressure to afford a crude which was purified by trituration with Et_2O. The resulting precipitate was collected by filtration, washed with fresh Et_2O and dried under *vacuum*, to yield the final compound as trifluoroacetate salt.

N-(5-methyl-1*H*-pyrazol-3-yl)propionamide trifluoroacetate (1, Scheme 1)
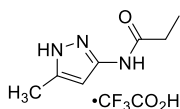
In line with the general procedure, treatment of **57** (0.17 g, 0.67 mmol) with TFA (2.05 mL, 26.8 mmol) in CH_2Cl_2 (7.0 mL) for 1 h afforded **1** as a white solid (0.07 g, 68 %); R_f 0.08 (PE/EtOAc 80:20). [1]**UPLC-MS**: t_R = 0.90 min (method A), *m/z*: 154.5 [M+H]$^+$ calcd for $C_7H_{12}N_3O$ 154.1. [1]**H-NMR** (400 MHz, CDCl$_3$) δ 10.20 (br. s, 1H, NHCO), 6.22 (br. s, 1H, CH-pyrazole), 2.26 (q, *J* = 7.2 Hz, 2H, CH$_2$), 2.18 (s, 3H, CH$_3$), 1.02 (t, *J* = 7.6 Hz, 3H, CH$_3$). [13]**C-NMR** (101 MHz, DMSO-d_6) δ 170.5, 146.8, 142.2, 95.2, 28.3, 10.5, 9.8. **UPLC-MS purity** > 99.5 % (λ = 215 nm).

### *N*-(5-methyl-1*H*-pyrazol-3-yl)pentanamide trifluoroacetate (2, Scheme 1)
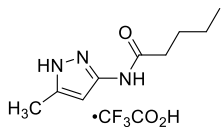
In line with the general procedure, treatment of **58** (0.17 g, 0.89 mmol) with TFA (2.73 mL, 35.6 mmol) in CH_2Cl_2 (9.0 mL) for 2 h afforded **2** as a white solid (0.05 g, 20 %); R_f 0.08 (PE/EtOAc 80:20). [1]**UPLC-MS**: t_R = 1.34 min (method A), *m/z*: 182.6 [M+H]$^+$ calcd for $C_9H_{16}N_3O$ 182.1. [1]**H-NMR** (400 MHz, DMSO-d_6) δ 10.28 (br. s, 1H, NHCO), 6.22 (s, 1H, CH-

pyrazole), 2.26 (t, J = 7.4 Hz, 2H, CH$_2$), 2.18 (s, 3H, CH$_2$), 1.52 (q, J = 7.6 Hz, 2H, CH$_2$), 1.28 (q, J = 7.6 Hz, 2H, CH$_2$), 0.87 (t, J = 7.3 Hz, 3H, CH$_3$). **^{13}C-NMR** (101 MHz, DMSO-d_6) δ 171.0, 147.5, 142.0, 95.3, 35.1, 27.1, 21.7, 13.8, 10.6. **UPLC-MS purity** > 99.5 % (λ = 215 nm).

### *N*-(5-phenyl-1*H*-pyrazol-3-yl)pentanamide trifluoroacetate (4, Scheme 1)
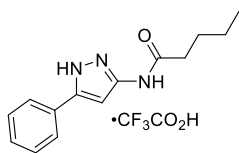
In line with the general procedure, treatment of **59** (0.02 g, 0.06 mmol) with TFA (0.18 mL, 2.4 mmol) in CH$_2$Cl$_2$ (1.0 mL) for 2 h afforded **4** as a yellowhish solid (0.01 g, 69 %); **R_f** 0.07 (PE/EtOAc 80:20). **^{1}UPLC-MS**: t$_R$ = 1.82 min (method A), *m/z*: 244.5 [M+H]$^+$ calcd for C$_{14}$H$_{18}$N$_3$O 244.1. **^{1}H-NMR** (400 MHz, DMSO-d_6) δ 10.37 (br. s, 1H, NHCO), 7.70 (d, J = 7.6 Hz, 2H, Ar), 7.45– 7.40 (m, 2H, Ar), 7.38– 7.30 (m, 1H, Ar), 6.84 (s, 1H, CH-pyrazole), 2.29 (t, J = 7.4 Hz, 2H, CH$_2$CO), 1.52- 1.29 (m, 2H, CH$_2$), 1.32 (q, J = 7.2 Hz, 2H, CH$_2$), 0.88 (t, J =7.2 Hz, 3H, CH$_3$). **^{13}C-NMR** (101 MHz, DMSO-d_6) δ 171.6, 147.8, 142.4, 136.6, 128.6, 128.2, 125.1, 90.9, 36.1, 27.0, 21.8, 13.8. **UPLC-MS purity** > 99.5 % (λ = 215 nm).

N-[5-(4-bromophenyl)-1*H*-pyrazol-3-yl]pentanamide trifluoroacetate (5, Scheme 1)
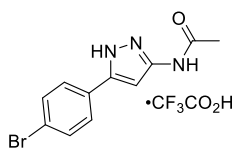
In line with the general procedure, treatment of **60** (0.10 g, 0.30 mmol) with TFA (0.92 mL, 12.0 mmol) in CH$_2$Cl$_2$ (3.0 mL) for 1 h afforded **5** as a white solid (0.05 g, 59 %); **R_f** 0.09 (PE/EtOAc 80:20). **^{1}H-NMR** (400 MHz, DMSO-d_6) δ 10.39 (br. s, 1H, NHCO), 7.70 (d, J = 8.4 Hz, 2H, Ar), 7.63 (d, J = 8.8 Hz, 2H, Ar), 6.67 (s, 1H, CH-pyrazole), 2.20 (s, 3H, COCH$_3$). **^{13}C-NMR** (101 MHz, DMSO-d_6) δ 169.9, 147.1, 142.1, 132.2, 130.4, 126.2, 123.2, 90.6, 24.2.

N-[5-(4-nitrophenyl)-1*H*-pyrazol-3-yl]pentanamide trifluoroacetate **(6, Scheme 1)**
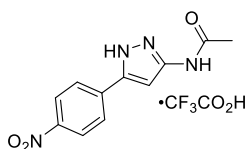

In line with the general procedure, treatment of **61** (0.01 g, 0.03 mmol) with TFA (0.09 mL, 1.2 mmol) in CH_2Cl_2 (1.0 mL) for 3 h afforded **6** as a yellow solid (0.005 g, 69 %); R_f 0.06 (PE/EtOAc 80:20). **^{1}H-NMR** (400 MHz, DMSO-d_6) δ 10.45 (br. s, 1H, NHCO), 8.30 (d, J = 8.8 Hz, 2H, Ar), 7.94 (d, J = 8.4 Hz, 2H, Ar), 7.04 (s, 1H, CH-pyrazole), 3.09 (s, 3H, COCH$_3$). **^{13}C-NMR** (101 MHz, DMSO-d_6) δ 169.6, 148.4, 146.7, 142.4, 136.2, 125.1, 124.2, 91.0, 24.1.

General procedure of *N*-acetylation: synthesis of 3-acetamidopyrazoles 3, 5-7 and 73-78 (Scheme 1 and 3)

To a stirred suspension of the corresponding 5-substituted-3-amino-pyrazole **48-52**, **68-72** (1.00 mmol) and K_2CO_3 (3.5 molar equiv) in CH_3CN (10.0 mL), a solution of acetyl chloride (1.5 molar equiv) in CH_3CN (1.0 M) was added dropwise at rt. The resulting reaction mixture was stirred under reflux for 1-6 h. The cooled suspension was concentrated under reduced pressure, then water (50.0 mL) was poured onto the residue. The resultant solid was filtered under *vacuum*, washed with fresh water and dried yielding the desired product.
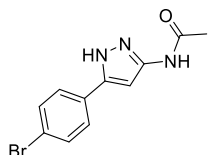
N-(5-phenyl-1*H*-pyrazol-3-yl)acetamide **(3, Scheme 1 and 3)**
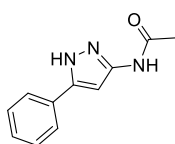
Following the general procedure, the title compound was synthetized starting from compound **49** (0.44 g, 2.76 mmol) and K_2CO_3 (1.33 g, 9.66 mmol) in CH_3CN (27.6 mL) treated with acetyl chloride (0.29 mL, 4.14 mmol) in CH_3CN (4.1 mL) for 4 h, to yield **3** as a white solid (0.51 g, 92 %); R_f 0.34 (CH_2Cl_2/CH_3OH/NH$_{3(aq)}$ 94:6:0.30). **^{1}H-NMR** (400 MHz, DMSO-d_6) δ 12.75 (br. s, 1H, NH), 10.41 (br. s, 1H, CONH), 7.70 (d, J = 7.6 Hz, 2H, Ph), 7.43 (dd, J = 7.6 and 7.2 Hz, 2H, Ph), 7.33 (dd, J = 7.6 and 7.2 Hz, 1H, Ph), 6.82

(br. s, 1H, CH-pyrazole), 2.02 (s, 3H, COCH$_3$). **^{13}C-NMR** (101 MHz, DMSO-d_6) δ 23.2, 93.4, 125.0 (2C), 128.0, 129.0 (2C), 129.9, 142.6, 147.5, 167.6.

### *N*-[5-(4-bromophenyl)-1*H*-pyrazol-3-yl]acetamide (5, Scheme 1 and 3)

Following the general procedure, the title compound was synthetized starting from the commercial compound **50** (1.00 g, 4.20 mmol) and K$_2$CO$_3$ (2.03 g, 14.70 mmol) in CH$_3$CN (42.0 mL) treated with acetyl chloride (0.46 mL, 6.30 mmol) in CH$_3$CN (6.3 mL) for 6 h, to yield **5** as a white solid (1.10 g, 93 %); R_f 0.30 (EtOAc). **^{1}H-NMR** (400 MHz, DMSO-d_6) δ 12.86 (br. s, 1H, NH), 10.42 (br. s, 1H, CONH), 7.71–7.57 (m, 4H, Ar), 6.90 (br. s, 1H, CH-pyrazole), 2.02 (s, 3H, COCH$_3$).

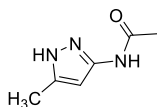### *N*-[5-(4-nitrophenyl)-1*H*-pyrazol-3-yl]acetamide (6, Scheme 1 and 3)
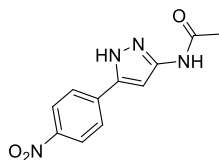
Following the general procedure, the title compound was synthetized starting from the commercial compound **51** (1.00 g, 4.90 mmol) and K$_2$CO$_3$ (2.37 g, 17.15 mmol) in CH$_3$CN (49.0 mL) treated with acetyl chloride (0.53 mL, 7.35 mmol) in CH$_3$CN (7.3 mL) for 6 h, to yield **6** as a yellow solid (0.54 g, 45 %); R_f 0.47 (EtOAc). **^{1}H-NMR** (400 MHz, DMSO-d_6) δ 13.18 (br. s, 1H, NH), 10.51 (br. s, 1H, CONH), 8.29 (d, J = 8.0 Hz, 2H, Ar), 7.99 (d, J = 8.4 Hz, 2H, Ar), 7.09 (br. s, 1H, CH-pyrazole), 2.03 (s, 3H, COCH$_3$).

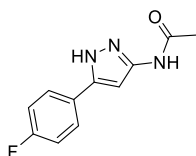### *N*-[5-(pyridin-2-yl)-1*H*-pyrazol-3-yl]acetamide (7, Scheme 1and 3)
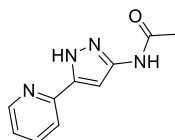
Following the general procedure, the title compound was synthetized starting from compound **52** (0.95 g, 5.93 mmol) and K$_2$CO$_3$ (2.86 g, 20.75 mmol) in CH$_3$CN (59.3 mL) treated with acetyl chloride (0.64 mL, 8.89 mmol) in CH$_3$CN (8.9 mL) for 5 h, to yield **7** as a beige solid (0.67 g, 56 %); R_f 0.40 (CH$_2$Cl$_2$/CH$_3$OH/NH$_{3(aq)}$ 92.5:7.5:0.375). **^{1}H-NMR** (400 MHz, DMSO-d_6) δ 12.98 (br. s, 1H, NH), 10.41 (br. s, 1H, CONH), 8.60 (d, J = 4.8 Hz, 1H, Ar), 7.90–7.82 (m, 1H, Ar), 7.79 (d, J = 7.6 Hz, 1H, Ar), 7.33 (t, J = 6.2 Hz, 1H, Ar), 7.06 (s, 1H, CH-pyrazole), 2.02 (s, 3H, COCH$_3$).

N-(5-methyl-1*H*-pyrazol-3-yl)acetamide (73, Scheme 3)

Following the general procedure, the title compound was synthetized starting from the commercial compound **48** (1.50 g, 15.44 mmol) and K_2CO_3 (7.46 g, 54.04 mmol) in CH_3CN (154.0 mL) treated with acetyl chloride (1.65 mL, 23.16 mmol) in CH_3CN (23.2 mL) for 6 h, to yield **73** as a white solid (1.20 g, 56 %); R_f 0.12 (CH_2Cl_2/CH_3OH 90:10). **¹H-NMR** (400 MHz, DMSO-d_6) δ 11.89 (br. s, 1H, NH), 10.20 (br. s, 1H, CONH), 6.22 (s, 1H, CH-pyrazole), 2.17 (s, 3H, CH_3), 1.96 (s, 3H, $COCH_3$).

N-[5-(4-fluorophenyl)-1*H*-pyrazol-3-yl]acetamide (74, Scheme 3)

Following the general procedure, the title compound was synthetized starting from the commercial compound **68** (1.00 g, 5.64 mmol) and K_2CO_3 (2.72 g, 19.74 mmol) in CH_3CN (56.4 mL) treated with acetyl chloride (0.61 mL, 8.46 mmol) in CH_3CN (8.5 mL) for 6 h, to yield **74** as a grey solid (1.11 g, 90 %); R_f 0.42 (EtOAc). **¹H-NMR** (400 MHz, DMSO-d_6) δ 12.76 (br. s, 1H, NH), 10.42 (br. s, 1H, CONH), 7.79–7.71 (m, 2H, Ar), 7.27 (t, J = 8.6 Hz, 2H, Ar), 6.81 (br. s, 1H, CH-pyrazole), 2.02 (s, 3H, $COCH_3$).

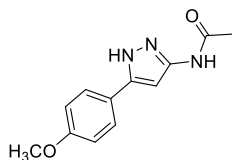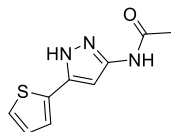### *N*-[5-(4-clorophenyl)-1*H*-pyrazol-3-yl]acetamide (75, Scheme 3)
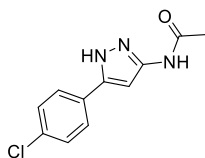
Following the general procedure, the title compound was synthetized starting from the commercial compound **69** (1.00 g, 5.16 mmol) and K_2CO_3 (2.49 g, 18.06 mmol) in CH_3CN (51.6 mL) treated with acetyl chloride (0.56 mL, 7.74 mmol) in CH_3CN (7.7 mL) for 6 h, to yield **75** as a white solid (1.20 g, 99 %); R_f 0.40 (EtOAc). **¹H-NMR** (400 MHz, DMSO-d_6) δ 12.90 (br. s, 1H, NH), 10.58 (br. s, 1H, CONH), 7.74 (d, J = 8.6 Hz, 2H, Ar), 7.48 (d, J = 8.6 Hz, 2H. Ar), 6.81 (br. s, 1H, CH-pyrazole), 2.02 (s, 3H, $COCH_3$).

N-[5-(4-methoxyphenyl)-1*H*-pyrazol-3-yl]acetamide (76, Scheme 3)

Following the general procedure, the title compound was synthetized starting from the commercial compound **70** (1.00 g, 5.28 mmol) and K_2CO_3 (2.55 g, 18.48 mmol) in CH_3CN (53.0 mL) treated with acetyl chloride (0.57 mL, 7.92 mmol) in CH_3CN (7.9 mL) for 6 h, to yield **76** as a white solid (0.84 g, 69 %); R_f 0.23 (EtOAc). **¹H-NMR** (400 MHz, DMSO-d_6) δ 12.61 (br. s, 1H, NH), 10.34 (br. s, 1H, CONH), 7.63 (d, J = 8.8 Hz, 2H, Ar), 6.99 (d, J = 8.8 Hz, 2H, Ar), 6.76 (br. s, 1H, CH-pyrazole), 3.78 (s, 3H, OCH$_3$), 2.01 (s, 3H, COCH$_3$).

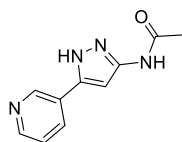### *N*-[5-(thiophen-2-yl)-1*H*-pyrazol-3-yl]acetamide (77, Scheme 3)

Following the general procedure, the title compound was synthetized starting from the commercial compound **72** (2.00 g, 12.10 mmol) and K_2CO_3 (5.84 g, 42.35 mmol) in CH_3CN (121.0 mL) treated with acetyl chloride (1.31 mL, 18.15 mmol) in CH_3CN (18.1 mL) for 6 h, to yield **77** as a beige solid (1.73 g, 69 %); R_f 0.46 (EtOAc). **¹H-NMR** (400 MHz, DMSO-d_6) δ 12.90 (br. s, 1H, NH), 10.35 (br. s, 1H, CONH), 7.50 (dd, J = 5.2 and 1.2 Hz, 1H, CH-thiophene), 7.39 (dd, J = 3.6 and 1.2 Hz, 1H, CH-thiophene), 7.10 (dd, J = 5.2 and 3.6 Hz, 1H, CH-thiophene), 6.59 (s, 1H, CH-pyrazole), 2.01 (s, 3H, COCH$_3$).

N-[5-(pyridin-3-yl)-1*H*-pyrazol-3-yl]acetamide (78, Scheme 3)

Following the general procedure, the title compound was synthetized starting from the commercial compound **71** (0.63 g, 3.93 mmol) and K_2CO_3 (1.90 g, 13.75 mmol) in CH_3CN (39.3 mL) treated with acetyl chloride (0.43 mL, 5.89 mmol) in CH_3CN (5.9 mL) for 1 h, to yield **78** as a white solid (0.49 mg, 62 %); R_f 0.44 (EtOAc). **¹H-NMR** (400 MHz, DMSO-d_6) δ 12.92 (br. s, 1H, NH), 10.47 (br. s, 1H, CONH), 8.94 (d, J = 2.3 Hz, 1H, Ar), 8.52 (dd, J = 4.8 and 1.6 Hz, 1H, Ar), 8.09 (dt, J = 8.0 and 2.0 Hz, 1H, Ar), 7.46 (dd, J = 8.0 and 4.8 Hz, 1H, Ar), 6.92 (br. s, 1H, CH-pyrazole), 2.03 (s, 3H, COCH$_3$).

General procedure for one-pot synthesis of oxalyl-based derivatives 8 and 9 (Scheme 2, Method I)

To a solution of the appropriate N^1-Boc-protected aminopyrazole **53** or **54** (1.00 mmol) and DIPEA (4.0 molar equiv) in dry CH_2Cl_2 (10.0 mL) at 0°C under N_2 atmosphere, a solution of oxalyl chloride (0.1 M in CH_2Cl_2, 1.0 molar equiv) was added dropwise, and the mixture was allowed to stir at rt for 2 h. After cooling at 0 °C, a solution of amine **137** (0.5 molar equiv) and DIPEA (2.0 molar equiv) in CH_2Cl_2 (5.0 mL) was then added dropwise, and the resulting mixture was warmed slowly to rt and stirred for 18 h. Upon reaction completion, the mixture was washed with 0.1 N NaOH aqueous solution (2 x 20.0 mL) and the organic phase was dried over Na_2SO_4, filtered and concentrated to dryness at reduced pressure. Purification of the crude product by typical silica gel flash chromatography followed by treatment with Et_2O allowed to obtain the pure compound.

N^1-{4-[4-(2,3-dichlorophenyl)piperazin-1-yl]butyl)-N^2-(5-methyl-1H-pyrazol-3-yl)oxalamide (8, Scheme 2)
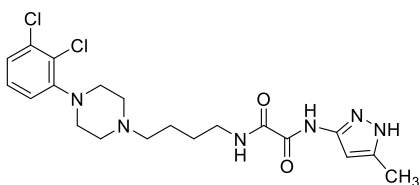
Following the general procedure, the title compound was synthetized starting from N^1-Boc-protected aminopyrazole **53** (0.20 g, 1.00 mmol), oxalyl chloride (0.08 mL, 1.00 mmol) and amine **137** (0.15 g, 0.50 mmol). Purification of the crude product by typical silica gel flash chromatography (CH_2Cl_2/CH_3OH 95:5) allowed to isolate **8** as a white solid (50 mg, 11 %); R_f 0.25 (CH_2Cl_2/CH_3OH 92.5:7.5). **UPLC-MS**: t_R = 1.73 min (method A), m/z: 453.5/455.5/457.5 $[M+H]^+$ calcd for $C_{20}H_{27}Cl_2N_6O_2$ 453.1/455.1/457.1. **^{1}H-NMR** (400 MHz, DMSO-d_6) δ 12.21 (br. s, 1H, NH), 10.18 (br. s, 1H, CONH), 8.98 (br. t, J = 6.0 Hz, 1H, $CH_2N\underline{H}CO$), 7.30–7.25 (m, 2H, Ar), 7.12 (dd, J = 6.8 and 3.2 Hz, 1H, Ar), 6.28 (br. s, 1H, CH-pyrazole), 3.21–3.16 (m, 2H, CH_2), 2.98 (br. s, 4H, $2CH_2$-piperazine), 2.53–2.50 (m, 4H, $2CH_2$-piperazine), 2.35 (t, J = 7.2 Hz, 2H, CH_2), 2.21 (s, 3H, CH_3), 1.53–1.45 (m, 4H, $2CH_2$). **^{13}C-NMR** (101 MHz, DMSO-d_6) δ 159.8, 157.8, 151.3, 147.3, 145.1, 140.6, 132.7,

128.6, 126.1, 124.4, 119.6, 95.8, 57.4, 52.9 (2C), 51.0 (2C), 26.7, 23.7, 10.9. **UPLC-MS purity** > 99.5 % (λ = 215 nm).

N^1-{4-[4-(2,3-dichlorophenyl)piperazin-1-yl]butyl}-N^2-(5-phenyl-1H-pyrazol-3-yl)oxalamide (9, Scheme 2)
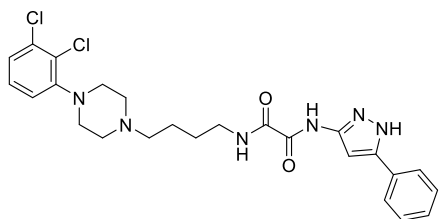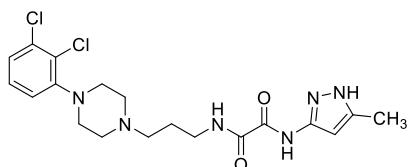

Following the general procedure, the title compound was synthetized starting from N^1-Boc-protected aminopyrazole **54** (0.26 g, 1.00 mmol), oxalyl chloride (0.08 mL, 1.00 mmol) and amine **137** (0.15 g, 0.50 mmol). Purification of the crude product by typical silica gel flash chromatography (CH$_2$Cl$_2$/CH$_3$OH 95:5) allowed to isolate **9** as a white solid (50 mg, 10 %); R_f 0.29 (CH$_2$Cl$_2$/CH$_3$OH 92.5:7.5). **UPLC-MS**: t$_R$ = 2.05 min (method A), *m/z*: 515.4/517.4/519.4 [M+H]$^+$ calcd for C$_{25}$H$_{29}$Cl$_2$N$_6$O$_2$ 515.2/517.2/519.2. **^{1}H-NMR** (400 MHz, DMSO-d_6) δ 13.05 (br. s, 1H, NH), 10.42 (br. s, 1H, CONH), 9.00 (br. s, 1H, CH$_2$N**H**CO), 7.73 (d, J = 7.2 Hz, 2H, Ar), 7.50–7.41 (m, 2H, Ar), 7.39–7.32 (m, 1H, Ar), 7.30–7.27 (m, 2H, Ar), 7.13 (dd, J = 6.0 and 3.2 Hz, 1H, Ar), 6.90 (br. s, 1H, CH-pyrazole), 3.22 (q, J = 6.4 Hz, 2H, CH$_2$), 2.98 (br. s, 4H, 2CH$_2$-piperazine), 2.53–2.50 (m, 4H, 2CH$_2$-piperazine), 2.36 (t, J = 6.8 Hz, 2H, CH$_2$), 1.60–1.47 (m, 4H, 2CH$_2$). **^{13}C-NMR** (101 MHz, DMSO-d_6) δ 160.7, 158.6, 149.4, 146.8, 142.4, 139.1, 129.9, 128.9 (2C), 128.2, 128.5, 126.4, 124.9 (2C), 124.3, 119.5, 90.4, 57.2, 52.4 (2C), 50.8 (2C), 38.8, 26.4, 23.5. **UPLC-MS purity** (UV 215 nm): > 99.5 %.

General procedure of *N*-THP deprotection: synthesis of final compounds 10, 12-26 and 28-30 (Scheme 2-4 and 6)

The appropriate *N*-THP protected intermediate **66**, **99-113**, **118-120** (1.00 mmol) was treated with TFA (40.0 molar equiv) in dry CH$_2$Cl$_2$ (10.0 mL) at 0°C. The ice-bath was removed, and the resulting mixture was stirred at rt for 2-18h. Upon reaction completion, the mixture was diluted with additional CH$_2$Cl$_2$ (10.0 mL) and washed twice (2 x 15.0 mL) with saturated NaHCO$_3$ aqueous solution (method **a**) or with 0.1 N NaOH aqueous solution (method **b**). The organic phase was dried over Na$_2$SO$_4$,

filtered and concentrated to dryness at reduced pressure. Purification of the crude product by trituration using appropriate solvent or solvents mixture or by typical silica gel flash chromatography followed by treatment with Et$_2$O allowed to obtain the desired product as free base.

N^1-{3-[4-(2,3-dichlorophenyl)piperazin-1-yl]propyl}-N^2-(5-methyl-1H-pyrazol-3-yl)oxalamide (10, Scheme 2)

Following the general procedure (method **a**), a mixture of **66** (0.08 g, 0.15 mmol) and TFA (0.46 mL, 6.00 mmol) in dry CH$_2$Cl$_2$ (2.0 mL) was allowed to react for 18 h. The crude product was dissolved in a minimal amount of MeOH and was precipitated by using Et$_2$O. Finally, filtration under *vacuum* and drying of the resultant beige solid gave **10** (0.05 g, 76 %); R_f 0.24 (CH$_2$Cl$_2$/CH$_3$OH 92.5:7.5). **UPLC-MS**: t_R = 1.77 min (method A), *m/z*: 439.4/441.3/443.4 [M+H]$^+$ calcd for C$_{19}$H$_{26}$Cl$_2$N$_6$O$_2$ 439.1/441.1/443.1. **^{1}H-NMR** (400 MHz, DMSO-d_6) δ 12.78 (br. s, 1H, NH), 10.38 (br. s, 1H, CONH), 7.70 (d, J = 7.6 Hz, 2H, Ph), 7.43 (t, J = 7.6 Hz, 2H, Ph), 7.34–7.29 (m, 3H, Ar), 7.16–7.11 (m, 1H, Ar), 6.89 (br. s, 1H, CH-pyrazole), 3.02 (br. s, 4H, 2CH$_2$-piperazine), 2.53–2.50 (m, 2H, CH$_2$), 2.68 (br. s, 4H, 2CH$_2$-piperazine), 2.35 (t, J = 7.0 Hz, 2H, CH$_2$), 1.66–1.49 (m, 4H, 2CH$_2$). **^{13}C-NMR** (101 MHz, DMSO-d_6) δ 160.7, 158.5, 149.6, 148.6, 141.0, 130.0, 127.5, 126.3, 125.9, 116.5, 93.3, 53.2, 52.5 (2C), 50.8 (2C), 39.7, 25.9, 10.5. **UPLC-MS purity** > 99.5 % (λ = 215 nm).

5-[4-(2,3-dichlorophenyl)piperazin-1-yl]-N-(5-methyl-1H-pyrazol-3-yl)pentanamide (12, Scheme 3)
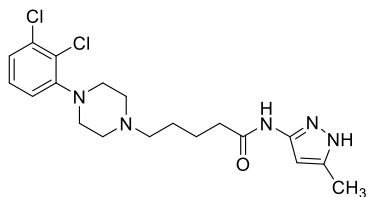
Following the general procedure (method **a**), a mixture of **99** (0.10 g, 0.202 mmol) and TFA (0.62 mL, 8.08 mmol) in dry CH$_2$Cl$_2$ (2.0 mL) was allowed to react for 18 h. The crude product was treated with Et$_2$O (4.0 mL) and the resulting precipitate was collected by filtration, washed with fresh Et$_2$O and

dried *under vacuum*, to yield **12** as a white solid (73 mg, 88 %); R_f 0.14 (CH$_2$Cl$_2$/CH$_3$OH 92:8). **UPLC-MS**: t$_R$ = 1.66 min (method A), *m/z*: 410.5/412.5/414.4 [M+H]$^+$ calcd for C$_{19}$H$_{26}$Cl$_2$N$_5$O 410.2/412.2/414.2. **^{1}H-NMR** (400 MHz, DMSO-d_6) δ 11.90 (br. s, 1H, NH), 10.12 (br. s, 1H, CONH), 7.32–7.27 (m, 2H, Ar), 7.15–7.10 (m, 1H, Ar), 6.25 (br. s, 1H, CH-pyrazole), 2.97 (t, *J* = 4.8 Hz, 4H, 2CH$_2$-piperazine), 2.53–2.50 (m, 4H, 2CH$_2$-piperazine), 2.34 (t, *J* = 7.1 Hz, 2H, CH$_2$), 2.27 (t, *J* = 7.3 Hz, 2H, CH$_2$), 2.17 (s, 3H, CH$_3$), 1.61–1.54 (m, 2H, CH$_2$), 1.48–1.41 (m, 2H, CH$_2$). **^{13}C-NMR** (151 MHz, DMSO-d_6) δ 170.2, 151.3, 145.6, 138.0, 132.6, 128.5, 126.0, 124.3, 119.6, 95.6, 57.5, 52.8 (2C), 51.0 (2C), 35.3, 25.8, 23.1, 10.7. **UPLC-MS purity** > 99.5 % (λ = 215 nm).
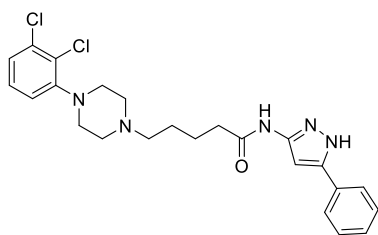
### 5-[4-(2,3-dichlorophenyl)piperazin-1-yl]-*N*-(5-phenyl-1*H*-pyrazol-3-yl)pentanamide (13, Scheme 3)

Following the general procedure (method **a**), a mixture of **100** (0.14 g, 0.25 mmol) and TFA (0.77 mL, 10.00 mmol) in dry CH$_2$Cl$_2$ (2.5 mL) was allowed to react for 2 h. The crude product was dissolved in a minimal amount of EtOAc and was precipitated by using *n*-hexane. Finally, filtration under *vacuum* and drying of the resultant white solid gave **9** (0.10 g, 85 %); R_f 0.41 (CH$_2$Cl$_2$/CH$_3$OH 92.5:7.5). **UPLC-MS**: t$_R$ = 1.98 min (method A), *m/z*: 472.5/474.5/476.5 [M+H]$^+$ calcd for C$_{24}$H$_{28}$Cl$_2$N$_5$O 472.2/474.2/476.2. **^{1}H-NMR** (400 MHz, DMSO-d_6) δ 12.78 (br. s, 1H, NH), 10.38 (br. s, 1H, CONH), 7.70 (d, *J* = 7.6 Hz, 2H, Ph), 7.43 (t, *J* = 7.6 Hz, 2H, Ph), 7.34–7.29 (m, 3H, Ar), 7.16–7.11 (m, 1H, Ar), 6.89 (br. s, 1H, CH-pyrazole), 3.02 (br. s, 4H, 2CH$_2$-piperazine), 2.53–2.50 (m, 2H, CH$_2$), 2.68 (br. s, 4H, 2CH$_2$-piperazine), 2.35 (t, *J* = 7.0 Hz, 2H, CH$_2$), 1.66–1.49 (m, 4H, 2CH$_2$). **^{13}C-NMR** (101 MHz, DMSO-d_6) δ 170.4, 150.9, 132.6, 129.0 (2C), 128.5 (2C), 128.0, 126.0, 124.9 (2C), 124.5, 119.6, 93.6, 57.1, 52.5 (2C), 50.4 (2C), 35.2, 25.3, 22.9. **UPLC-MS purity** > 99.5 % (λ = 215 nm).

5-[4-(2,3-dichlorophenyl)piperazin-1-yl]-*N*-[5-(4-fluorophenyl)-1*H*-pyrazol-3-yl]pentanamide (14, Scheme 3)
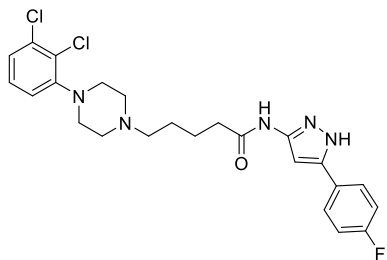
Following the general procedure (method **b**), a mixture of **101** (0.10 g, 0.174 mmol) and TFA (0.53 mL, 6.96 mmol) in dry CH_2Cl_2 (2.0 mL) was allowed to react for 4 h. The crude product was purified by trituration using a mixture of Et_2O/*n*-hexane (1:1, 4.0 mL) and the resulting precipitate was collected by filtration, washed with fresh Et_2O and dried *under vacuum*, to yield **14** as a white solid (50 mg, 60 %); R_f 0.33 (CH_2Cl_2/CH_3OH/$NH_{3(aq)}$ 90:10:0.5). **UPLC-MS**: t_R = 2.01 min (method A), *m/z*: 488.5/490.5/492.5 $[M+H]^+$ calcd for $C_{24}H_{27}Cl_2FN_5O$ 489.2/490.2/492.2. **^{1}H-NMR** (400 MHz, DMSO-d_6) δ 12.76 (br. s, 1H, NH), 10.35 (br. s, 1H, CONH), 7.75 (dd, J = 8.4 and 5.6 Hz, 2H, Ar), 7.34–7.23 (m, 4H, Ar), 7.13 (dd, J = 6.0 and 3.2 Hz, 1H, Ar), 6.88 (br. s, 1H, CH-pyrazole), 2.98 (br. s, 4H, 2CH$_2$-piperazine), 2.51 (br. s, 4H, 2CH$_2$-piperazine), 2.38–2.31 (m, 4H, 2CH$_2$), 1.61 (p, J = 7.6 Hz, 2H, CH$_2$), 1.49 (p, J = 7.2 Hz, 2H, CH$_2$). **^{13}C-NMR** (151 MHz, DMSO-d_6) δ 170.0, 161.8 (d, $J_{C\text{-}F}$ = 243.0 Hz), 150.8, 149.5, 137.0, 132.7, 128.6, 128.5 (d, $J_{Cm\text{-}F}$ = 8.2 Hz, 2C), 126.1, 126.0 (d, $J_{Cp\text{-}F}$ = 3.0 Hz), 125.3, 119.9, 115.9 (d, $J_{Co\text{-}F}$ = 22.5 Hz, 2C), 93.1, 60.5, 51.4 (2C), 48.1 (2C), 34.7, 26.7, 22.7. **UPLC-MS purity** > 99.5 % (λ = 215 nm).

N-[5-(4-chlorophenyl)-1*H*-pyrazol-3-yl]-5-[4-(2,3-dichlorophenyl)piperazin-1-yl]pentanamide (15, Scheme 3)
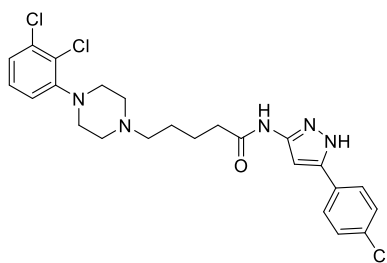
Following the general procedure (method **a**), a mixture of **102** (0.10 g, 0.169 mmol) and TFA (0.52 mL, 6.76 mmol) in dry CH_2Cl_2 (1.7 mL) was allowed to react for 18 h. The crude product was purified by trituration using Et_2O (3.0 mL) and the resulting precipitate was collected by filtration, washed with fresh Et_2O and dried *under vacuum*, to yield **15** as a white solid (60 mg, 70 %); R_f 0.36 (CH_2Cl_2/CH_3OH/$NH_{3(aq)}$

92.5:7.5:0.375). **UPLC-MS**: t_R = 2.21 min (method A), *m/z*: 506.2/508.2/510.1 [M+H]$^+$ calcd for $C_{24}H_{27}Cl_3N_5O$ 506.1/508.1/510.1. **^{1}H-NMR** (400 MHz, DMSO-d_6) δ 12.86 (br. s, 1H, NH), 10.40 (br. s, 1H, CONH), 7.73 (d, *J* = 8.4 Hz, 2H, Ar), 7.50 (d, *J* = 8.4 Hz, 2H, Ar), 7.35–7.26 (m, 2H, Ar), 7.14 (dd, *J* = 6.0 and 3.6 Hz, 1H, Ar), 6.93 (br. s, 1H, CH-pyrazole), 2.98 (br. s, 4H, 2CH$_2$-piperazine), 2.52 (br. s, 4H, 2CH$_2$-piperazine), 2.41–2.31 (m, 4H, 2CH$_2$), 1.61 (p, *J* = 7.6 Hz, 2H, CH$_2$), 1.54–1.44 (m, 2H, CH$_2$). **^{13}C-NMR** (101 MHz, DMSO-d_6) δ 170.4, 159.1, 151.2, 148.3, 141.7, 132.6 (2C), 128.5 (2C), 126.3, 126.0, 124.4, 122.1, 119.6, 114.4, 92.9, 56.9, 55.2 (2C), 50.4 (2C), 35.3, 25.7, 23.0. **UPLC-MS purity** > 99.5 % (λ = 215 nm).

5-[4-(2,3-dichlorophenyl)piperazin-1-yl]-*N*-[5-(4-methoxyphenyl)-1*H*-pyrazol-3-yl]pentanamide (16, Scheme 3)
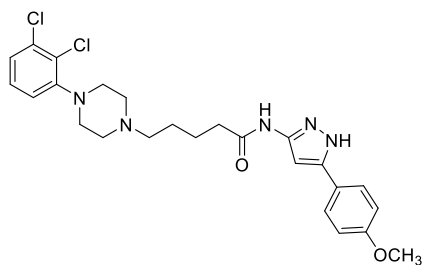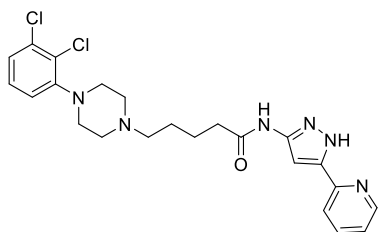

Following the general procedure (method **a**), a mixture of **103** (0.10 g, 0.17 mmol) and TFA (0.52 mL, 6.80 mmol) in dry CH$_2$Cl$_2$ (1.7 mL) was allowed to react for 18 h. The crude product was treated with *n*-hexane (5.0 mL) and the resulting solid was filtered off, washed with fresh *n*-hexane and dried *under vacuum*, to yield **16** as a white solid (70 mg, 82 %); *R$_f$* 0.33 (CH$_2$Cl$_2$/CH$_3$OH/NH$_{3(aq)}$ 92.5:7.5:0.375). **UPLC-MS**: t_R = 2.03 min (method A), *m/z*: 502.2/504.2/506.2 [M+H]$^+$ calcd for $C_{25}H_{30}Cl_2N_5O_2$ 502.2/504.2/506.1. **^{1}H-NMR** (400 MHz, DMSO-d_6) δ 12.62 (br. s, 1H, NH), 10.33 (br. s, 1H, CONH), 7.63 (d, *J* = 8.4 Hz, 2H, Ar), 7.32–7.26 (m, 2H, Ar), 7.13 (dd, *J* = 6.0 and 3.6 Hz, 1H, Ar), 7.00 (d, *J* = 8.4 Hz, 2H, Ar), 6.80 (s, 1H, CH-pyrazole), 3.78 (s, 3H, OCH$_3$), 2.98 (br. s, 4H, 2CH$_2$-piperazine), 2.51 (br. s, 4H, 2CH$_2$-piperazine), 2.39–2.28 (m, 4H, 2CH$_2$), 1.60 (p, *J* = 7.2 Hz, 2H, CH$_2$), 1.48 (p, *J* = 7.2 Hz, 2H, CH$_2$). **^{13}C-NMR** (151 MHz, DMSO-d_6) δ 170.4, 159.1, 151.2, 148.3, 141.7, 132.6, 128.5, 126.3 (2C), 126.0, 124.4, 122.1, 119.6, 114.4 (2C), 92.9, 57.3, 55.2, 52.7 (2C), 50.9 (2C), 35.3, 25.7, 23.0. **UPLC-MS purity** > 99.5 % (λ = 215 nm).

5-[4-(2,3-dichlorophenyl)piperazin-1-yl]-*N*-[5-(thiophen-2-yl)-1*H*-pyrazol-3-yl]pentanamide (17, Scheme 3)
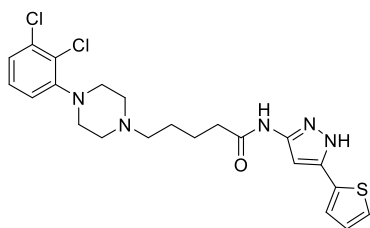
Following the general procedure (method **a**), a mixture of **104** (0.14 g, 0.249 mmol) and TFA (0.76 mL, 9.96 mmol) in dry CH_2Cl_2 (2.5 mL) was allowed to react for 18 h. The crude product was treated with Et_2O (5.0 mL) and the resulting precipitate was collected by filtration, washed with fresh Et_2O and dried under *vacuum*, to yield **17** as a white solid (90 mg, 76 %); R_f 0.25 (CH_2Cl_2/CH_3OH 94:6). **UPLC-MS**: t_R = 2.00 min (method A), *m/z*: 478.2/480.1/482.2 [M+H]$^+$ calcd for $C_{22}H_{26}Cl_2N_5OS$ 478.1/480.1/482.1. **^{1}H-NMR** (400 MHz, DMSO-d_6) *δ* 12.63 (br. s, 1H, NH), 10.54 (br. s, 1H, CONH), 7.52 (dd, *J* = 4.8 and 0.8 Hz, 1H, CH-thiophene), 7.40 (dd, *J* = 3.6 and 1.2 Hz, 1H, CH-thiophene), 7.32–7.27 (m, 2H, Ar), 7.13 (dd, *J* = 6.4 and 3.6 Hz, 1H, Ar), 7.11 (dd, *J* = 4.8 and 3.6 Hz, 1H, CH-thiophene), 6.62 (s, 1H, CH-pyrazole), 2.98 (br. s, 4H, 2CH$_2$-piperazine), 2.52 (br. s, 4H, 2CH$_2$-piperazine), 2.37–2.31 (m, 4H, 2CH$_2$), 1.61 (p, *J* = 7.4 Hz, 2H, CH$_2$), 1.48 (p, *J* = 7.2 Hz, 2H, CH$_2$). **^{13}C-NMR** (101 MHz, DMSO-d_6) *δ* 170.6, 151.2, 149.4, 146.0, 136.4, 132.6, 128.4, 127.9, 126.0, 125.4, 124.3, 124.0, 119.5, 92.9, 57.4, 52.8 (2C), 51.0 (2C), 35.3, 25.8, 23.0. **UPLC-MS purity** > 99.5 % (λ = 215 nm).

5-[4-(2,3-dichlorophenyl)piperazin-1-yl]-*N*-[5-(pyridin-2-yl)-1*H*-pyrazol-3-yl]pentanamide (18, Scheme 3)

Following the general procedure (method **a**), a mixture of **105** (0.04 g, 0.07 mmol) and TFA (0.22 mL, 2.69 mmol) in dry CH_2Cl_2 (1.0 mL) was allowed to react for 18 h. The crude product was purified by trituration using Et_2O (3.0 mL) and the resulting precipitate was collected by filtration, washed with fresh Et_2O and dried *under vacuum*, to yield **8** as a white solid (35 mg, 41 %); R_f 0.18 (CH_2Cl_2/CH_3OH 95:5). **^{1}H-NMR** (400 MHz, DMSO-d_6) *δ* 12.97 (br. s, 1H, NH), 10.40 (br. s, 1H, CONH), 8.65 (br. s, 1H, Ar), 7.88 (t, *J* = 7.6 Hz, 1H, Ar), 7.60 (d, *J* = 7.8 Hz, 1H, Ar), 7.32–7.27 (m, 3H, Ar), 7.14–7.10 (m, 2H, CH, Ar and

CH-pyrazole), 2.98 (br. s, 4H, 2CH$_2$-piperazine), 2.54 (br. s, 4H, 2CH$_2$-piperazine), 2.37–2.32 (m, 4H, 2CH$_2$), 1.65–1.58 (m, 2H, CH$_2$), 1.52–1.45 (m, 2H, CH$_2$). **^{13}C-NMR** (151 MHz, DMSO-d_6) δ 170.9, 151.5, 149.00, 148.7, 146.1, 138.4, 132.5, 132.4, 128.6, 126.1, 125.4, 124.4, 124.3, 119.6, 94.8, 57.5, 52.9 (2C), 51.0 (2C), 35.4, 25.9, 23.2.

5-[4-(2,3-dichlorophenyl)piperazin-1-yl]-*N*-[5-(pyridin-3-yl)-1*H*-pyrazol-3-yl]pentanamide (19, Scheme 4)
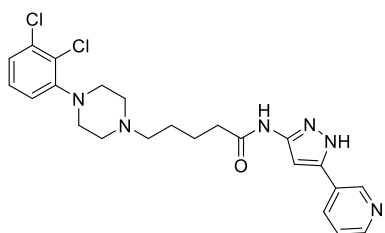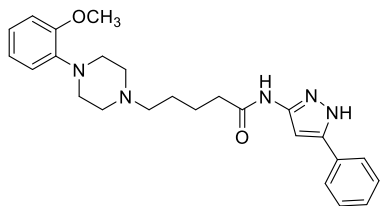

Following the general procedure (method **a**), a mixture of **113** (0.08 g, 0.143 mmol) and TFA (0.44 mL, 5.72 mmol) in dry CH$_2$Cl$_2$ (1.5 mL) was allowed to react for 2 h. The crude product was purified by trituration using Et$_2$O (2.0 mL) and the resulting precipitate was collected by filtration, washed with fresh Et$_2$O and dried under *vacuum*, to yield **19** as a white solid (43 mg, 64 %); R_f 0.20 (CH$_2$Cl$_2$/CH$_3$OH 95:5). **UPLC-MS**: t$_R$ = 1.72 min (method A), *m/z*: 473.0/475.0/477.0 [M+H]$^+$ calcd for C$_{23}$H$_{27}$Cl$_2$N$_6$O 473.2/475.2/477.2. **^{1}H-NMR** (400 MHz, DMSO-d_6) δ 12.95 (br. s, 1H, NH), 10.41 (br. s, 1H, CONH), 8.94 (br. s, 1H, Ar), 8.52 (d, *J* = 2.2 Hz, 1H, Ar), 8.09 (d, *J* = 7.8 Hz, 1H, Ar), 7.46 (br. s, 1H, Ar), 7.32–7.27 (m, 2H, Ar), 7.14–7.10 (m, 1H, CH, Ar), 7.01 (s, 1H, CH-pyrazole), 2.98 (br. s, 4H, 2CH$_2$-piperazine), 2.54 (br. s, 4H, 2CH$_2$-piperazine), 2.37–2.32 (m, 4H, 2CH$_2$), 1.65–1.58 (m, 2H, CH$_2$), 1.52–1.45 (m, 2H, CH$_2$). **^{13}C-NMR** (151 MHz, DMSO-d_6) δ 170.8, 151.3, 149.00, 148.6, 146.1, 138.9, 132.7, 132.4, 128.5, 126.1, 125.5, 124.4, 124.1, 119.6, 94.6, 57.5, 52.9 (2C), 51.0 (2C), 35.4, 25.9, 23.2. **UPLC-MS purity** 99.0 % (λ = 215 nm).

5-[4-(2-methoxyphenyl)piperazin-1-yl]-*N*-(5-methyl-1*H*-pyrazol-3-yl)pentanamide (20, Scheme 3)
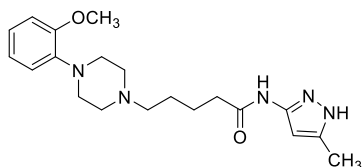
Following the general procedure (method **a**), a mixture of **106** (0.14 g, 0.31 mmol) and TFA (0.95 mL, 12.40 mmol) in dry CH_2Cl_2 (3.0 mL) was allowed to react for 18 h. The crude product was treated with Et_2O (5.0 mL) and the resulting precipitate was collected by filtration, washed with fresh Et_2O and dried *under vacuum*, to yield **20** as a beige solid (0.10 g, 87 %); R_f 0.17 (CH_2Cl_2/CH_3OH 90:10). **UPLC-MS**: t_R = 1.35 min (method A), *m/z*: 372.3 (M+H)$^+$ calcd for $C_{20}H_{30}N_5O_2$ 371.2. **¹H-NMR** (400 MHz, DMSO-d_6) δ 11.90 (br. s, 1H, NH), 10.12 (br. s, 1H, CONH), 6.98–6.84 (m, 4H, Ar), 6.26 (br. s, 1H, CH-pyrazole), 3.76 (s, 3H, OCH$_3$), 2.94 (br. s, 4H, 2CH$_2$-piperazine), 2.47 (br. s, 4H, 2CH$_2$-piperazine), 2.31 (t, *J* = 7.2 Hz, 2H, CH$_2$), 2.27 (t, *J* = 7.2 Hz, 2H, CH$_2$), 2.17 (s, 3H, CH$_3$), 1.57 (p, *J* = 7.4 Hz, 2H, CH$_2$), 1.48–1.41 (m, 2H, CH$_2$). **¹³C-NMR** (101 MHz, DMSO-d_6) δ 170.2, 152.0, 147.6, 141.3, 138.0, 122.3, 120.8, 117.9, 111.9, 95.6, 57.6, 55.3, 53.0 (2C), 50.1 (2C), 35.4, 25.9, 23.1, 10.7. **UPLC-MS purity** > 99.5 % (λ = 215 nm).

5-[4-(2-methoxyphenyl)piperazin-1-yl]-*N*-(5-phenyl-1*H*-pyrazol-3-yl)pentanamide (21, Scheme 3)

Following the general procedure (method **a**), a mixture of **107** (0.12 g, 0.23 mmol) and TFA (0.70 mL, 9.20 mmol) in dry CH_2Cl_2 (2.3 mL) was allowed to react for 18 h. Purification by typical silica gel flash chromatography ($CH_2Cl_2/CH_3OH/NH_{3(aq)}$ 95:5:0.25), followed by a trituration using Et_2O (3.0 mL) allowed to isolate **21** as a white solid (60 mg, 60 %); R_f 0.45 ($CH_2Cl_2/CH_3OH/NH_{3(aq)}$ 90:10:0.5). **UPLC-MS**: t_R = 1.66 min (method A), *m/z*: 434.4 [M+H]$^+$ calcd for $C_{25}H_{32}N_5O_2$ 434.3. **¹H-NMR** (400 MHz, DMSO-d_6) δ 12.78 (br. s, 1H, NH), 10.35 (br. s, 1H, CONH), 7.70 (d, *J* = 7.6 Hz, 2H, Ph), 7.44 (t, *J* = 7.4 Hz, 2H, Ph), 7.34 (t, *J* = 7.4 Hz, 1H, Ph), 6.91–6.86 (m, 5H, Ar and CH-pyrazole), 3.76 (s,

3H, OCH$_3$), 2.95 (br. s, 4H, 2CH$_2$-piperazine), 2.50 (br. s, 4H, 2CH$_2$-piperazine), 2.39–2.22 (m, 4H, 2CH$_2$), 1.61 (p, J = 7.4 Hz, 2H, CH$_2$), 1.47 (p, J = 7.4 Hz, 2H, CH$_2$). **^{13}C-NMR** (151 MHz, DMSO-d_6) δ 170.5, 152.0, 148.4, 141.7, 141.3, 129.4, 129.0 (2C), 128.1, 124.9 (2C), 122.3, 120.8, 117.9, 111.9, 93.7, 57.6, 55.3, 53.1 (2C), 50.1 (2C), 35.4, 25.9, 23.1. **UPLC-MS purity** > 99.5 % (λ = 215 nm).

### *N*-[5-(4-fluorophenyl)-1*H*-pyrazol-3-yl]-5-[4-(2-methoxyphenyl)piperazin-1-yl]pentanamide (22, Scheme 3)
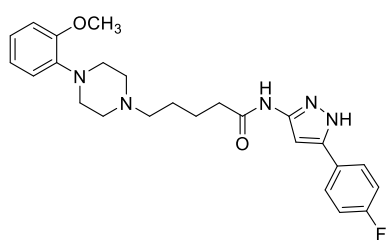
Following the general procedure (method **b**), a mixture of **108** (0.10 g, 0.205 mmol) and TFA (0.63 mL, 8.20 mmol) in dry CH$_2$Cl$_2$ (2.0 mL) was allowed to react for 4 h. The crude product was purified by trituration using a mixture of Et$_2$O/*n*-hexane (1:1, 4.0 mL) and the resulting precipitate was collected by filtration, washed with fresh Et$_2$O and dried under *vacuum*, to yield **22** as a white solid (70 mg, 76 %); R_f 0.38 (CH$_2$Cl$_2$/CH$_3$OH/NH$_{3(aq)}$ 90:10:0.5). **UPLC-MS**: t$_R$ = 1.72 min (method A), *m/z*: 452.4 [M+H]$^+$ calcd for C$_{25}$H$_{31}$FN$_5$O$_2$ 452.2. **^{1}H-NMR** (400 MHz, DMSO-d_6) δ 12.76 (br. s, 1H, NH), 10.35 (br. s, 1H, CONH), 7.75 (dd, J = 7.2 and 6.0 Hz, 2H, Ar), 7.28 (dd, J = 9.2 and 8.4 Hz, 2H, Ar), 6.93–6.85 (m, 5H, Ar and CH-pyrazole), 3.76 (s, 3H, OCH$_3$), 2.95 (br. s, 4H, 2CH$_2$-piperazine), 2.50 (br. s, 4H, 2CH$_2$-piperazine), 2.37–2.29 (m, 4H, 2CH$_2$), 1.65–1.43 (m, 4H, 2CH$_2$). **^{13}C-NMR** (151 MHz, DMSO-d_6) δ 170.5, 161.8 (d, $J_{C\text{-}F}$ = 243.0 Hz), 152.0, 148.4, 141.3, 140.8, 127.1 (d, $J_{Cm\text{-}F}$ = 9.0 Hz, 2C), 126.1 (d, $J_{Cp\text{-}F}$ = 3.0 Hz), 122.3, 120.8, 117.9, 115.9 (d, $J_{Co\text{-}F}$ = 22.5 Hz, 2C), 111.9, 93.8, 57.6, 55.3, 53.0 (2C), 50.1 (2C), 35.4, 25.9, 23.1. **UPLC-MS purity** > 99.5 % (λ = 215 nm).

N-[5-(4-bromophenyl)-1H-pyrazol-3-yl]-5-[4-(2-methoxyphenyl)piperazin-1-yl]pentanamide (23, Scheme 3)
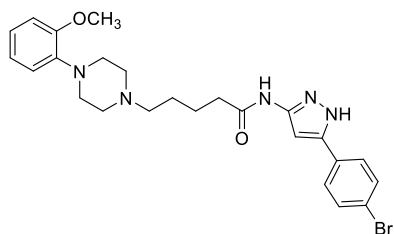
Following the general procedure (method **b**), a mixture of **109** (0.056 g, 0.09 mmol) and TFA (0.28 mL, 3.60 mmol) in dry CH_2Cl_2 (1.0 mL) was allowed to react for 2 h. The crude product was purified by trituration using Et_2O (3.0 mL) and the resulting precipitate was collected by filtration, washed with fresh Et_2O and dried *under vacuum*, to yield **23** as a white solid (40 mg, 87 %); R_f 0.45 ($CH_2Cl_2/CH_3OH/NH_{3(aq)}$ 90:10:0.5). **^{1}H-NMR** (400 MHz, DMSO-d_6) δ 12.85 (s, 1H, NH), 10.38 (s, 1H, CONH), 7.65 (d, J = 9.4 Hz, 5H, Ar and CH-pyrazole), 6.95 – 6.88 (m, 2H, Ar), 6.86 (d, J = 3.1 Hz, 2H, Ar), 3.76 (s, 3H, OCH$_3$), 2.94 (s, 4H, piperazine), 2.50 (br. s, 4H, piperazine), 2.37 – 2.29 (m, 4H), 1.60 (d, J = 7.8 Hz, 2H), 1.48 (d, J = 7.0 Hz, 2H).**^{13}C-NMR** (101 MHz, DMSO-d_6) δ 171.6, 146.5, 142.1, 140.8, 132.3, 130.5, 127.4 (2C), 124.3, 122.7, 121.3, 118.4 (2C), 113.0, 110.0, 90.5, 58.0, 55.8, 53.5 (2C), 50.5 (2C), 35.8, 26.3, 23.5.

N-[5-(4-methoxyphenyl)-1H-pyrazol-3-yl]-5-[4-(2-methoxyphenyl)piperazin-1-yl]pentanamide (24, Scheme 3)
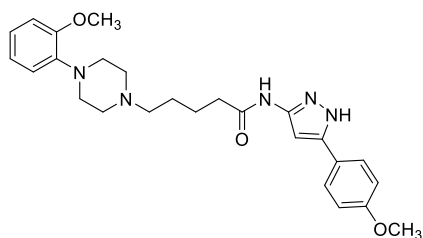
Following the general procedure (method **b**), a mixture of **110** (0.11 g, 0.201 mmol) and TFA (0.61 mL, 8.04 mmol) in dry CH_2Cl_2 (2.0 mL) was allowed to react for 3 h. Purification by typical silica gel flash chromatography ($CH_2Cl_2/CH_3OH/NH_{3(aq)}$ 95:5:0.25), followed by a trituration using Et_2O (2.0 mL) allowed to isolate **24** as a white solid (40 mg, 43 %); R_f 0.42 ($CH_2Cl_2/CH_3OH/NH_{3(aq)}$ 90:10:0.5). **UPLC-MS**: t_R = 1.66 min (method A), m/z: 464.4 [M+H]$^+$ calcd for $C_{26}H_{34}N_5O_3$ 464.3. **^{1}H-NMR** (400 MHz, DMSO-d_6) δ 12.60 (br. s, 1H, NH), 10.30 (br. s, 1H, CONH), 7.63 (d, J = 8.4 Hz, 2H, Ar), 7.00 (d, J = 8.4 Hz, 2H, Ar), 6.94–6.84 (m, 4H, Ar), 6.79 (s, 1H, CH-pyrazole), 3.78 (s, 3H, OCH$_3$), 3.76 (s, 3H, OCH$_3$), 2.95 (br. s, 4H, 2CH$_2$-piperazine), 2.50 (br. s, 4H, 2CH$_2$-

piperazine), 2.37–2.28 (m, 4H, 2CH$_2$), 1.64–1.43 (m, 4H, 2CH$_2$).**^{13}C-NMR** (151 MHz, DMSO-d_6) δ 170.5, 159.1, 152.0, 148.3, 141.7, 141.3, 126.4 (2C), 122.3, 122.2, 120.9, 117.9, 114.4 (2C), 111.9, 93.0, 57.6, 55.3, 55.2, 53.1 (2C), 50.1 (2C), 35.4, 25.9, 23.2. **UPLC-MS purity** > 99.5 % (λ = 215 nm).

5-[4-(2-methoxyphenyl)piperazin-1-yl]-*N*-[5-(4-nitrophenyl)-1*H*-pyrazol-3-yl]pentanamide (25, Scheme 6)
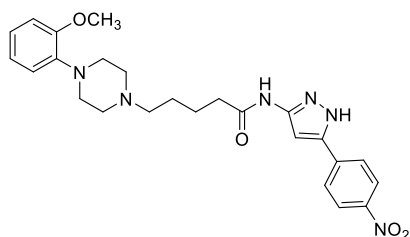
Following the general procedure (method **b**), a mixture of **111** (0.036 g, 0.06 mmol) and TFA (0.18 mL, 2.40 mmol) in dry CH$_2$Cl$_2$ (1.0 mL) was allowed to react for 2 h. The crude product was purified by trituration using Et$_2$O (3.0 mL) and the resulting precipitate was collected by filtration, washed with fresh Et$_2$O and dried under *vacuum*, to yield **25** as a white solid (20 mg, 70 %); *R_f* 0.48 (CH$_2$Cl$_2$/CH$_3$OH/NH$_{3(aq)}$ 90:10:0.5. **^{1}H-NMR** (400 MHz, DMSO-d_6) δ 12.61 (br. s, 1H, NH), 10.33 (br. s, 1H, CONH), 8.25 (d, *J* = 8.4 Hz, 2H, Ar), 7.78 (d, *J* = 8.4 Hz, 2H, Ar), 6.94–6.84 (m, 4H, Ar), 6.82 (s, 1H, CH-pyrazole), 3.78 (s, 3H, OCH$_3$), 3.76 (s, 3H, OCH$_3$), 2.96 (br. s, 4H, 2CH$_2$-piperazine), 2.51 (br. s, 4H, 2CH$_2$-piperazine), 2.37–2.28 (m, 4H, 2CH$_2$), 1.64–1.43 (m, 4H, 2CH$_2$).. **^{13}C-NMR** (101 MHz, DMSO-d_6) δ 171.7, 150.1, 148.1, 146.9, 142.4, 140.8, 137.1, 125.2, 124.0, 122.1, 121.7, 116.2, 113.1, 90.5, 56.2, 55.5, 52.5 (2C), 50.1 (2C), 36.7, 26.4.

5-[4-(2-methoxyphenyl)piperazin-1-yl]-*N*-[5-(thiophen-2-yl)-1*H*-pyrazol-3-yl]pentanamide (26, Scheme 3)
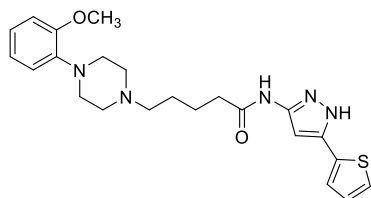
Following the general procedure (method **b**), a mixture of **112** (0.13 g, 0.248 mmol) and TFA (0.76 mL, 9.92 mmol) in dry CH$_2$Cl$_2$ (2.5 mL) was allowed to react for 18 h. Purification by typical silica gel flash chromatography (CH$_2$Cl$_2$/CH$_3$OH/NH$_{3(aq)}$ 95:5:0.25), followed by a trituration using Et$_2$O (2.0 mL) allowed to isolate **26** as a white solid (40 mg, 37 %); *R_f* 0.38

(CH_2Cl_2/CH_3OH/$NH_{3(aq)}$ 90:10:0.5). **UPLC-MS**: t_R = 1.58 min (method A), *m/z*: 440.3 [M+H]$^+$ calcd for $C_{23}H_{30}N_5O_2S$ 440.2. **^{1}H-NMR** (400 MHz, DMSO-d_6) δ 12.80 (br. s, 1H, NH), 10.38 (br. s, 1H, CONH), 7.56 (br. s, 1H, CH-thiophene), 7.42 (br. s, 1H, CH-thiophene), 7.12 (br. s, 1H, CH-thiophene), 6.97–6.81 (m, 4H, Ar), 6.73 (s, 1H, CH-pyrazole), 3.76 (s, 3H, OCH$_3$), 2.95 (br. s, 4H, 2CH$_2$-piperazine), 2.50 (br. s, 4H, 2CH$_2$-piperazine), 2.38–2.24 (m, 4H, 2CH$_2$), 1.64–1.43 (m, 4H, 2CH$_2$).**^{13}C-NMR** (151 MHz, DMSO-d_6) δ 170.5, 152.0, 148.2, 141.2, 136.2, 131.6, 128.1, 125.8, 124.2, 122.4, 120.8, 117.9, 111.9, 93.9, 57.5, 55.3, 52.9 (2C), 50.0 (2C), 35.3, 25.7, 23.0. **UPLC-MS purity** > 99.5 % (λ = 215 nm).

1-{4-[4-(2,3-dichlorophenyl)piperazin-1-yl]butyl}-3-(5-methyl-1*H*-pyrazol-3-yl)urea (28, Scheme 6)
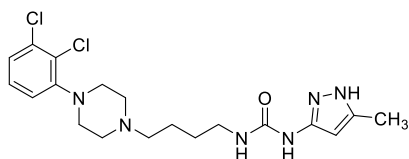
Following the general procedure (method **a**), a mixture of **118** (0.06 g, 0.12 mmol) and TFA (0.37 mL, 4.80 mmol) in dry CH_2Cl_2 (1.2 mL) was allowed to react for 18 h. Purification by typical silica gel flash chromatography (CH_2Cl_2/CH_3OH/$NH_{3(aq)}$ 95:5:0.25), followed by a trituration using Et$_2$O (3.0 mL) allowed to isolate **28** as a white solid (32 mg, 76 %); *R_f* 0.39 (CH_2Cl_2/CH_3OH/$NH_{3(aq)}$ 90:10:0.5). **^{1}H-NMR** (400 MHz, DMSO-d_6) δ 11.75 (br. s, 1H, NH), 8.57 (s, 1H, CONH-pyrazole), 7.35–7.26 (m, 2H, Ar), 7.14 (dd, *J* = 5.8 and 3.8 Hz, 1H, Ar), 7.10 (br. s, 1H, CH$_2$NHCO), 5.75 (s, 1H, CH-pyrazole), 3.13 (q, *J* = 6.4 Hz, 2H, CH$_2$NHCO), 3.01 (br. s, 4H, 2CH$_2$-piperazine), 2.69–2.61 (m, 4H, 2CH$_2$-piperazine), 2.53–2.47 (m, 2H, CH$_2$N), 2.14 (s, 3H, CH$_3$), 1.52–1.43 (m, 4H, 2CH$_2$). **^{13}C-NMR** (101 MHz, DMSO-d_6) δ 154.9, 151.0, 149.0, 138.7, 132.7, 128.5, 126.0, 124.5, 119.6, 93.2, 57.2, 52.6 (2C), 50.5 (2C), 38.9, 27.7, 23.3, 10.7.

1-{4-[4-(2-methoxyphenyl)piperazin-1-yl]butyl}-3-(5-methyl-1*H*-pyrazol-3-yl)urea (29, Scheme 6)
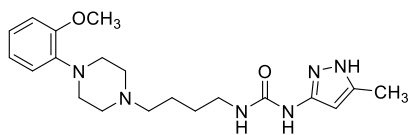
Following the general procedure (method **a**), a mixture of **119** (0.06 g, 0.13 mmol) and TFA (0.40

mL, 5.20 mmol) in dry CH_2Cl_2 (1.3 mL) was allowed to react for 18 h. Purification by typical silica gel flash chromatography ($CH_2Cl_2/CH_3OH/NH_{3(aq)}$ 95:5:0.25), followed by a trituration using Et_2O (3.0 mL) allowed to isolate **29** as a white solid (18 mg, 36 %); R_f 0.37 ($CH_2Cl_2/CH_3OH/NH_{3(aq)}$ 90:10:0.5). **¹H-NMR** (400 MHz, DMSO-d_6) δ 11.75 (br. s, 1H, NH), 8.55 (s, 1H, CONH-pyrazole), 7.11 (br. s, 1H, $CH_2N\underline{H}CO$), 6.95–6.80 (m, 4H, Ar), 5.75 (s, 1H, CH-pyrazole), 3.76 (s, 3H, OCH_3), 3.12 (d, $J = 5.6$ Hz, 2H, $C\underline{H}_2NHCO$), 2.94 (br. s, 4H, $2CH_2$-piperazine), 2.49 (br. s, 4H, $2CH_2$-piperazine), 2.30–2.27 (m, 2H, CH_2N), 2.14 (s, 3H, CH_3), 1.48–1.43 (m, 4H, $2CH_2$).**¹³C-NMR** (101 MHz, DMSO-d_6) δ 154.8, 152.0, 149.0, 141.3, 138.6, 122.3 (CH), 120.9 (CH), 117.9 (CH), 112.0 (CH), 93.2 (CH), 57.6 (CH_2), 55.3 (OCH_3), 53.0 ($2CH_2$), 50.1 ($2CH_2$), 38.9 (CH_2), 27.8 (CH_2),, 23.7 (CH_2), 10.6 (CH_3).

1-{4-[4-(2,3-dichlorophenyl)piperazin-1-yl]butyl}-3-(5-phenyl-1*H*-pyrazol-3-yl)urea (30, Scheme 6)
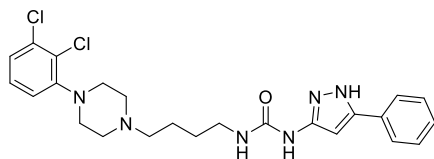
Following the general procedure (method **a**), a mixture of **120** (0.024 g, 0.042 mmol) and TFA (0.13 mL, 1.68 mmol) in dry CH_2Cl_2 (1.0 mL) was allowed to react for 18 h. The crude product was purified by trituration using Et_2O (2.0 mL) and the resulting precipitate was collected by filtration, washed with fresh Et_2O and dried under *vacuum*, to yield **25** as a white solid (15 mg, 73 %); R_f 0.13 ($CH_2Cl_2/CH_3OH/NH_{3(aq)}$ 92.5:7.5:0.375). **¹H-NMR** (400 MHz, DMSO-d_6) δ 12.59 (br. s, 1H, NH), 8.76 (s, 1H, CONH-pyrazole), 7.67 (d, $J = 7.8$ Hz, 2H, Ar), 7.44 (t, $J = 7.6$ Hz, 2H, Ar), 7.38 – 7.29 (m, 2H, Ar and $CH_2N\underline{H}CO$), 7.18 – 7.12 (m, 2H, Ar), 6.89 – 6.83 (m, 1H, Ar), 6.47 (s, 1H, CH-pyrazole), 3.16 (d, $J = 5.6$ Hz, 2H, $C\underline{H}_2NHCO$), 2.98 (br. s, 4H, $2CH_2$-piperazine), 2.49 (br. s, 4H, $2CH_2$-piperazine), 2.40–2.34 (m, 2H, CH_2N), 1.52–1.48 (m, 4H, $2CH_2$). **¹³C-NMR** (101 MHz, DMSO-d_6) δ 156.6, 150.1, 149.3, 142.3, 138.7, 130.2, 128.4 (2C), 128.3, 127.6, 126.4, 126.0, 125.3 (2C), 116.5, 90.2, 55.8, 52.4 (2C), 50.8 (2C), 39.0, 27.0, 25.0.

General procedure of HATU-mediated coupling reaction for amide bond formation: synthesis of final compound 11 (Scheme 2), 31, 34, 35, 38, (Scheme 8 and 9) and intermediates 66, 99-112 (Scheme 2 and 3)

To a mixture of the appropriate amine (1.00 mmol) and carboxylic acid (1.2 molar equiv) in dry DMF (10.0 mL), HATU (1.2 molar equiv) and DIPEA (3.2 or 2.2 molar equiv) were added. The reaction mixture (yellow solution) was allowed to react for 2-7 h at rt and, upon completion, was poured into water (100.0 mL) and was worked up applying one of the following methods:

a) the obtained precipitate was filtered off, washed with water and dried under *vacuum*;

b) the aqueous phase was extracted with EtOAc (3 x 25.0 mL), the combined organic layers were washed with brine, dried over Na_2SO_4 and the solvent was removed under reduced pressure.

In both cases, purification of the crude product by typical silica gel flash chromatography afforded the title compound.

N^1-{2-[4-(2,3-dichlorophenyl)piperazin-1-yl]ethyl}-N^2-(5-methyl-1H-pyrazol-3-yl)oxalamide (11, Scheme 2)
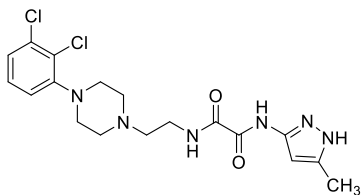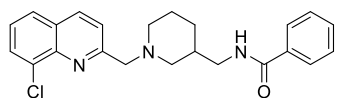

According to the general procedure (method **a**), a mixture of **135** (0.08 g, 0.30 mmol), **63** (0.06 g, 0.35 mmol), HATU (0.13 g, 0.35 mmol) and DIPEA (0.11 mL, 0.66 mmol) in dry DMF (3.0 mL) was stirred for 3 h. Purification by typical silica gel flash chromatography ($CH_2Cl_2/CH_3OH/NH_{3(aq)}$ 97.5:2.5:0.125) followed by a trituration using Et_2O (2.0 mL) allowed to isolate **11** as a white solid (0.03 g, 23 %); R_f 0.20 ($CH_2Cl_2/CH_3OH/NH_{3(aq)}$ 95:5:0.25). **UPLC-MS**: t_R = 1.95 min (method A), *m/z*: 425.4/427.3/429.3 [M+H]$^+$ calcd for $C_{18}H_{23}Cl_2N_6O_2$ 425.1/427.1/429.1. **^{1}H-NMR** (400 MHz, DMSO-d_6) δ 12.23 (br. s, 1H, NH), 10.21 (br. s, 1H, CONH), 8.80 (br. t, J = 6.0 Hz, 1H, CH$_2$NHCO), 7.31–7.28 (m, 2H, Ar), 7.15 (dd, J = 6.0 and 3.6 Hz, 1H, Ar), 6.30 (br. s, 1H, CH-pyrazole), 3.36–3.29 (m, 2H,

CH_2), 2.98 (br. s, 4H, $2CH_2$-piperazine), 2.59 (br. s, 4H, $2CH_2$-piperazine), 2.54–2.51 (m, 2H, CH_2), 2.22 (s, 3H, CH_3). **^{13}C-NMR** (101 MHz, DMSO-d_6) δ 160.4, 158.5, 149.7, 148.6, 141.0, 129.7, 127.8, 126.3, 125.8, 116.5, 93.4, 55.6, 52.4 (2C), 50.9 (2C), 37.3, 10.5. **UPLC-MS purity** > 99.5 % (λ = 215 nm).

N-((1-((8-chloroquinolin-2-yl)methyl)piperidin-3-yl)methyl)benzamide (31, Scheme 8)

According to the general procedure (method **b**), a mixture of **146** (0.07 g, 0.24 mmol) and benzoic acid (0.03 g, 0.29 mmol), in dry DMF (3.0 mL) was stirred for 4 h. Purification by typical silica gel flash chromatography (CH_2Cl_2/CH_3OH 98.5:1.5) allowed to isolate **31** as a yellow oil (0.06 g, 65 %). **^{1}H-NMR** (400 MHz, CDCl$_3$) δ 8.08 (d, J = 8.8 Hz, 1H, Ar), 7.80 (dd, J =1.2, 7.6 Hz, 1H, Ar), 7.67–7.71 (m, 4H, Ar), 7.40–7.48 (m, 2H, Ar), 7.33–7.37 (m, 2H, Ar), 6.36 (br. s, 1H, NH), 3.98–3.87 (m, 2H, CH_2N-piperidine), 3.44 (t, J = 6.4 Hz, 2H, C$\underline{H}_2$NHCO), 2.86 (d, J = 8.8 Hz, 1H, piperidine), 2.70–2.80 (m, 1H, piperidine), 2.36 (t, J = 10.6 Hz, 1H, piperidine), 2.17–2.22 (m, 1H, piperidine), 1.96–2.07 (m, 1H, piperidine), 1.72–1.84 (m, 3H, piperidine), 1.57–1.70 (m, 1H, piperidine). **^{13}C-NMR** (101 MHz, CDCl$_3$) δ 167.6, 159.0, 143.6, 135.9, 134.3, 131.7, 131.5, 129.3, 128.2, 128.0, 127.8, 126.9, 126.3, 121.9, 61.5, 57.1, 53.8, 44.1, 35.6, 27.1, 23.0.

N-(2-(1-((8-chloroquinolin-2-yl)methyl)piperidin-4-yl)ethyl)benzamide (34, Scheme 9)
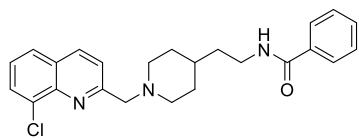
According to the general procedure (method **b**), a mixture of **150** (0.12 g, 0.32 mmol) and benzoic acid (0.46 g, 0.38 mmol), in dry DMF (3.0 mL) was stirred for 3 h. Purification by typical silica gel flash chromatography (CH_2Cl_2/CH_3OH 95:5) allowed to isolate **34** as a white solid (0.07 g, 55 %). **^{1}H-NMR** (400 MHz, DMSO-d_6) δ 8.37–8.44 (m, 2H, Ar and NH), 7.62–7.90 (m, 2H, Ar), 7.79–7.85 (m, 2H, Ar), 7.74 (d, J = 8.8 Hz, 1H, Ar), 7.42–7.56 (m, 4H, Ar), 3.78 (s, 2H, CH_2N-piperidine), 3.31–

3.36 (m, 2H, C$\underline{H}_2$NHCO), 2.83 (d, J =11.1 Hz, 2H, piperidine), 2.07 (t, J =11.3 Hz, 2H, piperidine), 1.70 (d, J =12.3 Hz, 2H, piperidine), 1.48 (q, J = 7.2 Hz, 2H, piperidine), 1.16-1.40 (m, 3H, piperidine). **^{13}C-NMR** (101 MHz, DMSO-d_6) δ 167.5, 159.0, 144.1, 135.8, 134.4, 131.7, 131.2, 129.3, 128.2, 127.8, 127.1, 126.9, 126.2, 122.0, 61.1, 52.9, 40.5, 34.9, 34.3, 30.2.

N-(2-(1-((8-chloroquinolin-2-yl)methyl)piperidin-4-yl)ethyl)-4-fluorobenzamide (35, Scheme 9)
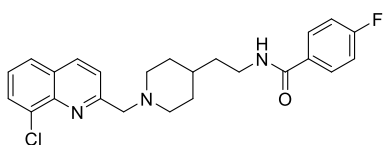
According to the general procedure (method **b**), a mixture of **150** (0.22g, 0.58 mmol) and 4-fluoro-benzoic acid (0.98 g, 0.70 mmol), in dry DMF (6.0 mL) was stirred for 4 h. Purification by typical silica gel flash chromatography (CH$_2$Cl$_2$/CH$_3$OH 95:5) allowed to isolate **35** as an orange oil (0.12 g, 50 %). **^{1}H-NMR** (400 MHz, DMSO-d_6) δ 8.43 (t, J = 6.0 Hz, 1H, NH), 8.41 (d, J =8.4 Hz, 1H, Ar), 7.88–7.96 (m, 4H, Ar), 7.74 (d, J = 8.8 Hz, 1H, Ar), 7.54 (t, J =7.6 Hz, 1H, Ar), 7.25–7.30 (m, 2H, Ar), 3.78 (s, 2H, CH$_2$N-piperidine), 3.31–3.36 (m, 2H,C$\underline{H}_2$NHCO), 2.83 (d, J =11.1 Hz, 2H, piperidine), 2.07 (t, J =11.3 Hz, 2H, piperidine), 1.70 (d, J =12.3 Hz, 2H, piperidine), 1.47 (q, J = 7.2 Hz, 2H, piperidine), 1.21–1.34 (m, 3H, piperidine). **^{13}C-NMR** (101 MHz, DMSO-d_6) δ 167.1, 165.4, 159.0, 144.4, 135.8, 131.8, 130.9, 129.8, 129.8, 129.3, 127.8, 126.9, 126.3, 121.9, 115.5, 115.3, 61.1, 52.7 (2C), 40.5, 35.2, 34.3, 30.3 (2C).

N-((1-((8-chloroquinolin-2-yl)methyl)piperidin-4-yl)methyl)benzamide (38, Scheme 8)
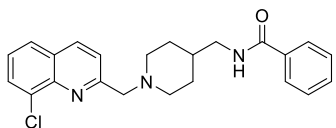
According to the general procedure (method **b**), a mixture of **147** (0.15 g, 0.51 mmol) and benzoic acid (0.74 g, 0.61 mmol), in dry DMF (5.0 mL) was stirred for 3 h. Purification by typical silica gel flash chromatography (CH$_2$Cl$_2$/CH$_3$OH 95:5) allowed to isolate **38** as an yellow oil (0.04 g, 20 %). **^{1}H-NMR** (400 MHz, CDCl$_3$) δ 8.13 (d, J = 8.4 Hz, 1H, Ar), 7.72–7.82 (m, 5H, Ar), 7.38–7.54 (m, 4H, Ar), 6.16 (br s, 1H, NH), 3.93 (s, 2H, CH$_2$N-piperidina), 3.41 (t, J = 6.4 Hz, 2H, C$\underline{H}_2$NHCO), 2.97 (d,

J = 11.6 Hz, 2H, piperidine), 2.14–2.27 (m, 2H, piperidine), 1.77 (d, J =12.6 Hz, 2H, piperidine), 1.55–1.62 (m, 2H, piperidine), 1.39–1.50 (m, 1H, piperidine). **^{13}C-NMR** (101 MHz, CDCl$_3$) δ 167.6, 159.0, 143.6, 136.0, 134.3, 131.7, 131.5, 129.3, 128.2, 128.2, 128.0, 127.8, 127.0, 126.2, 121.9, 61.1, 52.5, 44.7, 36.1, 28.6.

N^1-{3-[4-(2,3-dichlorophenyl)piperazin-1-yl]propyl}-N^2-[5-methyl-1-(tetrahydro-2H-pyran-2-yl)-1H-pyrazol-3-yl]oxalamide (66, Scheme 2)
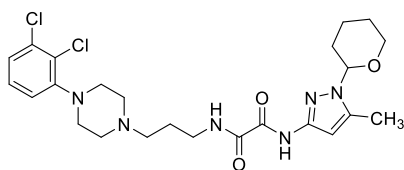
According to the general procedure (method **a**), a mixture of **136** (0.10 g, 0.28 mmol), **65** (0.08 g, 0.33 mmol), HATU (0.12 g, 0.33 mmol) and DIPEA (0.15 mL, 0.90 mmol) in dry DMF (3.0 mL) was stirred for 3 h to afford **66** as a beige solid (0.08 g, 55 %) without further purification; R_f 0.37 (CH$_2$Cl$_2$/CH$_3$OH/ 92.5:7.5). **^{1}H-NMR** (400 MHz, CDCl$_3$) δ 9.60 (br. s, 1H, CONH), 8.86 (br. s, 1H, CONH), 7.18–7.15 (m, 2H, Ar), 7.05 (t, J = 4.6 Hz, 1H, Ar), 6.55 (s, 1H, CH-pyrazole), 5.21 (dd, J = 10.0 and 2.0 Hz, 1H, CH, THP), 4.07 (d, J = 11.2 Hz, 1H, CH$_2$, THP), 3.65 (t, J = 11.4 Hz, 1H, CH$_2$, THP), 3.49 (q, J = 6.0 Hz, 2H, CH$_2$), 3.17 (br. s, 4H, 2CH$_2$-piperazine), 2.68 (br. s, 4H, 2CH$_2$-piperazine), 2.60 (t, J = 6.2 Hz, 2H, CH$_2$), 2.38–2.30 (m, 4H, CH$_3$ and CH$_2$-THP), 2.13–2.10 (m, 1H, CH$_2$, THP), 1.90–1.87 (m, 1H, CH$_2$, THP), 1.79 (t, J = 5.8 Hz, 2H, CH$_2$), 1.72–1.57 (m, 3H, CH$_2$, THP).

5-[4-(2,3-dichlorophenyl)piperazin-1-yl]-N-[5-methyl-1-(tetrahydro-2H-pyran-2-yl)-1H-pyrazol-3-yl]pentanamide (99, Scheme 3)
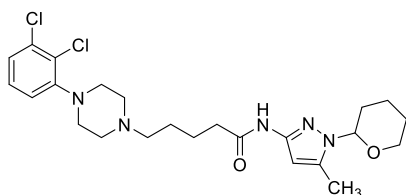
Following the general procedure (method **a**), a mixture of **89** (0.05 g, 0.25 mmol), **129** (0.11 g, 0.30 mmol), HATU (0.11 g, 0.30 mmol) and DIPEA (0.14 mL, 0.80 mmol) in dry DMF (2.50 mL) was allowed to react for 5 h, to afford **99** as a white solid (0.10 g, 80 %) without further purification; R_f 0.32 (CH$_2$Cl$_2$/CH$_3$OH 92.5:7.5). **^{1}H-NMR** (400 MHz, CDCl$_3$) δ 7.91 (br. s, 1H, CONH), 7.19–7.12 (m, 2H, Ar), 6.98 (dd, J = 7.4 and 2.2 Hz, 1H, Ar), 6.51

(s, 1H, CH-pyrazole), 5.15 (dd, J = 10.4 and 2.4 Hz, 1H, CH, THP), 4.08–4.04 (m, 1H, CH$_2$, THP), 3.63 (td, J = 11.2 and 2.4 Hz, 1H, CH$_2$, THP), 3.18 (br. t, J = 4.9 Hz, 4H, 2CH$_2$-piperazine), 2.80 (br. s, 4H, 2CH$_2$-piperazine), 2.59 (t, J = 7.2 Hz, 2H, CH$_2$), 2.37 (t, J = 6.8 Hz, 2H, CH$_2$), 2.30 (s, 3H, CH$_3$), 2.31–2.27 (m, 1H, CH$_2$, THP), 2.08–2.05 (m, 1H, CH$_2$, THP), 1.88–1.56 (m, 8H, 2CH$_2$ and 2CH$_2$-THP).

5-[4-(2-methoxyphenyl)piperazin-1-yl]-*N*-[5-methyl-1-(tetrahydro-2*H*-pyran-2-yl)-1*H*-pyrazol-3-yl]pentanamide (106, Scheme 3)
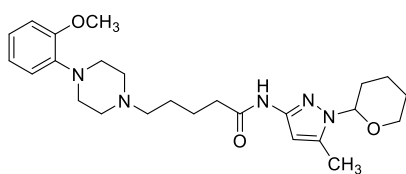
In line with the general procedure (method **b**), a mixture of **89** (0.07 g, 0.39 mmol), **130** (0.15 g, 0.47 mmol), HATU (0.18 g, 0.47 mmol) and DIPEA (0.22 mL, 1.25 mmol) in dry DMF (3.90 mL) was stirred for 5 h. Purification by typical silica gel flash chromatography (CH$_2$Cl$_2$/CH$_3$OH/NH$_{3(aq)}$ 97.5:2.5:0.125) allowed to isolate **106** as a beige solid (0.14 g, 79 %); R_f 0.32 (CH$_2$Cl$_2$/CH$_3$OH/NH$_{3(aq)}$ 95:5:0.25). **¹H-NMR** (400 MHz, CDCl$_3$) δ 7.85 (br. s, 1H, CONH), 7.03–6.82 (m, 4H, Ar), 6.52 (s, 1H, CH-pyrazole), 5.15 (dd, J = 10.2 and 1.8 Hz, 1H, CH, THP), 4.09–4.01 (m, 1H, CH$_2$, THP), 3.86 (s, 3H, OCH$_3$), 3.62 (td, J = 11.2 and 2.2 Hz, 1H, CH$_2$, THP), 3.11 (br. s, 4H, 2CH$_2$-piperazine), 2.65 (br. s, 4H, 2CH$_2$-piperazine), 2.43 (t, J = 7.2 Hz, 2H, CH$_2$), 2.35 (t, J = 7.2 Hz, 2H, CH$_2$), 2.30 (s, 3H, CH$_3$), 2.31–2.29 (m, 1H, CH$_2$, THP), 2.09–2.00 (m, 1H, CH$_2$, THP), 1.88–1.52 (m, 8H, 2CH$_2$ and 2CH$_2$-THP).

5-[4-(2,3-dichlorophenyl)piperazin-1-yl]-*N*-[5-phenyl-1-(tetrahydro-2*H*-pyran-2-yl)-1*H*-pyrazol-3-yl]pentanamide (100, Scheme 3)
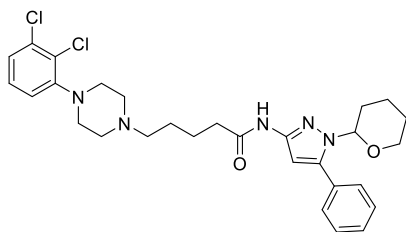
According to the general procedure (method **a**), a mixture of **90** (0.07 g, 0.29 mmol), **129** (0.13 g, 0.35 mmol), HATU (0.13 g, 0.35 mmol) and DIPEA (0.16 mL, 0.93 mmol) in dry DMF (2.90 mL) was stirred for 4 h and 30 minutes, to obtain **100** as a white solid (0.14 g, 87 %) without further purification; R_f 0.31

(CH$_2$Cl$_2$/CH$_3$OH/NH$_{3(aq)}$ 96.5:3.5:0.175). **^{1}H-NMR** (400 MHz, CDCl$_3$) δ 7.96 (br. s, 1H, CONH), 7.55–7.46 (m, 2H, Ph), 7.50–7.39 (m, 3H, Ph), 7.18–7.09 (m, 2H, Ar), 6.97 (dd, J = 6.8 and 3.2 Hz, 1H, Ar), 6.83 (s, 1H, CH-pyrazole), 5.14 (dd, J = 10.8 and 2.4 Hz, 1H, CH, THP), 4.16–4.08 (m, 1H, CH$_2$, THP), 3.57 (td, J = 11.6 and 2.0 Hz, 1H, CH$_2$, THP), 3.09 (br. s, 4H, 2CH$_2$-piperazine), 2.65 (br. s, 4H, 2CH$_2$-piperazine), 2.46 (t, J = 7.4 Hz, 2H, CH$_2$), 2.40 (t, J = 7.2 Hz, 2H, CH$_2$), 2.40–2.37 (m, 1H, CH$_2$, THP), 2.01–1.95 (m, 1H, CH$_2$, THP), 1.80–1.52 (m, 8H, 2CH$_2$ and 2CH$_2$-THP).

5-[4-(2-methoxyphenyl)piperazin-1-yl]-*N*-[5-phenyl-1-(tetrahydro-2*H*-pyran-2-yl)-1*H*-pyrazol-3-yl]pentanamide (107, Scheme 3)
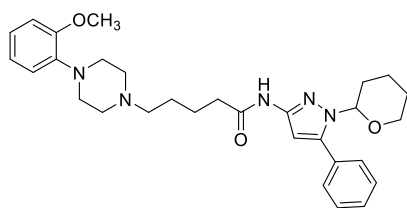
In line with the general procedure (method **a**), a mixture of **90** (0.08 g, 0.33 mmol), **130** (0.13 g, 0.39 mmol), HATU (0.15 g, 0.39 mmol) and DIPEA (0.18 mL, 1.06 mmol) in dry DMF (3.30 mL) was stirred for 4 h and 30 minutes, to obtain **107** as a white solid (0.12 g, 70 %) without further purification; *R_f* 0.18 (CH$_2$Cl$_2$/CH$_3$OH/NH$_{3(aq)}$ 95:5:0.25). **^{1}H-NMR** (400 MHz, CDCl$_3$) δ 7.96 (br. s, 1H, NHCO), 7.53–7.50 (m, 2H, Ph), 7.48–7.41 (m, 3H, Ph), 7.01–6.84 (m, 4H, Ar), 6.83 (s, 1H, CH-pyrazole), 5.14 (dd, J = 10.6 and 2.2 Hz, 1H, CH, THP), 4.16–4.08 (m, 1H, CH$_2$, THP), 3.86 (s, 3H, OCH$_3$), 3.57 (td, J = 11.6 and 2.2 Hz, 1H, CH$_2$, THP), 3.13 (br. s, 4H, 2CH$_2$-piperazine), 2.69 (br. s, 4H, 2CH$_2$-piperazine), 2.48 (t, J = 7.2 Hz, 2H, CH$_2$), 2.40 (t, J = 7.2 Hz, 2H, CH$_2$), 2.45–2.36 (m, 1H, CH$_2$, THP), 2.03–1.95 (m, 1H, CH$_2$, THP), 1.82–1.49 (m, 8H, 2CH$_2$ and 2CH$_2$-THP).

5-[4-(2,3-dichlorophenyl)piperazin-1-yl]-*N*-[5-(4-fluorophenyl)-1-(tetrahydro-2*H*-pyran-2-yl)-1*H*-pyrazol-3-yl]pentanamide (101, Scheme 3)
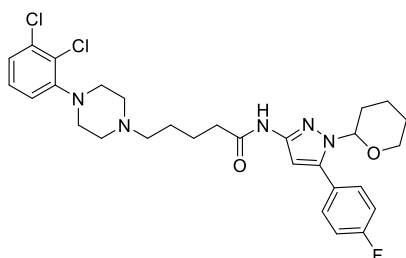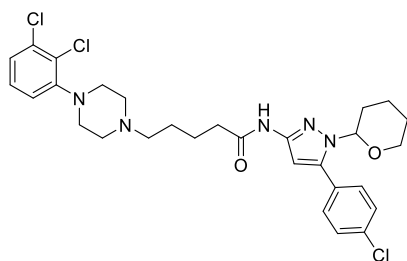
Following the general procedure (method **b**), a mixture of **91** (0.07 g, 0.27 mmol), **129** (0.12 g, 0.32 mmol), HATU (0.12 g, 0.32 mmol) and DIPEA (0.15 mL, 0.85 mmol) in dry DMF (2.70 mL) was allowed to react for 2 h. Purification by typical silica gel flash chromatography (CH$_2$Cl$_2$/CH$_3$OH/NH$_{3(aq)}$

95:5:0.25) allowed to isolate **101** as a white solid (0.10 g, 64 %); *R_f* 0.21 (CH$_2$Cl$_2$/CH$_3$OH/NH$_{3(aq)}$ 95:5:0.25). **^{1}H-NMR** (400 MHz, CDCl$_3$) δ 7.97 (br. s, 1H, NHCO), 7.54–7.46 (m, 2H, Ar), 7.19–7.09 (m, 4H, Ar), 6.97 (dd, *J* = 6.4 and 3.2 Hz, 1H, Ar), 6.81 (s, 1H, CH-pyrazole), 5.07 (dd, *J* = 10.4 and 2.4 Hz, 1H, CH, THP), 4.11 (d, *J* = 11.6 Hz, 1H, CH$_2$, THP), 3.55 (td, *J* = 10.4 and 2.4 Hz, 1H, CH$_2$, THP), 3.09 (br. s, 4H, 2CH$_2$-piperazine), 2.64 (br. s, 4H, 2CH$_2$-piperazine), 2.46 (t, *J* = 7.2 Hz, 2H, CH$_2$), 2.40 (t, *J* = 7.2 Hz, 2H, CH$_2$), 2.42–2.33 (m, 1H, CH$_2$, THP), 2.05–1.95 (m, 1H, CH$_2$, THP), 1.82–1.49 (m, 8H, 2CH$_2$ and 2CH$_2$-THP).

N-[5-(4-fluorophenyl)-1-(tetrahydro-2H-pyran-2-yl)-1H-pyrazol-3-yl]-5-[4-(2-methoxyphenyl)piperazin-1-yl]pentanamide (108, Scheme 3)
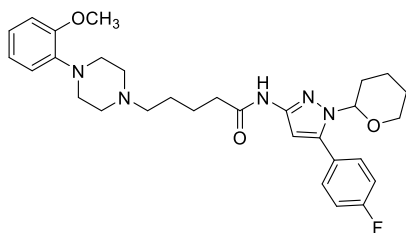
Following the general procedure (method **b**), a mixture of **91** (0.07 g, 0.27 mmol), **130** (0.10 g, 0.32 mmol), HATU (0.12 g, 0.32 mmol) and DIPEA (0.15 mL, 0.85 mmol) in dry DMF (2.70 mL) was allowed to react for 2 h. Purification by typical silica

gel flash chromatography (CH$_2$Cl$_2$/CH$_3$OH/NH$_{3(aq)}$ 95:5:0.25) allowed to isolate **108** as a white solid (0.10 g, 76 %); *R_f* 0.17 (CH$_2$Cl$_2$/CH$_3$OH/NH$_{3(aq)}$ 95:5:0.25). **^{1}H-NMR** (400 MHz, CDCl$_3$) δ 7.98 (br. s, 1H, NHCO), 7.54–7.46 (m, 2H, Ar), 7.15 (t, *J* = 8.4 Hz, 2H, Ar), 7.03–6.83 (m, 4H, Ar), 6.81 (s, 1H, CH-pyrazole), 5.06 (dd, *J* = 10.4 and 2.4 Hz, 1H, CH, THP), 4.16–4.07 (m, 1H, CH$_2$, THP), 3.86 (s, 3H, OCH$_3$), 3.55 (td, *J* = 11.6 and 2.2 Hz, 1H, CH$_2$, THP), 3.12 (br. s, 4H, 2CH$_2$-piperazine), 2.66 (br. s, 4H, 2CH$_2$-piperazine), 2.45 (t, *J* = 7.4 Hz, 2H, CH$_2$), 2.40 (t, *J* = 7.2 Hz, 2H, CH$_2$), 2.41–

2.35 (m, 1H, CH$_2$, THP), 2.03–1.96 (m, 1H, CH$_2$, THP), 1.82–1.49 (m, 8H, 2CH$_2$ and 2CH$_2$-THP).

N-[5-(4-chlorophenyl)-1-(tetrahydro-2*H*-pyran-2-yl)-1*H*-pyrazol-3-yl]-5-[4-(2,3-dichlorophenyl)piperazin-1-yl]pentanamide (102, Scheme 3)

According to the general procedure (method **b**), a mixture of **92** (0.15 g, 0.54 mmol), **129** (0.24 g, 0.65 mmol), HATU (0.25 g, 0.65 mmol) and DIPEA (0.30 mL, 1.73 mmol) in dry DMF (5.40 mL) was stirred for 3 h. Purification by typical silica gel flash chromatography (CH$_2$Cl$_2$/CH$_3$OH/NH$_{3(aq)}$ 97.5:2.5:0.125) allowed to isolate **102** as a white solid (0.26 g, 81 %); *R$_f$* 0.20 (CH$_2$Cl$_2$/CH$_3$OH/NH$_{3(aq)}$ 97.5:2.5:0.125). **^{1}H-NMR** (400 MHz, CDCl$_3$) δ 8.00 (br. s, 1H, NHCO), 7.50–7.39 (m, 4H, Ar), 7.19–7.09 (m, 2H, Ar), 6.97 (dd, *J* = 6.4 and 3.2 Hz, 1H, Ar), 6.83 (s, 1H, CH-pyrazole), 5.07 (dd, *J* = 10.6 and 2.2 Hz, 1H, CH, THP), 4.14–4.08 (m, 1H, CH$_2$, THP), 3.56 (td, *J* = 11.6 and 2.0 Hz, 1H, CH$_2$, THP), 3.09 (br. s, 4H, 2CH$_2$-piperazine), 2.64 (br. s, 4H, 2CH$_2$-piperazine), 2.46 (t, *J* = 7.2 Hz, 2H, CH$_2$), 2.40 (t, *J* = 7.4 Hz, 2H, CH$_2$), 2.41–2.32 (m, 1H, CH$_2$, THP), 2.00 (d, *J* = 12.4 Hz, 1H, CH$_2$, THP), 1.82–1.49 (m, 8H, 2CH$_2$ and 2CH$_2$-THP).

N-[5-(4-bromophenyl)-1-(tetrahydro-2*H*-pyran-2-yl)-1*H*-pyrazol-3-yl]-5-[4-(2-methoxyphenyl)piperazin-1-yl]pentanamide (109, Scheme 3)
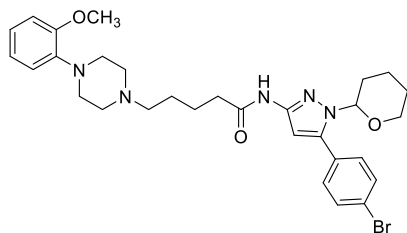
In line with the general procedure (method **a**), a mixture of **93** (0.04 g, 0.12 mmol), **130** (0.05 g, 0.15 mmol), HATU (0.06 g, 0.15 mmol) and DIPEA (0.07 mL, 0.38 mmol) in dry DMF (2.00 mL) was stirred for 4 h, to obtain **109** as a white solid (56 mg, 78 %) without further purification; *R$_f$* 0.31 (CH$_2$Cl$_2$/CH$_3$OH/NH$_{3(aq)}$ 95:5:0.25). **^{1}H-NMR** (400 MHz, CDCl$_3$) δ 8.00 (br. s, 1H, NHCO), 7.59 (d, *J* = 8.8 Hz, 2H, Ar), 7.40 (d, *J* = 8.8 Hz, 2H, Ar), 6.99–6.84 (m, 4H, Ar), 6.83 (s, 1H, CH-pyrazole), 5.07 (dd, *J*

= 10.8 and 2.4 Hz, 1H, CH, THP), 4.11 (d, J = 10.8 Hz, 1H, CH_2, THP), 3.86 (s, 3H, OCH_3), 3.61–3.51 (m, 1H, CH_2, THP), 3.12 (br. s, 4H, $2CH_2$-piperazine), 2.66 (br. s, 4H, $2CH_2$-piperazine), 2.45 (t, J = 7.2 Hz, 2H, CH_2), 2.40 (t, J = 7.2 Hz, 2H, CH_2), 2.42–2.35 (m, 1H, CH_2, THP), 2.00 (d, J = 12.4 Hz, 1H, CH_2, THP), 1.84–1.53 (m, 8H, $2CH_2$ and $2CH_2$-THP).

5-[4-(2,3-dichlorophenyl)piperazin-1-yl]-*N*-[5-(4-methoxyphenyl)-1-(tetrahydro-2*H*-pyran-2-yl)-1*H*-pyrazol-3-yl]pentanamide (103, Scheme 3)
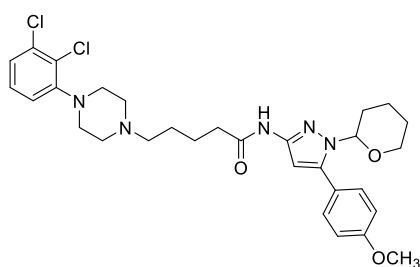
According to the general procedure (method **a**), a mixture of **94** (0.07 g, 0.26 mmol), **129** (0.11 g, 0.31 mmol), HATU (0.12 g, 0.31 mmol) and DIPEA (0.14 mL, 0.80 mmol) in dry DMF (2.60 mL) was stirred for 2 h and 40 minutes. Purification by typical silica gel flash chromatography (CH_2Cl_2/CH_3OH/$NH_{3(aq)}$ 97.5:2.5:0.125) allowed to isolate **103** as a white solid (0.11 g, 75 %); R_f 0.32 (CH_2Cl_2/CH_3OH/$NH_{3(aq)}$ 95:5:0.25). **¹H-NMR** (400 MHz, $CDCl_3$) δ 7.96 (br. s, 1H, NHCO), 7.48–7.40 (m, 2H, Ar), 7.18–7.09 (m, 2H, Ar), 7.02–6.93 (m, 3H, Ar), 6.77 (s, 1H, CH-pyrazole), 5.11 (dd, J = 10.6 and 2.2 Hz, 1H, CH, THP), 4.12 (dt, J = 11.6 and 2.4 Hz, 1H, CH_2, THP), 3.86 (s, 3H, OCH_3), 3.57 (td, J = 11.8 and 2.2 Hz, 1H, CH_2, THP), 3.09 (br. s, 4H, $2CH_2$-piperazine), 2.64 (br. s, 4H, $2CH_2$-piperazine), 2.46 (t, J = 7.2 Hz, 2H, CH_2), 2.39 (t, J = 7.4 Hz, 2H, CH_2), 2.39–2.31 (m, 1H, CH_2, THP), 1.99 (d, J = 12.8 Hz, 1H, CH_2, THP), 1.80–1.51 (m, 8H, $2CH_2$ and $2CH_2$-THP).

### *N*-(5-(4-methoxyphenyl)-1-(tetrahydro-2H-pyran-2-yl)-1H-pyrazol-3-yl)-5-(4-(2-methoxyphenyl)piperazin-1-yl)pentanamide (110, Scheme 3)
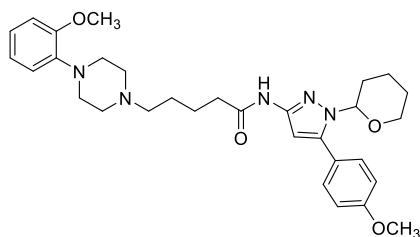
Following the general procedure (method **b**), a mixture of **94** (0.07 g, 0.26 mmol), **130** (0.10 g, 0.32 mmol), HATU (0.12 g, 0.32 mmol) and DIPEA (0.15 mL, 0.83 mmol) in dry DMF (2.60 mL) was allowed to react for 3 h and 30 minutes.
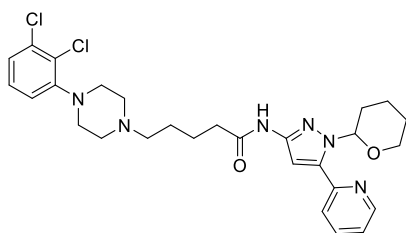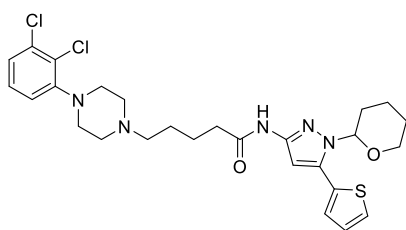
Purification by typical silica gel flash chromatography ($CH_2Cl_2/CH_3OH/NH_{3(aq)}$ 95:5:0.25) allowed to isolate **110** as a white solid (0.11 g, 77 %); R_f 0.27 ($CH_2Cl_2/CH_3OH/NH_{3(aq)}$ 95:5:0.25). **^{1}H-NMR** (400 MHz, CDCl$_3$) δ 7.93 (br. s, 1H, NHCO), 7.44 (d, J = 8.8 Hz, 2H, Ar), 7.03–6.82 (m, 6H, Ar), 6.77 (s, 1H, CH-pyrazole), 5.11 (d, J = 10.4 Hz, 1H, CH, THP), 4.12 (d, J = 11.2 Hz, 1H, CH$_2$, THP), 3.86 (s, 6H, 2OCH$_3$), 3.57 (t, J = 12.0 Hz, 1H, CH$_2$, THP), 3.12 (br. s, 4H, 2CH$_2$-piperazine), 2.66 (br. s, 4H, 2CH$_2$-piperazine), 2.45 (t, J = 7.2 Hz, 2H, CH$_2$), 2.39 (t, J = 7.2 Hz, 2H, CH$_2$), 2.42–2.35 (m, 1H, CH$_2$, THP), 1.99 (d, J = 10.8 Hz, 1H, CH$_2$, THP), 1.80–1.48 (m, 8H, 2CH$_2$ and 2CH$_2$-THP).

5-[4-(2-methoxyphenyl)piperazin-1-yl]-*N*-[5-(4-nitrophenyl)-1-(tetrahydro-2*H*-pyran-2-yl)-1*H*-pyrazol-3-yl]pentanamide (111, Scheme 3)
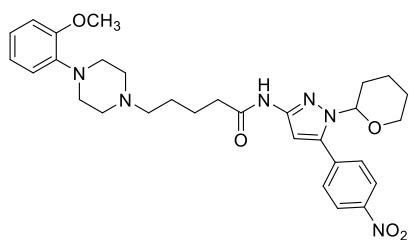
In line with the general procedure (method **a**), a mixture of **95** (0.05 g, 0.17 mmol), **130** (0.07 g, 0.21 mmol), HATU (0.08 g, 0.21 mmol) and DIPEA (0.09 mL, 0.54 mmol) in dry DMF (1.70 mL) was stirred for 4 h, to obtain **111** as a yellow solid (41 mg, 43 %) without further purification; R_f 0.28 ($CH_2Cl_2/CH_3OH/NH_{3(aq)}$ 95:5:0.25). **^{1}H-NMR** (400 MHz, CDCl$_3$) δ 8.32 (d, J = 8.8 Hz, 2H, Ar), 8.11 (br. s, 1H, NHCO), 7.72 (d, J = 8.8 Hz, 2H, Ar), 7.02–6.89 (m, 4H, Ar), 6.86 (s, 1H, CH-pyrazole), 5.07 (d, J = 8.00 Hz, 1H, CH, THP), 4.18–4.08 (m, 1H, CH$_2$, THP), 3.86 (s, 3H, OCH$_3$), 3.64–3.53 (m, 1H, CH$_2$, THP), 3.13 (br. s, 4H, 2CH$_2$-piperazine), 2.68 (br. s, 4H, 2CH$_2$-piperazine), 2.51–2.36 (m, 5H, 2CH$_2$ and CH$_2$-THP), 2.08–1.95 (m, 1H, CH$_2$, THP), 1.83–1.50 (m, 8H, 2CH$_2$ and 2CH$_2$-THP).

5-[4-(2,3-dichlorophenyl)piperazin-1-yl]-*N*-[5-(pyridin-2-yl)-1-(tetrahydro-2*H*-pyran-2-yl)-1*H*-pyrazol-3-yl]pentanamide (105, Scheme 3)

According to the general procedure (method **b**), a mixture of **97** (0.04 g, 0.16 mmol), **129** (0.07 g, 0.19 mmol), HATU (0.07 g, 0.19 mmol) and DIPEA (0.09 mL, 0.51 mmol) in dry DMF (1.60 mL) was stirred for 3 h. Purification by typical silica gel flash chromatography (EtOAc/CH$_3$OH/NH$_{3(aq)}$, gradient elution) allowed to isolate **105** (on elution with EtOAc/CH$_3$OH/NH$_{3(aq)}$ 95:5:0.25) as a white solid (0.11 g, 75 %); R_f 0.23 (CH$_2$Cl$_2$/CH$_3$OH/NH$_{3(aq)}$ 96:4:0.2). **^{1}H-NMR** (400 MHz, CDCl$_3$) δ 8.67 (d, J = 5.2 Hz, 1H, Ar) 8.03 (br. s, 1H, NHCO), 7.76 (td, J = 8.0 and 2.0 Hz, 1H, Ar), 7.64 (d, J = 8.0 Hz, 1H, Ar), 7.27–7.25 (m, 1H, Ar), 7.16–7.13 (m, 2H, Ar), 7.09 (s, 1H, CH-pyrazole), 6.97 (dd, J = 6.4 and 3.2 Hz, 1H, Ar), 6.32 (dd, J = 10.4 and 2.0 Hz, 1H, CH, THP), 4.08–4.03 (m, 1H, CH$_2$, THP), 3.60 (t, J = 11.6, 1H, CH$_2$, THP), 3.10 (br. s, 4H, 2CH$_2$-piperazine), 2.65 (br. s, 4H, 2CH$_2$-piperazine), 2.47 (t, J = 7.4 Hz, 2H, CH$_2$), 2.40 (t, J = 7.2 Hz, 2H, CH$_2$), 2.36–2.30 (m, 1H, CH$_2$, THP), 2.04–1.95 (m, 1H, CH$_2$, THP), 1.82–1.52 (m, 8H, 2CH$_2$ and 2CH$_2$-THP).

5-[4-(2,3-dichlorophenyl)piperazin-1-yl]-*N*-[1-(tetrahydro-2*H*-pyran-2-yl)-5-(thiophen-2-yl)-1*H*-pyrazol-3-yl]pentanamide (104, Scheme 3)

According to the general procedure (method **b**), a mixture of **96** (0.07 g, 0.28 mmol), **129** (0.12 g, 0.34 mmol), HATU (0.13 g, 0.34 mmol) and DIPEA (0.16 mL, 0.90 mmol) in dry DMF (2.80 mL) was stirred for 7 h. Purification by typical silica gel flash chromatography (CH$_2$Cl$_2$/CH$_3$OH/NH$_{3(aq)}$ 97:3:0.15) allowed to isolate **104** as a white solid (0.14 g, 89 %); R_f 0.24 (CH$_2$Cl$_2$/CH$_3$OH/NH$_{3(aq)}$ 95:5:0.25). **^{1}H-NMR** (400 MHz, CDCl$_3$) δ 7.98 (br. s, 1H, NHCO), 7.43 (dd, J = 5.2 and 1.2 Hz, 1H, CH-thiophene), 7.28–7.22 (m, 1H, CH-thiophene), 7.18–7.09 (m, 3H, Ar and CH-thiophene), 6.97 (dd, J = 6.8 and 3.2 Hz, 1H, Ar), 6.91 (s, 1H, CH-pyrazole), 5.32 (dd, J = 10.6 and 2.2 Hz, 1H, CH, THP), 4.15–4.06 (m, 1H, CH$_2$, THP), 3.65 (td, J = 11.6 and 2.0 Hz, 1H, CH$_2$, THP), 3.09 (br. t, J = 5.0 Hz, 4H, 2CH$_2$-piperazine), 2.64 (br. s, 4H, 2CH$_2$-piperazine),

2.46 (t, J = 7.2 Hz, 2H, CH$_2$), 2.40 (t, J = 7.2 Hz, 2H, CH$_2$), 2.39–2.35 (m, 1H, CH$_2$, THP), 2.03 (d, J = 12.6 Hz, 1H, CH$_2$, THP), 1.91–1.50 (m, 8H, 2CH$_2$ and 2CH$_2$-THP).

5-[4-(2-methoxyphenyl)piperazin-1-yl]-*N*-[1-(tetrahydro-2*H*-pyran-2-yl)-5-(thiophen-2-yl)-1*H*-pyrazol-3-yl]pentanamide (112, Scheme 3)
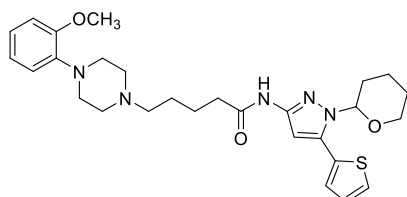
According to the general procedure (method **b**), a mixture of **96** (0.07 g, 0.28 mmol), **130** (0.11 g, 0.34 mmol), HATU (0.13 g, 0.34 mmol) and DIPEA (0.16 mL, 0.90 mmol) in dry DMF (2.80 mL) was stirred for 5 h. Purification by typical silica gel flash chromatography (CH$_2$Cl$_2$/CH$_3$OH/NH$_{3(aq)}$ 95:5:0.25) allowed to isolate **112** as a white solid (0.13 g, 89 %); R_f 0.25 (CH$_2$Cl$_2$/CH$_3$OH/NH$_{3(aq)}$ 95:5:0.25). **^{1}H-NMR** (400 MHz, CDCl$_3$) δ 7.97 (br. s, 1H, NHCO), 7.43 (dd, J = 5.2 and 1.2 Hz, 1H, CH-thiophene), 7.28–7.22 (m, 1H, CH-thiophene), 7.12 (dd, J = 5.2 and 3.6 Hz, 1H, CH-thiophene), 7.03–6.88 (m, 4H, Ar and CH-pyrazole), 6.85 (dd, J = 8.0 and 1.6 Hz, 1H, Ar), 5.31 (dd, J = 10.6 and 2.4 Hz, 1H, CH, THP), 4.15–4.06 (m, 1H, CH$_2$, THP), 3.86 (s, 3H, OCH$_3$), 3.65 (td, J = 11.6 and 2.0 Hz, 1H, CH$_2$, THP), 3.12 (br. s, 4H, 2CH$_2$-piperazine), 2.66 (br. s, 4H, 2CH$_2$-piperazine), 2.45 (t, J = 7.2 Hz, 2H, CH$_2$), 2.39 (t, J = 7.2 Hz, 2H, CH$_2$), 2.42–2.33 (m, 1H, CH$_2$, THP), 2.03 (d, J = 12.4 Hz, 1H, CH$_2$, THP), 1.89–1.52 (m, 8H, 2CH$_2$ and 2CH$_2$-THP).

### General procedure of urea formation: synthesis of final compound 27 and intermediates 118-120 (Scheme 6)

A mixture of the corresponding phenyl carbamate **114, 116** or **117** (1.00 mmol), the corresponding amine (1.5 molar equiv), and TEA (2.5 or 3.5 molar equiv) in CHCl$_3$ (10.0 mL) was stirred under reflux for 3-4 h. Upon reaction completion, the mixture was diluted with CH$_2$Cl$_2$ (10.0 mL) and washed with saturated NaHCO$_3$ aqueous solution (2 x 10.0 mL) and brine (2 x 10.0 mL). The organic phase was dried over Na$_2$SO$_4$, filtered and concentrated under reduced pressure to give a crude which was purified by typical silica gel flash chromatography, affording the desired product.

1-{3-[4-(2,3-dichlorophenyl)piperazin-1-yl]propyl}-3-(5-methyl-1*H*-pyrazol-3-yl)urea (27, Scheme 6)
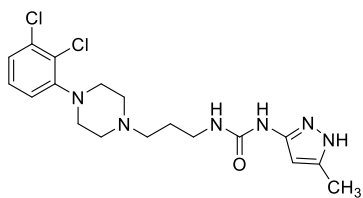
Following the general procedure, a mixture of phenyl carbamate **114** (0.05 g, 0.23 mmol), amine **136** (0.14 g, 0.35 mmol), and TEA (0.11 mL, 0.81 mmol) in CHCl$_3$ (2.3 mL) was stirred under reflux for 3 h. Purification by typical silica gel flash chromatography (CH$_2$Cl$_2$/PE/CH$_3$OH/NH$_{3(aq)}$ 80:15:5:0.25), followed by a trituration using Et$_2$O (3.0 mL) allowed to isolate **27** as a white solid (0.04 g, 28 %); R_f 0.19 (CH$_2$Cl$_2$/CH$_3$OH/NH$_{3(aq)}$ 92.5:7.5:0.375). **UPLC-MS**: t$_R$ = 1.37 min (method B), *m/z*: 411.4/413.5/415.0 [M+H]$^+$ calcd for C$_{18}$H$_{25}$Cl$_2$N$_6$O 411.1/413.1/415.1. **^{1}H-NMR** (400 MHz, DMSO-*d$_6$*) δ 11.74 (br. s, 1H, NH), 8.58 (br. s, 1H, CONH-pyrazole), 7.33–7.27 (m, 2H, Ar), 7.15–7.12 (m, 2H, Ar and CH$_2$NHCO), 5.74 (s, 1H, CH-pyrazole), 3.16 (q, *J* = 6.4 Hz, 2H, C$\underline{H}_2$NHCO), 2.98 (br. s, 4H, 2CH$_2$-piperazine), 2.52 (br. s, 4H, 2CH$_2$-piperazine), 2.37 (t, *J* = 7.2 Hz, 2H, CH$_2$N), 2.14 (s, 3H, CH$_3$), 1.65–1.57 (m, 2H, CH$_2$). **^{13}C-NMR** (101 MHz, DMSO-*d$_6$*) δ 154.8, 151.2, 134.0, 132.6, 128.4, 126.0, 124.3, 119.5, 104.3, 93.2, 55.3, 52.8 (2C), 50.9 (2C), 37.4, 26.9, 10.6. **UPLC-MS purity** > 99.5 % (λ = 215 nm).

1-{4-[4-(2,3-dichlorophenyl)piperazin-1-yl]butyl}-3-[5-methyl-1-(tetrahydro-2*H*-pyran-2-yl)-1*H*-pyrazol-3-yl]urea (118, Scheme 6)
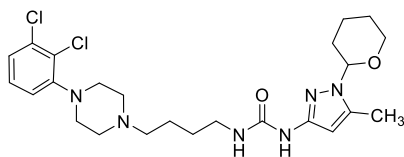
Following the general procedure, a mixture of phenyl carbamate **116** (0.05 g, 0.17 mmol), amine **137** (0.09 g, 0.26 mmol), and TEA (0.08 mL, 0.60 mmol) in CHCl$_3$ (1.7 mL) was stirred under reflux for 4 h. Purification by typical silica gel flash chromatography (CH$_2$Cl$_2$/CH$_3$OH/NH$_{3(aq)}$ 95:5:0.25), allowed to isolate **118** as an oil (0.06 g, 69 %); R_f 0.45 (CH$_2$Cl$_2$/CH$_3$OH/NH$_{3(aq)}$ 93:7:0.35). **^{1}H-NMR** (400 MHz, CDCl$_3$) δ 7.89 (br. s, 1H, CONH-pyrazole), 7.18–7.09 (m, 2H, Ar), 6.95 (dd, *J* = 6.4 and 3.2 Hz, 1H, Ar), 6.44 (s, 1H, CH-pyrazole), 5.57 (br. s, 1H, CH$_2$N$\underline{H}$CO), 5.15 (dd, *J* = 10.0 and 2.4 Hz, 1H, CH, THP), 4.06–3.99 (m, 1H, CH$_2$, THP), 3.68–3.58 (m, 1H, CH$_2$, THP), 3.42–3.30 (m, 2H, C$\underline{H}_2$NHCO), 3.06 (br. s, 4H, 2CH$_2$-piperazine),

2.63 (br. s, 4H, 2CH$_2$-piperazine), 2.46 (t, J = 6.8 Hz, 2H, CH$_2$N), 2.37–2.30 (m, 1H, CH$_2$, THP), 2.28 (s, 3H, CH$_3$), 2.11–2.08 (m, 1H, CH$_2$, THP), 1.99–1.91 (m, 1H, CH$_2$, THP), 1.74–1.61 (m, 7H, 2CH$_2$ and CH$_2$-THP).

1-{4-[4-(2,3-methoxyphenyl)piperazin-1-yl]butyl}-3-[5-methyl-1-(tetrahydro-2*H*-pyran-2-yl)-1*H*-pyrazol-3-yl]urea (119, Scheme 6)
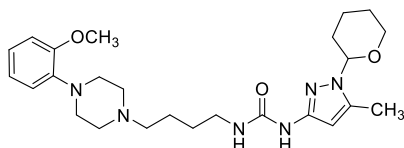
Following the general procedure, a mixture of phenyl carbamate **116** (0.05 g, 0.17 mmol), amine **138** (0.07 g, 0.26 mmol), and TEA (0.06 mL, 0.43 mmol) in CHCl$_3$ (1.7 mL) was stirred under reflux for 4 h. Purification by typical silica gel flash chromatography (CH$_2$Cl$_2$/CH$_3$OH/NH$_{3(aq)}$ 95:5:0.25), allowed to isolate **119** as an oil (0.06 g, 75 %); R_f 0.29 (CH$_2$Cl$_2$/CH$_3$OH/NH$_{3(aq)}$ 93:7:0.35). **¹H-NMR** (400 MHz, CDCl$_3$) δ 7.88 (br. s, 1H, CONH-pyrazole), 7.01–6.85 (m, 4H, Ar), 6.48 (s, 1H, CH-pyrazole), 5.57 (br. s, 1H, CH$_2$N<u>H</u>CO), 5.15 (dd, J = 9.6 and 2.0 Hz, 1H, CH, THP), 4.07–3.99 (m, 1H, CH$_2$, THP), 3.86 (s, 3H, OCH$_3$), 3.72–3.58 (m, 1H, CH$_2$, THP), 3.42–3.29 (m, 2H, C<u>H</u>$_2$NHCO), 3.09 (br. s, 4H, 2CH$_2$-piperazine), 2.65 (br. s, 4H, 2CH$_2$-piperazine), 2.44 (t, J = 6.8 Hz, 2H, CH$_2$N), 2.38–2.30 (m, 1H, CH$_2$, THP), 2.27 (s, 3H, CH$_3$), 2.13–2.06 (m, 1H, CH$_2$, THP), 1.99–1.90 (m, 1H, CH$_2$, THP), 1.71–1.56 (m, 7H, 2CH$_2$ and CH$_2$-THP).

1-{4-[4-(2,3-dichlorophenyl)piperazin-1-yl]butyl}-3-[3-phenyl-1-(tetrahydro-2*H*-pyran-2-yl)-1*H*-pyrazol-5-yl]urea (120, Scheme 6)
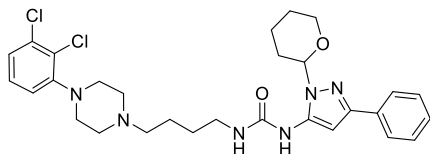
Following the general procedure, a mixture of phenyl carbamate **117** (0.03 g, 0.08 mmol), amine **137** (0.04 g, 0.12 mmol), and TEA (0.39 mL, 2.80 mmol) in CHCl$_3$ (2.0 mL) was stirred under reflux for 4 h. Purification by typical silica gel flash chromatography (CH$_2$Cl$_2$/CH$_3$OH/NH$_{3(aq)}$ 97:3:0.15), allowed to isolate **120** as an oil (0.024 g, 52 %); R_f 0.19 (CH$_2$Cl$_2$/CH$_3$OH/NH$_{3(aq)}$ 97:3:0.15). **¹H-NMR** (400 MHz, CDCl$_3$) δ 7.83 – 7.76 (m, 2H, Ar), 7.42 – 7.28 (m, 3H, Ar), 7.21 – 7.07 (m, 2H, Ar), 6.92 (dd, J = 7.6 and 2.0 Hz, 1H, Ar), 6.59 (br. s, 1H, CONH-pyrazole), 6.55 (s,

1H, CH-pyrazole), 5.45 (dd, J = 9.1 and 2.9 Hz, 1H, CH, THP), 5.39 (br. s, 1H, CH$_2$N<u>H</u>CO), 3.99 (d, J = 11.3 Hz, 1H, CH$_2$, THP), 3.70 (q, J = 12.6 and 10.4 Hz, 1H, CH$_2$, THP), 3.35–3.23 (m, 2H, C<u>H</u>$_2$NHCO), 3.03 (br. s, 4H, 2CH$_2$-piperazine), 2.62 (br. s, 4H, 2CH$_2$-piperazine), 2.45 (d, J = 6.3 Hz, 2H, CH$_2$N), 2.18–2.09 (m, 2H, CH$_2$, THP), 2.02 (d, J = 13.7 Hz, 1H, CH$_2$, THP), 1.74–1.61 (m, 7H, 2CH$_2$ and CH$_2$-THP).

Substitution reaction: synthesis of final compound 2-(2-(1-((8-chloroquinolin-2-yl)methyl)piperidin-4-yl)ethyl)isoindoline-1,3-dione (32, Scheme 9)
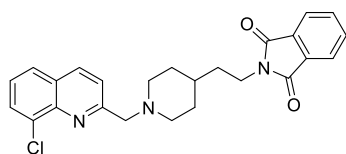
A solution of **149** (0.11 g, 0.34 mmol) and potassium phthalimide (0.08 g, 0.41 mmol) in DMF (3.5 mL) was stirred under reflux for 8 h. The reaction mixture was poured in H$_2$O and the resulting orange solid was filtered off, washed with fresh water and dried *under vacuum* to afford **32** as an orange solid (0.10 g, 68 %). **^{1}H-NMR** (400 MHz, DMSO-d_6) δ 8.41 (d, J = 8.5 Hz, 1H, Ar), 7.93 (ddd, J = 15.1, 7.9, 1.3 Hz, 2H, Ar), 7.91–7.79 (m, 4H, Ar), 7.73 (d, J = 8.5 Hz, 1H, Ar), 7.54 (t, J = 7.9 Hz, 1H. Ar), 3.79 (s, 2H, C<u>H</u>$_2$NH), 3.60 (t, J = 7.2 Hz, 2H, C<u>H</u>$_2$Pht), 2.83 (br. s, 1H, piperidine), 2.07 (br. s, 2H, piperidine), 1.73 (d, J = 10.6 Hz, 2H, piperidine), 1.54 (d, J = 6.3 Hz, 2H, piperidine), 1.24 (s, 4H). **^{13}C-NMR** (101 MHz, DMSO-d_6) δ 168.1, 159.0, 144.4, 135.7, 133.4, 132.4, 130.8, 129.3, 127.8, 126.9, 126.3, 123.3, 121.9, 61.1, 52.7, 38.6, 35.1, 33.0, 30.1.

General procedure of *N*-acylation reaction (method A): synthesis of quinoline-based compound 33, 36, 37 (Scheme 8 and 9) and N^1-protected 3(5)-acylaminopyrazole intermediates 57-62 and 64 (Scheme 1 and 2)

To a stirred solution of the corresponding amino quinoline-based intermediate **147**, **150** or 5-substituted-3-amino-pyrazole **53-56**, **89** (1.00 mmol) and DIPEA (3.0 molar equiv) in CH$_2$Cl$_2$ (10.0 mL) at 0 °C, a solution of the appropriate acyl chloride (1.3 molar equiv) in CH$_2$Cl$_2$ (2.0 M) was added dropwise. The resulting reaction mixture was stirred at room temperature for 2-7 h. Upon reaction completion, the mixture was

diluted with additional CH_2Cl_2 (10.0 mL) and washed with H_2O (2 x 20.0 mL) and then with saturated $NaHCO_3$ aqueous solution (2 x 20.0 mL). The organic phase was dried over Na_2SO_4, filtered and concentrated to dryness at reduced pressure to afford a crude which was purified by trituration using appropriate solvent or by typical silica gel flash chromatography to obtain the desired product.

N-(2-(1-((8-chloroquinolin-2-yl)methyl)piperidin-4-yl)ethyl)acetamide   (33, Scheme 9)
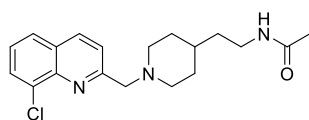
Following the general procedure, a mixture of amino intermediate **150** (0.10 g, 0.33 mmol), acetyl chloride (0.03 mL, 0.43 mmol) and DIPEA (0.17 mL, 0.99 mmol) in CH_2Cl_2 (4.0 mL) was allowed to react for 3 h. Purification by typical silica gel flash chromatography ($CH_2Cl_2/CH_3OH/NH_{3(aq)}$ 98:2:0.10) allowed to isolate **33** as an orange oil (0.05 g, 44 %); **^{1}H-NMR** (400 MHz, DMSO-d_6) δ 8.40 (d, $J = 8.5$ Hz, 1H, Ar), 7.98 – 7.88 (m, 2H, Ar), 7.74 (t, $J = 6.8$ Hz, 2H, Ar and NH), 7.55 (t, $J = 7.8$ Hz, 1H, Ar), 3.78 (s, 2H, C$\underline{H}_2$NH), 3.05 (q, $J = 6.6$ Hz, 2H, C$\underline{H}_2$NHCO), 2.82 (d, $J = 11.2$ Hz, 2H, piperidine), 2.07 (dd, $J = 22.0$ and 11.5 Hz, 2H, piperidine), 1.77 (s, 3H, COCH$_3$), 1.64 (d, $J = 12.4$ Hz, 2H, piperidine), 1.33 (q, $J = 7.0, 6.6$ Hz, 2H, piperidine), 1.21 (d, $J = 16.6$ Hz, 2H), 1.15 (d, $J = 9.1$ Hz, 1H).**^{13}C-NMR** (101 MHz, DMSO-d_6) δ 170.7, 158.5, 142.2, 135.9, 131.5, 129.2, 127.8, 127.1, 126.2, 121.9, 61.1, 52.8, 39.1, 34.9, 34.4, 30.0, 22.9.

N-((1-((8-chloroquinolin-2-yl)methyl)piperidin-4-yl)methyl)acetamide   (36, Scheme 8)
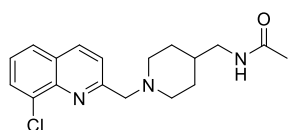
Following the general procedure, a mixture of amino intermediate **147** (0.19 g, 0.65 mmol), acetyl chloride (0.06 g, 0.84 mmol) and DIPEA (0.34 mL, 1.95 mmol) in CH_2Cl_2 (6.0 mL) was allowed to react for 6 h. Purification by typical silica gel flash chromatography (CH_2Cl_2/CH_3OH 97.5:2.5) allowed to isolate **36** as on oil (0.02 g, 9 %); **^{1}H-NMR** (400 MHz, CDCl$_3$) δ 8.15 (d, $J = 8.4$ Hz, 1H, Ar), 7.69-7.84 (m, 3H, Ar),

7.44 (t, J = 7.8 Hz, 1H, Ar), 5.75 (br. s, 1H, NH), 3.99 (s, 2H, CH$_2$N-piperidine), 3.18 (t, J = 6.3 Hz, 2H, C$\underline{H}$$_2$NHCO), 3.02 (d, J = 11.3 Hz, 2H, piperidine), 2.22–2.34 (m, 2H, piperidine), 2.18 (s, 3H, NHCOC$\underline{H}$$_3$), 1.72 (d, J = 12.9 Hz, 2H, piperidine), 1.37–1.62 (m, 3H, piperidine). ^{13}**C-NMR** (101 MHz, DMSO-d_6) δ 170.9, 158.9, 142.3, 136.1, 131.6, 129.3, 127.9, 126.8, 126.1, 121.9, 61.1, 51.7, 45.1, 34.8, 28.3, 22.9.

N-acetyl-N-((1-((8-chloroquinolin-2-yl)methyl)piperidin-4-yl)methyl)acetamide (37, Scheme 8)
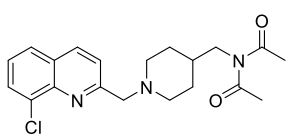
Following the general procedure, a mixture of amino intermediate **147** (0.19 g, 0.65 mmol), acetyl chloride (0.06 g, 0.84 mmol) and DIPEA (0.34 mL, 1.95 mmol) in CH$_2$Cl$_2$ (6.0 mL) was allowed to react for 6 h. Purification by typical silica gel flash chromatography (CH$_2$Cl$_2$/CH$_3$OH 97.5:2.5) allowed to isolate **37** as on oil (0.03 g, 13 %); ^{1}**H-NMR** (400 MHz, CDCl$_3$) δ 8.14 (d, J = 8.8 Hz, 1H, Ar), 7.78 (dd, J = 7.5 and 1.4 Hz, 1H, Ar), 7.70–7.75 (m, 2H, Ar), 7.43 (t, J = 7.9 Hz, 1H, Ar), 3.93 (s, 2H, CH$_2$N-piperidine), 3.63 (d, J =6.8 Hz, 2H, C$\underline{H}$$_2$N(COCH$_3$)$_2$), 2.97 (d, J =11.7 Hz, 2H, piperidine), 2.43 (s, 6H, NHCOC$\underline{H}$$_3$), 2.10–2.19 (m, 2H, piperidine), 1.56–1.65 (m, 3H, piperidine), 1.33–1.45 (m, 2H, piperidine). ^{13}**C-NMR** (101 MHz, DMSO-d_6) δ 171.4, 158.1, 143.1, 135.9, 131.6, 129.3, 127.8, 127.4, 126.3, 121.9.

tert-butyl 3-methyl-5-propionamido-1*H*-pyrazole-1-carboxylate (57, Scheme 1)
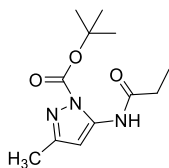
Following the general procedure, a mixture of N^1-Boc protected aminopyrazole **53** (0.20 g, 1.01 mmol), propionyl chloride (0.12 g, 1.31 mmol) and DIPEA (0.53 mL, 3.03 mmol) in CH$_2$Cl$_2$ (10.0 mL) was allowed to react for 6 h. Purification by typical silica gel flash chromatography (PE/EtOAc 80:20) allowed to isolate **57** as a white solid (0.18 g, 70 %); R_f 0.40 (PE/EtOAc 80:20). ^{1}**H-NMR** (400 MHz, CDCl$_3$) δ 10.18 (br. s, 1H, NHCO), 6.70 (s, 1H, CH-pyrazole), 2.45 (q, J = 7.6 Hz, 2H, COCH$_2$), 2.28 (s, 3H, CH$_3$), 1.68 (s, 9H, 3CH$_3$, Boc), 1.27 (t, J = 7.6 Hz, 3H, CH$_3$).

tert-butyl 3-methyl-5-pentanamido-1*H*-pyrazole-1-carboxylate (58, Scheme 1)
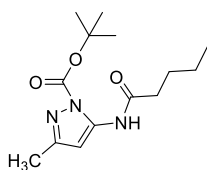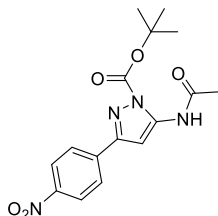
Following the general procedure, a mixture of N^1-Boc protected aminopyrazole **53** (0.25 g, 2.33 mmol), valeroyl chloride (0.36 mL, 3.03 mmol) and DIPEA (1.22 mL, 6.99 mmol) in CH$_2$Cl$_2$ (23.0 mL) was allowed to react for 3 h. Purification by typical silica gel flash chromatography (PE/EtOAc 90:10) allowed to isolate **58** as a yellow oil (0.32 g, 72 %); R_f 0.39 (PE/EtOAc 70:30). **^{1}H-NMR** (400 MHz, CDCl$_3$) δ 10.15 (br. s, 1H, NHCO), 6.69 (s, 1H, CH-pyrazole), 2.42 (t, J = 7.6 Hz, 2H, COCH$_2$), 2.27 (s, 3H, CH$_3$), 1.75–1.69 (m, 2H, CH$_2$), 1.67 (s, 9H, 3CH$_3$, Boc), 1.44–1.38 (m, 2H, CH$_2$), 0.95 (t, J = 6.8 Hz, 3H, CH$_3$).

tert-butyl 3-phenyl-5-pentanamido-1*H*-pyrazole-1-carboxylate (59, Scheme 1)
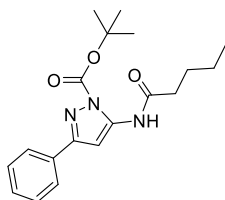
Following the general procedure, a mixture of N^1-Boc protected aminopyrazole **54** (0.10 g. 0.39 mmol), valeroyl chloride (0.06 mL, 0.50 mmol) and DIPEA (0.20 mL, 1.17 mmol) in CH$_2$Cl$_2$ (4.0 mL) was allowed to react for 5 h. Purification by typical silica gel flash chromatography (PE/EtOAc 90:10) allowed to isolate **59** as a white solid (0.04 g, 30 %); R_f 0.34 (PE/EtOAc 90:10). **^{1}H-NMR** (400 MHz, CDCl$_3$) δ 10.24 (br. s, 1H, NHCO), 7.91–7.80 (m, 2H, Ar), 7.44–7.37 (m, 3H, Ar), 7.27 (s, 1H, CH-pyrazole), 2.46 (t, J = 7.6 Hz, 2H, COCH$_2$), 1.77–1.75 (m, 2H, CH$_2$), 1.71 (s, 9H, 3CH$_3$, Boc), 1.43 (q, J = 7.6 Hz, 2H, CH$_2$), 0.97 (t, J = 7.6 Hz, 3H, CH$_3$).

tert-butyl 5-acetamido-3-(4-bromophenyl)-1*H*-pyrazole-1-carboxylate (60, Scheme 1)
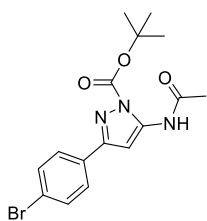
Following the general procedure, a mixture of N^1-Boc protected aminopyrazole **55** (0.08 g. 0.24 mmol), acetyl chloride (0.02 mL, 0.31 mmol) and DIPEA (0.12 mL, 0.72 mmol) in CH$_2$Cl$_2$ (2.5 mL) was allowed to react for 7 h. Purification by typical silica gel flash chromatography (PE/EtOAc 80:20) allowed to isolate **60** as a white solid (0.04 g, 44 %); R_f 0.45

(PE/EtOAc 80:20). **^{1}H-NMR** (400 MHz, CDCl$_3$) δ 10.24 (br. s, 1H, NHCO), 7.60 (d, J = 8.4 Hz, 2H, Ar), 7.48 (d, J = 8.6 Hz, 2H, Ar), 7.31 (s, 1H, CH-pyrazole), 2.29 (s, 3H, CH$_3$), 1. 70 (s, 9H, 3CH$_3$, Boc).

***tert*-butyl   5-acetamido-3-(4-nitrophenyl)-1*H*-pyrazole-1-carboxylate   (61, Scheme 1)**

Following the general procedure, a mixture of N^1-Boc protected aminopyrazole **56** (0.08 g. 0.26 mmol), acetyl chloride (0.02 mL, 0.34 mmol) and DIPEA (0.14 mL, 0.78 mmol) in CH$_2$Cl$_2$ (2.6 mL) was allowed to react for 7 h. Purification by typical silica gel flash chromatography (PE/EtOAc 80:20) allowed to isolate **61** as a white solid (0.04 g, 44 %); R_f 0.48 (PE/EtOAc 70:30). **^{1}H-NMR** (400 MHz, CDCl$_3$) δ 10.21 (br. s, 1H, NHCO), 8.28 (d, J = 8.4 Hz, 2H, Ar), 8.06 (d, J = 8.8 Hz, 2H, Ar), 7.30 (s, 1H, CH-pyrazole), 2.28 (s, 3H, CH$_3$), 1. 72 (s, 9H, 3CH$_3$, Boc).

***tert*-butyl   5-(2-ethoxy-2-oxoacetamido)-3-methyl-1*H*-pyrazole-1-carboxylate (62, Scheme 2, Method IIa)**
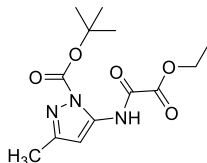
Following the general procedure, a mixture of N^1-Boc protected aminopyrazole **53** (0.50 g, 2.53 mmol), ethylchloroxoacetate (0.37 mL, 3.29 mmol) and DIPEA (1.32 mL, 7.59 mmol) in CH$_2$Cl$_2$ (25.0 mL) was allowed to react for 2 h. Purification by typical silica gel flash chromatography (toluene/acetone 90:10) allowed to isolate **62** as an oil (0.41 g, 55 %); R_f 0.32 (PE/EtOAc 70:30). **^{1}H-NMR** (400 MHz, CDCl$_3$) δ 11.53 (br. s, 1H, NHCO), 6.78 (s, 1H, CH-pyrazole), 4.43 (q, J = 7.2 Hz, 2H, OCH$_2$), 2.30 (s, 3H, CH$_3$), 1.69 (s, 9H, 3CH$_3$, Boc), 1.43 (t, J = 7.2 Hz, 3H, CH$_3$).

ethyl   2-{[5-methyl-1-(tetrahydro-2*H*-pyran-2-yl)-1*H*-pyrazol-3-yl]amino}-2-oxoacetate (64, Scheme 2, Method IIb)
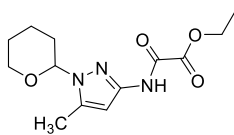
Following the general procedure, a mixture of N^1-THP protected aminopyrazole **89** (0.48 g, 2.65 mmol), ethylchloroxoacetate (0.38 mL, 3.44 mmol) and DIPEA (1.38 mL, 7.94 mmol) in CH_2Cl_2 (26.5 mL) was allowed to react for 2 h. The crude product was washed with *n*-hexane (2 x 20.0 mL) affording **64** as a yellow oil (0.60 g, 80 %); R_f 0.60 (CH_2Cl_2/CH_3OH 95:5). **^{1}H-NMR** (400 MHz, CDCl$_3$) δ 9.26 (br. s, 1H, NHCO), 6.62 (s, 1H, CH-pyrazole), 5.21 (dd, *J* = 10.4 and 2.8 Hz, 1H, CH, THP), 4.39 (q, *J* = 7.2 Hz, 2H, OCH$_2$), 4.07 (d, *J* = 11.6 Hz, 1H, CH$_2$, THP), 3.65 (td, *J* = 11.2 and 2.4 Hz, 1H, CH$_2$, THP), 2.36–2.30 (m, 4H, CH$_3$ and CH$_2$-THP), 2.12–2.08 (m, 1H, CH$_2$, THP), 1.88 (dd, *J* = 13.6 and 2.4 Hz, 1H, CH$_2$, THP), 1.71–1.57 (m, 3H, CH$_2$, THP),1.41 (t, *J* = 7.0 Hz, 3H, CH$_3$).

General procedure of *N*-acylation reaction (method B): synthesis of 5-[4-(2,3-dichlorophenyl)piperazin-1-yl]-*N*-[3-(pyridin-3-yl)-1-(tetrahydro-2*H*-pyran-2-yl)-1*H*-pyrazol-5-yl]pentanamide (113, Scheme 4)
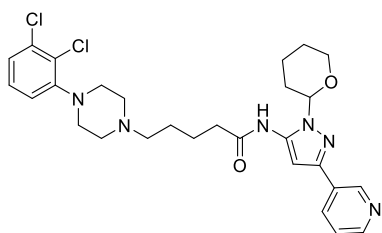
The suspension of the freshly prepared acyl chloride **139** (0.178 g, 0.51 mmol) in dry 1,4-dioxane (3.0 mL) was added dropwise to a stirred solution of amine **98** (0.125 g, 0.51 mmol) and TEA (0.21 mL) in dry 1,4-dioxane (2.5 mL) at rt under an nitrogen atmosphere. The resulting mixture was stirred for 48 h at the same temperature. The reaction mixture was concentrated to dryness, was diluted with CH_2Cl_2, was washed with aqueous NaOH solution (0.1 N), was dried over Na_2SO_4 and was evaporated under reduced pressure. Purification of the crude product by typical silica gel flash chromatography by employing a gradient 0-3 % of NH$_3$ solution (1 N in CH$_3$OH) in EtOAc afforded **113** (81 mg, 28 %); **^{1}H-NMR** (400 MHz, CDCl$_3$) δ 9.03 (d, *J* = 2.2 Hz, 1H, Ar), 8.67 (br. s, 1H, NH), 8.53 (dd, *J* = 4.8 and 1.7 Hz, 1H, Ar), 8.07 (dt, *J* = 7.9 and 2.0 Hz, 1H, Ar), 7.30 (dd, *J* = 7.9 and 4.8 Hz, 1H, Ar), 7.20–7.07 (m, 2H, Ar), 7.03–6.88 (m, 2H, 2CH, Ar and CH-pyrazole), 5.57 (d, *J* = 7.7 Hz, 1H, CH, THP), 4.03–3.98 (m, 1H, CH$_2$, THP), 3.82–3.68 (m, 1H, CH$_2$, THP), 3.13 (br. s, 4H, 2CH$_2$-

piperazine), 2.75 (br. s, 4H, 2CH$_2$-piperazine), 2.57 (br. s, 2H, CH$_2$), 2.48 (t, J = 7.2 Hz, 2H, CH$_2$), 2.40-2.24 (m, 1H, CH$_2$, THP), 2.17-2.12 (m, 1H, CH$_2$, THP), 1.89-1.55 (m, 8H, 2CH$_2$ and 2CH$_2$-THP).

General procedure of LDA-assisted Claisen condensation: synthesis of β-ketonitriles 44-47 (Scheme 1)

To a solution of CH$_3$CN (1.05 molar equiv) in dry THF (1.0 mL) at −78 °C under N$_2$ atmosphere, LDA (2.0 M in THF, 1.1 molar equiv) was added dropwise, and the mixture was stirred for 1 h at the same temperature. A solution of appropriate methyl ester (1.00 mmol) in dry THF (0.5 mL) was then added dropwise, maintaining the temperature below −60 °C. After addition, the reaction mixture was warmed slowly to rt and stirred for 18 h. Upon completion, the resulting beige suspension was quenched with 10% citric acid aqueous solution (2.0 mL) and diluted with additional H$_2$O (10.0 mL). The aqueous phase was extracted with EtOAc (3 x 10.0 mL), dried over Na$_2$SO$_4$, filtered, and concentrated under reduced pressure to afford a crude which was purified by typical silica gel flash chromatography (PE/EtOAc 70:30), yielding the title compound.

3-oxo-3-phenylpropanenitrile (44, Scheme 1)
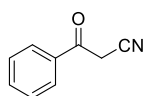
In line with the general procedure, the title compound was synthetized starting from methyl benzoate **40** (0.89 g, 6.55 mmol), CH$_3$CN (0.36 mL, 6.88 mmol) and LDA (3.60 mL, 7.21 mmol) in dry THF (7.0 mL), to yield **44** as a yellow solid (0.27 g, 28 %); R_f 0.10 (PE/EtOAc 90:10). **^{1}H-NMR** (400 MHz, CDCl$_3$) δ 7.93 (d, J = 8.8 Hz, 2H, Ar), 7.68 (t, J = 7.2 Hz, 1H, Ar), 7.54 (t, J = 7.2 Hz, 2H, Ar), 4.09 (s, 2H, CH$_2$CN).

3-(4-bromophenyl)-3-oxopropanenitrile (45, Scheme 1)
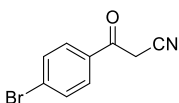
In line with the general procedure, the title compound was synthetized starting from methyl 4-bromobenzoate **41** (1.37 g, 6.37 mmol), CH$_3$CN (0.35 mL, 6.69 mmol) and LDA (3.50 mL, 7.01 mmol) in dry

THF (6.4 mL), to yield **45** as a yellow solid (0.54 g, 35 %); R_f 0.10 (PE/EtOAc 90:10). **^{1}H-NMR** (400 MHz, CDCl$_3$) δ 7.80 (d, J = 8.8 Hz, 2H, Ar), 7.69 (d, J = 8.4 Hz, 2H, Ar), 4.05 (s, 2H, CH$_2$CN).

3-(4-nitrophenyl)-3-oxopropanenitrile (46, Scheme 1)
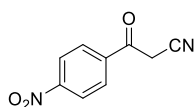
In line with the general procedure, the title compound was synthetized starting from methyl 4-nitrobenzoate **42** (1.00 g, 5.52 mmol), CH$_3$CN (0.30 mL, 5.80 mmol) and LDA (3.19 mL, 6.38 mmol) in dry THF (5.5 mL), to yield **46** as a brown solid (0.20 g, 18 %); R_f 0.11 (PE/EtOAc 80:20). **^{1}H-NMR** (400 MHz, CDCl$_3$) δ 8.35 (d, J = 9.2 Hz, 2H, Ar), 8.11 (d, J = 8.4 Hz, 2H, Ar), 4.20 (s, 2H, CH$_2$CN),

3-oxo-3-(pyridin-2-yl)propanenitrile (47, Scheme 1)
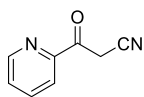
In line with the general procedure, the title compound was synthetized starting from methyl picolinate **43** (1.70 g, 12.40 mmol), CH$_3$CN (0.68 mL, 13.01 mmol) and LDA (6.82 mL, 13.64 mmol) in dry THF (12.4 mL), to yield **47** as a brown solid (1.51 g, 83 %) without further purification; R_f 0.53 (PE/EtOAc 50:50). **^{1}H-NMR** (400 MHz, CDCl$_3$) δ 8.69 (ddd, J = 4.8, 2.0 and 1.2 Hz, 1H, Ar), 8.11 (dt, J = 8.0 and 1.2 Hz, 1H, Ar), 7.91 (td, J = 8.0 and 1.6 Hz, 1H, Ar), 7.57 (ddd, J = 7.6, 4.8 and 1.2 Hz, 1H, Ar), 4.39 (s, 2H, CH$_2$CN).

General procedure for the synthesis of amino-pyrazole derivatives 49-52 (Scheme 1)

To a solution of the appropriate β-ketonitrile intermediate **44-47** (1.00 mmol) in EtOH (10.0 mL) hydrazine monohydrate (2.0 molar equiv) was added dropwise, and the mixture was stirred under reflux for 4-10 h. After cooling at rt, the mixture was concentrated under reduced pressure to afford a crude which was purified by trituration using a mixture of PE/EtOAc (9:1) or by typical silica gel flash chromatography.

3-(phenyl)-1*H*-pyrazol-5-amine (49, Scheme 1)
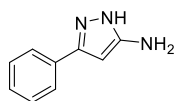
Following the general procedure, β-ketonitrile **44** (0.17 g, 1.17 mmol) was treated with hydrazine monohydrate (0.11 mL, 2.34 mmol) in EtOH (12.0 mL) for 4 h. The crude product was purified by trituration using a mixture of PE/EtOAc (9:1, 10.0 mL), to isolate **49** as a beige solid (0.11 g, 59 %); R_f 0.15 (CH$_2$Cl$_2$/CH$_3$OH 95:5). **^{1}H-NMR** (400 MHz, acetone-d_6) δ 7.74 (d, J = 7.6 Hz, 2H, Ar), 7.41 (t, J = 7.6 Hz, 2H, Ar), 7.30 (t, J = 7.6 Hz, 1H, Ar), 5.91 (s, 1H, CH-pyrazole).

3-(4-bromophenyl)-1*H*-pyrazol-5-amine (50, Scheme 1)
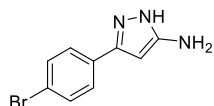
Following the general procedure, β-ketonitrile **45** (0.50 g, 2.08 mmol) was treated with hydrazine monohydrate (0.20 ml, 4.16 mmol) in EtOH (20.0 mL) for 4 h. The crude product was purified by trituration using a mixture of PE/EtOAc (9:1, 20.0 mL), to give **50** as a beige solid (0.17 g, 32 %); R_f 0.17 (CH$_2$Cl$_2$/CH$_3$OH 95:5). **^{1}H-NMR** (400 MHz, acetone-d_6) δ 7.70 (d, J = 8.8 Hz, 2H, Ar), 7.57 (d, J = 8.4 Hz, 2H, Ar), 5.90 (s, 1H, CH-pyrazole), 3.79 (br. s, NH$_2$).

3-(4-nitrophenyl)-1*H*-pyrazol-5-amine (51, Scheme 1)
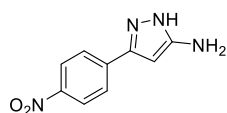
Following the general procedure, β-ketonitrile **46** (0.20 g, 1.05 mmol) was treated with hydrazine monohydrate (0.10 mL, 2.10 mmol) in EtOH (10.0 mL) for 5 h. The crude product was purified by trituration using a mixture of PE/EtOAc (9:1, 10.0 mL), to give **51** as a brown solid (0.22 g, 97 %); R_f 0.36 (CH$_2$Cl$_2$/CH$_3$OH 90:10). **^{1}H-NMR** (400 MHz, CDCl$_3$) δ 8.23 (d, J = 8.8 Hz, 2H, Ar), 8.13 (d, J = 8.8 Hz, 2H, Ar), 6.50 (s, 1H, CH-pyrazole).

3-(pyridin-2-yl)-1*H*-pyrazol-5-amine (52, Scheme 1)
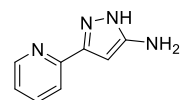
Following the general procedure, β-ketonitrile **47** (1.51 g, 10.33 mmol) was treated with hydrazine monohydrate (1.00 mL, 20.66 mmol) in EtOH (103.0 mL) for 10 h. Purification of the crude product by typical silica

gel flash chromatography (CH$_2$Cl$_2$/CH$_3$OH/NH$_{3(aq)}$ 95:5:0.25) allowed to isolate **52** as a beige solid (1.00 g, 60 %); *R$_f$* 0.15 (CH$_2$Cl$_2$/CH$_3$OH/NH$_{3(aq)}$ 93:7:0.35). **¹H-NMR** (400 MHz, CDCl$_3$) δ 8.61 (ddd, *J* = 4.8, 2.0 and 1.2 Hz, 1H, Ar), 7.71 (dt, *J* = 8.0 and 1.2 Hz, 1H, Ar), 7.53 (d, *J* = 8.0, 1H, Ar), 7.21 (ddd, *J* = 7.6, 4.8 and 1.2 Hz, 1H, Ar), 6.08 (s, 1H, CH-pyrazole), 3.81 (br. s, NH$_2$).

General procedure of *N*-Boc protection: synthesis of N¹-Boc-protected aminopyrazoles 53-56 (Scheme 1) and intermediates 157 and 158 (Scheme 10)

To a solution of the appropriate amino compound (1.00 mmol) in a mixture of CH$_2$Cl$_2$/THF (4:1, 10.0 mL) was added portion-wise di-*tert*-butyl dicarbonate (1.05 molar equiv) and the reaction mixture was stirred at rt for 16 h. Upon completion, the solution was concentrated under reduced pressure and the resulting residue was purified by typical silica gel flash chromatography to afford the title compound.
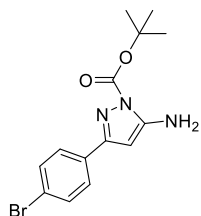
tert-butyl 5-amino-3-methyl-1*H*-pyrazole-1-carboxylate (53, Scheme 1)
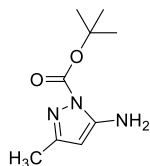
In line with the general procedure, the title compound was synthetized starting from commercially available 3-amino-5-methyl-pyrazole **48** (0.50 g, 5.15 mmol) and di-*tert*-butyl decarbonate (1.18 g, 5.41 mmol) in a mixture of CH$_2$Cl$_2$/THF (52.0 mL). Purification by typical silica gel flash chromatography (PE/Et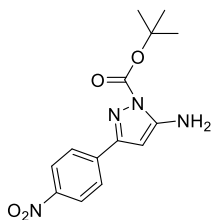OAc, gradient elution) allowed to isolate **53** (on elution with PE/EtOAc 50:50) as a white solid (0.88 g, 87 %); *R$_f$* 0.40 (PE/EtOAc 50:50). **¹H-NMR** (400 MHz, CDCl$_3$) δ 5.30 (br. s, 2H, NH$_2$), 5.24 (s, 1H, CH-pyrazole), 2.17 (s, 3H, CH$_3$), 1.65 (s, 9H, 3CH$_3$, Boc).

tert-butyl 5-amino-3-phenyl-1*H*-pyrazole-1-carboxylate (54, Scheme 1)
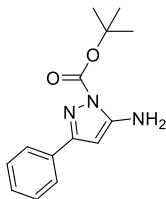
In line with the general procedure, the title compound was synthetized starting from 3-amino-5-phenyl-pyrazole **49** (0.50 g, 3.14 mmol) and di-*tert*-butyl decarbonate (0.72 g, 3.30 mmol) in a mixture of CH$_2$Cl$_2$/THF (31.0 mL). Purification by typical silica gel flash chromatography (PE/EtOAc, gradient elution) allowed to isolate **54** (on elution

with PE/EtOAc 80:20) as a white solid (0.50 g, 61 %); R_f 0.30 (PE/EtOAc 80:20). **¹H-NMR** (400 MHz, CDCl₃) δ 7.83 (d, J = 7.2 Hz, 2H, Ar), 7.42–7.34 (m, 3H, Ar), 5.78 (s, 1H, CH-pyrazole), 5.35 (br. s, 2H, NH₂), 1.70 (s, 9H, 3CH₃, Boc).

tert-butyl 5-amino-3-(4-bromophenyl)-1*H*-pyrazole-1-carboxylate (55, Scheme 1)

In line with the general procedure, the title compound was synthetized starting from commercially available 3-amino-5-methyl-pyrazole **50** (0.17 g, 0.67 mmol) and di-*tert*-butyl decarbonate (0.15 g, 0.70 mmol) in a mixture of CH₂Cl₂/THF (7.0 mL). Purification by typical silica gel flash chromatography (CH₂Cl₂) allowed to isolate **55** as a white solid (0.15 g, 66 %); R_f 0.35 (PE/EtOAc 80:20). **¹H-NMR** (400 MHz, CDCl₃) δ 7.69 (d, J = 8.4 Hz, 2H, Ar), 7.51 (d, J = 8.6 Hz, 2H, Ar), 5.74 (s, 1H, CH-pyrazole), 5.35 (br. s, 2H, NH₂), 1.69 (s, 9H, 3CH₃, Boc).

tert-butyl 5-amino-3-(4-nitrophenyl)-1*H*-pyrazole-1-carboxylate (56, Scheme 1)

In line with the general procedure, the title compound was synthetized starting from commercially available 3-amino-5-methyl-pyrazole **51** (0.22 g, 1.07 mmol) and di-*tert*-butyl decarbonate (0.24 g, 1.12 mmol) in a mixture of CH₂Cl₂/THF (10.0 mL). Purification by typical silica gel flash chromatography (PE/EtOAc, gradient elution) allowed to isolate **56** (on elution with PE/EtOAc 80:20) as a white solid (0.08 g, 22 %); R_f 0.50 (PE/EtOAc 80:20). **¹H-NMR** (400 MHz, CDCl₃) δ 8.25 (d, J = 9.2 Hz, 2H, Ar), 7.98 (d, J = 9.2 Hz, 2H, Ar), 5.83 (s, 1H, CH-pyrazole), 5.41 (br. s, 2H, NH₂), 1.70 (s, 9H, 3CH₃, Boc).

### *tert*-butyl ((1-benzylpiperidin-3-yl)methyl)carbamate (157, Scheme 10)
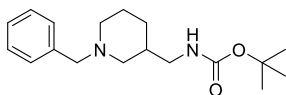
In line with the general procedure, the title compound was synthetized starting from **155** (0.38 g, 1.86 mmol) and di-*tert*-

butyl decarbonate (0.43 g, 1.95 mmol) in a mixture of CH_2Cl_2/THF (18.0 mL). Purification by typical silica gel flash chromatography (PE/EtOAc, gradient elution) allowed to isolate **157** (on elution with PE/EtOAc 80:20) as a yellow oil (0.22 g, 39 %). **^{1}H-NMR** (400 MHz, CDCl$_3$) δ 0.99 (d, J = 10.0 Hz, 1H,), 1.41 (s, 9H, 3CH$_3$), 1.63-1.78 (m, 4H), 2.00 (q, J = 10.4 Hz, 1H), 2.70 (d, J = 11.20 Hz, 2H), 2.76 (d, J = 8.4 Hz, 2H), 3.01 (d, 2H, CH$_2$-Ph), 3.43-3.51 (m, 2H), 4.61 (br. s, 1H, NH), 7.22-7.25 (m, 1H, Ar), 7.29 (d, 1H, J =4.4 Hz, Ar).

tert-butyl ((1-benzylpiperidin-4-yl)methyl)carbamate (158, Scheme 10)
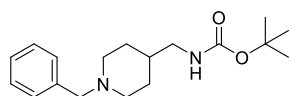
In line with the general procedure, the title compound was synthetized starting from **156** (0.71 g, 3.48 mmol) and di-*tert*-butyl decarbonate (0.80 g, 3.65 mmol) in a mixture of CH_2Cl_2/THF (35.0 mL), affording **158** as a brown oil (0.95 g, 87 %), without any further purification. **^{1}H-NMR** (400 MHz, CDCl$_3$) δ 1.43 (s, 9H, 3CH$_3$), 1.47 (t, 1H, J = 7.2 Hz, 1H), 1.52 (d, J = 6.0 Hz, 2H), 1.67 (d, J = 12.8 Hz, 2H), 2.03 (t, J =11.2 Hz, 2H), 2.94 (d, J = 11.6 Hz, 2H), 3.01 (t, J = 6.4 Hz, 2H), 3.56 (s, 2H, CH$_2$-Ph), 4.60 (s, 1H, NH), 7.24-7.35 (m, 5H, Ar).

General procedure of ester hydrolysis reaction: synthesis of aminopyrazole intermediates 63 and 65 (Scheme 2) and arylpiperazine carboxylic acid derivatives 129 and 130 (Scheme 7)

A solution of the corresponding ester (1.00 mmol) in THF/H$_2$O (1:1, 10.0 mL) was treated with LiOH (1.1 or 2.2 molar equiv) and the resulting mixture was stirred at rt for 1-2 h. Upon completion, the solution was concentrated under reduced pressure to remove THF and the alkaline aqueous phase was neutralized with HCl aqueous solution (0.5 or 6 N). The resulting precipitate was collected by filtration and dried under *vacuum* to afford the desired carboxylic acid as hydrochloride salt or free base.

2-[(5-methyl-1*H*-pyrazol-3-yl)amino]-2-oxoacetic acid (63, Scheme 2)
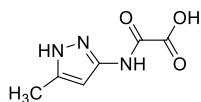
In line with the general procedure, treatment of ester **62** (0.38 g, 1.28 mmol) with LiOH (0.03 g, 1.41 mmol) in a mixture of

THF/H$_2$O (13.0 mL) for 1 h afforded **63** as a white solid (0.06 g, 28 %); R_f 0.07 (CH$_2$Cl$_2$/CH$_3$OH 90:10). **^{1}H-NMR** (400 MHz, DMSO-d_6) δ 12.06 (br. s, 1H, NH), 9.83 (br. s, 1H, NHCO), 6.26 (s, 1H, CH-pyrazole), 2.18 (s, 3H, CH$_3$).

2-{[5-methyl-1-(tetrahydro-2*H*-pyran-2-yl)-1*H*-pyrazol-3-yl]amino}-2-oxoacetic acid (65, Scheme 2)
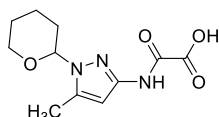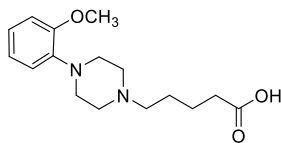
 In line with the general procedure, treatment of ester **64** (0.60 g, 2.13 mmol) with LiOH (0.06 g, 2.35 mmol) in a mixture of THF/H$_2$O (20.0 mL) for 1 h afforded **65** as a white solid (0.45 g, 83 %); R_f 0.36 (CH$_2$Cl$_2$/CH$_3$OH 90:10). **^{1}H-NMR** (400 MHz, DMSO-d_6) δ 9.87 (s, 1H, NHCO), 6.38 (s, 1H, CH-pyrazole), 5.28 (dd, J = 10.0 and 2.4 Hz, 1H, CH, THP), 3.87 (d, J = 11.6 Hz, 1H, CH$_2$, THP), 3.66–3.55 (m, 1H, CH$_2$, THP), 2.26 (s, 3H, CH$_3$), 2.25–2.10 (m, 1H, CH$_2$, THP), 1.97 (d, J = 14.0 Hz, 1H, CH$_2$, THP), 1.80 (dd, J = 13.6 and 3.2 Hz, 1H, CH$_2$, THP), 1.70–1.59 (m, 1H, CH$_2$, THP), 1.52–1.47 (m, 2H, CH$_2$, THP).

5-[4-(2,3-dichlorophenyl)piperazin-1-yl]pentanoic acid hydrochloride (129, Scheme 7)
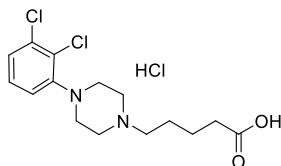
 In line with the general procedure, treatment of ester **127** (0.40 g, 1.01 mmol) with LiOH (0.05 g, 2.22 mmol) in a mixture of THF/H$_2$O (10.0 mL) for 2 h afforded **129** as a beige solid (0.34 g, 92 %); R_f 0.11 (CH$_2$Cl$_2$/CH$_3$OH 90:10). **^{1}H-NMR** (400 MHz, DMSO-d_6) δ 7.39–7.32 (m, 2H, Ar), 7.23–7.17 (m, 1H, Ar), 3.54 (br. s, 2H, CH$_2$), 3.39 (br. s, 2H, CH$_2$), 3.22–3.12 (m, 6H, 3CH$_2$), 2.29 (t, J = 7.2 Hz, 2H, CH$_2$), 1.78–1.69 (m, 2H, CH$_2$), 1.58–1.50 (m, 2H, CH$_2$).

### 5-[4-(2-methoxyphenyl)piperazin-1-yl]pentanoic acid (130, Scheme 7)

 In line with the general procedure, treatment of ester **128** (1.38 g, 4.31 mmol) with LiOH (0.23 g, 9.48 mmol) in a mixture of THF/H$_2$O (43.0 mL) for 2 h afforded **130** as a

white solid (1.01 g, 80 %); R_f 0.08 (CH$_2$Cl$_2$/CH$_3$OH 90:10). **^{1}H-NMR** (400 MHz, DMSO-d_6) δ 6.99–6.79 (m, 4H, Ar), 3.75 (s, 3H, OCH$_3$), 2.97 (br. s, 4H, 2CH$_2$-piperazine), 2.56 (br. s, 4H, 2CH$_2$-piperazine), 2.39 (t, J = 6.6 Hz, 2H, CH$_2$), 2.22 (t, J = 6.6 Hz, 2H, CH$_2$), 1.53–1.45 (m, 4H, 2CH$_2$).

General procedure of *N*-THP protection: synthesis of intermediates 79-88 (Scheme 3)

To a mixture of the intermediate **3, 5-7, 73-78** (1.00 mmol) in CH$_3$CN (10.0 mL), 3,4-dihydro-2*H*-pyran (2.5 molar equiv) was added dropwise followed by addition of catalytic amount of TFA (0.02 molar equiv). The resulting mixture was stirred under reflux for 6-24 h. Upon completion, the reaction mixture was cooled down to rt and was concentrated under reduced pressure. Purification of the crude product by trituration using Et$_2$O or by typical silica gel flash chromatography followed by treatment with an appropriate solvent or solvents mixture allowed to obtain the desired product.

**N-[5-methyl-1-(tetrahydro-2H-pyran-2-yl)-1H-pyrazol-3-yl]acetamide** (**79b, Scheme 3**)
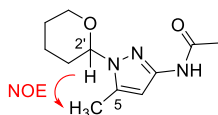
According to the previously described general procedure, a mixture of **73** (1.15 g, 8.26 mmol), 3,4-dihydro-2*H*-pyran (1.88 mL, 20.66 mmol) and TFA (12 µL, 0.16 mmol) in CH$_3$CN (83 mL) was allowed to react for 6 h. The crude product was treated with Et$_2$O (25.0 mL) and the resulting precipitate was collected by filtration, washed with fresh Et$_2$O and dried under vacuum affording **79** as a white solid (0.84 g, 46 %); R_f 0.50 (CH$_2$Cl$_2$/CH$_3$OH/NH$_{3(aq)}$ 94:6:0.30). **^{1}H-NMR** (400 MHz, CDCl$_3$) δ 7.99 (br. s, 1H, CONH), 6.50 (s, 1H, CH-pyrazole), 5.14 (d, J = 10.2 Hz, 1H, CH, THP), 4.03 (d, J = 11.6 Hz, 1H, CH$_2$, THP), 3.61 (t, J = 10.4 Hz, 1H, CH$_2$, THP), 2.29–2.21 (m, 4H, CH$_3$ and CH$_2$-THP), 2.09–2.01 (m, 4H, COCH$_3$ and CH$_2$-THP), 1.86–1.82 (m, 1H, CH$_2$, THP), 1.64–1.56 (m, 3H, CH$_2$, THP). A **2D-NOESY** experiment was performed to confirm the compound

regiochemistry; **diagnostic NOE contact:** H-2 (THP) *vs* CH$_3$-5 (aminopyrazole). See *Appendix*.

N-[3-phenyl-1-(tetrahydro-2H-pyran-2-yl)-1H-pyrazol-5-yl]acetamide **(80a)** **and N-[5-phenyl-1-(tetrahydro-2H-pyran-2-yl)-1H-pyrazol-3-yl]acetamide (80b, Scheme 3)**

Following the general procedure, a mixture of **3** (0.50 g, 2.48 mmol), 3,4-dihydro-2H-pyran (0.57 mL, 6.21 mmol) and TFA (4 μL, 0.05 mmol) in CH$_3$CN (25.0 mL) was allowed to react for 10 h. A final purification by typical silica gel flash chromatography (CH$_2$Cl$_2$/CH$_3$OH/NH$_{3(aq)}$ 99:1:0.05), followed by a trituration using *n*-hexane allowed to isolate two different isomers (regioisomer **80a** and regioisomer **80b**).
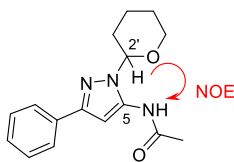
80a (white solid, 0.20 g, 28 %): R_f 0.71 (CH$_2$Cl$_2$/CH$_3$OH/NH$_{3(aq)}$ 95:5:0.25). **^{1}H-NMR** (400 MHz, DMSO-d_6) δ 9.96 (br. s, 1H, CONH), 7.77 (d, J = 7.2 Hz, 2H, Ph), 7.40 (t, J = 7.6 Hz, 2H, Ph), 7.33–7.29 (m, 1H, Ph), 6.72 (s, 1H, CH-pyrazole), 5.44 (dd, J = 9.2 and 2.0 Hz, 1H, CH, THP), 3.90 (d, J = 11.6 Hz, 1H, CH$_2$, THP), 3.69–3.63 (m, 1H, CH$_2$, THP), 2.38–2.29 (m, 1H, CH$_2$, THP), 2.11 (s, 3H, COCH$_3$), 2.07–2.02 (m, 1H, CH$_2$, THP), 1.88–1.82 (m, 1H, CH$_2$, THP), 1.70–1.54 (m, 3H, CH$_2$, THP). A **2D-NOESY** experiment was performed to confirm the compound regiochemistry; **diagnostic NOE contacts:** H-2 (THP) *vs* CO<u>NH</u>. See *Appendix*.
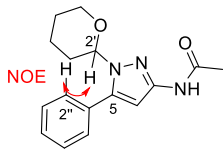

80b (oil, 0.15 g, 21 %): R_f 0.34 (CH$_2$Cl$_2$/CH$_3$OH/NH$_{3(aq)}$ 95:5:0.25). **^{1}H-NMR** (400 MHz, DMSO-d_6) δ 10.53 (br. s, 1H, CONH), 7.52–7.44 (m, 5H, Ph), 6.66 (s, 1H, CH-pyrazole), 5.14 (dd, J = 10.0 and 2.0 Hz, 1H, CH, THP), 3.98 (d, J = 11.2 Hz, 1H, CH$_2$, THP), 3.54–4.47 (m, 1H, CH$_2$, THP), 2.35–2.26 (m, 1H, CH$_2$, THP), 2.01 (s, 3H, COCH$_3$), 1.96–1.88 (m, 1H, CH$_2$, THP), 1.82–1.74 (m, 1H, CH$_2$, THP), 1.62–1.46 (m, 3H, CH$_2$, THP). A **2D-NOESY** experiment was performed to confirm the compound regiochemistry; **diagnostic NOE contact:** H-2 (THP) *vs* H-2′ (Ph). See *Appendix*.

N-[**3**-(**4**-fluorophenyl)-**1**-(tetrahydro-**2***H*-pyran-**2**-yl)-**1***H*-pyrazol-**5**-yl]acetamide (81a) and *N*-[**5**-(**4**-fluorophenyl)-**1**-(tetrahydro-**2***H*-pyran-**2**-yl)-**1***H*-pyrazol-**3**-yl]acetamide (81b, Scheme 3)

In line with the general procedure, a mixture of **74** (1.04 g, 4.74 mmol), 3,4-dihydro-2H-pyran (1.08 mL, 11.85 mmol) and TFA (7 μL, 0.09 mmol) in CH_3CN (47.0 mL) was allowed to react for 23 h. A final purification by typical silica gel flash chromatography ($CH_2Cl_2/CH_3OH/NH_{3(aq)}$ 99:1:0.05), followed by a trituration using *n*-hexane allowed to isolate two different isomers (regioisomer **81a** and regioisomer **81b**).
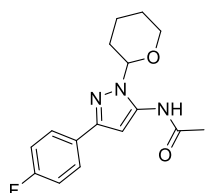
81a (white solid, 0.09 g, 6 %): R_f 0.70 ($CH_2Cl_2/CH_3OH/NH_{3(aq)}$ 95:5:0.25). **¹H-NMR** (400 MHz, CDCl₃) δ 8.42 (br. s, 1H, CONH), 7.78–7.74 (m, 2H, Ar), 7.07–7.03 (m, 2H, Ar), 6.88 (s, 1H, CH-pyrazole), 5.52 (dd, *J* = 7.6 and 2.4 Hz, 1H, CH, THP), 4.01–3.97 (m, 1H, CH₂, THP), 3.76–3.73 (m, 1H, CH₂, THP), 2.62–2.49 (m, 1H, CH₂, THP), 2.20 (s, 3H, COCH₃), 2.13–2.10 (m, 2H, CH₂, THP), 1.88–1.57 (m, 3H, CH₂, THP).
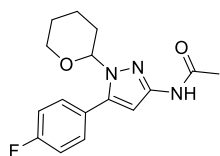

81b (white solid, 0.55 g, 38 %): R_f 0.43 ($CH_2Cl_2/CH_3OH/NH_{3(aq)}$ 95:5:0.25). **¹H-NMR** (400 MHz, CDCl₃) δ 7.79 (br. s, 1H, CONH), 7.55–7.45 (m, 2H, Ar), 7.20–7.11 (m, 2H, Ar), 6.79 (s, 1H, CH-pyrazole), 5.07 (dd, *J* = 10.6 and 2.2 Hz, 1H, CH, THP), 4.16–4.08 (m, 1H, CH₂, THP), 3.56 (td, *J* = 11.6 and 2.0 Hz, 1H, CH₂, THP), 2.48–2.34 (m, 1H, CH₂, THP), 2.15 (s, 3H, COCH₃), 2.03 (d, *J* = 10.8 Hz, 1H, CH₂, THP), 1.82–1.65 (m, 2H, CH₂, THP), 1.58–1.49 (m, 2H, CH₂, THP).
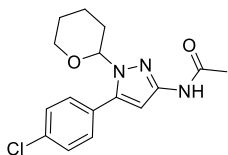
N-[**3**-(**4**-chlorophenyl)-**1**-(tetrahydro-**2***H*-pyran-**2**-yl)-**1***H*-pyrazol-**5**-yl]acetamide (82a) and *N*-[**5**-(**4**-chlorophenyl)-**1**-(tetrahydro-**2***H*-pyran-**2**-yl)-**1***H*-pyrazol-**3**-yl]acetamide (82b, Scheme 3)

In line with the general procedure, a mixture of **75** (1.13 g, 4.79 mmol), 3,4-dihydro-2H-pyran (1.09 mL, 11.97 mmol) and TFA (8 μL, 0.10 mmol) in CH_3CN (48.0

mL) was allowed to react for 23 h. A final purification by typical silica gel flash chromatography (CH$_2$Cl$_2$/CH$_3$OH/NH$_{3(aq)}$ 99:1:0.05), followed by a trituration using *n*-hexane allowed to isolate two different isomers (regioisomer **82a** and regioisomer **82b**).
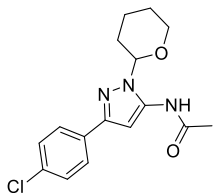
82a (white solid, 0.09 g, 6 %): **R_f** 0.69 (CH$_2$Cl$_2$/CH$_3$OH/NH$_{3(aq)}$ 95:5:0.25). **^{1}H-NMR** (400 MHz, CDCl$_3$) δ 8.42 (br. s, 1H, CONH), 7.73 (d, J = 8.4 Hz, 2H, Ar), 7.34 (d, J = 8.8 Hz, 2H, Ar), 6.91 (s, 1H, CH-pyrazole), 5.53 (dd, J = 7.8 and 2.6 Hz, 1H, CH, THP), 3.99 (dd, J = 11.6 and 4.0 Hz, 1H, CH$_2$, THP), 3.79–3.68 (m, 1H, CH$_2$, THP), 2.32–2.27 (m, 1H, CH$_2$, THP), 2.21 (s, 3H, COCH$_3$), 2.17–2.10 (m, 2H, CH$_2$, THP), 1.74–1.65 (m, 3H, CH$_2$,).

82b (white solid, 0.23 g, 15 %): **R_f** 0.39 (CH$_2$Cl$_2$/CH$_3$OH/NH$_{3(aq)}$ 95:5:0.25). **^{1}H-NMR** (400 MHz, CDCl$_3$) δ 7.72 (br. s, 1H, CONH), 7.50–7.40 (m, 4H, Ar), 6.81 (s, 1H, CH-pyrazole), 5.08 (dd, J = 10.4 and 2.0 Hz, 1H, CH, THP), 4.16–4.08 (m, 1H, CH$_2$, THP), 3.62–3.51 (m, 1H, CH$_2$, THP), 2.48–2.34 (m, 1H, CH$_2$, THP), 2.15 (s, 3H, COCH$_3$), 2.06–2.01 (m, 1H, CH$_2$, THP), 1.79–1.68 (m, 2H, CH$_2$, THP), 1.59–1.52 (m, 2H, CH$_2$, THP).

N-[3-(4-bromophenyl)-1-(tetrahydro-2*H*-pyran-2-yl)-1*H*-pyrazol-5-yl]acetamide (83a) and *N*-[5-(4-bromophenyl)-1-(tetrahydro-2*H*-pyran-2-yl)-1*H*-pyrazol-3-yl]acetamide (83b, Scheme 3)

Following the general procedure, a mixture of **5** (1.04 g, 3.71 mmol), 3,4-dihydro-2H-pyran (0.85 mL, 9.27 mmol) and TFA (6 µL, 0.07 mmol) in CH$_3$CN (47.0 mL) was stirred for 13 h. The crude product was purified by typical silica gel flash chromatography (CH$_2$Cl$_2$/CH$_3$OH/NH$_{3(aq)}$ 99:1:0.05), affording two different isomers (regioisomer **83a** and regioisomer **83b**).
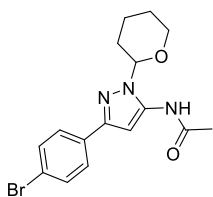
83a (oil, 0.32 g, 24 %): R_f 0.73 (CH$_2$Cl$_2$/CH$_3$OH/NH$_{3(aq)}$ 95:5:0.25). **^{1}H-NMR** (400 MHz, CDCl$_3$) δ 8.43 (br. s, 1H, CONH), 7.67 (d, J = 8.4 Hz, 2H, Ar), 7.49 (d, J = 8.0 Hz, 2H, Ar), 6.91 (s, 1H, CH-pyrazole), 5.52 (dd, J = 7.8 and 2.6 Hz, 1H, CH, THP), 4.05–3.97 (m, 1H, CH$_2$, THP), 3.77–3.67 (m, 1H, CH$_2$, THP), 2.33–2.24 (m, 1H, CH$_2$, THP), 2.21 (s, 3H, COCH$_3$), 2.17–2.09 (m, 2H, CH$_2$, THP), 1.78–1.69 (m, 3H, CH$_2$,).
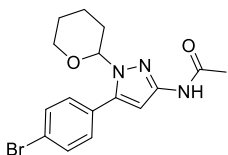
83b (oil, 0.15 g, 11 %): R_f 0.47 (CH$_2$Cl$_2$/CH$_3$OH/NH$_{3(aq)}$ 95:5:0.25). **^{1}H-NMR** (400 MHz, CDCl$_3$) δ 7.79 (br. s, 1H, CONH), 7.59 (d, J = 8.4 Hz, 2H, Ar), 7.39 (d, J = 8.4 Hz, 2H, Ar), 6.81 (s, 1H, CH-pyrazole), 5.07 (dd, J = 10.4 and 2.4 Hz, 1H, CH, THP), 4.16–4.07 (m, 1H, CH$_2$, THP), 3.59–3.53 (m, 1H, CH$_2$, THP), 2.45–2.35 (m, 1H, CH$_2$, THP), 2.15 (s, 3H, COCH$_3$), 2.06–2.01 (m, 1H, CH$_2$, THP), 1.78–1.66 (m, 2H, CH$_2$, THP), 1.60–1.51 (m, 2H, CH$_2$, THP).

N-[3-(4-methoxyphenyl)-1-(tetrahydro-2*H*-pyran-2-yl)-1*H*-pyrazol-5-yl]acetamide (84a) and *N*-[5-(4-methoxyphenyl)-1-(tetrahydro-2*H*-pyran-2-yl)-1*H*-pyrazol-3-yl]acetamide (84b, Scheme 3)

According to the general procedure, a mixture of **76** (0.80 g, 3.46 mmol), 3,4-dihydro-2H-pyran (0.79 mL, 8.65 mmol) and TFA (5 µL, 0.07 mmol) in CH$_3$CN (35.0 mL) was allowed to react for 23 h. Purification of the crude product by typical silica gel flash chromatography (CH$_2$Cl$_2$/CH$_3$OH/NH$_{3(aq)}$ 99:1:0.05) allowed to isolate two different isomers (regioisomer **84a** and regioisomer **84b**).
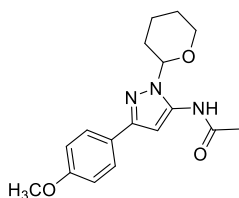
84a (oil, 0.21 g, 19 %): R_f 0.71 (CH$_2$Cl$_2$/CH$_3$OH/NH$_{3(aq)}$ 95:5:0.25). **^{1}H-NMR** (400 MHz, CDCl$_3$) δ 8.42 (br. s, 1H, CONH), 7.73 (d, J = 8.8 Hz, 2H, Ar), 6.91 (d, J = 8.4 Hz, 2H, Ar), 6.86 (s, 1H, CH-pyrazole), 5.52 (dd, J = 8.0 and 2.8 Hz, 1H, CH, THP), 4.01–3.96 (m, 1H, CH$_2$, THP), 3.83 (s, 3H, OCH$_3$), 3.80–3.70 (m, 1H, CH$_2$,

THP), 2.35–2.30 (m, 1H, CH$_2$, THP), 2.20 (s, 3H, COCH$_3$), 2.18–2.12 (m, 2H, CH$_2$, THP), 1.73–1.64 (m, 3H, CH$_2$,).
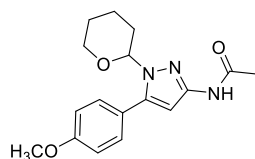
84b (white solid, 0.30 g, 27 %): R_f 0.50 (CH$_2$Cl$_2$/CH$_3$OH/NH$_{3(aq)}$ 95:5:0.25). **^{1}H-NMR** (400 MHz, CDCl$_3$) δ 7.79 (br. s, 1H, CONH), 7.45 (d, J = 8.4 Hz, 2H, Ar), 6.98 (d, J = 8.4 Hz, 2H, Ar), 6.75 (s, 1H, CH-pyrazole), 5.12 (dd, J = 10.6 and 1.8 Hz, 1H, CH, THP), 4.17–4.08 (m, 1H, CH$_2$, THP), 3.86 (s, 3H, OCH$_3$), 3.57 (td, J = 11.6 and 2.2 Hz, 1H, CH$_2$, THP), 2.48–2.33 (m, 1H, CH$_2$, THP), 2.15 (s, 3H, COCH$_3$), 2.01 (d, J = 12.0 Hz, 1H, CH$_2$, THP), 1.78–1.65 (m, 2H, CH$_2$, THP), 1.57–1.50 (m, 2H, CH$_2$, THP).

N-[3-(4-nitrophenyl)-1-(tetrahydro-2*H*-pyran-2-yl)-1*H*-pyrazol-5-yl]acetamide (85a) and *N*-[5-(4-nitrophenyl)-1-(tetrahydro-2*H*-pyran-2-yl)-1*H*-pyrazol-3-yl]acetamide (85b, Scheme 3)

In line with the general procedure, a mixture of **6** (0.80 g, 3.46 mmol), 3,4-dihydro-2H-pyran (0.79 mL, 8.65 mmol) and TFA (5 μL, 0.07 mmol) in CH$_3$CN (35.0 mL) was allowed to react for 24 h. Purification of the crude product by typical silica gel flash chromatography (CH$_2$Cl$_2$/CH$_3$OH/NH$_{3(aq)}$ 99:1:0.05) allowed to isolate two different isomers (regioisomer **85a** and regioisomer **85b**).
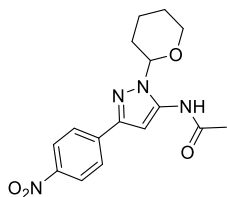
85a (yellowish solid, 0.40 g, 60 %): R_f 0.70 (CH$_2$Cl$_2$/CH$_3$OH/NH$_{3(aq)}$ 95:5:0.25). **^{1}H-NMR** (400 MHz, CDCl$_3$) δ 8.46 (br. s, 1H, CONH), 8.24 (d, J = 8.8 Hz, 2H, Ar), 7.96 (d, J = 9.2 Hz, 2H, Ar), 7.04 (s, 1H, CH-pyrazole), 5.57 (dd, J = 7.6 and 2.4 Hz, 1H, CH, THP), 3.99–3.96 (m, 1H, CH$_2$, THP), 3.80–3.74 (m, 1H, CH$_2$, THP), 2.35–2.29 (m, 1H, CH$_2$, THP), 2.23 (s, 3H, COCH$_3$), 2.18–2.13 (m, 2H, CH$_2$, THP), 1.77–1.56 (m, 3H, CH$_2$,).
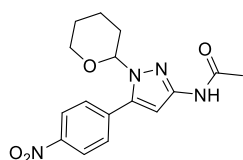
85b (yellow oil, 0.06 g, 9 %): R_f 0.52 (CH$_2$Cl$_2$/CH$_3$OH/NH$_{3(aq)}$ 95:5:0.25). **¹H-NMR** (400 MHz, CDCl$_3$) δ 8.33 (d, J = 8.8 Hz, 2H, Ar), 7.75–7.71 (m, 3H, Ar and CONH), 6.94 (s, 1H, CH-pyrazole), 5.09 (dd, J = 10.2 and 2.6 Hz, 1H, CH, THP), 4.17–4.12 (m, 1H, CH$_2$, THP), 3.57 (td, J = 11.8 and 2.4 Hz, 1H, CH$_2$, THP), 2.49–2.38 (m, 1H, CH$_2$, THP), 2.17 (s, 3H, COCH$_3$), 2.10–2.01 (m, 1H, CH$_2$, THP), 1.76–1.55 (m, 4H, CH$_2$, THP).

N-[1-(tetrahydro-2H-pyran-2-yl)-3-(thiophen-2-yl)-1H-pyrazol-5-yl]acetamide (86a) and N-[1-(tetrahydro-2H-pyran-2-yl)-5-(thiophen-2-yl)-1H-pyrazol-3-yl]acetamide (86b, Scheme 3)

In line with the general procedure, a mixture of **77** (1.66 g, 8.00 mmol), 3,4-dihydro-2H-pyran (1.82 mL, 20.00 mmol) and TFA (12 µL, 0.16 mmol) in CH$_3$CN (80.0 mL) was stirred for 23 h. A final purification by typical silica gel flash chromatography (CH$_2$Cl$_2$/CH$_3$OH/NH$_{3(aq)}$ 99:1:0.05), followed by a trituration using n-hexane allowed to isolate two different isomers (regioisomer **86a** and regioisomer **86b**).
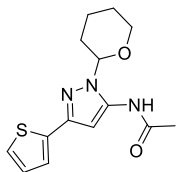
86a (white solid, 0.20 g, 9 %): R_f 0.69 (CH$_2$Cl$_2$/CH$_3$OH/NH$_{3(aq)}$ 95:5:0.25). **¹H-NMR** (400 MHz, CDCl$_3$) δ 8.49 (br. s, 1H, CONH), 7.30 (dd, J = 3.6 and 0.8 Hz, 1H, CH-thiophene), 7.21 (d, J = 4.8 Hz, 1H, CH-thiophene), 7.02 (dd, J = 5.2 and 3.6 Hz, 1H, CH-thiophene), 6.84 (s, 1H, CH-pyrazole), 5.51 (dd, J = 7.6 and 2.4 Hz, 1H, CH, THP), 4.01–3.97 (m, 1H, CH$_2$, THP), 3.79–3.62 (m, 1H, CH$_2$, THP), 2.22–2.19 (m, 4H, CH$_2$-THP and COCH$_3$), 2.12–2.08 (m, 2H, CH$_2$, THP), 1.80–1.64 (m, 3H, CH$_2$,).
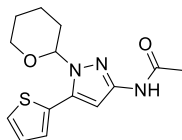
86b (white solid, 0.48 g, 21 %): R_f 0.49 (CH$_2$Cl$_2$/CH$_3$OH/NH$_{3(aq)}$ 95:5:0.25). **¹H-NMR** (400 MHz, CDCl$_3$) δ 8.20 (br. s, 1H, CONH), 7.42 (dd, J = 5.2 and 1.2 Hz, 1H, CH-thiophene), 7.25 (dd, J = 3.6 and 1.2 Hz, 1H, CH-thiophene), 7.11 (dd, J = 5.2 and 3.2 Hz, 1H, CH-thiophene), 6.90 (s, 1H, CH-pyrazole), 5.30 (dd, J = 10.0 and 2.4 Hz, 1H, CH, THP), 4.09 (dd, J = 11.2
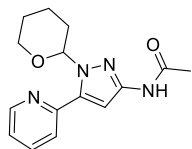
and 2.4 Hz, 1H, CH_2, THP), 3.64 (td, J = 11.2 and 2.0 Hz, 1H, CH_2, THP), 2.44–2.34 (m, 1H, CH_2, THP), 2.14 (s, 3H, $COCH_3$), 2.07–1.99 (m, 1H, CH_2, THP), 1.88–1.79 (m, 1H, CH_2, THP), 1.74–1.61 (m, 1H, CH_2, THP), 1.65–1.50 (m, 2H, CH_2, THP).

N-[3-(4-methoxyphenyl)-1-(tetrahydro-2*H*-pyran-2-yl)-1*H*-pyrazol-5-yl]acetamide (87a) and *N*-[5-(4-methoxyphenyl)-1-(tetrahydro-2*H*-pyran-2-yl)-1*H*-pyrazol-3-yl]acetamide (87b, Scheme 5)

According to the general procedure, a mixture of **7** (0.16 g, 0.79 mmol), 3,4-dihydro-2H-pyran (0.18 mL, 1.97 mmol) and TFA (1.2 µL, 0.016 mmol) in CH_3CN (8.0 mL) was allowed to react for 12 h. Purification of the crude product by typical silica gel flash chromatography (EtOAc/CH_3OH/$NH_{3(aq)}$ 99:1:0.05) allowed to isolate two different isomers (regioisomer **87a** and regioisomer **87b**).
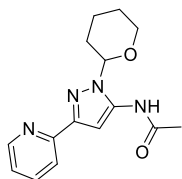

87a (white solid, 0.06 g, 26 %): R_f 0.41 (CH_2Cl_2/CH_3OH/$NH_{3(aq)}$ 95:5:0.25). **¹H-NMR** (400 MHz, $CDCl_3$) δ 8.65 (d, J = 4.0 Hz, 1H, Ar), 8.43 (br. s, 1H, CONH), 7.88 (d, J = 7.6 Hz, 1H, Ar), 7.72–7.68 (m, 1H, Ar), 7.21–7.18 (m, 2H, Ar and CH-pyrazole), 5.59 (d, J = 6.0 Hz, 1H, CH, THP), 4.05 (d, J = 11.6 Hz, 1H, CH_2, THP), 3.79–3.72 (m, 1H, CH_2, THP), 2.30–2.25 (m, 1H, CH_2, THP), 2.22 (s, 3H, $COCH_3$), 2.18–2.10 (m, 2H, CH_2, THP), 1.78–1.62 (m, 3H, CH_2,).

87b (white solid, 0.06 g, 26 %): R_f 0.48 (CH_2Cl_2/CH_3OH/$NH_{3(aq)}$ 95:5:0.25). **¹H-NMR** (400 MHz, $CDCl_3$) δ 8.66 (dd, J = 4.2 and 1.0 Hz, 1H, Ar), 7.81 (br. s, 1H, CONH), 7.77 (td, J = 7.6 and 1.6 Hz, 1H, Ar), 7.66 (d, J = 8.0 Hz, 1H, Ar), 7.29–7.25 (m, 1H, Ar), 7.08 (s, 1H, CH-pyrazole), 6.33 (dd, J = 10.4 and 2.4 Hz, 1H, CH, THP), 4.07 (dt, J = 11.2 and 2.0 Hz, 1H, CH_2, THP), 3.62 (td, J = 12.0 and 2.4 Hz, 1H, CH_2, THP), 2.38–2.32 (m, 1H, CH_2, THP), 2.16 (s, 3H, $COCH_3$), 2.00 (d, J = 12.8 Hz, 1H, CH_2, THP), 1.76–1.67 (m, 2H, CH_2, THP), 1.56–1.53 (m, 2H, CH_2, THP).

### *N*-[3-(pyridin-3-yl)-1-(tetrahydro-2*H*-pyran-2-yl)-1*H*-pyrazol-5-yl]acetamide (88, Scheme 3)
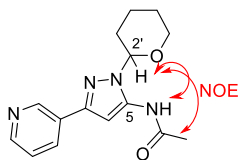
According to the previously described general procedure, a mixture of **78** (0.49 g, 2.42 mmol), 3,4-dihydro-2*H*-pyran (0.89 mL, 9.68 mmol) and TFA in CH$_3$CN (24.0 mL) was allowed to react for 22 h. Purification by typical silica gel flash chromatography (CH$_2$Cl$_2$/CH$_3$OH/NH$_{3(aq)}$ 99:1:0.05) gave a product that was dissolved in a minimal amount of CH$_2$Cl$_2$ and was precipitated by using PE. Finally, filtration under *vacuum* and drying of the resultant solid gave **88** as a white solid (0.28 g, 40 %); *R$_f$* 0.50 (CH$_2$Cl$_2$/CH$_3$OH/NH$_{3(aq)}$ 94:6:0.30). **^{1}H-NMR** (400 MHz, DMSO-*d$_6$*) *δ* 10.00 (br. s, 1H, CONH), 8.97 (d, *J* = 2.2 Hz, 1H, Ar), 8.51 (dd, *J* = 4.8 and 1.7 Hz, 1H, Ar), 8.13 (dt, *J* = 7.9 and 2.0 Hz, 1H, Ar), 7.42 (dd, *J* = 7.9 and 4.8 Hz, 1H, Ar), 6.83 (s, 1H, CH-pyrazole), 5.48 (dd, *J* = 9.6 and 2.6 Hz, 1H, CH, THP), 4.04–3.79 (m, 1H, CH$_2$, THP), 3.77–3.57 (m, 1H, CH$_2$, THP), 2.41–2.27 (m, 1H, CH$_2$, THP), 2.11 (s, 3H, COCH$_3$), 2.08–1.97 (m, 1H, CH$_2$, THP), 1.88–1.82 (m, 1H, CH$_2$, THP), 1.74–1.48 (m, 3H, CH$_2$, THP). A **2D-NOESY** experiment was performed to confirm the compound regiochemistry. **diagnostic NOE contacts:** H-2 (THP) *vs* CO<u>NH</u>. See *Appendix*.

### General procedure of *N*-deacetylation: synthesis of intermediates 89-98 and 115 (Scheme 3, 4 and 6)

The appropriate *N*-acetylated intermediate (1.00 mmol) was treated with KOH (10.0 molar equiv) in a mixture of EtOH/H$_2$O (2:3, 10.0 mL). The resulting reaction mixture was stirred under reflux for 8-48 h. Then, the solution was concentrated under reduced pressure to remove EtOH and the alkaline aqueous phase was extracted with CH$_2$Cl$_2$ (3 x 25.0 mL). The combined organic phase was dried over Na$_2$SO$_4$ and was evaporated to dryness affording the desired compound.

### 5-methyl-1-(tetrahydro-2*H*-pyran-2-yl)-1*H*-pyrazol-3-amine (89, Scheme 3)
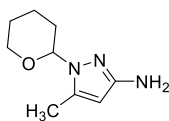
According to the previously described general procedure, treatment of **79b** (0.77 g, 3.45 mmol) with KOH (1.93 g, 34.50 mmol) in a mixture of EtOH/H_2O (35.0 mL) for 11 h afforded **89** as an oil (0.56 g, 90 %); R_f 0.31 (CH_2Cl_2/CH_3OH/$NH_{3(aq)}$ 95:5:0.25). **^{1}H-NMR** (400 MHz, CDCl$_3$) δ 5.41 (s, 1H, CH-pyrazole), 5.02 (dd, J = 10.6 and 2.2 Hz, 1H, CH, THP), 4.02 (ddt, J = 11.2, 4.4 and 2.2 Hz, 1H, CH_2, THP), 3.58 (td, J = 11.6 and 2.4 Hz, 1H, CH_2, THP), 3.45 (br. s, 2H, NH_2), 2.39–2.29 (m, 1H, CH_2, THP), 2.20 (s, 3H, CH_3), 2.04–1.99 (m, 1H, CH_2, THP), 1.88–1.78 (m, 1H, CH_2, THP), 1.71–1.45 (m, 3H, CH_2, THP).

5-phenyl-1-(tetrahydro-2*H*-pyran-2-yl)-1*H*-pyrazol-3-amine (90, Scheme 3)
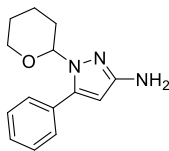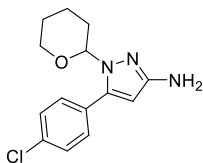
In line with the general procedure, treatment of **80b** (0.10 g, 0.35 mmol) with KOH (0.20 g, 3.50 mmol) in a mixture of EtOH/H_2O (3.50 mL) for 24 h gave **90** as an oil (0.08 g, 94 %); R_f 0.56 (EtOAc/CH_3OH/$NH_{3(aq)}$ 99:1:0.05). **^{1}H-NMR** (400 MHz, CDCl$_3$) δ 7.51–7.37 (m, 5H, Ph), 5.72 (s, 1H, CH-pyrazole), 5.04 (dd, J = 10.4 and 2.0 Hz, 1H, CH, THP), 4.14–4.10 (m, 1H, CH_2, THP), 3.71 (br. s, 2H, NH_2), 3.54 (td, J = 11.6 and 2.0 Hz, 1H, CH_2, THP), 2.52–2.41 (m, 1H, CH_2, THP), 2.02–1.84 (m, 1H, CH_2, THP), 1.80–1.69 (m, 2H, CH_2, THP), 1.56–1.49 (m, 2H, CH_2, THP).

### 5-(4-fluorophenyl)-1-(tetrahydro-2*H*-pyran-2-yl)-1*H*-pyrazol-3-amine (91, Scheme 3)
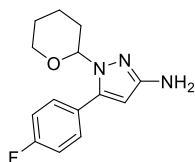
Following the general procedure, treatment of **81b** (0.55 g, 1.81 mmol) with KOH (1.01 g, 18.10 mmol) in a mixture of EtOH/H_2O (18.00 mL) for 48 h gave **91** as an oil (0.46 g, 97 %); R_f 0.49 (EtOAc). **^{1}H-NMR** (400 MHz, CDCl$_3$) δ 7.53–7.40 (m, 2H, Ar), 7.19–7.08 (m, 2H, Ar), 5.69 (s, 1H, CH-pyrazole), 4.96 (dd, J = 10.4 and 2.4 Hz, 1H, CH, THP), 4.10 (ddt, J = 11.2, 4.4 and 2.4 Hz, 1H, CH_2, THP), 3.70 (br. s, 2H, NH_2), 3.52 (td, J = 12.2 and 2.0 Hz, 1H, CH_2, THP), 2.48–2.40 (m, 1H, CH_2, THP), 2.06–1.96 (m, 1H, CH_2, THP), 1.83–1.65 (m, 2H, CH_2, THP), 1.57–1.47 (m, 2H, CH_2, THP).

### 5-(4-chlorophenyl)-1-(tetrahydro-2*H*-pyran-2-yl)-1*H*-pyrazol-3-amine (92, Scheme 3)

According to the general procedure, treatment of **82b** (0.16 g, 0.50 mmol) with KOH (0.28 g, 5.00 mmol) in a mixture of EtOH/H$_2$O (5.00 mL) for 48 h gave **92** as an oil (0.14 g, quantitative yield); R_f 0.58 (EtOAc). **^{1}H-NMR** (400 MHz, CDCl$_3$) δ 7.42 (s, 4H, Ar), 5.71 (s, 1H, CH-pyrazole), 4.97 (dd, *J* = 10.4 and 2.4 Hz, 1H, CH, THP), 4.11 (dt, *J* = 11.6 and 2.8 Hz, 1H, CH$_2$, THP), 3.52 (td, *J* = 12.2 and 2.0 Hz, 1H, CH$_2$, THP), 3.08 (br. s, 2H, NH$_2$), 2.53–2.38 (m, 1H, CH$_2$, THP), 2.01 (d, *J* = 12.4 Hz, 1H, CH$_2$, THP), 1.80–1.67 (m, 2H, CH$_2$, THP), 1.57–1.47 (m, 2H, CH$_2$, THP).

5-(4-bromophenyl)-1-(tetrahydro-2*H*-pyran-2-yl)-1*H*-pyrazol-3-amine (93, Scheme 3)
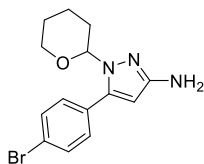
In line with the general procedure, **83b** (0.15 g, 0.41 mmol) was treated with KOH (0.23 g, 4.10 mmol) in a mixture of EtOH/H$_2$O (4.00 mL) for 24 h. Purification by typical silica gel flash chromatography (CH$_2$Cl$_2$/CH$_3$OH/NH$_{3(aq)}$ 97.5:2.5:0.125) of the crude gave **93** as a yellow oil (0.05 g, 38 %); R_f 0.31 (EtOAc). **^{1}H-NMR** (400 MHz, CDCl$_3$) δ 7.57 (dd, *J* = 8.4 and 2.0 Hz, 2H, Ar), 7.35 (dd, *J* = 8.6 Hz and 2.0, 2H, Ar), 5.71 (s, 1H, CH-pyrazole), 4.97 (dd, *J* = 10.4 and 2.4 Hz, 1H, CH, THP), 4.15–4.06 (m, 1H, CH$_2$, THP), 3.70 (br. s, 2H, NH$_2$), 3.58–3.43 (m, 1H, CH$_2$, THP), 2.53–2.38 (m, 1H, CH$_2$, THP), 2.01 (d, *J* = 11.6 Hz, 1H, CH$_2$, THP), 1.81–1.67 (m, 2H, CH$_2$, THP), 1.55–1.45 (m, 2H, CH$_2$, THP).

5-(4-methoxyphenyl)-1-(tetrahydro-2*H*-pyran-2-yl)-1*H*-pyrazol-3-amine (94, Scheme 3)
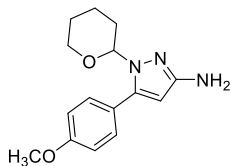
According to the general procedure, treatment of **84b** (0.30 g, 0.95 mmol) with KOH (0.53 g, 9.50 mmol) in a mixture of EtOH/H$_2$O (9.50 mL) for 48 h gave **94** as a white solid (0.22

g, 85 %); R_f 0.40 (EtOAc). **¹H-NMR** (400 MHz, CDCl₃) δ 7.40 (d, J = 8.8 Hz, 2H, Ar), 6.97 (d, J = 8.8 Hz, 2H, Ar), 5.67 (s, 1H, CH-pyrazole), 5.01 (dd, J = 10.4 and 2.4 Hz, 1H, CH, THP), 4.16–4.07 (m, 1H, CH₂, THP), 3.86 (s, 3H, OCH₃), 3.68 (br. s, 2H, NH₂), 3.54 (td, J = 12.0 and 2.4 Hz, 1H, CH₂, THP), 2.51–2.40 (m, 1H, CH₂, THP), 2.04–1.96 (m, 1H, CH₂, THP), 1.86–1.66 (m, 2H, CH₂, THP), 1.59–1.43 (m, 2H, CH₂, THP).

### 5-(4-nitrophenyl)-1-(tetrahydro-2*H*-pyran-2-yl)-1*H*-pyrazol-3-amine   (95, Scheme 3)
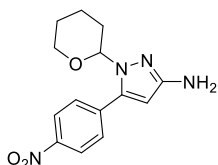
According to the general procedure, treatment of **85b** (0.06 g, 0.18 mmol) with KOH (0.10 g, 1.80 mmol) in a mixture of EtOH/H₂O (2.00 mL) for 48 h gave **95** as a yellow oil (0.05 g, 96 %); R_f 0.45 (EtOAc). **¹H-NMR** (400 MHz, CDCl₃) δ 8.31 (d, J = 8.4 Hz, 2H, Ar), 7.67 (d, J = 8.8 Hz, 2H. Ar), 5.83 (s, 1H, CH-pyrazole), 4.98 (dd, J = 10.6 and 2.2 Hz, 1H, CH, THP), 4.18–4.09 (m, 1H, CH₂, THP), 3.74 (br. s, 2H, NH₂), 3.55 (td, J = 11.4 and 2.4 Hz, 1H, CH₂, THP), 2.55–2.40 (m, 1H, CH₂, THP), 2.08–1.98 (m, 1H, CH₂, THP), 1.86–1.46 (m, 4H, 2CH₂, THP).

### 1-(tetrahydro-2*H*-pyran-2-yl)-5-(thiophen-2-yl)-1*H*-pyrazol-3-amine   (96, Scheme 3)
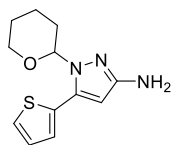
In line with the general procedure, treatment of **86b** (0.25 g, 0.86 mmol) with KOH (0.48 g, 8.60 mmol) in a mixture of EtOH/H₂O (8.60 mL) for 8 h gave **96** as a white solid (0.21 g, 98 %); R_f 0.50 (EtOAc). **¹H-NMR** (400 MHz, CDCl₃) δ 7.39 (dd, J = 5.2 and 1.2 Hz, 1H, CH-thiophene), 7.20 (dd, J = 3.6 and 1.2 Hz, 1H, CH-thiophene), 7.11 (dd, J = 5.2 and 3.6 Hz, 1H, CH-thiophene), 5.80 (s, 1H, CH-pyrazole), 5.22 (dd, J = 10.4 and 2.4 Hz, 1H, CH, THP), 4.10 (ddt, J = 11.6, 4.4 and 2.4 Hz, 1H, CH₂, THP), 3.69 (br. s, 2H, NH₂), 3.62 (td, J = 11.6 and 2.4 Hz, 1H, CH₂, THP), 2.53–2.38 (m, 1H, CH₂, THP), 2.09–2.00 (m, 1H, CH₂, THP), 1.88–1.82 (m, 1H, CH₂, THP),1.78–1.67 (m, 1H, CH₂, THP), 1.66–1.53 (m, 1H, CH₂, THP), 1.57–1.48 (m, 1H, CH₂, THP).

**5-(pyridin-2-yl)-1-(tetrahydro-2*H*-pyran-2-yl)-1*H*-pyrazol-3-amine** **(97, Scheme 3)**
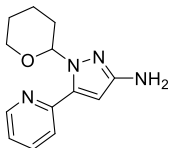
According to the general procedure, treatment of **87b** (0.06 g, 0.21 mmol) with KOH (0.12 g, 2.10 mmol) in a mixture of EtOH/H_2O (2.00 mL) for 27 h gave **97** as an oil (0.04 g, 78 %); R_f 0.22 (EtOAc). **^{1}H-NMR** (400 MHz, CDCl$_3$) δ 8.66 (d, J = 4.8 Hz, 1H, Ar), 7.78–7.72 (m, 1H, Ar), 7.53 (d, J = 8.0 Hz, 1H, Ar), 7.28–7.23 (m, 1H, Ar), 6.00 (dd, J = 10.0 and 2.0 Hz, 1H, CH, THP), 5.96 (s, 1H, CH-pyrazole), 4.06 (d, J = 11.2 Hz, 1H, CH$_2$, THP), 3.71 (br. s, 2H, NH$_2$), 3.60–3.53 (m, 1H, CH$_2$, THP), 2.50–2.39 (m, 1H, CH$_2$, THP), 2.05–2.00 (m, 1H, CH$_2$, THP), 1.76–1.49 (m, 4H, 2CH$_2$, THP).

3-(pyridin-3-yl)-1-(tetrahydro-2*H*-pyran-2-yl)-1*H*-pyrazol-5-amine **(98, Scheme 4)**
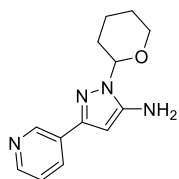
Following the general procedure, treatment of **88a** (0.29 g, 1.00 mmol) with KOH (0.56 g, 10.00 mmol) in a mixture of EtOH/H_2O (10.00 mL) for 48 h gave **98** as an oil (0.24 g, 98 %); R_f 0.22 (EtOAc). **^{1}H-NMR** (400 MHz, DMSO-d_6) δ 8.88 (dd, J = 2.3 and 0.8 Hz, 1H, Ar), 8.45 (dd, J = 4.8 and 1.7 Hz, 1H, Ar), 8.03 (dt, J = 7.9 and 2.0 Hz, 1H, Ar), 7.37 (dd, J = 7.9 and 4.8 Hz, 1H, Ar), 5.78 (s, 1H, CH-pyrazole), 5.43 (br. s, 2H, NH$_2$), 5.29 (dd, J = 9.8 and 2.5 Hz, 1H, CH, THP), 3.96–3.76 (m, 1H, CH$_2$, THP), 3.68–3.61 (m, 1H, CH$_2$, THP), 2.39–2.19 (m, 1H, CH$_2$, THP), 2.05–1.96 (m, 1H, CH$_2$, THP), 1.84–1.78 (m, 1H, CH$_2$, THP), 1.69–1.45 (m, 3H, CH$_2$, THP).

3-phenyl-1-(tetrahydro-2*H*-pyran-2-yl)-1*H*-pyrazol-5-amine (115, Scheme 6)
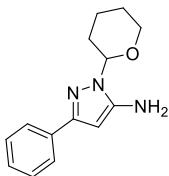
In line with the general procedure, treatment of **80a** (0.18 g, 0.63 mmol) with KOH (0.35 g, 6.30 mmol) in a mixture of EtOH/H_2O (6.30 mL) for 29 h gave **115** as yellowish solid (0.15 g, 98 %); R_f 0.70 (CH$_2$Cl$_2$/CH$_3$OH/NH$_{3(aq)}$ 98.5:1.5:0.075). **^{1}H-NMR** (400 MHz, CDCl$_3$) δ 7.74 (d, J = 6.8 Hz, 2H, Ph), 7.35 (t, J = 7.6 Hz, 2H, Ph), 7.28–7.24

(m, 1H, Ph), 5.84 (s, 1H, CH-pyrazole), 5.40 (dd, J = 9.0 and 3.0 Hz, 1H, CH, THP), 4.02 (br. s, 2H, NH$_2$), 4.01–3.98 (m, 1H, CH$_2$, THP), 3.71–3.66 (m, 1H, CH$_2$, THP), 2.48–2.38 (m, 1H, CH$_2$, THP), 2.18–2.04 (m, 2H, CH$_2$, THP), 1.73–1.62 (m, 3H, CH$_2$, THP).

General procedure of phenyl carbamate formation: synthesis of intermediates 114, 116 and 117 (Scheme 6)

To a solution of the corresponding amine **48**, **89** or **115** (1.00 mmol) in pyridine (5.0 mL) at 0 °C under nitrogen atmosphere, phenyl chloroformate (1.0 molar equiv) was added dropwise over a period of 10 minutes. The resulting reaction mixture (yellow solution) was warmed to rt and was stirred for 12 h at the same temperature. The mixture was quenched with water (100.0 mL) and was worked up applying one of the following methods:

   a) the obtained precipitate was filtered off, washed with water and dried under *vacuum* to give the desired product;

   b) the aqueous phase was extracted with Et$_2$O (3 x 25.0 mL); the combined organic layers were washed with brine, dried over Na$_2$SO$_4$ and concentrated to dryness under reduced pressure to give a crude which was purified by typical silica gel flash chromatography, affording the title compound.

**phenyl (5-methyl-1H-pyrazol-3-yl)carbamate (114, Scheme 6)**
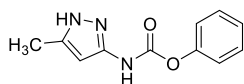
 The title compound was synthetized according to the general procedure (method **a**) using 3-amino-5-methylpyrazole **48** (0.50 g, 5.15 mmol) and phenyl chloroformate (0.65 mL, 5.15 mmol) in pyridine (25.7 mL), to yield **114** as a white solid (0.10 g, 9 %) without further purification; R_f 0.15 (CH$_2$Cl$_2$/CH$_3$OH 95:5). **^{1}H-NMR** (400 MHz, CDCl$_3$) δ 8.45 (br. s, 1H, NHCO), 7.42–7.39 (m, 2H, Ph), 7.25–7.19 (m, 3H, Ph), 6.37 (s, 1H, CH-pyrazole), 2.31 (s, 3H, CH$_3$).

phenyl [5-methyl-1-(tetrahydro-2H-pyran-2-yl)-1H-pyrazol-3-yl]carbamate (116, Scheme 6)
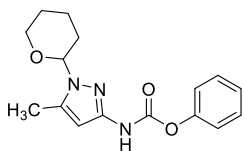
The title compound was synthetized according to the general procedure (method **b**) starting from amine **89** (0.25 g, 1.38 mmol) and phenyl chloroformate (0.17 mL, 1.38 mmol) in pyridine (6.9 mL). Purification by typical silica gel flash chromatography (PE/EtOAc 80:20) allowed to isolate **116** as a white solid (0.12 g, 29 %); R_f 0.26 (PE/EtOAc 70:30). **¹H-NMR** (400 MHz, CDCl₃) δ 7.42–7.33 (m, 3H, Ph and NHCO), 7.27–7.18 (m, 1H, Ph), 7.22–7.13 (m, 2H, Ph), 6.36 (s, 1H, CH-pyrazole), 5.17 (dd, J = 10.0 and 2.4 Hz, 1H, CH, THP), 4.10–4.04 (m, 1H, CH₂, THP), 3.64 (td, J = 11.6 and 2.8 Hz, 1H, CH₂, THP), 2.43–2.33 (m, 1H, CH₂, THP), 2.31 (s, 3H, CH₃), 2.14–2.06 (m, 1H, CH₂, THP), 1.93–1.84 (m, 1H, CH₂, THP), 1.80–1.69 (m, 1H, CH₂, THP), 1.69–1.57 (m, 2H, CH₂, THP).

phenyl [3-phenyl-1-(tetrahydro-2*H*-pyran-2-yl)-1*H*-pyrazol-5-yl]carbamate (117, Scheme 6)
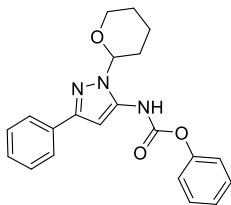
The title compound was synthetized according to the general procedure (method **b**) using amine **115** (0.07 g, 0.29 mmol) and phenyl chloroformate (0.04 mL, 0.29 mmol) in pyridine (1.5 mL). Purification by typical silica gel flash chromatography (PE/EtOAc 80:20) allowed to isolate **117** as a white solid (0.05 g, 47 %); R_f 0.45 (PE/EtOAc 80:20). **¹H-NMR** (400 MHz, DMSO-d_6) δ 7.91–7.75 (m, 2H, Ph), 7.49–7.40 (m, 6H, Ph and NHCO), 7.38–7.28 (m, 3H, Ph), 7.21 (s, 1H, CH-pyrazole), 5.76 (dd, J = 9.2 and 2.8 Hz, 1H, CH, THP), 3.94 (d, J = 11.2 Hz, 1H, CH₂, THP), 3.81–3.75 (m, 1H, CH₂, THP), 2.41–2.26 (m, 1H, CH₂, THP), 2.15–1.70 (m, 3H, CH₂, THP), 1.65–1.56 (m, 2H, CH₂, THP).

General procedure of *N*-alkylation reaction: synthesis of arylpiperazine intermediates 127, 128 and 131-134 (Scheme 7)

1) A stirred mixture of commercially available arylpiperazine **122** or **123** (1.00 mmol), *N*-(chloroalkyl)phthalimide **124** or **126** (2.0 molar equiv) and K₂CO₃ (3.5 molar equiv) in CH₃CN (10.0 mL) was stirred under reflux for 14 h. Upon

145

completion, the hot suspension was filtered, and the residue washed with acetone several times. The collected filtrate was concentrated under reduced pressure to give the desired product after appropriate purification.

2) A microwave vial was loaded with commercially available arylpiperazine **122** or **123** (1.00 mmol) and the appropriate commercial alkyl bromide derivative **121** or **125** (1.05 molar equiv), followed by CH$_3$CN (2.0 mL) and TEA (3.0 molar equiv). The vial was heated at 100 °C under MW irradiation for 40 min. The resulting solid was filtered, and the filtrate was concentrated under reduced pressure to obtain a crude residue which was worked up applying one of the following methods:

   a) the crude was portioned between water (10.0 mL) and CH$_2$Cl$_2$ (10.0 mL). After stirring the mixture for 5 minutes at rt, the separated organic layer was dried over Na$_2$SO$_4$, filtered and evaporated to dryness. The resulting residue was suspended in HCl 2N aqueous solution (10.0 mL) and the mixture was stirred 1 h at rt. The aqueous layer was extracted first with Et$_2$O (2 x 10.0 mL) and then with CH$_2$Cl$_2$ (3 x 10.0 mL). The combined CH$_2$Cl$_2$ phases were dried over Na$_2$SO$_4$, filtered and concentrated to dryness to give the desired compound as a hydrochloride salt.

   b) The crude was dissolved in CH$_2$Cl$_2$ (10.0 mL) and washed with H$_2$O (2 x 10.0 mL) and saturated NaHCO$_3$ aqueous solution (2 x 10.0 mL). The organic phase was dried over Na$_2$SO$_4$, filtered and concentrated to dryness to afford the title compound as a free base.

ethyl 5-[4-(2,3-dichlorophenyl)piperazin-1-yl]pentanoate hydrochloride (127, Scheme 7)
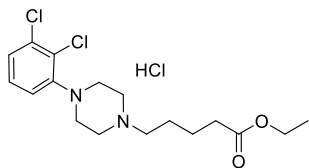
In line with the general procedure (method **2a**), the title compound was synthetized starting from 1-(2,3-dichlorophenyl)piperazine hydrochloride **122** (0.50 g, 1.87 mmol), ethyl 5-bromovalerate **121** (0.31 mL, 1.96 mmol) and TEA (0.78 mL, 5.61

mmol) in CH_3CN (3.7 mL), to yield **127** as a white solid (0.40 g, 54 %); $\boldsymbol{R_f}$ 0.27 (CH_2Cl_2/CH_3OH 95:5). **^{1}H-NMR** (400 MHz, $CDCl_3$) δ 7.25-7.18 (m, 2H, Ar), 7.04 (d, J = 6.8 Hz, 1H, Ar), 4.15 (q, J = 6.8 Hz, 2H, CH_2), 3.72–3.61 (m, 4H, $2CH_2$-piperazine), 3.38 (br. d, J = 12.0 Hz, 2H, CH_2), 3.11–3.02 (m, 4H, $2CH_2$-piperazine), 2.41 (t, J = 7.2 Hz, 2H, CH_2), 2.09–1.99 (m, 2H, CH_2), 1.77–1.71 (m, 2H, CH_2), 1.27 (t, J = 7.2 Hz, 3H, CH_3).

ethyl 5-[4-(2-methoxyphenyl)piperazin-1-yl]pentanoate (128, Scheme 7)
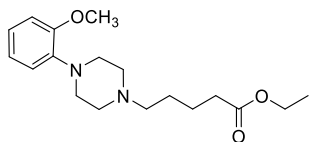
Following the general procedure (method **2b**), the title compound was synthetized starting from 1-(2-methoxyphenyl)piperazine **123** (2.00 g, 11.55 mmol), ethyl 5-bromovalerate **121** (2.00 g, 11.55 mmol) and TEA (5.58 g, 40.42 mmol) in CH_3CN (115.0 mL), to yield **128** as a white solid (1.50 g, 60 %); $\boldsymbol{R_f}$ 0.33 (EtOAc). **^{1}H-NMR** (400 MHz, $CDCl_3$) δ 7.00–6.87 (m, 3H, Ar), 6.84 (dd, J = 8.0 and 1.6 Hz, 1H, Ar), 4.12 (q, J = 7.2 Hz, 2H, CH_2), 3.85 (s, 3H, OCH_3), 3.08 (br. s, 4H, $2CH_2$-piperazine), 2.63 (br. s, 4H, $2CH_2$-piperazine), 2.41 (t, J = 7.6 Hz, 2H, CH_2), 2.33 (t, J = 7.2 Hz, 2H, CH_2), 1.73–1.62 (m, 2H, CH_2), 1.62–1.49 (m, 2H, CH_2), 1.25 (t, J = 7.2 Hz, 3H, CH_3).

### 2-{2-[4-(2,3-dichlorophenyl)piperazin-1-yl]ethyl}isoindoline-1,3-dione hydrochloride (131, Scheme 7)
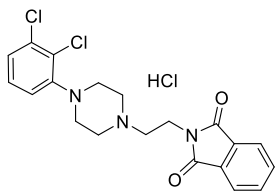
Following the general procedure (method **1**), the title compound was prepared starting from 1-(2,3-dichlorophenyl)piperazine hydrochloride **122** (0.66 g, 2.85 mmol), *N*-(2-chloroethyl)phthalimide **124** (1.19 g, 5.70 mmol), and K_2CO_3 (1.38 g, 9.98 mmol) in CH_3CN (28.5 mL). The resulting crude was suspended in HCl 2N aqueous solution (25.0 mL), and the mixture stirred 1 h at rt. The aqueous layer was extracted with CH_2Cl_2 (3 x 25.0 mL), and the combined organic phases were dried over Na_2SO_4, filtered and concentrated to dryness. Treatment of the obtained residue with Et_2O afforded a precipitate, which was collected by filtration,

washed with fresh Et₂O, and dried under *vacuum* to give **131** as a hydrochloride salt (white solid, 0.27 g, 21 %); R_f 0.23 (PE/EtOAc 70:30). **¹H-NMR** (400 MHz, DMSO-d_6) δ 10.62 (br. s, 1H, NH⁺), 7.92–7.85 (m, 4H, Ar), 7.38–7.34 (m, 2H, Ar), 7.21 (dd, J = 9.6 and 3.6 Hz, 1H, Ar), 4.03 (br. s, 2H, CH₂), 3.74 (br. d, J = 9.2 Hz, 2H, CH₂), 3.53–3.45 (m, 4H, 2CH₂), 3.31–3.22 (m, 2H, CH₂), 3.16–3.10 (m, 2H, CH₂).

2-{3-[4-(2,3-dichlorophenyl)piperazin-1-yl]propyl}isoindoline-1,3-dione (132, Scheme 7)
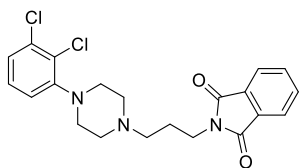
In line with the general procedure (method **2b**), the title compound was synthetized starting from 1-(2,3-dichlorophenyl)piperazine hydrochloride **122** (1.00 g, 3.74 mmol), *N*-(3-bromopropyl)phthalimide **125** (1.05 g, 3.92 mmol), and TEA (1.56 mL, 11.22 mmol) in CH₃CN (7.5 mL). Purification by typical silica gel flash chromatography (CH₂Cl₂/CH₃OH, gradient elution) allowed to isolate **132** (on elution with CH₂Cl₂/CH₃OH 97.5:2.5) as a beige solid (0.90 g, 58 %); R_f 0.50 (CH₂Cl₂/CH₃OH/NH₃₍aq₎ 95:5:0.25). **¹H-NMR** (hydrochloride analogue, 400 MHz, DMSO-d_6) δ 10.62 (br. s, 1H, NH⁺), 7.92–7.85 (m, 4H, Ar), 7.38–7.34 (m, 2H, Ar), 7.21 (dd, J = 9.6 and 3.6 Hz, 1H, Ar), 4.03 (br. s, 2H, CH₂), 3.74 (br. d, J = 9.2 Hz, 2H, CH₂), 3.53–3.45 (m, 4H, 2CH₂), 3.31–3.22 (m, 2H, CH₂), 3.16–3.10 (m, 2H, CH₂).
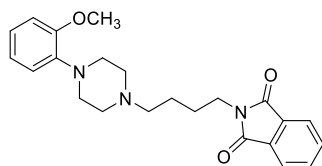
2-{4-[4-(2,3-dichlorophenyl)piperazin-1-yl]butyl}isoindoline-1,3-dione (133, Scheme 7)
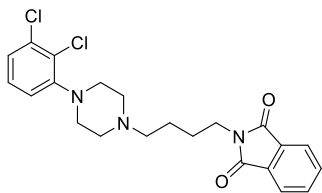
Following the general procedure (method **1**), the title compound was prepared starting from 1-(2,3-dichlorophenyl)piperazine hydrochloride **122** (2.55 g, 9.34 mmol), *N*-(4-chlorobuthyl)phthalimide **126** (4.44 g, 18.68 mmol), and K₂CO₃ (4.51 g, 32.69 mmol) in CH₃CN (93.4 mL). Purification of the crude product by typical silica gel flash chromatography (CH₂Cl₂/CH₃OH, gradient elution) allowed to isolate **133** (on elution with CH₂Cl₂/CH₃OH 95:5) as a white solid (3.32 g, 82 %); R_f 0.45 (CH₂Cl₂/CH₃OH/NH₃₍aq₎ 98:2:0.1). **¹H-NMR** (400 MHz,

DMSO-d_6) δ 7.90–7.82 (m, 4H, Ar), 7.37–7.23 (m, 2H, Ar), 7.15–7.10 (m, 1H, Ar), 3.61 (t, J = 7.0 Hz, 2H, CH$_2$), 2.97–2.94 (m, 4H, 2CH$_2$-piperazine), 2.53–2.51 (m, 4H, 2CH$_2$-piperazine), 2.36 (t, J = 7.2 Hz, 2H, CH$_2$), 1.64 (p, J = 7.1 Hz, 2H, CH$_2$), 1.47 (p, J = 7.3 Hz, 2H, CH$_2$).

### 2-{4-[4-(2-methoxyphenyl)piperazin-1-yl]butyl}isoindoline-1,3-dione (134, Scheme 7)

Following the general procedure (method **1**), the title compound was prepared starting from 1-(2-methoxyphenyl)piperazine **123** (1.00 g, 5.20 mmol), *N*-(4-chlorobuthyl)phthalimide **126** (2.47 g, 10.40 mmol), and K$_2$CO$_3$ (2.51 g, 18.20 mmol) in CH$_3$CN (52.0 mL). Purification of the crude product by typical silica gel flash chromatography (CH$_2$Cl$_2$/CH$_3$OH/NH$_{3(aq)}$ 98:2:0.1) allowed to isolate **134** as a yellow oil (0.75 g, 37 %); R_f 0.24 (CH$_2$Cl$_2$/CH$_3$OH/NH$_{3(aq)}$ 98:2:0.1). **^{1}H-NMR** (400 MHz, CDCl$_3$) δ 7.85 (dd, J = 5.4 and 3.0 Hz, 2H, Ar), 7.72 (dd, J = 5.6 and 3.2 Hz, 2H, Ar), 7.02–6.89 (m, 3H, Ar), 6.86 (d, J = 8.0 Hz, 1H, Ar), 3.86 (s, 3H, OCH$_3$), 3.74 (t, J = 7.2 Hz, 2H, CH$_2$), 3.09 (br. s, 4H, 2CH$_2$-piperazine), 2.65 (br. s, 4H, 2CH$_2$-piperazine), 2.45 (t, J = 7.6 Hz, 2H, CH$_2$), 1.81–1.71 (m, 2H, CH$_2$), 1.63–1.55 (m, 2H, CH$_2$).

General procedure of hydrazinolysis reaction: synthesis of arylpiperazine amine derivatives 135-138 (Scheme 7) and intermediate 150 (Scheme 9)

To a suspension of the corresponding phthalimide intermediate **131-134** or **32** (1.00 mmol) in EtOH (4.0 mL), hydrazine monohydrate (3.0 molar equiv) was added dropwise and the resulting mixture was stirred under reflux for 3-5 h. After cooling at rt, the reaction mixture was concentrated under reduced pressure and the residue was suspended in CH$_2$Cl$_2$. The resulting white solid was filtered under *vacuum* and washed several times with fresh CH$_2$Cl$_2$. The collected filtrate was evaporated under reduced pressure to obtain the desired compound without further purification.

2-[4-(2,3-dichlorophenyl)piperazin-1-yl]ethan-1-amine (135, Scheme 7)
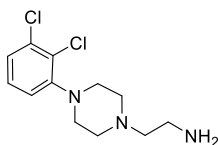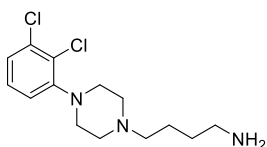
In line with the general procedure, treatment of phthalimide intermediate **131** (0.27 g, 0.67 mmol) with hydrazine monohydrate (0.10 mL, 2.01 mmol) in EtOH (2.7 mL) for 4 h afforded **135** as a yellowish oil (0.14 g, 76 %); R_f 0.11 (CH_2Cl_2/CH_3OH 90:10). **^{1}H-NMR** (400 MHz, $CDCl_3$) δ 7.15–7.11 (m, 2H, Ar), 6.94 (d, $J = 9.2$ Hz, 1H, Ar), 3.08 (br. s, 4H, 2CH_2-piperazine), 2.99 (t, $J = 6.0$ Hz, 2H, CH_2), 2.87 (br. s, 2H, NH_2), 2.69 (br. s, 4H, 2CH_2-piperazine), 2.64 (t, $J = 5.4$ Hz, 2H, CH_2).

3-[4-(2,3-dichlorophenyl)piperazin-1-yl]propan-1-amine hydrochloride (136, Scheme 7)
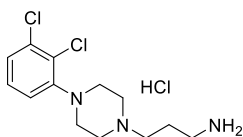
In line with the general procedure, phthalimide intermediate **132** (0.90 g, 2.15 mmol) was treated with hydrazine monohydrate (0.31 mL, 6.45 mmol) in EtOH (8.6 mL) for 5 h. To the hot mixture was added HCl 2N aqueous solution until pH 2, and reflux was continued for one more hour. After cooling to rt, the mixture was filtrated, the residue washed with CH_3OH, and the filtrate evaporated to dryness. Treatment of the obtained residue with Et_2O afforded a precipitate, which was collected by filtration, washed with fresh Et_2O, and dried under *vacuum* to give **136** as a hydrochloride salt (beige solid, 0.50 g, 64 %); R_f 0.05 (CH_2Cl_2/CH_3OH 92.5:7.5). **^{1}H-NMR** (400 MHz, DMSO-d_6) δ 7.98 (br. s, 3H, NH_3^+), 7.38–7.34 (m, 2H, Ar), 7.21 (d, $J = 5.6$ Hz, 1H, Ar), 3.57 (br. d, $J = 10.4$ Hz, 2H, CH_2), 3.44 (br. d, $J = 12.0$ Hz, 2H, CH_2), 3.26–3.20 (m, 6H, 3CH_2), 2.98–2.88 (m, 2H, CH_2), 2.10–2.01 (m, 2H, CH_2).
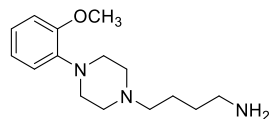
4-[4-(2,3-dichlorophenyl)piperazin-1-yl]butan-1-amine (137, Scheme 7)

In line with the general procedure, treatment of phthalimide intermediate **133** (0.20 g, 0.46 mmol) with hydrazine monohydrate (0.07 mL, 1.38 mmol) in EtOH (1.8 mL) for 3 h afforded **137** as a red oil (0.13 g, 93 %); R_f 0.09 (CH_2Cl_2/CH_3OH 90:10). **^{1}H-NMR** (400 MHz, $CDCl_3$) δ 7.10–7.08 (m, 2H, Ar), 6.90 (t, $J = 5.2$ Hz, 1H, Ar), 3.20–3.17

(m, 2H, CH$_2$), 3.01 (br. s, 4H, 2CH$_2$-piperazine), 2.58 (br. s, 4H, 2CH$_2$-piperazine), 2.40 (t, J = 7.6 Hz, 2H, CH$_2$), 1.66–1.51 (m, 4H, 2CH$_2$).

4-[4-(2-methoxyphenyl)piperazin-1-yl]butan-1-amine (138, Scheme 7)

In line with the general procedure, treatment of phthalimide intermediate **134** (0.72 g, 1.83 mmol) with hydrazine monohydrate (0.27 mL, 5.49 mmol) in EtOH (7.3 mL) for 3 h afforded **138** as an orange oil (0.45 g, 93 %); R_f 0.08 (CH$_2$Cl$_2$/CH$_3$OH 90:10). **^{1}H-NMR** (400 MHz, CDCl$_3$) δ 7.01–6.97 (m, 1H, Ar), 6.94–6.90 (m, 2H, Ar), 6.85 (d, J = 7.6 Hz, 1H, Ar), 3.86 (s, 3H, OCH$_3$), 3.09 (br. s, 4H, 2CH$_2$-piperazine), 2.77 (t, J = 6.4 Hz, 2H, CH$_2$), 2.66 (br. s, 4H, 2CH$_2$-piperazine), 2.42 (t, J = 7.2 Hz, 2H, CH$_2$), 1.66–1.53 (m, 4H, 2CH$_2$).

### 2-(1-((8-chloroquinolin-2-yl)methyl)piperidin-4-yl)ethan-1-amine (150, Scheme 9)
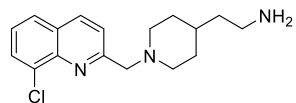
In line with the general procedure, treatment of phthalimide intermediate **32** (0.15 g, 0.34 mmol) with hydrazine monohydrate (0.05 mL, 1.02 mmol) in EtOH (3.4 mL) for 3 h afforded **150** as an orange oil (0.10 g, 97 %); R_f 0.09 (CH$_2$Cl$_2$/CH$_3$OH 90:10). **^{1}H-NMR** (400 MHz, DMSO-d_6) δ 8.41 (d, J = 8.5 Hz, 1H, Ar), 7.98 – 7.85 (m, 2H, Ar), 7.78 (t, J = 6.8 Hz, 1H, Ar), 7.55 (t, J = 7.8 Hz, 1H, Ar), 3.78 (s, 2H, CH$_2$NH), 2.82 (d, J = 11.2 Hz, 2H, piperidine), 2.75 (q, J = 6.6 Hz, 2H, CH$_2$NH$_2$), 2.07 (dd, J = 22.0, 11.5 Hz, 2H, piperidine), 1.64 (d, J = 12.4 Hz, 2H, piperidine), 1.33 (q, J = 7.0, 6.6 Hz, 2H, piperidine), 1.21 (d, J = 16.6 Hz, 2H), 1.15-10 (m, 3H).

Acyl chloride formation: synthesis of 5-[4-(2,3-dichlorophenyl)piperazin-1-yl]pentanoyl chloride (139, Scheme 4)

To a heterogeneous solution of acid **129** (0.20 g, 0.544 mmol) in dry CH_2CH_2 (1.86 ml), cooled down to 0 °C, dry DMF (0.001 ml, 0.02 mmol) was added dropwise followed by the slow addition of oxalyl chloride (0.06 ml, 0.664 mmol). After ice-bath removal, the resulting mixture was allowed to stir for 1 h at rt. Evaporation of the volatiles under reduced pressure gave **139** crude (0.544 mmol, assumed 100%), which was employed in the next synthetic step without further purification.
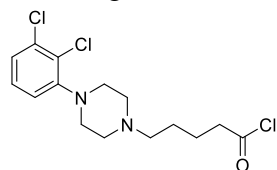
**Chlorination reaction: synthesis of 8-chloro-2-(chloromethyl)quinoline (141, Scheme 8)**
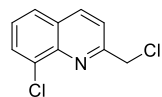
A microwave vial was loaded with commercially available 8-chloromethylquinoline (1.00 g, 5.63 mmol, 1.0 molar equiv), TBAI (2.08 g, 5.63 mmol, 1.00 molar equiv) ed urea (0.34 mg, 5.63 mmol, 1.00 molar equiv) in DCE (28.0 mL). The vial was heated at 110 °C under MW irradiation for 30 min. Upon completion, the solvent was removed under reduced pressure affording a crude which was purified by typical silica gel flash chromatography (toluene), to yield 141 as a white solid (0.40 g, 67 %). **^{1}H-NMR** (400 MHz, CDCl$_3$) δ 8.20 (d, J = 8.4 Hz, 1H, Ar), 7.82(dd, J = 7.6 Hz, 1.2 Hz, 1H, Ar), 7.73 (dd, 1H, J = 8.0 Hz, 1.2 Hz, 1H, Ar), 7.70 (d, J = 8.4 Hz, 1H, Ar), 7.47 (t, J=8.0 Hz, 1H, Ar), 4.91 (s, 2H, ClCH$_2$).

General procedure of N-debenzylation reaction: synthesis of intermediate 142 and 143 (Scheme 10)

To a solution of the corresponding *N*-benzyl intermediate **157** or **158** (1.00 mmol) in EtOH (10.0 mL), hydrazine monohydrate (2.0 molar equiv) was added dropwise, followed by catalytic amount of Pd/C 10 % (5-10 % molar equiv). The resulting mixture was heated at 80°C for 5 h. After cooling at rt, the reaction mixture was filtered to remove the catalyst. The collected filtrate was evaporated under reduced pressure to obtain the desired compound without further purification.

tert-butyl (piperidin-3-ylmethyl)carbamate (142, Scheme 10)
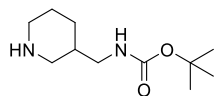
In line with the general procedure, treatment of benzyl intermediate **157** (0.30 g, 0.98 mmol) with hydrazine monohydrate (0.09 g, 1.77 mmol) afforded **142** as an oil (0.25 g, 87 %). **¹H-NMR** (400 MHz, CDCl₃) δ 4.61 (br s, 1H, NH), 3.06 (d, J = 12.40 Hz, 1H, piperidine), 2.99 (t, J = 6.80 Hz, 3H, piperidine), 2.52-2.59 (m, 1H, piperidine), 1.98-2.06 (m, 1H, piperidine), 1.79 (d, J=13.20 Hz, 1H, piperidine), 1.58-1.69 (m, 2H, piperidine), 1.43 (s, 9H, 3CH₃), 1.09 (q, J = 3.20 Hz, 1H, piperidine).

tert-butyl (piperidin-4-ylmethyl)carbamate (143, Scheme 10)
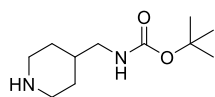
In line with the general procedure, treatment of benzyl intermediate **158** (0.95 g, 3.12 mmol) with hydrazine monohydrate (0.31 g, 6.25 mmol) afforded **143** as an oil (0.39 g, 40 %). **¹H-NMR** (400 MHz, CDCl₃) δ 4.65 (br. s, 1H, NH), 3.42 (d, J = 12.4 Hz, 2H, piperidine), 3.02 (t, J = 6.4 Hz, 2H, piperidine), 2.68 (t, J = 11.2 Hz, 2H, piperidine), 6.88 (t, J = 14.0 Hz, 2H, piperidine), 1.50 (s, 1H, NH, piperidina), 1.44 (s, 9H, 3CH₃), 1.33-1.40 (m, 2H, piperidine), 1.22-1.32 (m, 1 H, piperidine).

General procedure of N-alkylation reaction: synthesis of intermediate 144, 145 (Scheme 8) and 148 (Scheme 9)

A solution of chloromethyl derivative **141** (1.00 mmol), the appropriate amine **142**, **143** or 4-piperidine-ethanol (1.00 or 2.00 molar equiv), and NEt₃ (2.5 or 3.0 molar equiv) in CH₃CN (10.0 mL) was stirred under reflux for 14 h. Upon completion, the reaction mixture was dried under reduced pressure and the obtained crude was purified by typical silica gel flash chromatography, to afford the title compounds.

tert- butyl ((1-((8-chloroquinolin-2-yl)methyl)piperidin-3-yl)methyl)carbamate (144, Scheme 8)
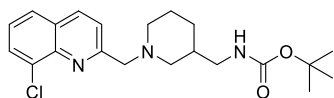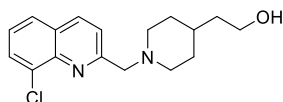
In line with the general procedure, reaction of amine **142** (0.24 g, 1.11 mmol) with chloromethyl **141** (0.22 g, 1.11 mmol) gave a crude which was purified by typical silica gel flash chromatography (CH_2Cl_2/CH_3OH/$NH_{3(aq)}$ 97.5:2.5:0.125), to yield **144** as an oil (0.27 g, 62 %). **^{1}H-NMR** (400 MHz, $CDCl_3$) δ 1.43 (s, 9H, 3CH$_3$), 1.62-1.73 (m, 5H, piperidine), 1.75 (s, 1H, piperidine), 2.20 (d, J = 15.2 Hz, 1H, piperidine), 2.77 (d, J = 10.4 Hz, 1H, piperidine), 2.85 (d, J = 8.8 Hz, 1H, piperidine), 3.05 (t, J = 6.8 Hz, 2H, CH$_2$), 3.90 (s, 2H, C$\underline{H}_2$NH), 4.80 (s, 1H, NH), 7.42 (t, J = 8.0 Hz, 1H, Ar), 7.71-7.75 (m, 2H, Ar), 7.80 (q, J = 1.60 Hz, 1H, Ar), 8.13 (d, J = 8.8 Hz, 1H, Ar).

tert- butyl ((1-((8-chloroquinolin-2-yl)methyl)piperidin-4-yl)methyl)carbamate (145, Scheme 8)
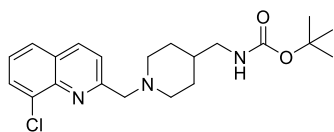
In line with the general procedure, reaction of amine **143** (0.39 g, 1.83 mmol) with chloromethyl **141** (0.37 g, 1.83 mmol) gave a crude which was purified by typical silica gel flash chromatography (CH_2Cl_2/CH_3OH/$NH_{3(aq)}$ 97.5:2.5:0.125), to yield **145** as yellow solid (0.47 g, 66 %). **^{1}H-NMR** (400 MHz, $CDCl_3$) δ 1.31-1.35 (m, 2H, piperidine), 1.44 (s, 10H, 3CH$_3$ and H-piperidine), 1.69 (d, J = 11.2 Hz, 2H, piperidine), 2.17 (t, J = 10.8 Hz, 2H, piperidine), 2.94 (d, J = 11.6 Hz, 2H, piperidine), 3.04 (t, J = 6.0 Hz, 2H, C$\underline{H}_2$NHBoc), 3.92 (s, 2H, C$\underline{H}_2$NH), 4.65 (br. s, 1H, NH), 7.27-7.43 (m, 1H, Ar), 7.72 (dd, J = 8.8 and 1.6 Hz, 2H, Ar), 7.80 (d, J = 7.6 Hz, 1H, Ar), 8.13 (d, J = 8.4 Hz, 1H, Ar).

### 2-(1-((8-chloroquinolin-2-yl)methyl)piperidin-4-yl)ethan-1-ol (148, Scheme 9)

In line with the general procedure, reaction of 4-piperidine-ethanol (0.99 g, 7.72 mmol) with chloromethyl **141** (0.82 g, 3.86 mmol) gave a crude which was purified by typical silica gel flash chromatography (CH_2Cl_2/CH_3OH/$NH_{3(aq)}$ 97.5:2.5:0.125), to yield **148** as yellow oil (0.46 g, 39 %). **^{1}H-NMR** (400 MHz, $CDCl_3$)

δ 1.20-1.82 (m, 9H, piperidine), 2.19 (t, J = 11.6 Hz, 2H, piperidine), 2.94 (d, J = 11.6 Hz, 2H, piperidine), 3.71 (t, J = 6.0 Hz, 2H, C<u>H</u>$_2$OH), 3.92 (s, 2H, C<u>H</u>$_2$NH), 7.41 (t, J = 8.0 Hz, 1H, Ar), 7.71-7.81 (m, 3H, Ar), 8.13 (d, J = 8.4 Hz, 1H, Ar).

**General procedure of N-Boc cleavage: synthesis of intermediate 146 and 147 (Scheme 8)**

To a suspension of **144** or **145** (1.00 mmol) in a mixture of 1,4-dioxane/CH$_3$OH (1.5:1, 10.0 mL), cooled down to 0 °C, a solution of HCl (4 M) in 1,4-dioxane (30.0 molar equiv) was added dropwise. The resulting reaction mixture was warmed to rt and was stirred at the same temperature for 8 h. Upon completion, evaporation of the reaction solvent mixture gave a residue, which was purified by typical silica gel flash chromatography (CH$_2$Cl$_2$/CH$_3$OH/NH$_{3(aq)}$ 96.0:4.0:0.2), to yield the desired product.

(1-((8-chloroquinolin-2-yl)methyl)piperidin-3-yl)methanamine (146, Scheme 8)
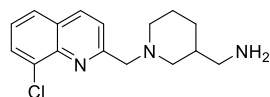
Following the general procedure, treatment of Boc-protected **144** (0.27 g, 0.69 mmol) with HCl (4 M) in 1,4-dioxane (5.18 mL, 20.70 mmol) gave **146** as a yellow oil (0.27 g, 62 %). **^{1}H-NMR** (400 MHz, CDCl$_3$) 1.03-1.10 (m, 1H, piperidine), 1.64-1.69 (m, 4H, piperidine), 1.91-1.96 (m, 1H, piperidine), 2.18 (d, 1H, J = 6.8 Hz, piperidine), 2.59 (d, 2H, J = 3.6 Hz, C<u>H</u>$_2$NH$_2$), 2.83 (d, J = 11.2 Hz, 1H, piperidine), 2.93 (d, J = 10.0 Hz, 1H, piperidine), 3.92 (s, 2H, CH$_2$-piperidine), 7.40-7.51 (m, 1H, Ar), 7.74-7.82 (m, 3H, Ar), 8.13 (d, J = 8.4 Hz, 1H, Ar).

**(1-((8-chloroquinolin-2-yl)methyl)piperidin-4-yl)methanamine (147, Scheme 8)**
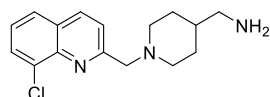
Following the general procedure, treatment of Boc-protected **145** (0.47 g, 1.20 mmol) with HCl (4 M) in 1,4-dioxane (9.00 mL, 36.00 mmol) gave **147** as a white oil (0.25 g, 40 %). **^{1}H-NMR** (400 MHz, CDCl$_3$) 1.36-1-40 (m, 1H, piperidina), 1.66 (t, J = 8.0 Hz, 2H, piperidine), 1.92

(d, J = 15.2 Hz, 1H, piperidine), 2.10 (d, J = 12.8 Hz, 2H, piperidine), 2.14 (br. s, 1H, piperidina), 2.72 (t, J = 6.0 Hz, 2H, C$\underline{H}_2$NH$_2$), 3.26 (d, J = 9.6 Hz, 2H, piperidine), 4.70 (s, 2H, CH$_2$-Ph), 7.66 (t, J = 7.6 Hz, 1H, Ar), 7.94 (d, J = 8.4 Hz, 1H, Ar), 8.03 (t, J = 8.4 Hz, 2H, Ar), 8.19 (br. s, 2H, NH$_2$), 8.58 (d, J = 8.0 Hz, 1H, Ar).

**Nucleophilic substitution reaction: synthesis of intermediate 149 (Scheme 9)**
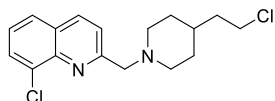
To a stirred solution of **148** (0.46 g, 1.50 mmol, 1.00 eq) in CH$_2$Cl$_2$ (15.0 mL) at 0 °C, SOCl$_2$ (0.35 g, 3.00 mmol, 2.00 eq, 0.21 mL) was added dropwise. The resulting reaction mixture was stirred at room temperature for 5 h. Upon reaction completion, the mixture was diluted with additional CH$_2$Cl$_2$ (10.0 mL) and washed with H$_2$O (2 x 20.0 mL) and then with saturated NaHCO$_3$ aqueous solution (2 x 20.0 mL). The organic phase was dried over Na$_2$SO$_4$, filtered and concentrated to dryness at reduced pressure to afford **149** without any further purification (0.20 g, 47 %). **^{1}H-NMR** (400 MHz, CDCl$_3$) δ 1.73 (t, J = 8.0 Hz, 2H, piperidine), 1.80-1.95 (m, 5H, piperidine), 2.26 (br. s, 2H, piperidine), 2.97 (d, J = 8.8 Hz, 2H, CH$_2$), 3.58 (t, 2H, J = 6.8 Hz, piperidine), 3.96 (s, 2H, piperidine), 7.45 (t, J= 7.6 Hz, 1H, Ar), 7.72-7.82 (m, 3H, Ar), 8.14 (d, 1H, J= 8.4 Hz, Ar).

**General procedure of *N*-benzylation reaction: synthesis of intermediate 152 and 156 (Scheme 10)**

To a solution of 3-piperidine-methanol **151** or 4-methylamine-piperidine **159** (1.00 mmol) and NEt$_3$ (2.0 molar equiv) in CH$_3$CN (2.0 mL), benzyl bromide (1.0 molar equiv) was added dropwise. The resulting reaction mixture was stirred under reflux for 3 h. Upon completion, the mixture was concentrated to dryness and the obtained crude was diluted with CH$_2$Cl$_2$ (10.0 mL), washed with H$_2$O (2 x 20.0 mL) and then with saturated NaHCO$_3$ aqueous solution (2 x 20.0 mL). The organic phase was dried over Na$_2$SO$_4$, filtered and concentrated to dryness at reduced pressure to afford the title compound without any further purification.

**(1-benzylpiperidin-3-yl)methanol (152, Scheme 10)**
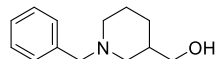
In line with the general procedure, the title compound was synthetized starting from 3-piperidine-methanol **151** (3.00 g, 26.04 mmol) and benzyl bromide (2.10 mL, 26.04 mmol,), to yield **152** as an orange oil (3.53 g, 81 %). **^{1}H-NMR** (400 MHz, CDCl$_3$) δ 1.18-1.21 (m, 1H), 1.56-1.81 (m, 4H), 2.07-2.23 (m, 2H), 2.56-2.58 (m, 1H), 2.77 (d, J = 8.4 Hz, 1H), 3.49 (s, 2H), 3.54-3.65 (m, 2H), 7.24-7.31 (m, 5H).

(1-benzylpiperidin-4-yl)methanamine (156, Scheme 10)
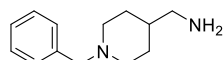
In line with the general procedure, the title compound was synthetized starting from 3-piperidine-methanol **159** (1.00 g, 8.75 mmol) and benzyl bromide (0.71 mL, 8.75 mmol,), to yield **156** as a red oil (0.71 g, 40 %). **^{1}H-NMR** (400 MHz, CDCl$_3$) δ 1.22-1.28 (m, 2H, CH$_2$), 1.50 (t, J = 7.2 Hz, 1H, CH), 1.69 (d, J = 10.8 Hz, 2H), 1.77 (s, 2H, NH$_2$), 1.96 (q, J = 8.0 Hz, 2H, CH$_2$), 2.54 (q, J = 6.4 Hz, 2H, CH$_2$), 2.90 (d, J = 11.6 Hz, 2H, CH$_2$), 3.77 (s, 2H, CH$_2$-Ph), 7.23-7.25 (m, 1H, Ar), 7.27-7.32 (m, 4H, Ar).

**Mesylation of alcohol: synthesis of intermediate 153 (Scheme 10)**
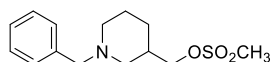
To a solution of **152** (1.23 g, 6.43 mmol, 1.00 eq) and NEt$_3$ (1.79 mL, 12.86 mmol, 2.00 eq) in dry CH$_2$Cl$_2$ (60.0 mL) at 0 °C, methanesulfonyl chloride (0.57 mL, 7.39 mmol, 1.15 eq) was added dropwise. The resulting reaction mixture was stirred at rt for 12 h. Upon reaction completion, the mixture was diluted with additional CH$_2$Cl$_2$ (10.0 mL) and washed with saturated NaHCO$_3$ aqueous solution (2 x 20.0 mL). The organic phase was dried over Na$_2$SO$_4$, filtered and concentrated to dryness at reduced pressure to afford **153** as an orange oil without any further purification (1.41 g, 77 %). **^{1}H-NMR** (400 MHz, CDCl$_3$) δ 1.16-1.20 (m, 1H), 1.54-1.82 (m, 4H), 2.06-2.21 (m, 2H), 2.56-2.58 (m, 1H), 2.74 (d, J = 8.4 Hz, 1H), 3.52 (s, 2H), 3.67-3.75 (m, 2H), 7.25-7.30 (m, 5H).

**Substitution reaction: synthesis of intermediate 154 (Scheme 10)**
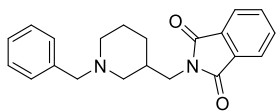
A solution of **152** (1.91 g, 4.98 mmol, 1.00 eq) and potassium phthalimide (1.10 g, 5.97 mmol, 1.20 eq) in DMF (24.0 mL) was stirred at 100 °C for 4 h. The reaction mixture was poured in H_2O and the resulting white solid was filtered off, washed with fresh water and dried *under vacuum* to afford **154** as a solid (0.87 g, 53 %). **^{1}H-NMR** (400 MHz, CDCl$_3$) δ 1.07 (d, *J* = 9.2 Hz, 1H), 1.53 (br. s, 1H), 1.68 (t, 2H, *J* = 9.6 Hz), 1.96 (t, *J* = 10.8 Hz, 2H), 2.05 (br. s, 1H), 2.12 (d, *J* = 3.2 Hz, 2H), 3.40 (d, *J* = 13.2 Hz, 2H), 3.52 (s, 2H), 7.20-7.29 (m, 3H, Ar), 7.28-7.71 (m, 3H, Ar), 7.83-7.87 (m, 3H, Ar).
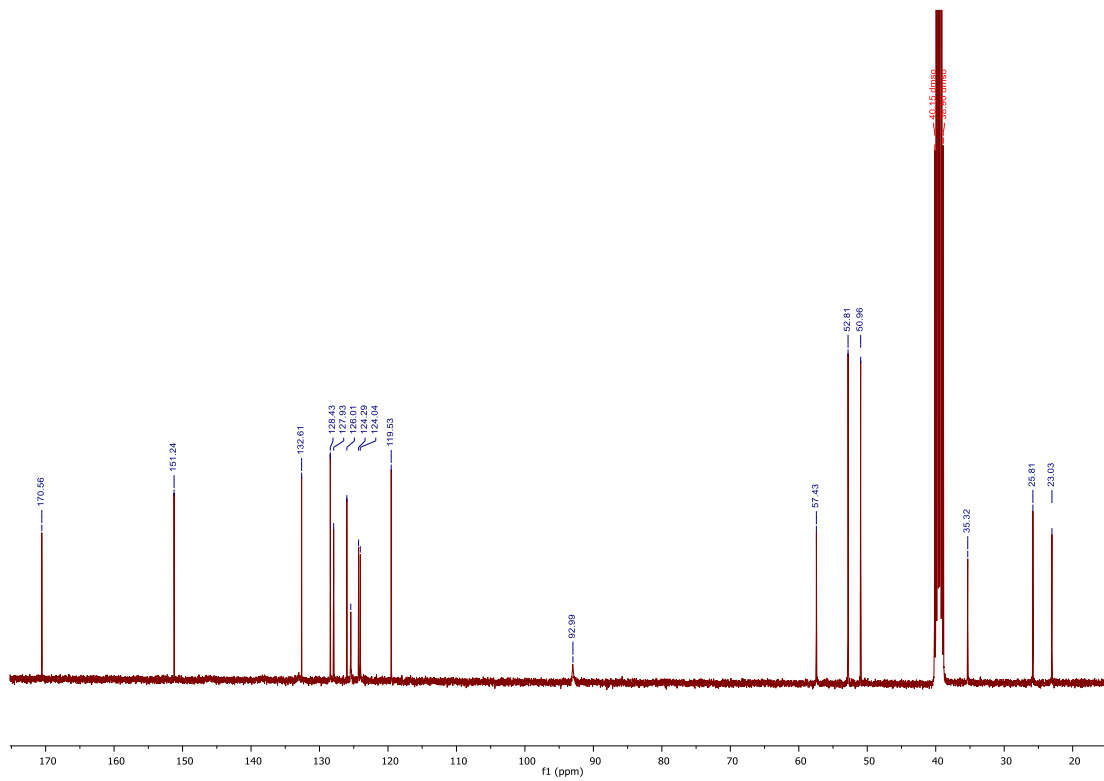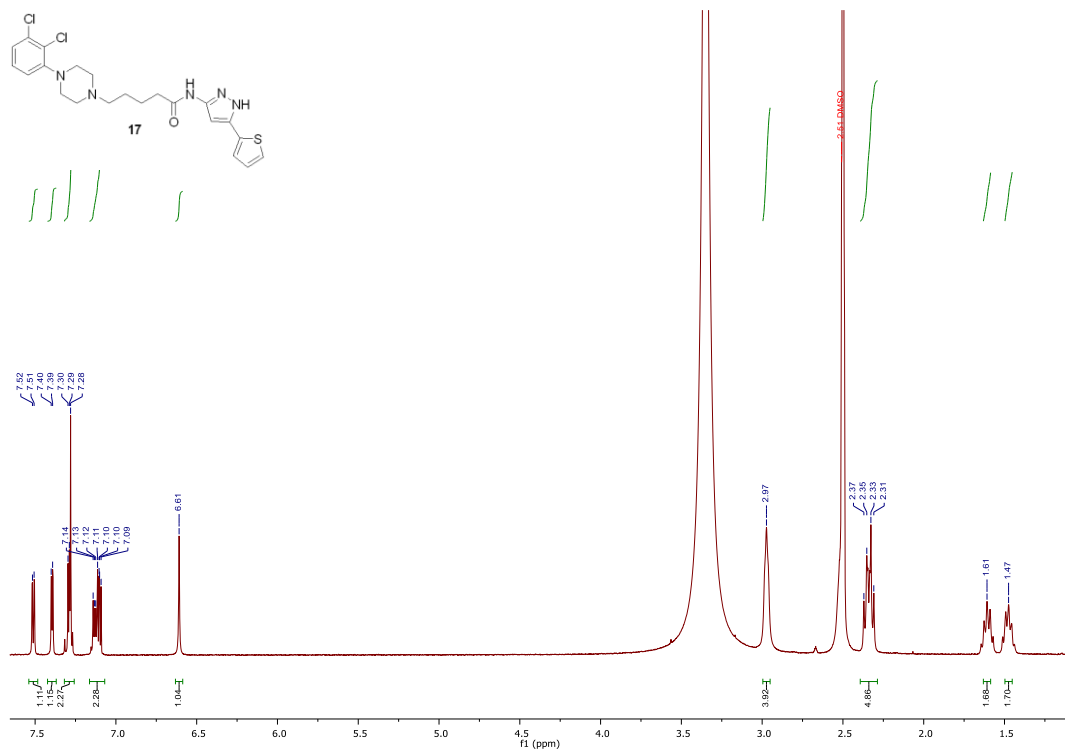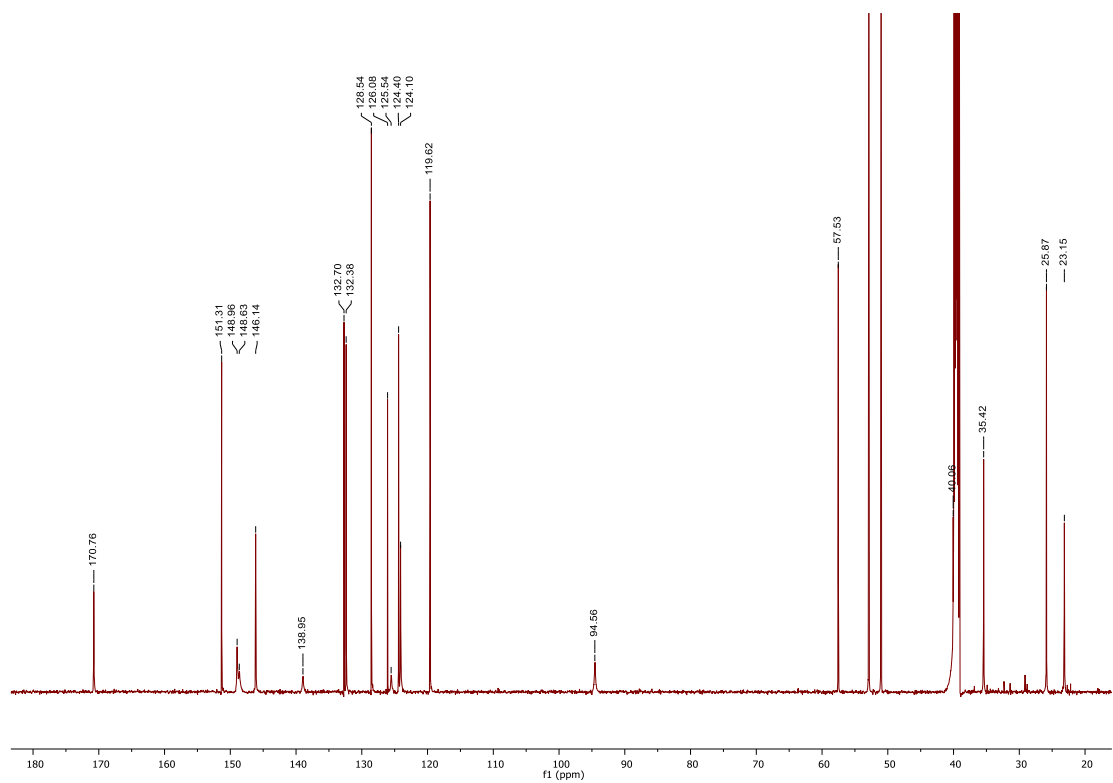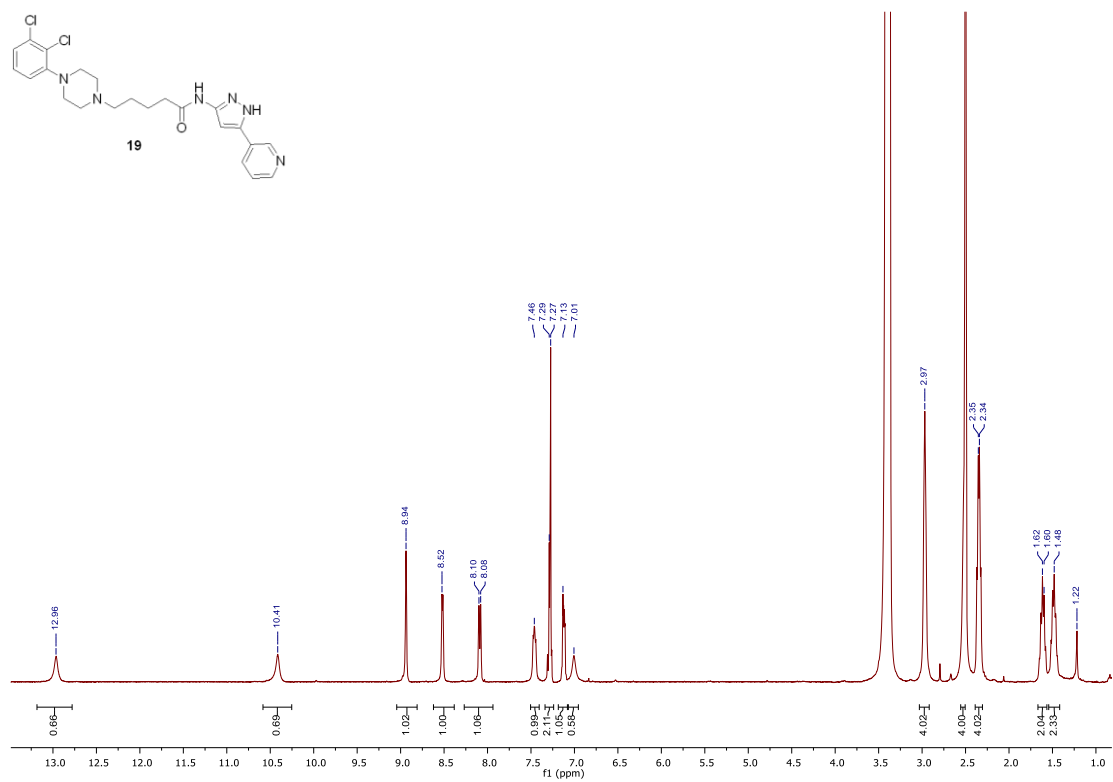
APPENDIX

Representative Spectra

80a

H-2 THP

NH
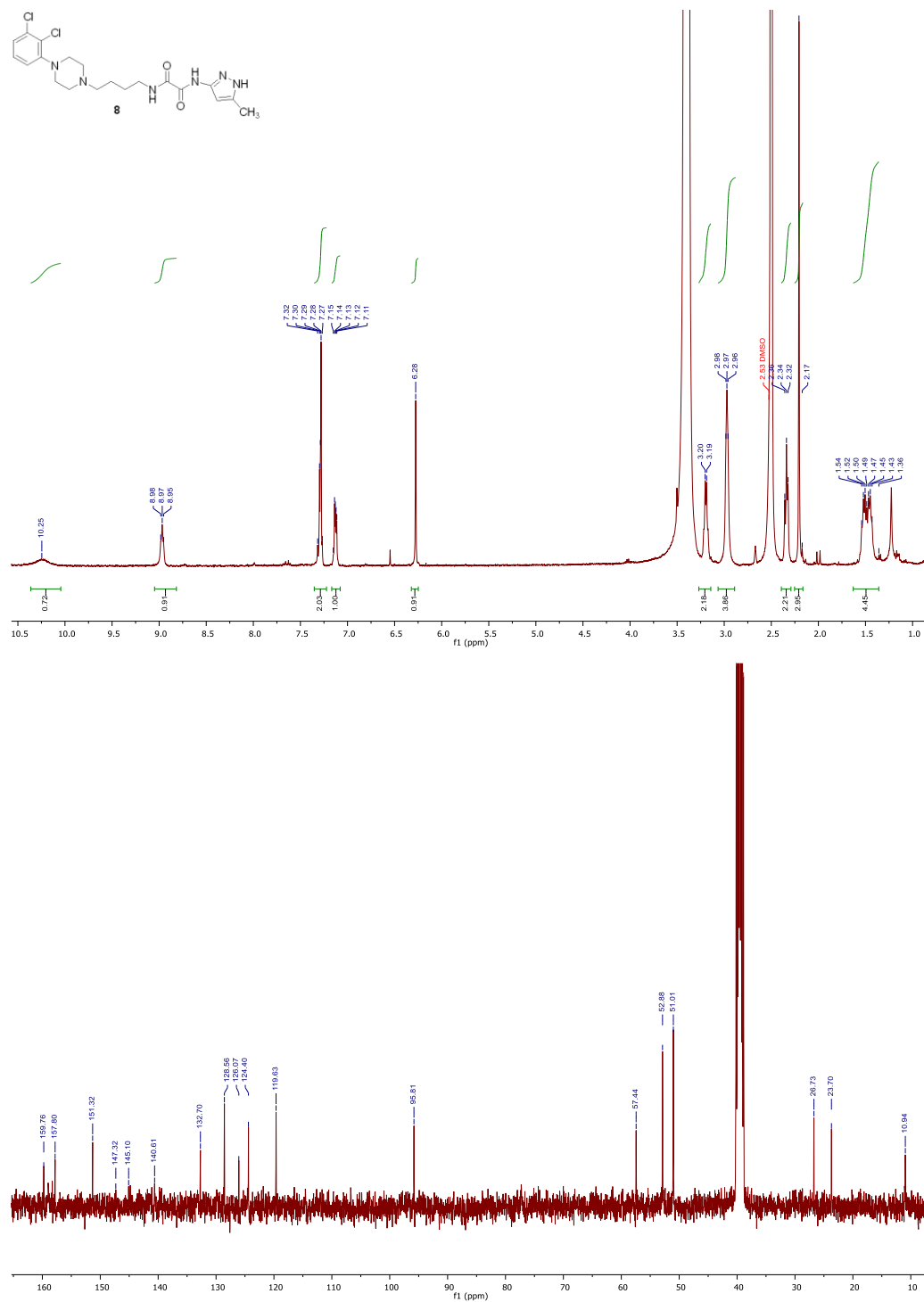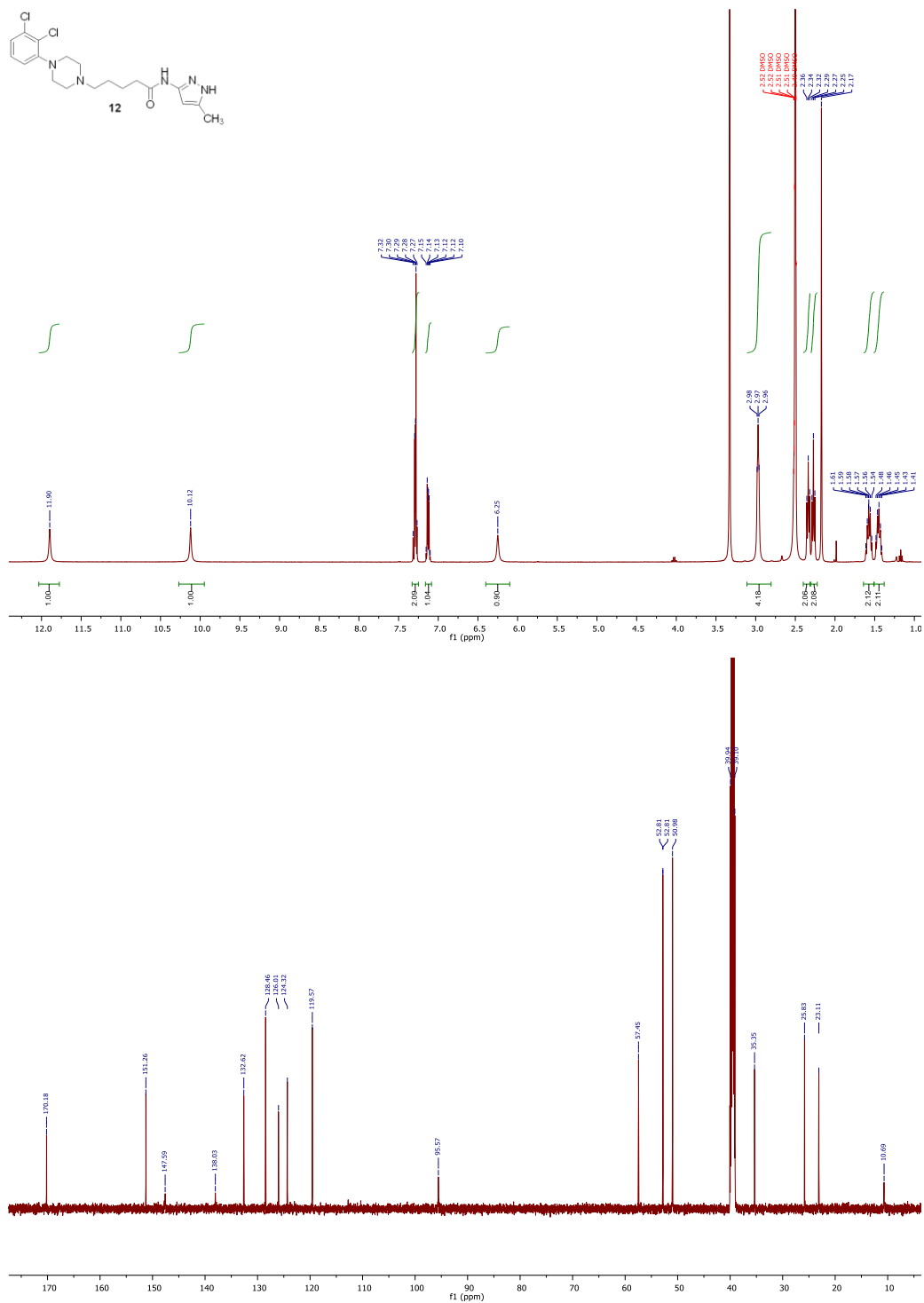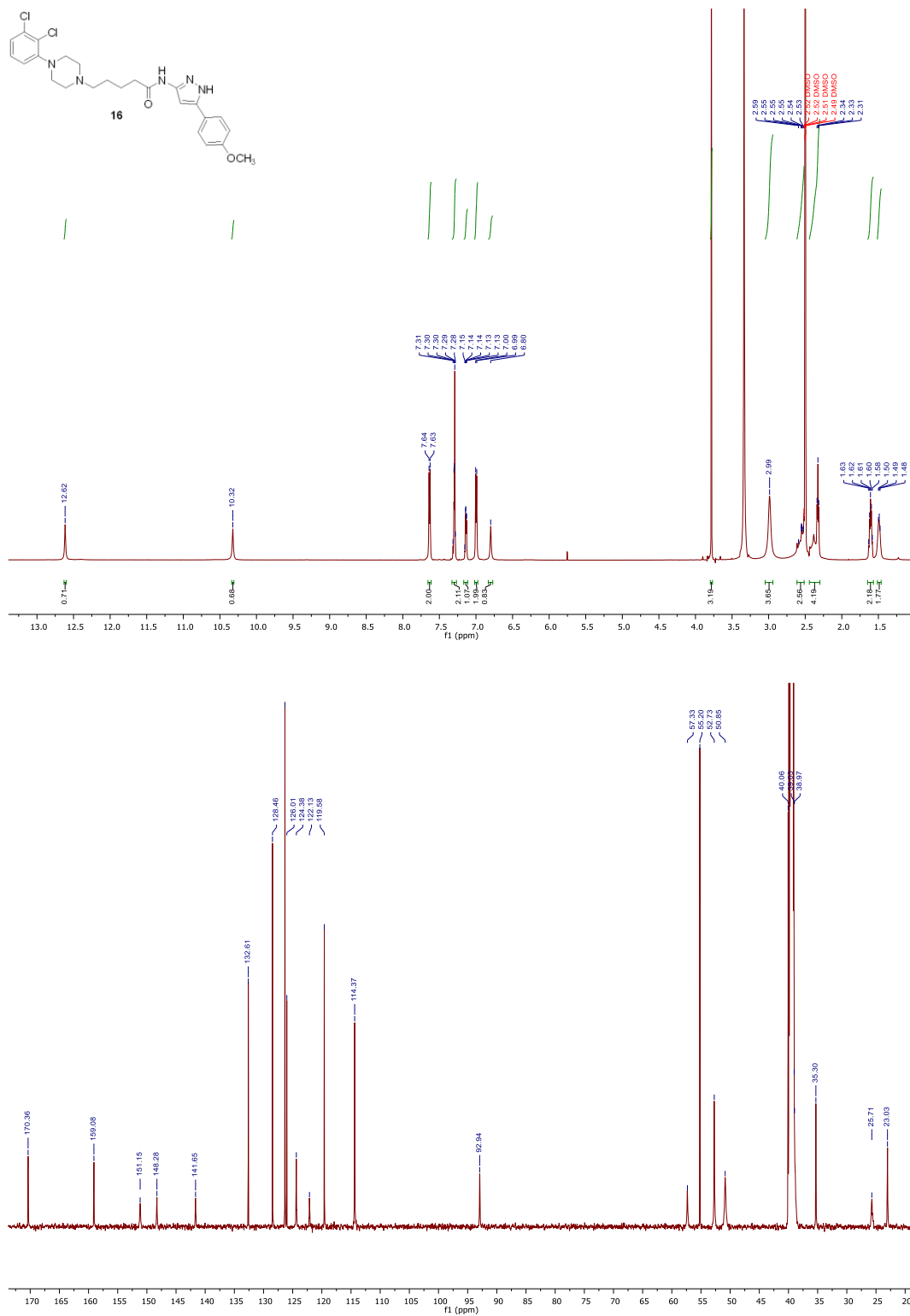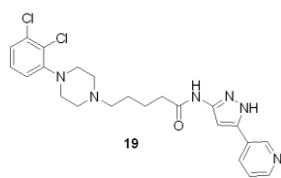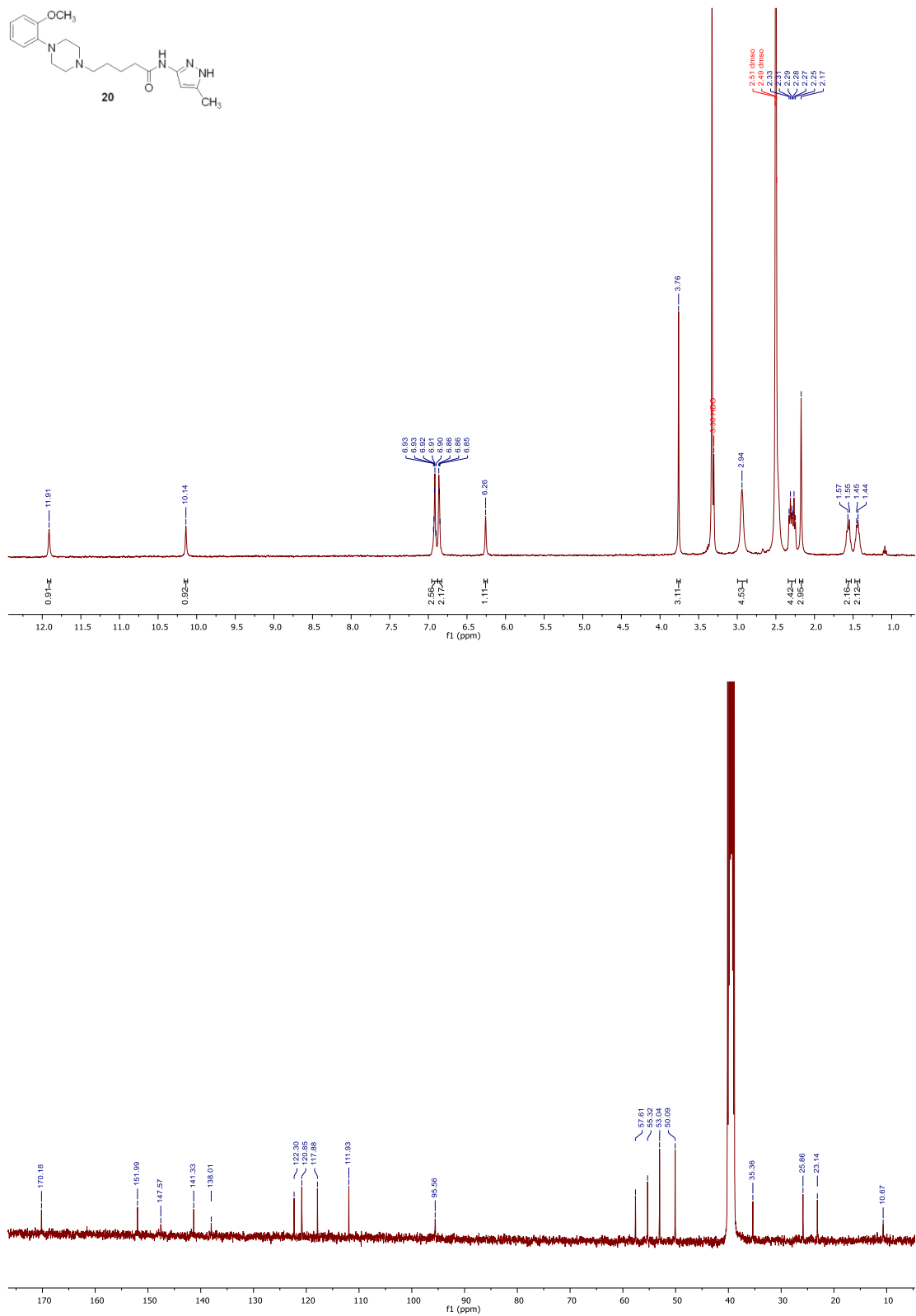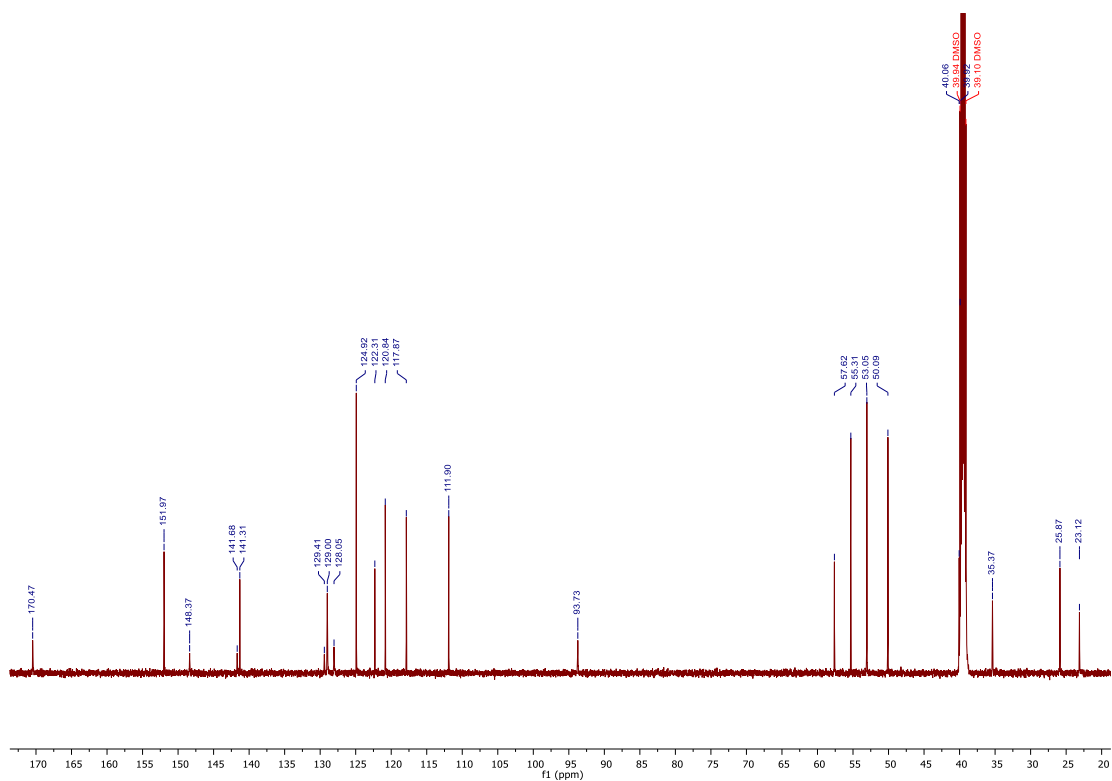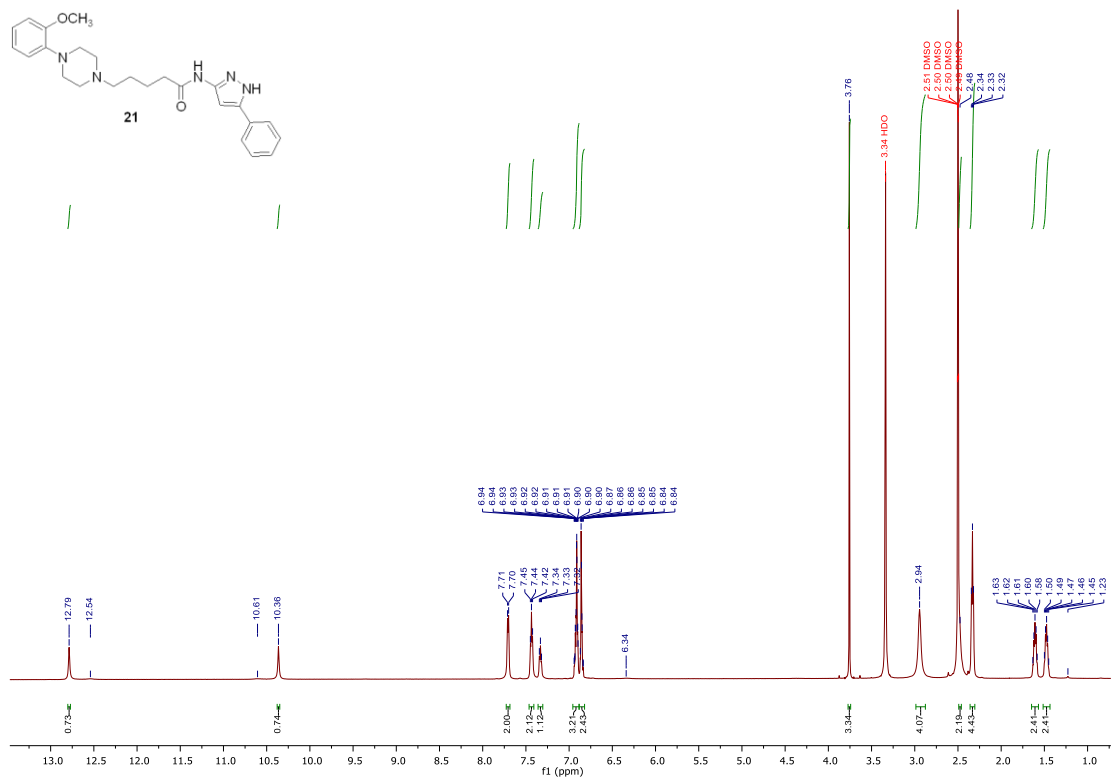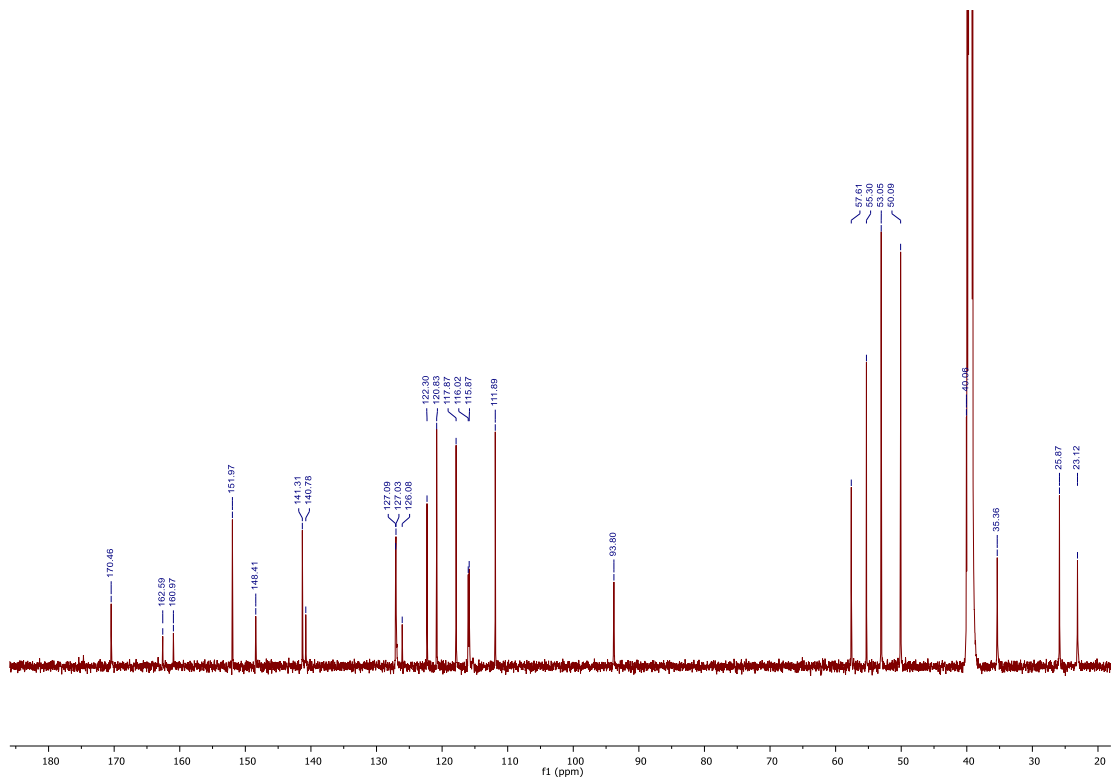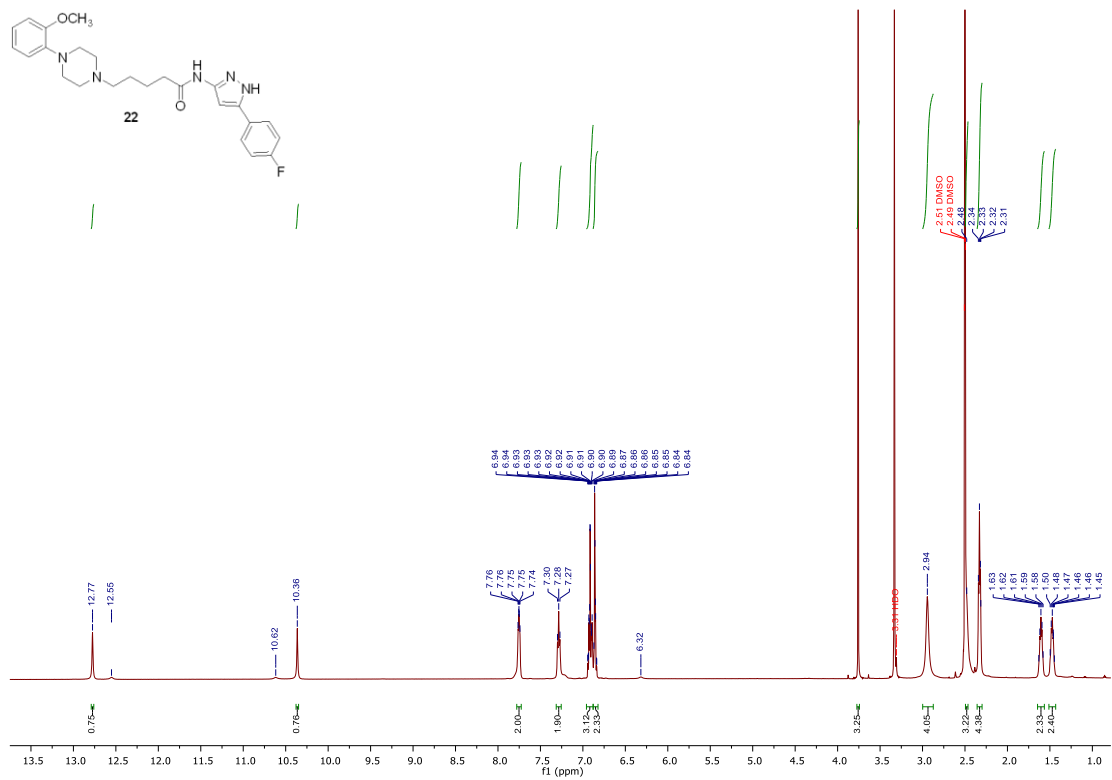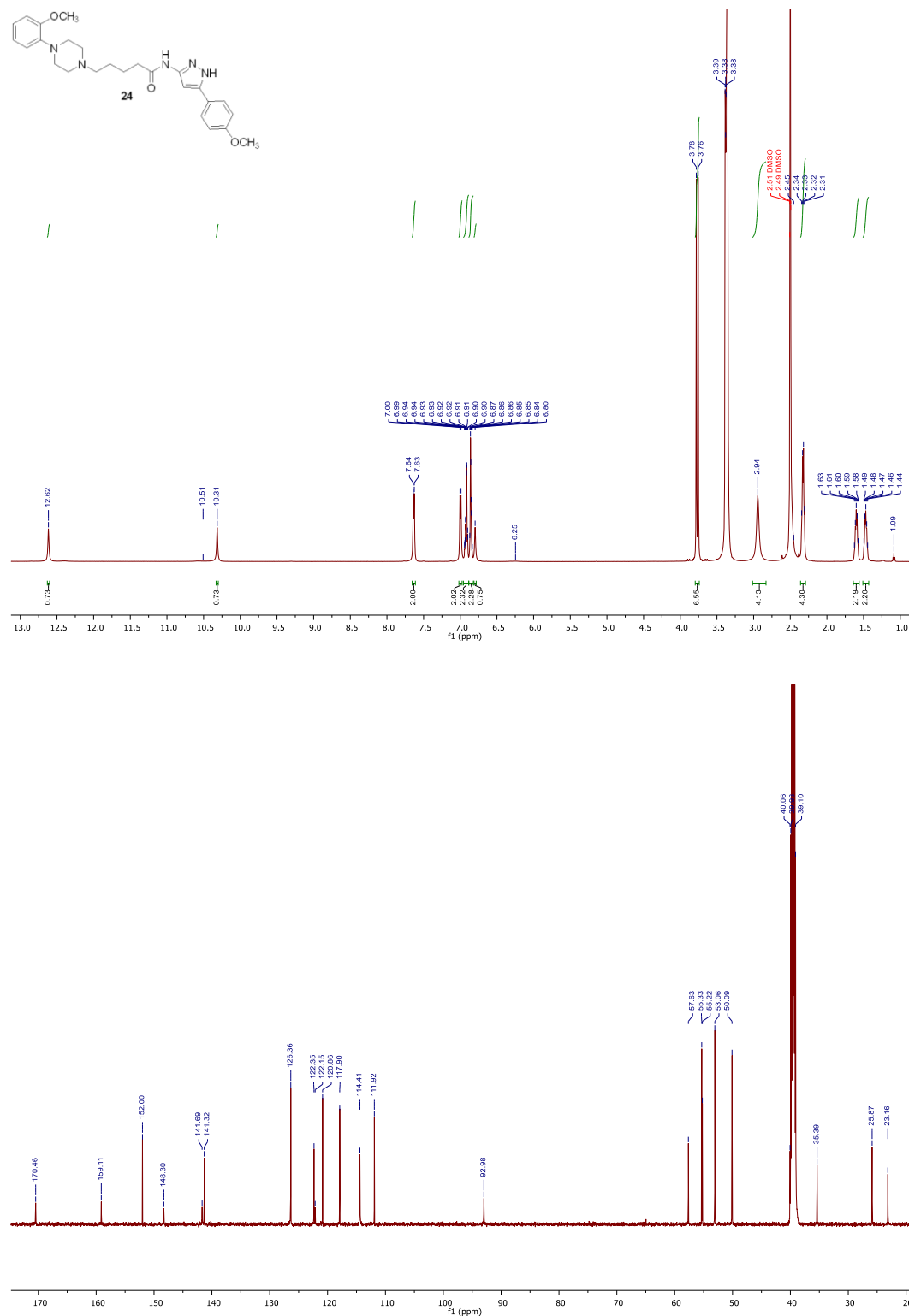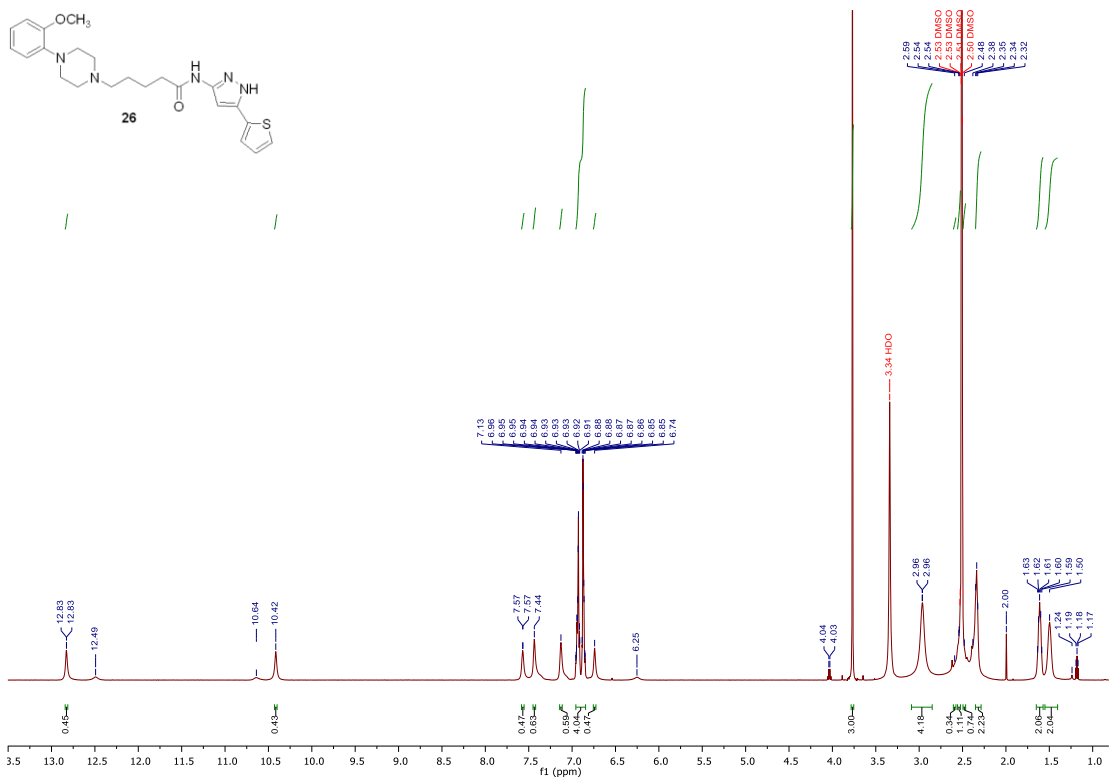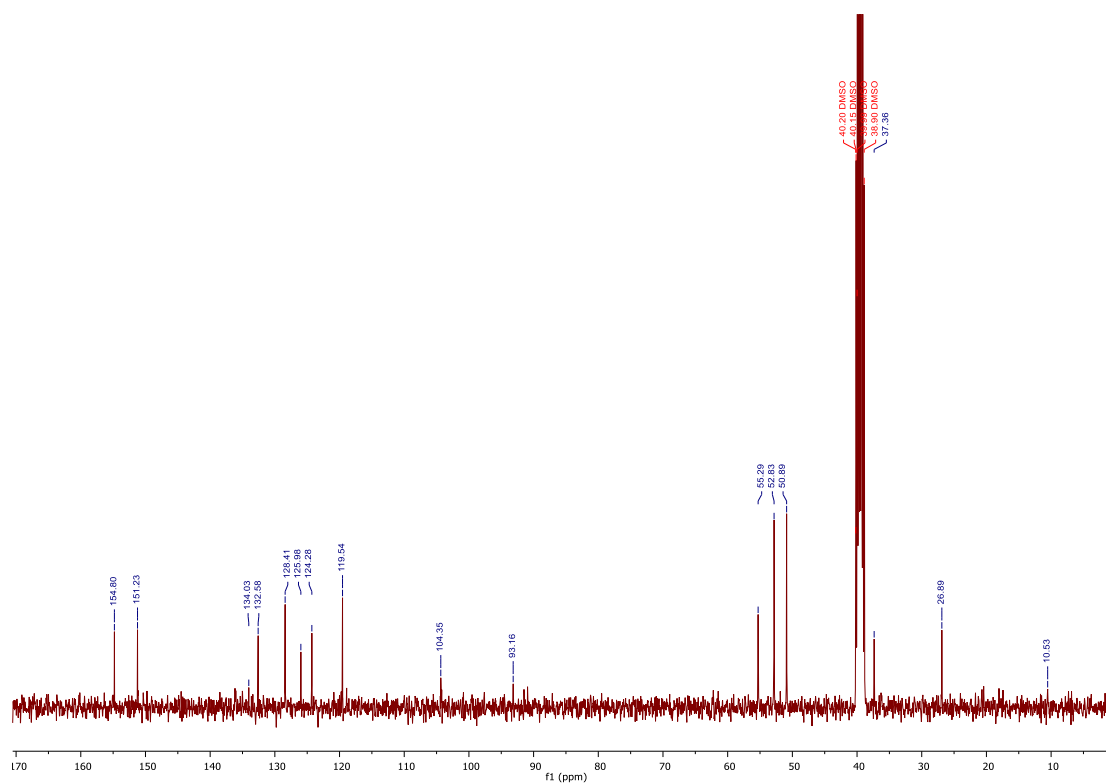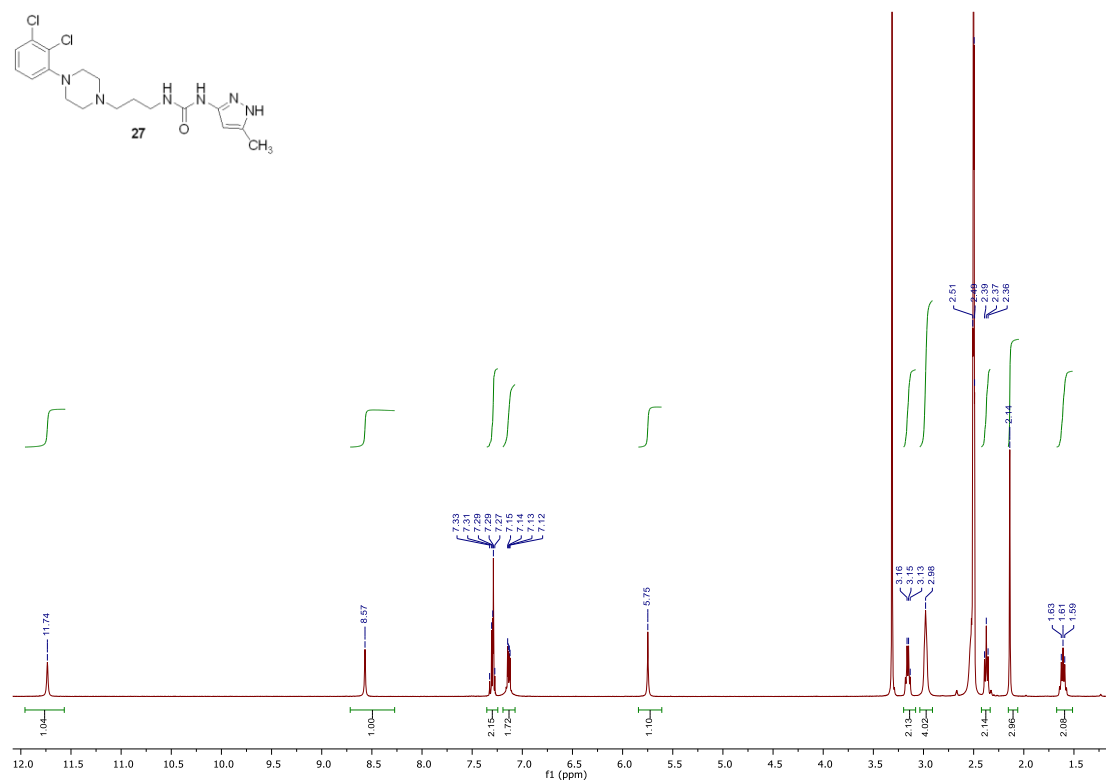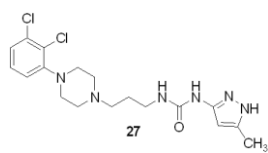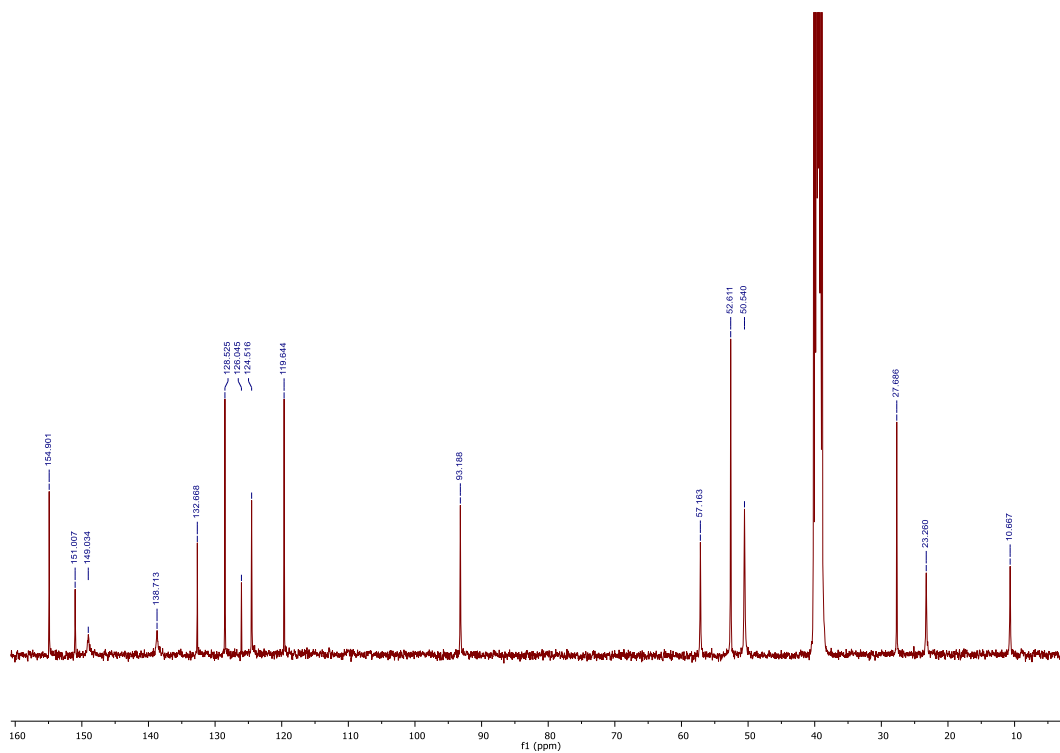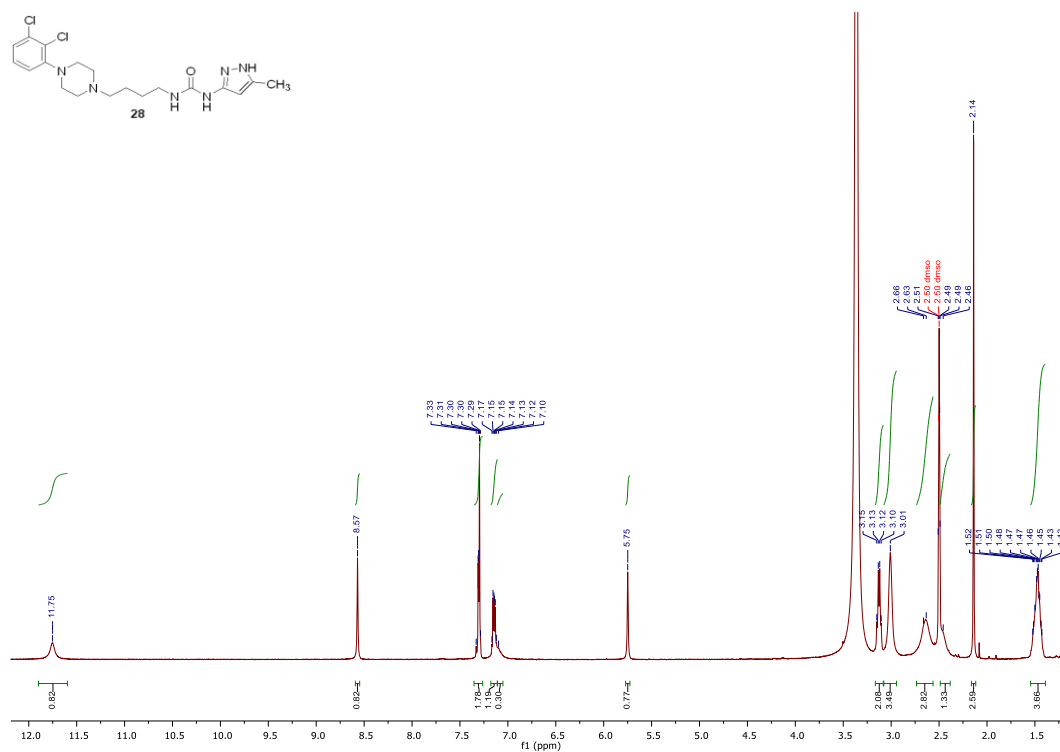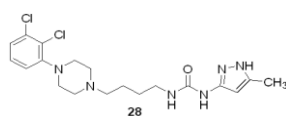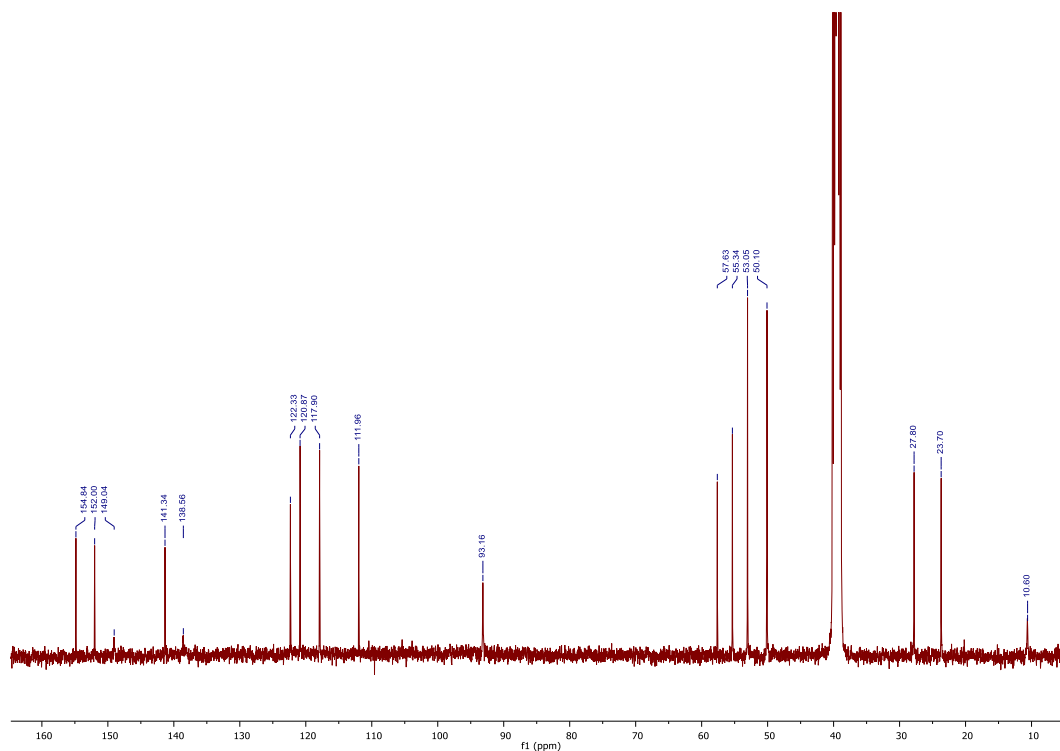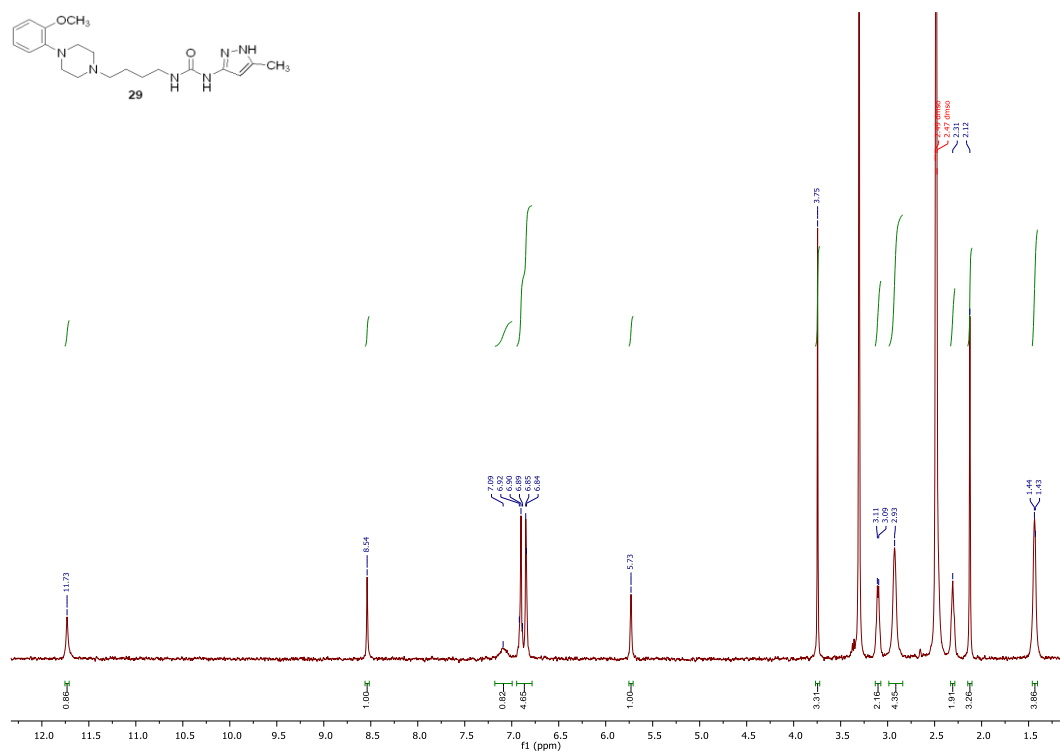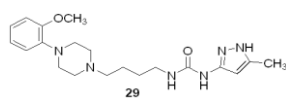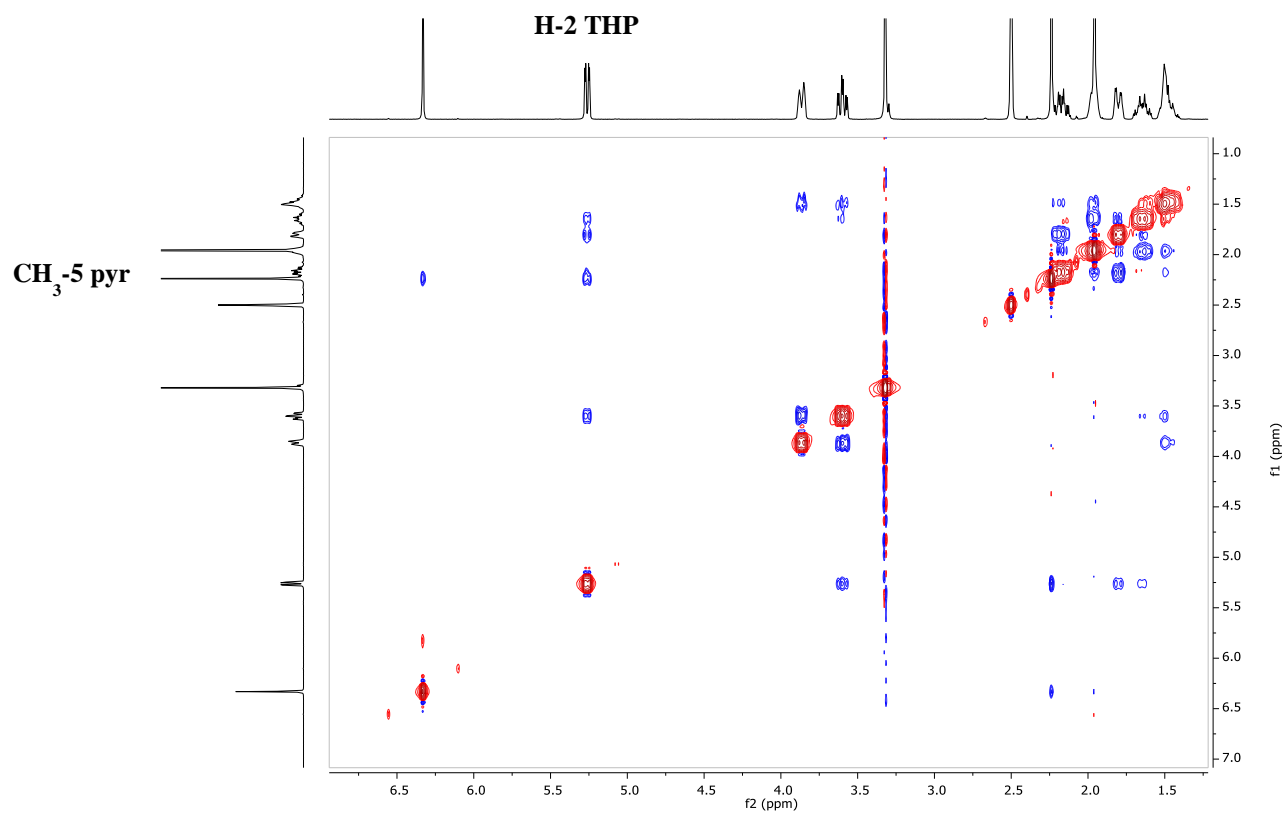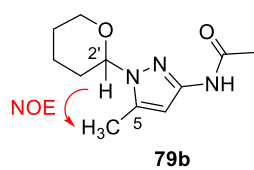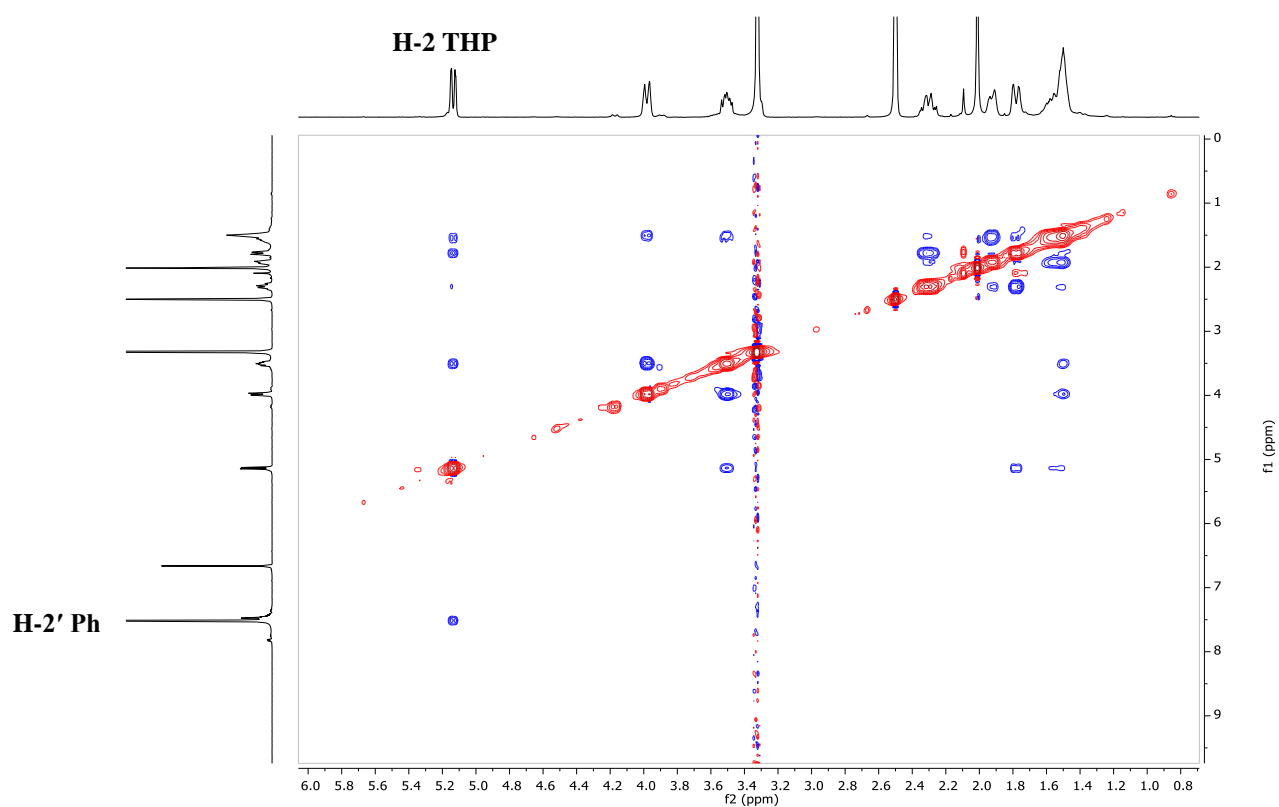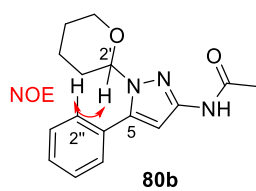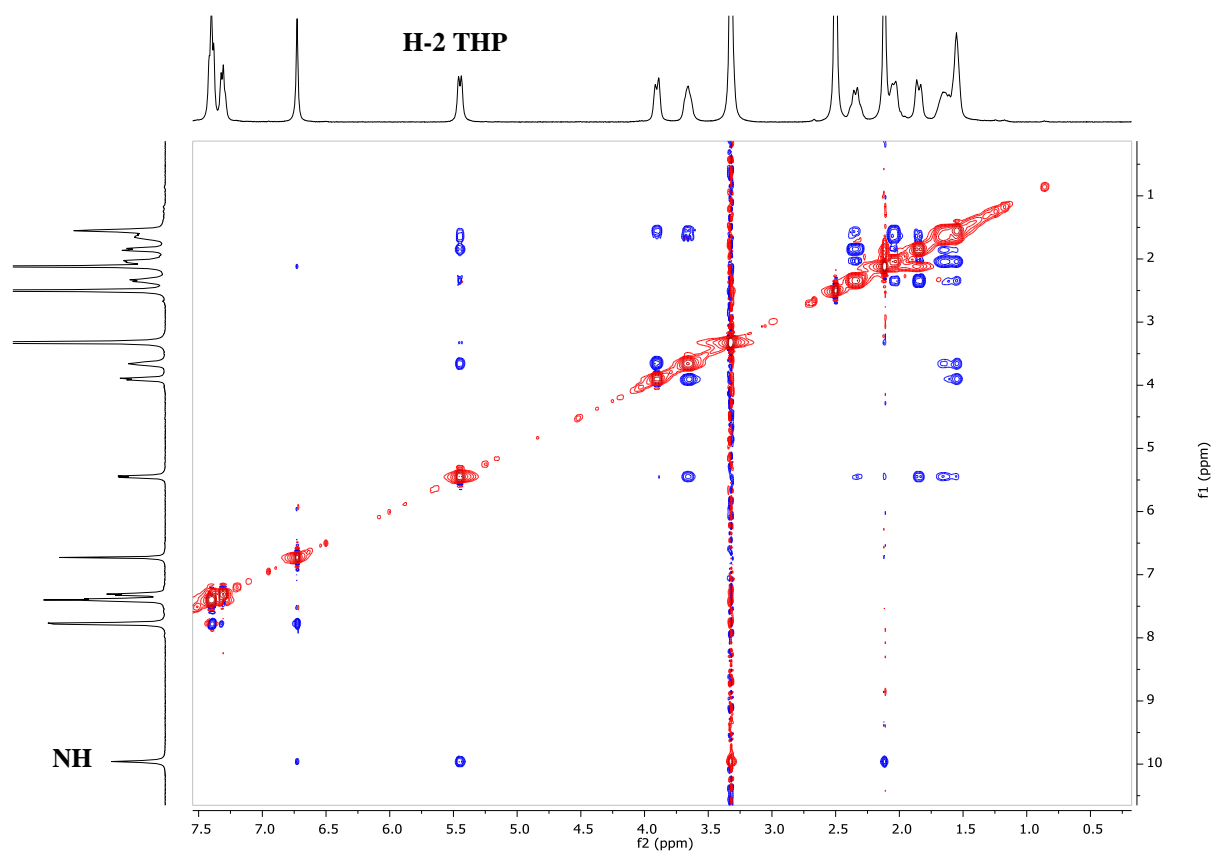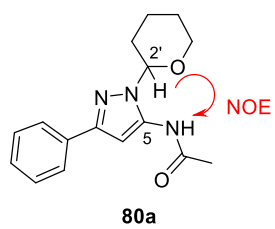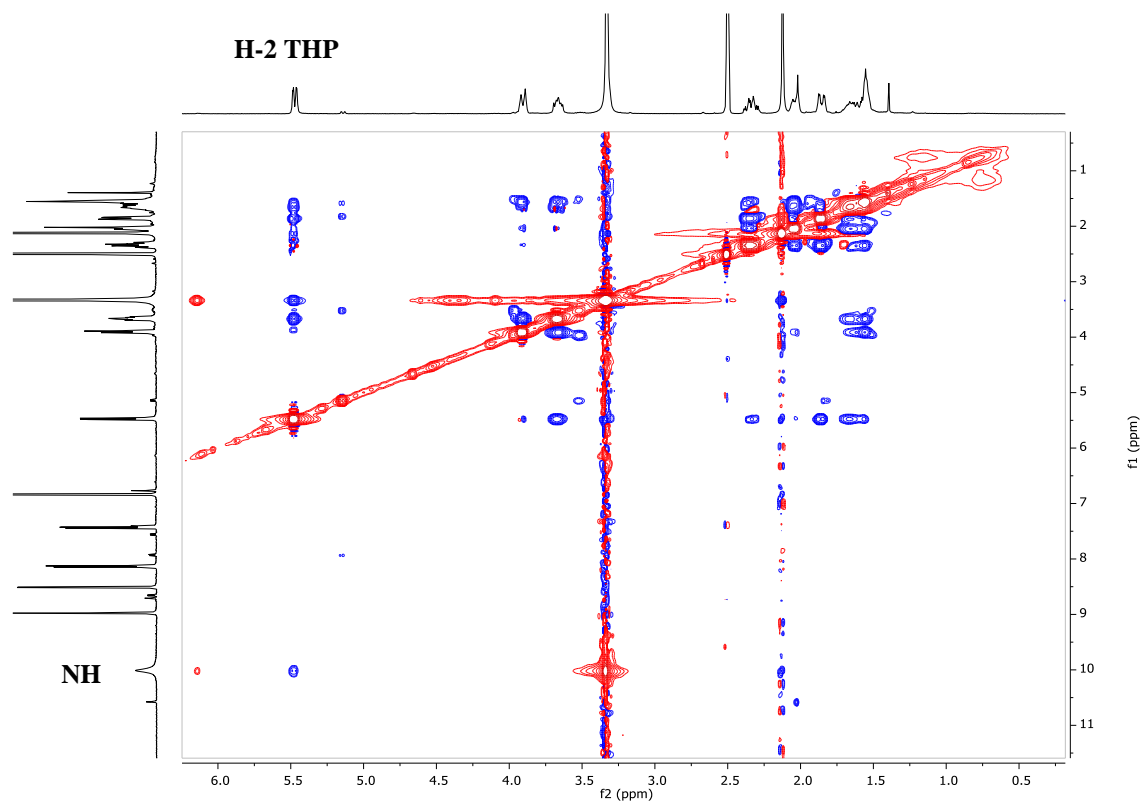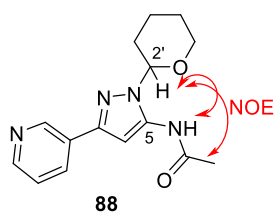
Bibliografy

1.   Paykel, E., Manic-depressive illness: Bipolar disorders and recurrent depression (2nd edn). *British Journal of Psychiatry* **2008,** *193* (1), 86-87.

2.   Martinez-Aran, A.; Vieta, E.; Torrent, C.; Sanchez-Moreno, J.; Goikolea, J.; Salamero, M.; Malhi, G.; Gonzalez-Pinto, A.; Daban, C.; Alvarez-Grandi, S.; Fountoulakis, K.; Kaprinis, G.; Tabares-Seisdedos, R.; Ayuso-Mateos, J., Functional outcome in bipolar disorder: the role of clinical and cognitive factors. *Bipolar Disorders* **2007,** *9* (1-2), 103-113.

3.   Alonso, J.; Petukhova, M.; Vilagut, G.; Chatterji, S.; Heeringa, S.; Ustun, T.; Alhamzawi, A.; Viana, M.; Angermeyer, M.; Bromet, E.; Bruffaerts, R.; de Girolamo, G.; Florescu, S.; Gureje, O.; Haro, J.; Hinkov, H.; Hu, C.; Karam, E.; Kovess, V.; Levinson, D.; Medina-Mora, M.; Nakamura, Y.; Ormel, J.; Posada-Villa, J.; Sagar, R.; Scott, K.; Tsang, A.; Williams, D.; Kessler, R., Days out of role due to common physical and mental conditions: results from the WHO World Mental Health surveys. *Molecular Psychiatry* **2011,** *16* (12), 1234-1246.

4.   Grande, I.; Berk, M.; Birmaher, B.; Vieta, E., Bipolar disorder. *Lancet* **2016,** *387* (10027), 1561-1572.

5.   Phillips, M.; Kupfer, D., Bipolar Disorder 2 Bipolar disorder diagnosis: challenges and future directions. *Lancet* **2013,** *381* (9878), 1663-1671.

6.   Roshanaei-Moghaddam, B.; Katon, W., Premature Mortality From General Medical Illnesses Among Persons With Bipolar Disorder: A Review. *Psychiatric Services* **2009,** *60* (2), 147-156.

7.   Miller, S.; Dell'Osso, B.; Ketter, T., The prevalence and burden of bipolar depression. *Journal of Affective Disorders* **2014,** *169*, S3-S11.

8.   McIntyre, R.; Konarski, J.; Yatham, L., Comorbidity in bipolar disorder: a framework for rational treatment selection. *Human Psychopharmacology-Clinical and Experimental* **2004,** *19* (6), 369-386.

9.   Merikangas, K.; Akiskal, H.; Angst, J.; Greenberg, P.; Hirschfeld, R.; Petukhova, M.; Kessler, R., Lifetime and 12-month prevalence of bipolar spectrum disorder in the national comorbidity survey replication. *Archives of General Psychiatry* **2007,** *64* (5), 543-552.

10.   Hirschfeld, R.; Lewis, L.; Vornik, L., Perceptions and impact of bipolar disorder: How far have we really come? Results of the National Depressive and Manic-Depressive Association 2000 survey of individuals with bipolar disorder. *Journal of Clinical Psychiatry* **2003,** *64* (2), 161-174.

11.   Baldessarini, R.; Tondo, L.; Baethge, C.; Lepri, B.; Bratti, I., Effects of treatment latency on response to maintenance treatment in manic-depressive disorders. *Bipolar Disorders* **2007,** *9* (4), 386-393.

12.   Sigitova, E.; Fisar, Z.; Hroudova, J.; Cikankova, T.; Raboch, J., Biological hypotheses and biomarkers of bipolar disorder. *Psychiatry and Clinical Neurosciences* **2017,** *71* (2), 77-103.

13.   Schloesser, R.; Huang, J.; Klein, P.; Manji, H., Cellular plasticity cascades in the pathophysiology and treatment of bipolar disorder. *Neuropsychopharmacology* **2008,** *33* (1), 110-133.

14.	McGuffin, P.; Rijsdijk, F.; Andrew, M.; Sham, P.; Katz, R.; Cardno, A., The heritability of bipolar affective disorder and the genetic relationship to unipolar depression. *Archives of General Psychiatry* **2003,** *60* (5), 497-502.

15.	Kerner, B., Toward a deeper understanding of the genetics of bipolar disorder. *Frontiers in Psychiatry* **2015,** *6*.

16.	Kato, T., Molecular genetics of bipolar disorder and depression. *Psychiatry and Clinical Neurosciences* **2007,** *61* (1), 3-19.

17.	Aas, M.; Etain, B.; Bellivier, F.; Henry, C.; Lagerberg, T.; Ringen, A.; Agartz, I.; Gard, S.; Kahn, J.; Leboyer, M.; Andreassen, O.; Melle, I., Additive effects of childhood abuse and cannabis abuse on clinical expressions of bipolar disorders. *Psychological Medicine* **2014,** *44* (8), 1653-1662.

18.	Martinowich, K.; Schloesser, R.; Manji, H., Bipolar disorder: from genes to behavior pathways. *Journal of Clinical Investigation* **2009,** *119* (4), 726-736.

19.	KATO, T.; SHIOIRI, T.; MURASHITA, J.; HAMAKAWA, H.; INUBUSHI, T.; TAKAHASHI, S., P-31 MAGNETIC-RESONANCE SPECTROSCOPY AND VENTRICULAR ENLARGEMENT IN BIPOLAR DISORDER. *Psychiatry Research-Neuroimaging* **1994,** *55* (1), 41-50.

20.	Brambilla, P.; Nicoletti, M.; Harenski, K.; Sassi, R.; Mallinger, A.; Frank, E.; Kupfer, D.; Keshavan, M.; Soares, J., Anatomical MRI study of subgenual prefrontal cortex in bipolar and unipolar subjects. *Neuropsychopharmacology* **2002,** *27* (5), 792-799.

21.	Hibar, D.; Westlye, L.; van Erp, T.; Rasmussen, J.; Leonardo, C.; Faskowitz, J.; Haukvik, U.; Hartberg, C.; Doan, N.; Agartz, I.; Dale, A.; Gruber, O.; Kramer, B.; Trost, S.; Liberg, B.; Abe, C.; Ekman, C.; Ingvar, M.; Landen, M.; Fears, S.; Freimer, N.; Bearden, C.; Sprooten, E.; Glahn, D.; Pearlson, G.; Emsell, L.; Kenney, J.; Scanlon, C.; McDonald, C.; Cannon, D.; Almeida, J.; Versace, A.; Caseras, X.; Lawrence, N.; Phillips, M.; Dima, D.; Delvecchio, G.; Frangou, S.; Satterthwaite, T.; Wolf, D.; Houenou, J.; Henry, C.; Malt, U.; Boen, E.; Elvsashagen, T.; Young, A.; Lloyd, A.; Goodwin, G.; Mackay, C.; Bourne, C.; Bilderbeck, A.; Abramovic, L.; Boks, M.; van Haren, N.; Ophoff, R.; Kahn, R.; Bauer, M.; Pfennig, A.; Alda, M.; Hajek, T.; Mwangi, B.; Soares, J.; Nickson, T.; Dimitrova, R.; Sussmann, J.; Hagenaars, S.; Whalley, H.; McIntosh, A.; Thompson, P.; Andreassen, O.; Gen, C. R. C. C.; Gr, E. B. D. W.; Gen, C. R. C. C.; Gr, E. B. D. W., Subcortical volumetric abnormalities in bipolar disorder. *Molecular Psychiatry* **2016,** *21* (12), 1710-1716.

22.	ALTSHULER, L.; CURRAN, J.; HAUSER, P.; MINTZ, J.; DENICOFF, K.; POST, R., T-2 HYPERINTENSITIES IN BIPOLAR DISORDER - MAGNETIC-RESONANCE-IMAGING COMPARISON AND LITERATURE METAANALYSIS. *American Journal of Psychiatry* **1995,** *152* (8), 1139-1144.

23.	Vargas, C.; Lopez-Jaramillo, C.; Vieta, E., A systematic literature review of resting state network-functional MRI in bipolar disorder. *Journal of Affective Disorders* **2013,** *150* (3), 727-735.

24.	SCHILDKRAUT, J., THE CATECHOLAMINE HYPOTHESIS OF AFFECTIVE-DISORDERS - A REVIEW OF SUPPORTING EVIDENCE (REPRINTED FROM AMERICAN JOURNAL OF PSYCHIATRY, VOL 122, PG 509-522, 1965). *Journal of Neuropsychiatry and Clinical Neurosciences* **1995,** *7* (4), 524-533.

25.   Heninger, G.; Delgado, P.; Charney, D., The revised monoamine theory of depression: A modulatory role for monoamines, based on new findings from monoamine depletion experiments in humans. *Pharmacopsychiatry* **1996,** *29* (1), 2-11.

26.   Ashok, A.; Marques, T.; Jauhar, S.; Nour, M.; Goodwin, G.; Young, A.; Howes, O., The dopamine hypothesis of bipolar affective disorder: the state of the art and implications for treatment. *Molecular Psychiatry* **2017,** *22* (5), 666-679.

27.   Rees, J.; Florang, V.; Anderson, D.; Doorn, J., Lipid peroxidation products inhibit dopamine catabolism yielding aberrant levels of a reactive intermediate. *Chemical Research in Toxicology* **2007,** *20* (10), 1536-1542.

28.   Berman, S.; Hastings, T., Dopamine oxidation alters mitochondrial respiration and induces permeability transition in brain mitochondria: Implications for Parkinson's disease. *Journal of Neurochemistry* **1999,** *73* (3), 1127-1137.

29.   Stokes, A.; Hastings, T.; Vrana, K., Cytotoxic and genotoxic potential of dopamine. *Journal of Neuroscience Research* **1999,** *55* (6), 659-665.

30.   Grima, G.; Benz, B.; Parpura, V.; Cuenod, M.; Do, K., Dopamine-induced oxidative stress in neurons with glutathione deficit: implication for schizophrenia. *Schizophrenia Research* **2003,** *62* (3), 213-224.

31.   Meyer, J.; Wilson, A.; Sagrati, S.; Miler, L.; Rusjan, P.; Bloomfield, P.; Clark, M.; Sacher, J.; Voineskos, A.; Houle, S., Brain Monoamine Oxidase A Binding in Major Depressive Disorder Relationship to Selective Serotonin Reuptake Inhibitor Treatment, Recovery, and Recurrence. *Archives of General Psychiatry* **2009,** *66* (12), 1304-1312.

32.   Selvaraj, S.; Murthy, N.; Bhagwagar, Z.; Bose, S.; Hinz, R.; Grasby, P.; Cowen, P., Diminished brain 5-HT transporter binding in major depression: a positron emission tomography study with [C-11]DASB. *Psychopharmacology* **2011,** *213* (2-3), 555-562.

33.   Yuksel, C.; Ongur, D., Magnetic Resonance Spectroscopy Studies of Glutamate-Related Abnormalities in Mood Disorders. *Biological Psychiatry* **2010,** *68* (9), 785-794.

34.   Kato, T., Mitochondrial dysfunction as the molecular basis of bipolar disorder - Therapeutic implications. *Cns Drugs* **2007,** *21* (1), 1-11.

35.   Kim, H.; Rapoport, S.; Rao, J., Altered expression of apoptotic factors and synaptic markers in postmortem brain from bipolar disorder patients. *Neurobiology of Disease* **2010,** *37* (3), 596-603.

36.   Fernandes, B.; Gama, C.; Cereser, K.; Yatham, L.; Fries, G.; Colpo, G.; de Lucena, D.; Kunz, M.; Gomes, F.; Kapczinski, F., Brain-derived neurotrophic factor as a state-marker of mood episodes in bipolar disorders: A systematic review and meta-regression analysis. *Journal of Psychiatric Research* **2011,** *45* (8), 995-1004.

37.   Polyakova, M.; Stuke, K.; Schuemberg, K.; Mueller, K.; Schoenknecht, P.; Schroeter, M., BDNF as a biomarker for successful treatment of mood disorders: A systematic & quantitative meta-analysis. *Journal of Affective Disorders* **2015,** *174*, 432-440.

38.   Harry, G.; Kraft, A., Microglia in the developing brain: A potential target with lifetime effects. *Neurotoxicology* **2012,** *33* (2), 191-206.

39.   Prinz, M.; Priller, J., Microglia and brain macrophages in the molecular age: from origin to neuropsychiatric disease. *Nature Reviews Neuroscience* **2014,** *15* (5), 300-312.

40.   Streit, W.; Mrak, R.; Griffin, W., Microglia and neuroinflammation: a pathological perspective. *Journal of Neuroinflammation* **2004,** *1*.

41.   Bezchlibnyk, Y.; Wang, J.; McQueen, G.; Young, L., Gene expression differences in bipolar disorder revealed by cDNA array analysis of post-mortem frontal cortex. *Journal of Neurochemistry* **2001,** *79* (4), 826-834.

42.   Rao, J.; Harry, G.; Rapoport, S.; Kim, H., Increased excitotoxicity and neuroinflammatory markers in postmortem frontal cortex from bipolar disorder patients. *Molecular Psychiatry* **2010,** *15* (4), 384-392.

43.   Hamdani, N.; Doukhan, R.; Kurtlucan, O.; Tamouza, R.; Leboyer, M., Immunity, Inflammation, and Bipolar Disorder: Diagnostic and Therapeutic Implications. *Current Psychiatry Reports* **2013,** *15* (9).

44.   Stertz, L.; Magalhaes, P.; Kapczinski, F., Is bipolar disorder an inflammatory condition? The relevance of microglial activation. *Current Opinion in Psychiatry* **2013,** *26* (1), 19-26.

45.   Mahadik, S.; Evans, D.; Lal, H., Oxidative stress and role of antioxidant and omega-3 essential fatty acid supplementation in schizophrenia. *Progress in Neuro-Psychopharmacology & Biological Psychiatry* **2001,** *25* (3), 463-493.

46.   Berk, M.; Kapczinski, F.; Andreazza, A.; Dean, O.; Giorlando, F.; Maes, M.; Yucel, M.; Gama, C.; Dodd, S.; Dean, B.; Magalhaes, P.; Amminger, P.; McGorry, P.; Malhi, G., Pathways underlying neuroprogression in bipolar disorder: Focus on inflammation, oxidative stress and neurotrophic factors. *Neuroscience and Biobehavioral Reviews* **2011,** *35* (3), 804-817.

47.   Kunz, M.; Gama, C.; Andreazza, A.; Salvador, M.; Cereser, K.; Gomes, F.; Belmonte-De-Abreu, P.; Berk, M.; Kapczinski, F., Elevated serum superoxide dismutase and thiobarbituric acid reactive substances in different phases of bipolar disorder and in schizophrenia. *Progress in Neuro-Psychopharmacology & Biological Psychiatry* **2008,** *32* (7), 1677-1681.

48.   Gergerlioglu, H.; Savas, H.; Bulbul, F.; Selek, S.; Uz, E.; Yumru, M., Changes in nitric oxide level and superoxide dismutase activity during antimanic treatment. *Progress in Neuro-Psychopharmacology & Biological Psychiatry* **2007,** *31* (3), 697-702.

49.   Kapczinski, F.; Dal-Pizzol, F.; Teixeira, A.; Magalhaes, P.; Kauer-Sant'Anna, M.; Klamt, F.; Moreira, J.; Pasquali, M.; Fries, G.; Quevedo, J.; Gama, C.; Post, R., Peripheral biomarkers and illness activity in bipolar disorder. *Journal of Psychiatric Research* **2011,** *45* (2), 156-161.

50.   Taylor, D.; Cornelius, V.; Smith, L.; Young, A., Comparative efficacy and acceptability of drug treatments for bipolar depression: a multiple-treatments meta-analysis. *Acta Psychiatrica Scandinavica* **2014,** *130* (6), 452-469.

51.   Miura, T.; Noma, H.; Furukawa, T.; Mitsuyasu, H.; Tanaka, S.; Stockton, S.; Salanti, G.; Motomura, K.; Shimano-Katsuki, S.; Leucht, S.; Cipriani, A.; Geddes, J.; Kanba, S., Comparative efficacy and tolerability of pharmacological treatments in the maintenance treatment of bipolar disorder: a systematic review and network meta-analysis. *Lancet Psychiatry* **2014,** *1* (5), 351-359.

52.   Yatham, L.; Kennedy, S.; Parikh, S.; Schaffer, A.; Bond, D.; Frey, B.; Sharma, V.; Goldstein, B.; Rej, S.; Beaulieu, S.; Alda, M.; MacQueen, G.; Milev, R.; Ravindran, A.; O'Donovan, C.; McIntosh, D.; Lam, R.; Vazquez, G.; Kapczinski, F.; McIntyre, R.; Kozicky, J.; Kanba, S.; Lafer, B.; Suppes, T.; Calabrese, J.; Vieta, E.; Malhi, G.; Post, R.; Berk, M., Canadian Network for Mood and Anxiety Treatments (CANMAT) and International Society for Bipolar Disorders (ISBD) 2018 guidelines for the management of patients with bipolar disorder. *Bipolar Disorders* **2018,** *20* (2), 97-170.

53.   Kanba, S.; Kato, T.; Terao, T.; Yamada, K.; Mood, C. T. G.; Disorders, J. S. M.; Mood, C. T. G.; Disorders, J. S. M., Guideline for treatment of bipolar disorder by the Japanese Society of Mood Disorders, 2012. *Psychiatry and Clinical Neurosciences* **2013,** *67* (5), 285-300.

54.   Vieta, E.; Locklear, J.; Gunther, O.; Ekman, M.; Miltenburger, C.; Chatterton, M.; Astrom, M.; Paulsson, B., Treatment Options for Bipolar Depression A Systematic Review of Randomized, Controlled Trials. *Journal of Clinical Psychopharmacology* **2010,** *30* (5), 579-590.

55.   Young, L.; Joffe, R.; Robb, J.; MacQueen, G.; Marriott, M.; Patelis-Siotis, I., Double-blind comparison of addition of a second mood stabilizer versus an antidepressant to an initial mood stabilizer for treatment of patients with bipolar depression. *American Journal of Psychiatry* **2000,** *157* (1), 124-126.

56.   Geddes, J.; Calabrese, J.; Goodwin, G., Lamotrigine for treatment of bipolar depression: independent meta-analysis and meta-regression of individual patient data from five randomised trials. *British Journal of Psychiatry* **2009,** *194* (1), 4-9.

57.   ALTSHULER, L.; POST, R.; LEVERICH, G.; MIKALAUSKAS, K.; ROSOFF, A.; ACKERMAN, L., ANTIDEPRESSANT-INDUCED MANIA AND CYCLE ACCELERATION - A CONTROVERSY REVISITED. *American Journal of Psychiatry* **1995,** *152* (8), 1130-1138.

58.   SACHS, G.; LAFER, B.; STOLL, A.; BANOV, M.; THIBAULT, A.; TOHEN, M.; ROSENBAUM, J., A DOUBLE-BLIND TRIAL OF BUPROPION VERSUS DESIPRAMINE FOR BIPOLAR DEPRESSION. *Journal of Clinical Psychiatry* **1994,** *55* (9), 391-393.

59.   Malhi, G.; Tanious, M.; Das, P.; Coulston, C.; Berk, M., Potential Mechanisms of Action of Lithium in Bipolar Disorder Current Understanding. *Cns Drugs* **2013,** *27* (2), 135-153.

60.   Drevets, W., Neuroimaging and neuropathological studies of depression: implications for the cognitive-emotional features of mood disorders. *Current Opinion in Neurobiology* **2001,** *11* (2), 240-249.

61.   Yucel, K.; Taylor, V.; McKinnon, M.; MacDonald, K.; Alda, M.; Young, L.; MacQueen, G., Bilateral hippocampal volume increase in patients with bipolar disorder and short-term lithium treatment. *Neuropsychopharmacology* **2008,** *33* (2), 361-367.

62.   Chang, K.; Barnea-Goraly, N.; Karchemskiy, A.; Simeonova, D.; Barnes, P.; Ketter, T.; Reiss, A., Cortical magnetic resonance imaging findings in familial pediatric bipolar disorder. *Biological Psychiatry* **2005,** *58* (3), 197-203.

63.   Manji, H.; Chen, G., PKC, MAP kinases and the bcl-2 family of proteins as long-term targets for mood stabilizers. *Molecular Psychiatry* **2002,** *7*, S46-S56.

64.   Harwood, A., Lithium and bipolar mood disorder: the inositol-depletion hypothesis revisited. *Molecular Psychiatry* **2005,** *10* (1), 117-126.

65.   Gould, T.; Chen, G.; Manji, H., In vivo evidence in the brain for lithium inhibition of glycogen synthase kinase-3. *Neuropsychopharmacology* **2004,** *29* (1), 32-38.

66.   Hedgepeth, C.; Conrad, L.; Zhang, J.; Huang, H.; Lee, V.; Klein, P., Activation of the wnt signaling pathway: A molecular mechanism for lithium action. *Developmental Biology* **1997,** *185* (1), 82-91.

67.   Lovestone, S.; Davis, D.; Webster, M.; Kaech, S.; Brion, J.; Matus, A.; Anderton, B., Lithium reduces tau phosphorylation: Effects in living cells and in neurons at therapeutic concentrations. *Biological Psychiatry* **1999,** *45* (8), 995-1003.

68.   Cui, J.; Shao, L.; Young, L.; Wang, J., Role of glutathione in neuroprotective effects of mood stabilizing drugs lithium and valproate. *Neuroscience* **2007,** *144* (4), 1447-1453.

69.   Chang, Y.; Rapoport, S.; Rao, J., Chronic Administration of Mood Stabilizers Upregulates BDNF and Bcl-2 Expression Levels in Rat Frontal Cortex. *Neurochemical Research* **2009,** *34* (3), 536-541.

70.   Ketter, T.; Manji, H.; Post, R., Potential mechanisms of action of lamotrigine in the treatment of bipolar disorders. *Journal of Clinical Psychopharmacology* **2003,** *23* (5), 484-495.

71.   Stefani, A.; Spadoni, F.; Bernardi, G., Voltage-activated calcium channels: Targets of antiepileptic drug therapy? *Epilepsia* **1997,** *38* (9), 959-965.

72.   Chateauvieux, S.; Morceau, F.; Dicato, M.; Diederich, M., Molecular and Therapeutic Potential and Toxicity of Valproic Acid. *Journal of Biomedicine and Biotechnology* **2010**.

73.   Bachmann, R.; Wang, Y.; Yuan, P.; Zhou, R.; Li, X.; Alesci, S.; Du, J.; Manji, H., Common effects of lithium and valproate on mitochondrial functions: protection against methamphetamine-induced mitochondrial damage. *International Journal of Neuropsychopharmacology* **2009,** *12* (6), 805-822.

74.   Chen, G.; Huang, L.; Jiang, Y.; Manji, H., The mood-stabilizing agent valproate inhibits the activity of glycogen synthase kinase-3. *Journal of Neurochemistry* **1999,** *72* (3), 1327-1330.

75.   MELTZER, H.; MATSUBARA, S.; LEE, J., CLASSIFICATION OF TYPICAL AND ATYPICAL ANTIPSYCHOTIC-DRUGS ON THE BASIS OF DOPAMINE D-1, D-2 AND SEROTONIN2 PKI VALUES. *Journal of Pharmacology and Experimental Therapeutics* **1989,** *251* (1), 238-246.

76.   Meltzer, H.; Caskey, C., Update on Typical and Atypical Antipsychotic Drugs. *Annual Review of Medicine, Vol 64* **2013,** *64*, 393-406.

77.   Kusumi, I.; Boku, S.; Takahashi, Y., Psychopharmacology of atypical antipsychotic drugs: From the receptor binding profile to neuroprotection and neurogenesis. *Psychiatry and Clinical Neurosciences* **2015,** *69* (5), 243-258.

78.   Kato, T.; Monji, A.; Mizoguchi, Y.; Hashioka, S.; Horikawa, H.; Seki, Y.; Kasai, M.; Utsumi, H.; Kanba, S., Anti-Inflammatory Properties of Antipsychotics Via Microglia Modulations: Are Antipsychotics a 'Fire Extinguisher' in the Brain of Schizophrenia? *Mini-Reviews in Medicinal Chemistry* **2011,** *11* (7), 565-574.

79.   Berk, M.; Dodd, S.; Kauer-Sant'Anna, M.; Malhi, G.; Bourin, M.; Kapczinski, F.; Norman, T., Dopamine dysregulation syndrome: implications for a dopamine hypothesis of bipolar disorder. *Acta Psychiatrica Scandinavica* **2007,** *116*, 41-49.

80.   Wittenborn, J. R., Deductive approaches to the catecholamine hypothesis of affective disorders. *J Nerv Ment Dis* **1974,** *158* (5), 320-4.

81.   Tissot, R., The common pathophysiology of monaminergic psychoses: a new hypothesis. *Neuropsychobiology* **1975,** *1* (4), 243-60.

82.   Singh, M. M., A unifying hypothesis on the biochemical basis of affective disorder. *Psychiatr Q* **1970,** *44* (4), 706-24.

83.   Cousins, D. A.; Butts, K.; Young, A. H., The role of dopamine in bipolar disorder. *Bipolar Disord* **2009,** *11* (8), 787-806.

84.   Howes, O.; Egerton, A.; Allan, V.; McGuire, P.; Stokes, P.; Kapur, S., Mechanisms Underlying Psychosis and Antipsychotic Treatment Response in Schizophrenia: Insights from PET and SPECT Imaging. *Current Pharmaceutical Design* **2009,** *15* (22), 2550-2559.

85.   Rangel-Barajas, C.; Coronel, I.; Floran, B., Dopamine Receptors and Neurodegeneration. *Aging and Disease* **2015,** *6* (5), 349-368.

86.   Missale, C.; Nash, S.; Robinson, S.; Jaber, M.; Caron, M., Dopamine receptors: From structure to function. *Physiological Reviews* **1998,** *78* (1), 189-225.

87.   Maramai, S.; Gemma, S.; Brogi, S.; Campiani, G.; Butini, S.; Stark, H.; Brindisi, M., Dopamine D3 Receptor Antagonists as Potential Therapeutics for the Treatment of Neurological Diseases. *Frontiers in Neuroscience* **2016,** *10*.

88.   Levant, B., The D-3 dopamine receptor: Neurobiology and potential clinical relevance. *Pharmacological Reviews* **1997,** *49* (3), 231-252.

89.   Chien, E.; Liu, W.; Zhao, Q.; Katritch, V.; Han, G.; Hanson, M.; Shi, L.; Newman, A.; Javitch, J.; Cherezov, V.; Stevens, R., Structure of the Human Dopamine D3 Receptor in Complex with a D2/D3 Selective Antagonist. *Science* **2010,** *330* (6007), 1091-1095.

90.   Sokoloff, P.; Le Foll, B., The dopamine D3 receptor, a quarter century later. *European Journal of Neuroscience* **2017,** *45* (1), 2-19.

91.   SOKOLOFF, P.; GIROS, B.; MARTRES, M.; ANDRIEUX, M.; BESANCON, R.; PILON, C.; BOUTHENET, M.; SOUIL, E.; SCHWARTZ, J., LOCALIZATION AND FUNCTION OF THE D(3) DOPAMINE RECEPTOR. *Arzneimittel-Forschung/drug Research* **1992,** *42-1* (2A), 224-230.

92.   SOKOLOFF, P.; GIROS, B.; MARTRES, M.; BOUTHENET, M.; SCHWARTZ, J., MOLECULAR-CLONING AND CHARACTERIZATION OF A NOVEL DOPAMINE RECEPTOR (D3) AS A TARGET FOR NEUROLEPTICS. *Nature* **1990,** *347* (6289), 146-151.

93.   Newman, A.; Grundt, P.; Cyriac, G.; Deschamps, J.; Taylor, M.; Kumar, R.; Ho, D.; Luedtke, R., N-(4-(4-(2,3-Dichloro- or 2-methoxyphenyl)piperazin-1-yl)butyl)heterobiarylcarboxamides with Functionalized Linking Chains as High Affinity and Enantioselective D3 Receptor Antagonists. *Journal of Medicinal Chemistry* **2009,** *52* (8), 2559-2570.

94.   Visanji, N.; Millan, M.; Brotchie, J., BP897, a "selective" dopamine D-3 receptor partial agonist, has actions in addition to attenuation of D-3 transmission in modulating locomotion induced by L-dopa in monoamine depleted rats. *Movement Disorders* **2004,** *19* (9), 1132-1132.

95.   Yuan, J.; Chen, X.; Brodbeck, R.; Primus, R.; Braun, J.; Wasley, J.; Thurkauf, A., NGB 2904 and NGB 2849: Two highly selective dopamine D-3 receptor antagonists. *Bioorganic & Medicinal Chemistry Letters* **1998,** *8* (19), 2715-2718.

96.   Xi, Z.; Gardner, E., Pharmacological actions of NGB 2904, a selective dopamine D-3 receptor antagonist, in animal models of drug addiction. *Cns Drug Reviews* **2007,** *13* (2), 240-259.

97.   Bettinetti, L.; Schlotter, K.; Hubner, H.; Gmeiner, P., Interactive SAR studies: Rational discovery of super-potent and highly selective dopamine D3 receptor antagonists and partial agonists. *Journal of Medicinal Chemistry* **2002,** *45* (21), 4594-4597.

98.   Thanos, P.; Katana, J.; Ashby, C.; Michaelides, M.; Gardner, E.; Heidbreder, C.; Volkow, N., The selective dopamine D3 receptor antagonist SB-277011-A attenuates ethanol consumption in ethanol preferring (P) and non-preferring (NP) rats. *Pharmacology Biochemistry and Behavior* **2005,** *81* (1), 190-197.

99.   Grundt, P.; Carlson, E.; Cao, J.; Bennett, C.; McElveen, E.; Taylor, M.; Luedtke, R.; Newman, A., Novel heterocyclic trans olefin analogues of N-{4-[4-(2,3-dichlorophenyl)piperazin-1-yl]butyl}arylcarboxamides as selective probes with high affinity for the dopamine D3 receptor. *Journal of Medicinal Chemistry* **2005,** *48* (3), 839-848.

100.   Kiss, B.; Horvath, A.; Nemethy, Z.; Schmidt, E.; Laszlovszky, I.; Bugovics, G.; Fazekas, K.; Hornok, K.; Orosz, S.; Gyertyan, I.; Agai-Csongor, E.; Domany, G.; Tihanyi, K.; Adham, N.; Szombathelyi, Z., Cariprazine (RGH-188), a Dopamine D-3 Receptor-Preferring, D-3/D-2 Dopamine Receptor Antagonist-Partial Agonist Antipsychotic Candidate: In Vitro and Neurochemical Profile. *Journal of Pharmacology and Experimental Therapeutics* **2010,** *333* (1), 328-340.

101.   Newman, A.; Beuming, T.; Banala, A.; Donthamsett, P.; Pongetti, K.; LaBounty, A.; Levy, B.; Cao, J.; Michino, M.; Luedtke, R.; Javitch, J.; Shi, L., Molecular Determinants of Selectivity and Efficacy at the Dopamine D3 Receptor. *Journal of Medicinal Chemistry* **2012,** *55* (15), 6689-6699.

102.   Geneste, H.; Amberg, W.; Backfisch, G.; Beyerbach, A.; Braje, W.; Delzer, E.; Haupt, A.; Hutchins, C.; King, L.; Sauer, D.; Unger, L.; Wernet, W., Synthesis and SAR of highly potent and selective dopamine D-3-receptor antagonists: Variations on the 1H-pyrimidin-2-one theme. *Bioorganic & Medicinal Chemistry Letters* **2006,** *16* (7), 1934-1937.

103.   Macdonald, G.; Branch, C.; Hadley, M.; Johnson, C.; Nash, D.; Smith, A.; Stemp, G.; Thewlis, K.; Vong, A.; Austin, N.; Jeffrey, P.; Winborn, K.; Boyfield, I.; Hagan, J.; Middlemiss, D.; Reavill, C.; Riley, G.; Watson, J.; Wood, M.; Parker, S.; Ashby, C., Design and synthesis of trans-3-(2-(4-((3-(3-(5-methyl-1,2,4-oxadiazolyl))phenyl)carboxamido)cyclohexyl)ethyl)-7-methylsulfonyl-2,3,4,5-tetrahydro-1H-3-benzazepine (SB-414796): A potent and selective dopamine D-3 receptor antagonist. *Journal of Medicinal Chemistry* **2003,** *46* (23), 4952-4964.

104.   Micheli, F.; Arista, L.; Bonanomi, G.; Blaney, F.; Braggio, S.; Capelli, A.; Checchia, A.; Damiani, F.; Di-Fabio, R.; Fontana, S.; Gentile, G.; Griffante, C.; Hamprecht, D.; Marchioro, C.; Mugnaini, M.; Piner, J.; Ratti, E.; Tedesco, G.; Tarsi, L.; Terreni, S.; Worby, A.; Ashby, C.; Heidbreder, C., 1,2,4-Triazolyl Azabicyclo[3.1.0]hexanes: A New Series of Potent and Selective Dopamine D-3 Receptor Antagonists. *Journal of Medicinal Chemistry* **2010,** *53* (1), 374-391.

105.   Hong, M.; Chen, D.; Klein, P.; Lee, V., Lithium reduces tau phosphorylation by inhibition of glycogen synthase kinase-3. *Journal of Biological Chemistry* **1997,** *272* (40), 25326-25332.

106.   SUTHERLAND, C.; LEIGHTON, I.; COHEN, P., INACTIVATION OF GLYCOGEN-SYNTHASE KINASE-3-BETA BY PHOSPHORYLATION - NEW KINASE CONNECTIONS IN INSULIN AND GROWTH-FACTOR SIGNALING. *Biochemical Journal* **1993,** *296*, 15-19.

107.   Fang, X.; Yu, S.; Lu, Y.; Bast, R.; Woodgett, J.; Mills, G., Phosphorylation and inactivation of glycogen synthase kinase 3 by protein kinase A. *Proceedings of the National Academy of Sciences of the United States of America* **2000,** *97* (22), 11960-11965.

108.   CROSS, D.; ALESSI, D.; COHEN, P.; ANDJELKOVICH, M.; HEMMINGS, B., INHIBITION OF GLYCOGEN-SYNTHASE KINASE-3 BY INSULIN-MEDIATED BY PROTEIN-KINASE-B. *Nature* **1995,** *378* (6559), 785-789.

109.   GOODE, N.; HUGHES, K.; WOODGETT, J.; PARKER, P., DIFFERENTIAL REGULATION OF GLYCOGEN-SYNTHASE KINASE-3-BETA BY PROTEIN-KINASE-C ISOTYPES. *Journal of Biological Chemistry* **1992,** *267* (24), 16878-16882.

110.   Ding, V.; Chen, R.; McCormick, F., Differential regulation of glycogen synthase kinase 3 beta by insulin and Wnt signaling. *Journal of Biological Chemistry* **2000,** *275* (42), 32475-32481.

111.   ter Haar, E.; Coll, J. T.; Austen, D. A.; Hsiao, H. M.; Swenson, L.; Jain, J., Structure of GSK3beta reveals a primed phosphorylation mechanism. *Nat Struct Biol* **2001,** *8* (7), 593-6.

112.   Lu, S.; Jiang, Y.; Zou, J.; Wu, T., Dissection of the difference between the group I metal ions in inhibiting GSK3 beta: a computational study. *Physical Chemistry Chemical Physics* **2011,** *13* (15), 7014-7023.

113.   Jope, R. S., Glycogen synthase kinase-3 in the etiology and treatment of mood disorders. *Front Mol Neurosci* **2011,** *4*, 16.

114.   Ryves, W. J.; Harwood, A. J., Lithium inhibits glycogen synthase kinase-3 by competition for magnesium. *Biochem Biophys Res Commun* **2001,** *280* (3), 720-5.

115.   Jope, R. S., Lithium and GSK-3: one inhibitor, two inhibitory actions, multiple outcomes. *Trends Pharmacol Sci* **2003,** *24* (9), 441-3.

116.   Dandekar, M. P.; Valvassori, S. S.; Dal-Pont, G. C.; Quevedo, J., Glycogen Synthase Kinase-3β as a Putative Therapeutic Target for Bipolar Disorder. *Curr Drug Metab* **2018,** *19* (8), 663-673.

117.   Gould, T. D.; Einat, H.; Bhat, R.; Manji, H. K., AR-A014418, a selective GSK-3 inhibitor, produces antidepressant-like effects in the forced swim test. *Int J Neuropsychopharmacol* **2004,** *7* (4), 387-90.

118.   McInnes, C.; Fischer, P., Strategies for the design of potent and selective kinase inhibitors. *Current Pharmaceutical Design* **2005,** *11* (14), 1845-1863.

119.   Martinez, A.; Alonso, M.; Castro, A.; Perez, C.; Moreno, F. J., First non-ATP competitive glycogen synthase kinase 3 beta (GSK-3beta) inhibitors: thiadiazolidinones (TDZD) as potential drugs for the treatment of Alzheimer's disease. *Journal of medicinal chemistry* **2002,** *45* (6), 1292-9.

120.	Mazanetz, M.; Fischer, P., Untangling tau hyperphosphorylation in drug design for neurodegenerative diseases. *Nature Reviews Drug Discovery* **2007,** *6* (6), 464-479.

121.	Perez, D. I.; Conde, S.; Perez, C.; Gil, C.; Simon, D.; Wandosell, F.; Moreno, F. J.; Gelpi, J. L.; Luque, F. J.; Martinez, A., Thienylhalomethylketones: Irreversible glycogen synthase kinase 3 inhibitors as useful pharmacological tools. *Bioorg. Med. Chem.* **2009,** *17* (19), 6914.

122.	Veselinović, T.; Paulzen, M.; Gründer, G., Cariprazine, a new, orally active dopamine D2/3 receptor partial agonist for the treatment of schizophrenia, bipolar mania and depression. *Expert Rev Neurother* **2013,** *13* (11), 1141-59.

123.	Kozikowski, A. P.; Gaisina, I. N.; Yuan, H.; Petukhov, P. A.; Blond, S. Y.; Fedolak, A.; Caldarone, B.; McGonigle, P., Structure-based design leads to the identification of lithium mimetics that block mania-like effects in rodents. possible new GSK-3beta therapies for bipolar disorders. *J Am Chem Soc* **2007,** *129* (26), 8328-32.

124.	De Simone, A.; Russo, D.; Ruda, G. F.; Micoli, A.; Ferraro, M.; Di Martino, R. M.; Ottonello, G.; Summa, M.; Armirotti, A.; Bandiera, T.; Cavalli, A.; Bottegoni, G., Design, Synthesis, Structure-Activity Relationship Studies, and Three-Dimensional Quantitative Structure-Activity Relationship (3D-QSAR) Modeling of a Series of O-Biphenyl Carbamates as Dual Modulators of Dopamine D3 Receptor and Fatty Acid Amide Hydrolase. *J Med Chem* **2017,** *60* (6), 2287-2304.

125.	Bottegoni, G.; Veronesi, M.; Bisignano, P.; Kacker, P.; Favia, A. D.; Cavalli, A., Development and Application of a Virtual Screening Protocol for the Identification of Multitarget Fragments. *ChemMedChem* **2016,** *11* (12), 1259-63.

126.	Seelen, W.; Schafer, M.; Ernst, A., Selective ring N-protection of aminopyrazoles. *Tetrahedron Letters* **2003,** *44* (24), 4491-4493.

127.	Kroth, H.; Ansaloni, A.; Varisco, Y.; Jan, A.; Sreenivasachary, N.; Rezaei-Ghaleh, N.; Giriens, V.; Lohmann, S.; López-Deber, M. P.; Adolfsson, O.; Pihlgren, M.; Paganetti, P.; Froestl, W.; Nagel-Steger, L.; Willbold, D.; Schrader, T.; Zweckstetter, M.; Pfeifer, A.; Lashuel, H. A.; Muhs, A., Discovery and structure activity relationship of small molecule inhibitors of toxic β-amyloid-42 fibril formation. *J Biol Chem* **2012,** *287* (41), 34786-800.

128.	Ivanova, A.; Burgart, Y.; Saloutin, V., Synthesis and Antibacterial Activity of N-Alkyl-Substituted 4-Aryldiazenylpyrazoles. *Chemistry of Heterocyclic Compounds* **2013,** *49* (8), 1128-1135.

129.	Bidon-Chanal, A.; Fuertes, A.; Alonso, D.; Pérez, D. I.; Martínez, A.; Luque, F. J.; Medina, M., Evidence for a new binding mode to GSK-3: allosteric regulation by the marine compound palinurin. *Eur J Med Chem* **2013,** *60*, 479-89.

130.	Kockeritz, L.; Doble, B.; Patel, S.; Woodgett, J. R., Glycogen synthase kinase-3--an overview of an over-achieving protein kinase. *Curr Drug Targets* **2006,** *7* (11), 1377-88.